Exploitation de la réactivité de l'or via le design des ligands : stabilisation des intermédiaires réactionnels et développement de nouveaux processus catalytiques Au(I)/Au(III)

Abdallah Zeineddine

Université Fédérale
Toulouse Midi-Pyrénées

THÈSE

En vue de l'obtention du

DOCTORAT DE L'UNIVERSITÉ DE TOULOUSE

Délivré par :

Université Toulouse 3 Paul Sabatier (UT3 Paul Sabatier)

Présentée et soutenue par :
Abdallah ZEINEDDINE
le 20 Décembre 2017

Titre :
Harnessing the Reactivity of Gold *via* Ligand Design: Stabilization of Reactive Intermediates and Development of New Au(I)/Au(III) Catalytic Pathways

---

École doctorale et discipline ou spécialité :
ED SDM : Chimie moléculaire - CO 046

Unité de recherche :
Laboratoire Hétérochimie Fondamentale et Appliquée

Directeur/trice(s) de Thèse :
Didier BOURISSOU
Abderrahmane AMGOUNE

Jury :
Xavi RIBAS, Professeur de l'Université de Gérone, Espagne (Rapporteur)
Corinne GOSMINI, Directrice de Recherche C.N.R.S à Paris (Rapporteur)
Michel ETIENNE, Professeur de l'Université de Toulouse
Abderrahmane AMGOUNE, Professeur de l'Université de Lyon
Didier BOURISSOU, Directeur de Recherche C.N.R.S à Toulouse

Université Fédérale
Toulouse Midi-Pyrénées

THÈSE

En vue de l'obtention du

DOCTORAT DE L'UNIVERSITÉ DE TOULOUSE

Délivré par :

Université Toulouse 3 Paul Sabatier (UT3 Paul Sabatier)

Présentée et soutenue par :
Abdallah ZEINEDDINE
le 20 Décembre 2017

Titre :
Harnessing the Reactivity of Gold *via* Ligand Design: Stabilization of Reactive Intermediates and Development of New Au(I)/Au(III) Catalytic Pathways

---

École doctorale et discipline ou spécialité :
ED SDM : Chimie moléculaire - CO 046

Unité de recherche :
Laboratoire Hétérochimie Fondamentale et Appliquée

Directeur/trice(s) de Thèse :
Didier BOURISSOU
Abderrahmane AMGOUNE

Jury :
Xavi RIBAS, Professeur de l'Université de Gérone, Espagne (Rapporteur)
Corinne GOSMINI, Directrice de Recherche C.N.R.S à Paris (Rapporteur)
Michel ETIENNE, Professeur de l'Université de Toulouse
Abderrahmane AMGOUNE, Professeur de l'Université de Lyon
Didier BOURISSOU, Directeur de Recherche C.N.R.S à Toulouse

“Learn from yesterday, live for today, hope for tomorrow.
The important thing is not to stop questioning.”

Albert Einstein

For my family,

Acknowledgments

First, I would like to express my sincere gratitude to the member of the jury, Dr. Xavi Ribas, Dr. Corinne Gosmini and Pr. Michel Etienne for accepting to judge my work with enthusiasm and for the scientific discussion we had during the defense. I would then like to thank Didier and Abder for giving me the chance to do my master's internship and this thesis four years ago. Working at your side and under your supervision was a real pleasure.

Didier, I would like to thank you for giving me this precious opportunity to join your team. Your rigorous research approach and your encouraging attitude have always pulled me up, allowed me to go beyond my limits and to progress throughout these four years. At the end of this wonderful experience, I learned to be more organized, more rigorous and, thanks to you, I'm more armed to face my future challenges.

Abder, I had an incredible chance to work with you, and few lines would not be enough to thank you. You have always been there for me during the good and the bad moments, your unconditional support and your confidence in me have allowed me to accomplish this thesis. I will definitely miss your advices (and not only the scientific ones!!), your sense of humor, your constant positive attitude, and all the discussions we had!!!

I especially thank Ghenwa since without her I will most probably not have come to the LHFA for my master's internship. Thank you for all the discussions we shared (and not just the scientific ones), for all your advices, for your reassuring attitude, and for your constant support during these four years. I will miss you a lot, and I'm sure that we will stay in touch.

Blanca, thank you for taking the time to answer all my questions, for the valuable advices that you gave me during my stay in the lab, and for all the enriching scientific discussions we had.

Julien, thank you for your cheerfulness attitude and the good vibes you installed every day during all my stay in the lab. I will really miss all the political / series (I will make sure to discuss the last season of GoT with you!!) / movies / silly discussions we had.

During my thesis, I also had the chance to meet permanent staff from other teams. Nicolas, it was really a great pleasure to meet you and share the lunch and coffee breaks with you. Your kindness and your sense of humor contributed to the good times I spent in this laboratory. Noel, thank you for always being available to discuss chemistry and for all the advices that you gave to me!! Marie, although you arrived late to the lab, I really appreciate the moments and the discussions we shared during the lunch and coffee breaks!! Montserrat, thank you for taking the time to answer all my questions especially when I started to work with the GC.

I would like also to show my gratitude to Isabelle Favier, Christian Pradel, Olivier Thillaye De Boullay and Julien Babinot for being here ready to help with a smile every time I had a question or a problem. I would like to thank Romaric Lenk for his contribution and for helping me on this project. I would also like to thank Olivier Volpato for all the discussions we had, for your constant smile and positive mood, and of course for your big contribution to the proper functioning of the laboratory. Maryse Béziat and Sérah Noel thank you for your efficiency regarding the administrative formalities of the lab and for your kindness.

During the four years I spent at the LHFA, I had the chance to meet and work with many wonderful colleagues. I want to thank these people for all the pleasant moments we spent together in and outside the lab (for some unfortunately they arrived at the end of my stay): Laura, Gwen, Amos, Noel Angel, Max, Marc, Sitze, Anthony C., Natalia, Isabel, Katya, Raphael (the kind), Sébastien, Richard, Marta, Mattia, Julian, Florian, Nicolas, Pillar, Sophie, Jean, Aymeric, Nicolas, Anthony P. and Lorena. Another big special thanks to Franck,

Antonio and Alexandre for all the laughter, parties and moments we had together and you guys were always here for me whenever I needed to relax or to cheer up.

A big thank you to the current LBPB team. Charlie, Paul and Maxime, I've been hanging out with you guys almost every day for the past last two years (whether in the lab or outside) and I'm going to miss you a lot. We had very crazy/funny/stupid/inappropriate (Paul the last one is mainly for you hahahahaha) conversations and we spent an amazing time together. I consider myself very lucky to know you guys and of course we will stay in touch (P.S. Charlie this mean that I won't stop insulting you or threatening you to kick your ass). Rigoulette, I'm really happy that I had the chance to know you and it was a great pleasure to work with you over the past year. You are full of positive energy and you always manage to keep a smile on your face. Stay like this and best of luck for your stay at the LHFA. Saam, my favorite Thai!! Thank you for all the time we had together, for the food you cooked, for organizing basketball games, and for being a good friend!! Jessica, I'm happy that I met you and that we worked together for this past year. I wish you the best of luck for your future career. Cyril, although we didn't have the chance to spend a lot of time together, but I already consider you as a friend. I wish you the best of luck for your thesis and I hope that we will stay in touch (Iceland this summer??). Maryne, first I'm sorry I made you fill useless data sheets when you first arrived to the lab :D. I'm really glad that I met you and I wish you the best of luck for your thesis (go copper girl!!!). Enrico, you are a very cool and funny guy and I'm pleased to meet you. Best of luck for your Post-Doc and hope to see you again.

Maria, thank you for this one year we spent together. You always managed to pull me up even in the worst moments ever (I don't even know how you managed to do that!!!). Thank you for all the discussions we had, for all the laughter, for putting up with me (which strike is this one?), for all the parties….for everything really. I don't know what would I have done

without you this last year (probably I would have been bored but I would still have my ears functioning well hahahahahaha). I will miss you a lot!!!

Gustave, I don't even know where to start. You are the first friend I met in France (more than five years ago already!!) and we shared so many good moments together during our master studies (worst lab and study partner I ever had), at the LHFA and especially outside the lab. Thank you for being here (especially when I first arrived to Toulouse) whenever I needed a favor, a cheering talk, an advice, a laugh.....you are simply a great friend Gus Gus.

Feriel, you already know what I think about you, so I will try to be brief. I want to thank you for all the moments we shared in the office and in the lab. We had an amazing time together, but what I mostly appreciated is that when we had a fight (and of course it was always your fault! "non mais alors laaa…"), it took us few minutes to make peace and go back to enjoy each other companies. Thank you for the advices you gave me during all my stay in the lab, always here to listen and help, you are a true "golden" friend and I miss you a lot!!!

Finally, the people who matter the most in my life. My childhood friends (Walid, Amer, Malek, Yehya and Jad), although our future has separated us and each one of us is in a different country, but we don't need to see each other often to know that I can count on you guys and that you are always here for me, as much as I'm here for you. I love you my brothers. And of course the Zeineddine family: Mom, Dad, Maya and Hiba, I love you to the moon and back. I will have never be here today and would have never accomplished this thesis if it wasn't for your unconditional love and support. I'm very lucky to have you as my family and I miss you every day.

Table Of Contents

General Remarks ..... **- 11 -**

Experimental Conditions ..... - 11 -

List of Abbreviations ..... - 13 -

List of Compounds ..... - 15 -

1 General Introduction ..... **- 18 -**

1.1 Characteristics of Gold Chemistry ..... - 18 -

1.2 Reactivity of Gold Towards Elementary Organometallic Reactions ..... - 20 -

1.2.1 Oxidative Addition of Si-Si Bonds ..... - 21 -

1.2.2 Migratory Insertion ..... - 22 -

1.2.3 β-Hydride Elimination Reaction ..... - 25 -

1.3 Bidentate or Tridentate Ligands for the Characterization of Gold Intermediates - 28 -

1.4 Gold Catalysis with Bidentate Gold Complexes ..... - 31 -

1.4.1 (P,P) Bidentate Ligand ..... - 31 -

1.4.2 (C,C) Bidentate Ligand ..... - 35 -

1.4.3 (C,O) Bidentate Ligand ..... - 39 -

1.4.4 (P,N) Bidentate Ligand ..... - 41 -

1.5 Research Objectives and Thesis Outline ..... - 43 -

1.6 References ..... - 45 -

2 Ligand Design to Trigger the Oxidative Addition to Gold(I) ..... **- 47 -**

2.1 Historical Background ..... - 47 -

2.2 Intermolecular Oxidative Addition: Design Principles ..... - 53 -

2.3 Synthesis and Reactivity of (P,P) Au(I) Complex ..... - 57 -

2.3.1 Synthesis of Diphosphine-*o*-carborane Gold(I) Complexes ..... - 57 -

2.3.2 Influence of Phosphorus Substituents on the Oxidative Addition Reaction . - 58 -

2.3.3 Influence of the Counter anion on the Oxidative Addition Reaction ..... - 61 -

2.3.4 Oxidative Addition to Complex 6: Scope and Limitations ..... - 64 -

2.4 From (P,P) -Ligand to Simpler Hemi-Labile (P,L) Ligands ..... - 71 -

2.4.1 Design Principles ..... - 71 -

2.4.2 Preliminary Results with Different (P,N) Ligands ..... - 71 -

2.4.3 (P,N) Ligands Screening ..... - 79 -

2.4.4 Influence of the Counter Anion on the Oxidative Addition Reaction ..... - 80 -

2.4.5 Influence of Phosphorus Substituents on the Oxidative Addition Reaction . - 83 -

2.4.6 Oxidative Addition to Complex 10: Scope and Limitations ..... - 85 -

2.5 Conclusion ..... - 92 -

2.6 Experimental Part ..... - 94 -

2.7 Computational Details ..... - 120 -

2.8 References ..... - 121 -

3 Development of C-C Cross Coupling Reactions with Ar-X ..... - 124 -

3.1 State of the Art of Cross Coupling with Gold ..... - 124 -

3.1.1 Cross Coupling with External Oxidants ..... - 126 -

3.1.2 Cross-Coupling with Strong Electrophiles ..... - 135 -

3.2 Rational Construction of a Csp^2-Csp^2 Catalytic Cycle ..... - 141 -

3.2.1 Model Stoichiometric Reactions ..... - 142 -

3.2.2 Towards Catalysis ..... - 148 -

3.3 Conclusion ..... - 165 -

3.4 Experimental Part ..... - 166 -

3.5 References ..... - 179 -

4 Isolation of Reactive Gold(I) Carbene Complex ..... - 181 -

4.1 State of the Art ..... - 181 -

4.2 Characterization of α-oxo gold(I) carbene ..... - 188 -

4.2.1 With (P,N) Ligand ..... - 188 -

4.2.2 With (P,P) Ligand ..... - 190 -

4.3 Reactivity of α-oxo Gold(I) Carbenes ..... - 199 -

4.3.1 Towards Styrene ..... - 200 -

4.3.2 Towards Phosphine-Borane ..... - 201 -

4.3.3 Towards Phenol ..... - 202 -

4.4 Conclusion ..... - 206 -

4.5 Experimental Part ..... - 208 -

4.5.1 General Remarks ..... - 208 -

4.6 Computational Details ..... - 216 -

4.7 References ..... - 217 -

5 General Conclusion and Perspectives ..... - 219 -

6 Compte-rendu en Langue Française ..... - 227 -

6.1 Introduction Générale ..... - 227 -

6.2 Objectif du Projet de Thèse ..... - 228 -

6.3 Design de Ligand pour Déclencher l'Addition Oxydante à l'Or(I) ..... - 228 -

6.3.1 Introduction ..... - 228 -

6.3.2 Synthèse et Réactivité du complexe (P,P)Au(I) ..... - 229 -

6.3.3 Synthèse et Réactivité du complexe (P,N)Au(I) ..... - 234 -

6.4 Développement de Réactions de Couplage Croisé C-C avec Ar-X ..... - 237 -

6.4.1 Réactions Stœchiométriques Modèles ..... - 238 -

6.4.2 De la Stœchiométrie à la Catalyse ..... - 240 -

6.5 Isolation d'un Carbène d'or(I) Réactif ..... - 243 -

6.5.1 Introduction ..... - 243 -

6.5.2 Caractérisation d'un complexe α-oxo carbène d'or(I) ..... - 244 -

6.6 Conclusion ..... - 249 -

Résumé

Ce travail de thèse porte sur la chimie organométallique des complexes d'or(I) et sur l'étude de leurs réactivités. Plus particulièrement, le travail présenté ici dans ce manuscrit avait pour objectif d'approfondir nos connaissances sur l'impact des ligands utilisés sur la réactivité de l'or vis-à-vis (i) de l'addition oxydante intermoléculaire et (ii) la possibilité de stabiliser des intermédiaires d'or(I) hautement réactifs.

Dans la première partie de ce manuscrit, l'addition oxydante intermoléculaire des halogénures d'aryle (iodure et bromure) à des complexes moléculaires d'or(I) a été étudiée en détails. Nous avons pu montrer que cette étape élémentaire de la chimie organométallique, considéré comme impossible avec l'or, était en fait un processus favorable lorsqu'un ligand adéquat est employé, et deux stratégies différentes ont été élaborées. La première consiste à utiliser un ligand bis-phosphine bidenté qui impose une géométrie coudée autour de l'or, tandis que la deuxième stratégie implique l'utilisation d'un ligand hémi-labile bidenté avec des groupements donneurs doux et dur. Les deux stratégies ont été fructueuses, et les complexes d'or(III) issus des réactions d'addition oxydante ont été caractérisés spectroscopiquement et structuralement.

Dans la deuxième partie, ayant à notre disposition deux complexes d'or(I) capable d'effectuer l'addition oxydante, nous voulions aller au-delà de cette étape élémentaire. Dans cet objectif, nous avons construit un nouveau cycle catalytique Au(I)/Au(III) impliquant une séquence d'addition oxydante Csp^2-X, de Csp^2-H auration et d'élimination réductrice, illustrant le premier exemple d'arylation directe d'arènes avec des halogénures d'aryle catalysée à l'or.

Enfin, dans la dernière partie, nous avons tenté de stabiliser et de caractériser des intermédiaires d'or(I) très instables, comme le α-oxo carbène d'or(I). Cette espèce hautement électrophile est proposée comme un intermédiaire clés dans des nombreuses transformations catalytiques, mais n'a jamais été isolé ou caractérisé (en solution ou à l'état solide). L'utilisation d'un ligand bis-phosphine bidenté nous a permis de caractériser spectroscopiquement et structuralement le carbène α-oxo d'or(I) pour la première fois. Nous avons ensuite étudié sa réactivité vis-à-vis des réactions d'insertion et de cyclopropanation.

Mots clés: chimie de l'or ; addition oxydante ; arylation directe ; carbène α-oxo d'or(I)

Abstract

The present work is an organometallic study concerning the chemistry of gold(I) complexes and their reactivity. Of particular interest was to gain further knowledge on the impact of the ligands employed on the reactivity of gold towards (i) the intermolecular oxidative addition of aryl halides and (ii) the possibility of stabilizing high reactive gold(I) intermediates.

In the first part of the manuscript, the intermolecular oxidative addition of aryl halides (iodide and bromide) with molecular gold(I) complexes was investigated in detail. We showed that this organometallic elementary step, usually considered to be impossible for gold, is actually a favorable process when an adequate ligand is employed and two different strategies have been elaborated. The first one consists in the use of a bis-phosphine bidentate ligand that forces a bent geometry around gold, whereas the second strategy implicates the use of a hemi-labile bidentate ligand bearing a soft and a hard donor group. Both strategies were found fruitful, and the gold(III) complexes stemming from oxidative addition reactions were characterized by spectroscopic and structural means.

In the second part, having in hands two gold(I) complexes that undergo the oxidative addition reaction, we wanted to go beyond this elementary step. In that objective, we constructed a new Au(I)/Au(III) catalytic cycle involving a sequence of Csp^2-X oxidative addition, Csp^2-H auration and reductive elimination, allowing the first example of gold-catalyzed direct arylation of arenes with aryl halides.

Finally, in the last part, we attempted to stabilize and characterize high reactive gold(I) intermediates, like the α-oxo gold(I) carbenes. This electrophilic species is proposed in many catalytic transformations as key intermediates, but has never been isolated or characterized (in solution or in solid state). The use of a bidentate diphosphine ligand allowed the characterization of the α-oxo gold(I) carbene for the first time by means of multinuclear NMR spectroscopy, X-ray diffraction analysis and high resolution mass spectroscopy (ESI+). We then investigated the reactivity of the α-oxo gold(I) carbene towards insertion and cyclopropanation reactions. Interestingly, the reactivity of the generated gold(I) carbenes can be modulated depending on the electronic properties of the aryl ethyl diazoacetate used.

Keywords: gold chemistry; oxidative addition; direct arylation; α-oxo gold(I) carbenes.

General Remarks

The work presented in this manuscript was carried out in the Laboratoire Hétérochimie Fondamentale et Appliquée (UMR 5069) at the Université de Toulouse III – Paul Sabatier under the supervision of Pr. Abderrahmane Amgoune and Dr. Didier Bourissou from January 2014 to July 2017. Computational studies were performed by Dr. Karinne Miqueu and coworkers at the Institut des Sciences Analytiques et Physisco-Chimique pour l'Environnement et les Matériaux (UMR 5254).

Experimental Conditions

General Procedures

Unless otherwise stated, all reactions and manipulations were carried out under an inert atmosphere of dry argon using standard Schlenk techniques or in a glovebox under an inert atmosphere. Dry, oxygen-free solvents were dried by passage through activated molecular sieves (3 Å), using an MBraun SPS-800 solvent purification system. 1,2-dichlorobenzene and deuterated solvents were dried with activated powdered molecular sieves (3 Å). All solvents were degassed by multiple freeze-pump-thaw cycles. 1,2-dicarba-*closo*-dodecarborane was purchased from KatChem (Prague, Czech Republic). All starting materials were purchased from Sigma Aldrich.

Melting Points

Melting points were determined with a calibrated Stuart SMP40 apparatus.

NMR Spectroscopy

Solution ^{1}H, ^{13}C, ^{11}B, ^{19}F and ^{31}P NMR spectra were recorded on Bruker Avance 300, 400 or 500 spectrometers at 298 K, unless otherwise stated. Chemical shifts (δ) are expressed with a positive sign, in parts per million. ^{1}H and ^{13}C chemical shifts reported are referenced internally to residual portio- (^{1}H) or deutero- (^{13}C) solvent, while ^{11}B, ^{19}F and ^{31}P chemical shifts are relative to $BF_3.OEt_2$, $CFCl_3$ and 85% H_3PO_4, respectively. The following abbreviations and their combinations are used: br, broad; s, singlet; d, doublet; t, triplet; q, quartet; m, multiplet. The ^{1}H and ^{13}C resonance signals were attributed by means of 2D HSQC and HMBC experiments.

Mass Spectroscopy and GC-MS Analysis

Mass spectra were recorded on a Waters UPLC Xevo G2 Q TOF apparatus. GC-MS analyses were performed on a MS Perkin Elmer Clarus MS560, GC Perkin Elmer Clarus 500 and Agilent HP6890.

X-ray Crystallography

Crystallographic data were collected on a Bruker-AXS APEX II or on a Bruker Kappa APEX II. The structures were solved by direct methods (SHELXS-97), and refined using the least-squares method on F^2.

List of Abbreviations

Ar	Generic aryl group
$AgNTf_2$	Silver bis(trifluoromethanesulfonyl)imide
AgOTf	Silver trifluoromethanesulfonate
$AgSbF_6$	Silver hexafluoroantimonate
BAr^F	Tetrakis(bis(3,5-trifluoromethyl)phenyl)borate
BINOL	1,1'-bi(2-naphtol)
CDA	Charge-decomposition analysis
CSA	Camphorsulfonic acid
CT	Charge transfer
DavePhos	2-dicyclohexylphosphino-2'-(*N*,*N*-dimethylamino)biphenyl
DCB	1,2-dichlorobenzene
DFT	Density functional theory
ESI	Electrospray ionization
EDG	Electron-donating group
eq.	Equivalent
EWG	Electron-withdrawing group
GC-MS	Gas chromatography-Mass spectrometry
HOMO	Highest occupied molecular orbital
HRMS	High resolution mass spectrometry
*i*Pr	Isopropyl
IR	Infrared
L	Generic neutral, 2-electron donor ligand
LUMO	Lowest unoccupied molecular orbital

M	Transition metal
MeDalphos	Di(1-adamantyl)-2-dimethylaminophenylphosphine
MorDalphos	Di(1-adamantyl)-2-morpholinophenylphosphine
NFSI	*N*-fluorobenzenesulfonimide
NLMO	Natural localized molecular orbital
NHC	*N*-heterocyclic carbene
NMR	Nuclear magnetic resonance
Nu	Nucleophile
Selectfluor	1-chloromethyl-4-fluoro-1,4-diazoniabicyclo[2.2.2]octane bis(tetrafluoroborate)
SMD	Universal salvation model
THT	Tetrahydrothiophene
TMB	1,3,5-trimethoxybenzene
VdW	Van der Waals
Xantphos	4,5-bis(diphenylphosphino)-9,9-dimethylxanthene
XRD	X-ray diffraction

List of Compounds

1

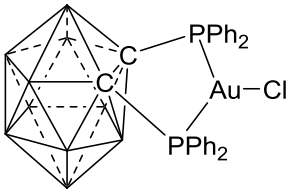

2

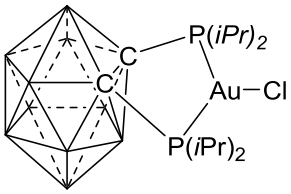

3

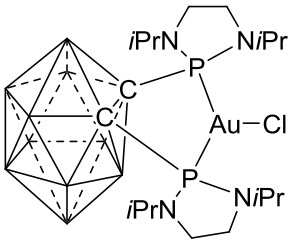

4

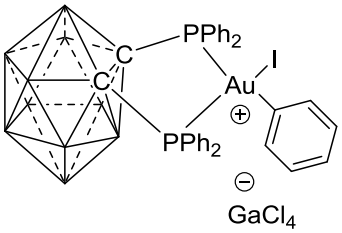

5

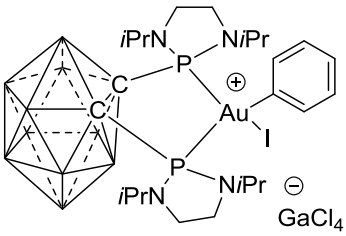

6

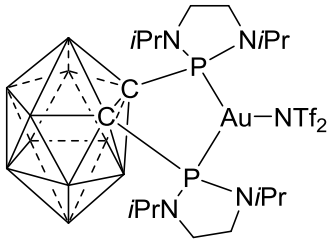

7

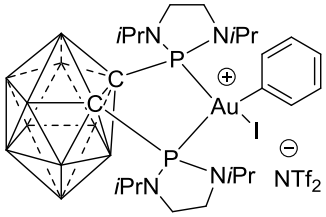

8

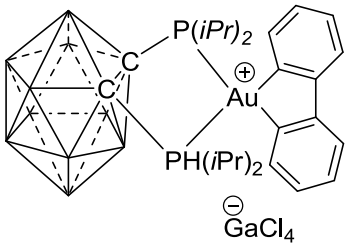

9

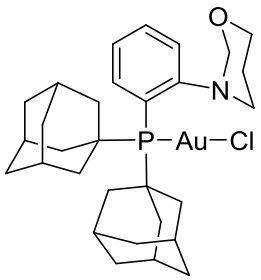

10

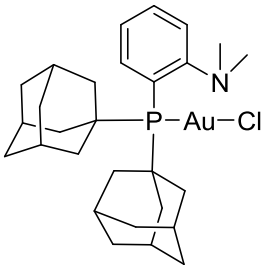

10-I

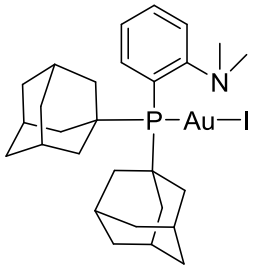

11

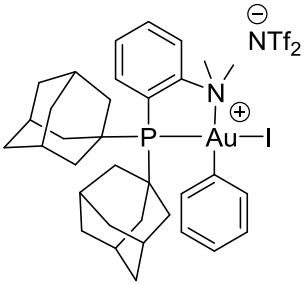

12

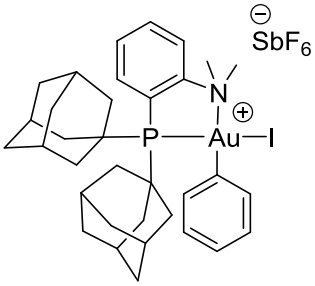

13

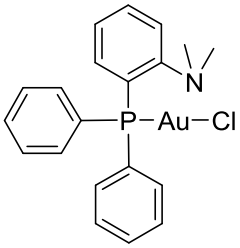

14

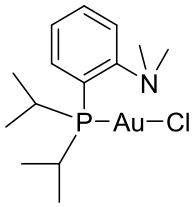

15

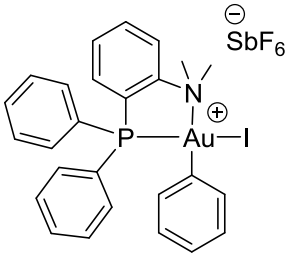

16

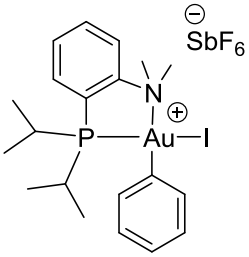

17

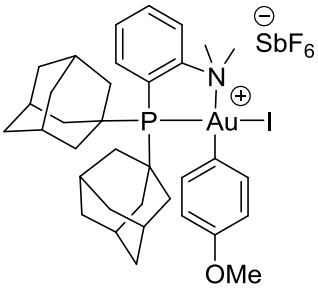

17’

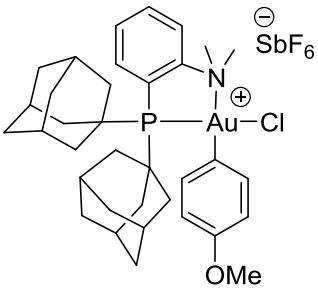

18

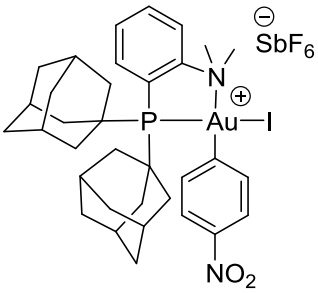

18’

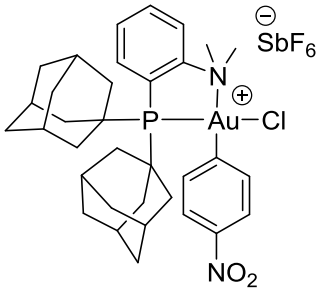
SbF6
N
P
Au
Cl
NO2

19

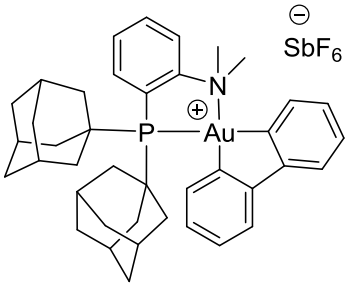
SbF6
N
P
Au

20

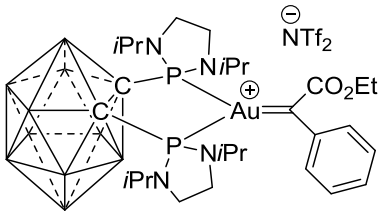
iPrN
P
NiPr
NTf2
C
C
Au
CO2Et
P
NiPr
iPrN

21

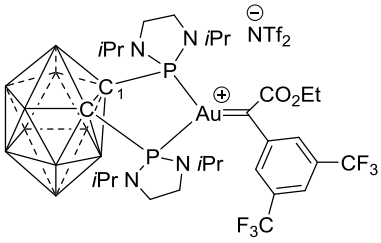
iPr N
N iPr
NTf2
P
C1
C
Au
CO2Et
P
N iPr
iPr N
CF3
F3C

1 General Introduction

1.1 Characteristics of Gold Chemistry

Gold is undoubtedly one of the first metals known to the human kind. As a result of its shinny color that never tarnishes, its ductility and malleability, gold's usage was ornamental in early civilizations. Over the decades, gold found many applications like in monetary exchange systems, odontology and electronics due to its high resistance to corrosion and its excellent electrical conductivity. In all these applications, gold is used in its metallic state. Despite the availability of other stable oxidation states, mainly the +I and +III states, the use of gold in chemistry remained undeveloped for a long time. Mononuclear gold(II) complexes are very scarce, and usually in the +II oxidation state, gold forms multinuclear species stabilized by Au-Au interactions.[1,2]

Gold can be distinguished from other transition metals when looking at its general properties, at the structure of its compound, and at its reactivity. These differences are the direct or indirect consequences of relativistic effects. In fact, due to a large number of protons in the nuclei of certain elements, electrons' velocity increases and approaches the speed of light and consequently, Einstein's theory of relativity has to be considered. Therefore, these "speedy" electrons have a relativistic mass that is greater than the non-relativistic mass. The direct consequence of a mass increase results in the contraction of the s and p shells (more pronounced for the s orbitals) since the Bohr radius of an electron is inversely proportional to its mass. This contraction is followed by the decrease in the effective nuclear charge Z_{eff} and as an outcome all orbitals are expanded. This destabilization affects the most the d orbitals and leads to an indirect stabilization (relativistic deshielding) of s and p orbitals. The relativistic deshielding attains its maximum for a filled d orbital, which explains why the relativistic effects are more noticeable with the heavier group 10 and 11 metals, namely Pt

and Au. Moreover, theoretical calculations stated that the most pronounced impact of relativistic effects is reached for the atomic number 79, *i.e.* gold.[3-6]

The fallouts of the relativistic effect on gold chemistry are several. First, due to the relatively smaller energy gap between the 5d and 6s orbitals, gold absorbs blue and violet and reflects red and yellow, giving this bright "golden" color to gold (in contrast to silver that absorbs in the ultraviolet region due to a larger energy gap between the 4d and 5s).[7] The smaller covalent radius of gold (1.36 Å) when compared to silver (1.45 Å) is also a consequence of relativistic effects.[8] Moreover, in contrast to copper and silver, the +III oxidation state of gold is more accessible thanks to the destabilization of the d orbitals.[9] Finally, the high electronegativity of gold (*vs.* other metals) and its soft character are also linked to relativistic effects.[1,10]

The soft and electronegative natures of gold are the reason behind its success. In fact, after being considered as chemically inert for so long, gold was found, in the late 1990's, to be a powerful carbophilic Lewis acid well suited for the activation of soft electrophiles such as π bonds towards nucleophilic attacks (Scheme 2.1).[11]

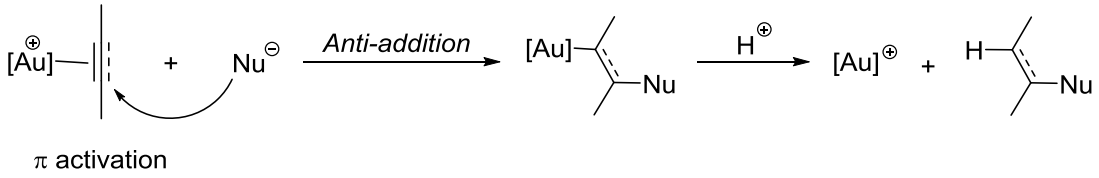

Scheme 2.1 Nucleophilic attack on a gold-activated π bond.

After this major breakthrough, we witnessed a gold rush in catalysis. In all these transformations, electro-deficient gold cationic complexes featuring monodentate ligands (L = R_3P or NHC) with the general formula [LAu^+], were used as active species.[12-14] The

coordination of π substrates affords two coordinate Au(I) intermediates with a favorable linear geometry. For a while, ligand modulation and structure/reactivity relationship investigations were limited to these monodentate ligands. However, more recently, multidentate ligands have also been shown to be very suitable for gold(I) and gold(III) species, opening promising perspectives in gold chemistry.[15-17] Thus, new reactivities and new catalytic transformations have been reported with gold complexes thanks to the use of bi- and tri-dentate ligands.[18-20]

In this study, we will particularly focus on the use of bidentate ligands to trigger the reactivity of gold beyond π-bond activation processes. A non-exhaustive bibliographic survey of recent reports, from our group and others, on the reactivity of gold(I) complexes bearing bidentate ligands will be presented in this chapter.

1.2 Reactivity of Gold Towards Elementary Organometallic Reactions

Until recently, the classical elementary steps of organometallic chemistry, well known and understood for almost all late transition metals, were unexplored with gold and even considered to be impossible. Combining experimental and theoretical studies, our team has developed over the years an expertise in the design of polydentate ligands and their application for the characterization and isolation of reactive species. Using this strategy, the reactivity of gold towards conventional elementary steps, such as oxidative addition and migratory insertion, were investigated in details. The following section will be dedicated to outline the results previously obtained in our team using bidentate gold complexes.

1.2.1 Oxidative Addition of Si-Si Bonds

The oxidative addition reaction is a key elementary step in transition metal chemistry. It is well known and understood for late transition metals, but oxidative addition at gold remains very elusive. A more detailed historical background of this reaction with gold will be discussed in the next chapter, and only the oxidative addition of Si-Si bonds will be considered in this chapter.

First, our team focused on the intramolecular oxidative addition of σ-Si-Si bond. The approach consisted in the use of bidentate diphosphine ligand that supports a Si-Si bond. This strategy was found fruitful with copper and allowed the first structural characterization of a σ-complex with a coinage metal.[21] However, a different reactivity was observed with gold. In fact, upon coordination of the diphosphine disilane moiety to gold, we gained evidence for the spontaneous oxidative addition at -80°C of the σ-Si-Si bond to form a bis(silyl)gold(III) complex.[22] This complex was completely characterized by multinuclear NMR spectroscopy at -60°C due to its instability. Gratifyingly, addition of one equivalent of $GaCl_3$ to abstract the chloride from the gold center afforded a stable cationic gold(III) complex that can be isolated in a 81% yield and was further characterized in the solid state *via* X-ray diffraction analysis (Scheme 2.2).

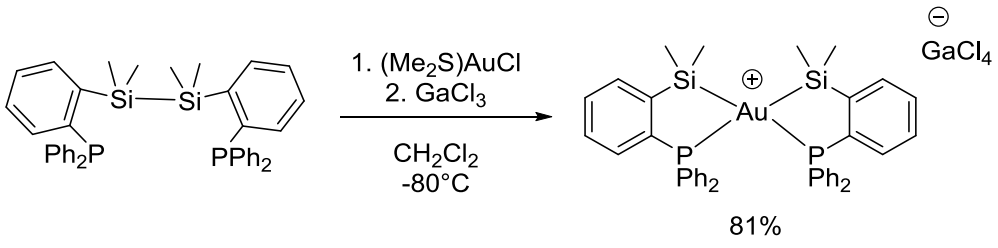

Scheme 2.2 Spontaneous oxidative addition of the σ-Si-Si bond to gold.

It is worth mentioning that after this unprecedented intramolecular oxidative addition, our team reported as well the intermolecular version of the σ-Si-Si bond activation but this time using a monophosphine gold(I) chloride complex. The resulting gold(III) species were highly instable and decomposed rapidly above -80°C, but they were unambiguously characterized at low temperature.[23]

1.2.2 Migratory Insertion

Migratory *syn* insertion reactions of C-C multiple bonds in metal-element bonds are ubiquitous with transition metals, but remain elusive for gold. As mentioned before, usually gold reacts with multiple bonds to form π-complexes which are activated towards nucleophilic attack to generate vinylgold species. The outcome of this reaction pathway is *trans* configurated products, indicating that the nucleophilic attack proceeds in an *anti* manner (Scheme 2.3).

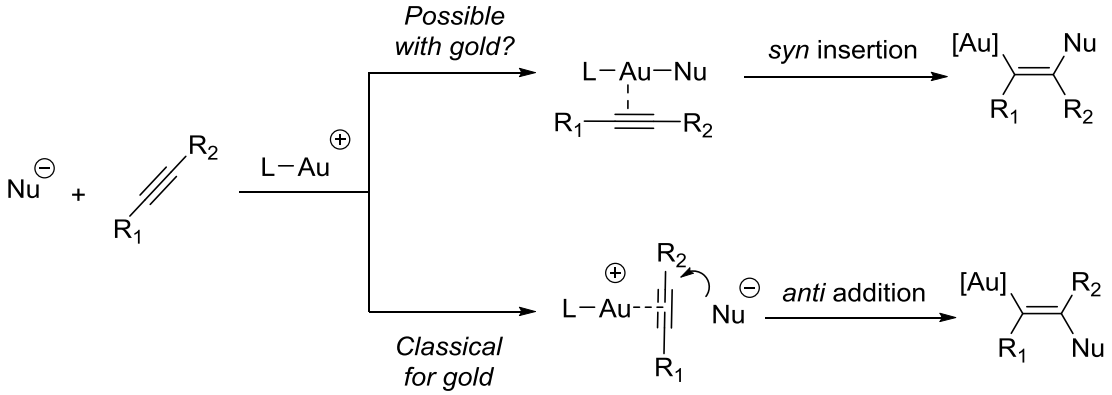

Scheme 2.3 The two possible reaction pathways with multiple bonds and nucleophiles in the presence of gold(I).

Moreover, the migratory insertion reaction in the metal-carbon bond is a key step found in major catalytic transformations like the Ziegler-Natta type polymerization of olefins and the

Mirozoki-Heck cross coupling reaction. Even though the *syn* addition reaction was proposed as a possible pathway for several gold-catalyzed functionalization reactions, most computational and experimental data favor the nucleophilic attack on the π-complex in *anti* to gold (outer-sphere mechanism). Hence, this step is well documented with early and late transition metals, but unprecedented with gold.

Gold(I) complexes generally react towards π-bonds following the outer-sphere mechanism due to their preference for the dicoordinated geometry (coordination of an olefin to a linear L-Au-Nu is not favorable), except for one example reported by our group.[24] However, with gold(III) complexes, one could imagine the feasibility of this transformation.

1.2.2.1 Migratory Insertion with Gold(III) Complexes

After having substantiated the *syn* insertion with gold(I) complexes, the next step for our team was to investigate the insertion of alkenes in the Au(III)-C bond. To do that, a well defined gold(III) complex with a rigid backbone was synthesized by the unprecedented intramolecular oxidative addition of aryl halides (see 2.1). This (P,C) bidentate ligand not only allowed the easy access to the +III oxidation state of gold and its stabilization, but it offered the possibility to have an alkyl group in *cis* position to a free coordination site, which is ideal for migratory insertion reactions. Thus, bidentate (P,C) gold(III)-alkyl complexes featuring a free coordination site were prepared by our group. At -90°C, addition of norbornene to the cationic (P,C) gold(III)-Me complex resulted in the formation of a new major phosphorus containing species. An extensive low temperature NMR spectroscopic analysis indicated the coordination of the olefin to the gold(III) complex, which is a rare example of characterized gold(III) olefin species.[25] Besides NMR spectroscopy, detailed computational analysis of the gold(III) π-olefin intermediate was performed and it indicated that compared with group 10 metal

complexes, the contribution of metal → $\pi^*_{C=C}$ backdonation in the bonding of the olefin is much weaker. This substantiates the key role of the rigid bidentate (P,C) ligand in stabilizing this reactive gold(III) π-olefin complex. Increasing the temperature from -90°C to -80°C resulted in the fast insertion of two norbornene units in the Au(III)-Me bond. The structure of the three-coordinated gold(III) norbornyl complex was confirmed by NMR spectroscopy at low temperature due to its instability.[26] Interestingly, a number of NMR signals were diagnostic of a γ-C-H agostic interaction, a fundamental organometallic mode of interaction that had never been reported with gold. Computational data were in agreement with the experimental observations, and confirmed for the first time the existence of agostic interactions with gold complexes.[27] The unstable gold(III) norbornyl complex could be trapped with pyridine or chloride to afford thermally stable four-coordinated species that were fully characterized (Scheme 2.4).

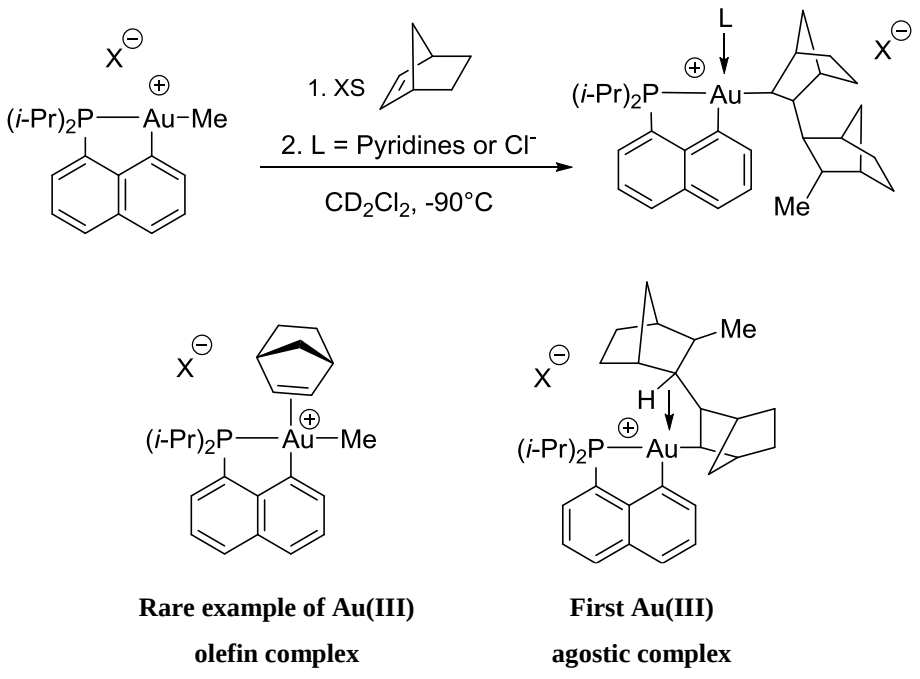

Scheme 2.4 Insertion of norbornene int o Au(III)-Me bond and characterization of gold(III) key reactive intermediates with the (P,C) bidentate ligand.

The double insertion of norbornene in the Au-Me bond is consistent with what was observed previously with Pd-Me species, and indicates that the gold-norbornyl species formed after the first insertion is more reactive than the gold-methyl complex.

Moreover, original cationic tricoordinated (P,C) cyclometallated gold(III) aryl complex were synthesized, and norbornene was shown to insert as well in the Au(III)-Csp^2 bond (Scheme 2.5).[28] In this case, one norbornene unit was inserted and surprisingly the resulting tricoordinated complexes were stable at room temperature. NMR spectroscopy, XRD analysis, along with DFT calculations revealed that after insertion of norbornene, the remote aryl group was η^2-coordinated to gold, which explains the stability observed experimentally. This mode of coordination has never been observed with gold(III), and once again, this highlight the key role of the (P,C) bidentate ligand in stabilizing reactive species. Finally, other C-C multiple bonds (ethylene, styrene and diphenylacetylene) were shown to undergo the migratory insertion reaction.

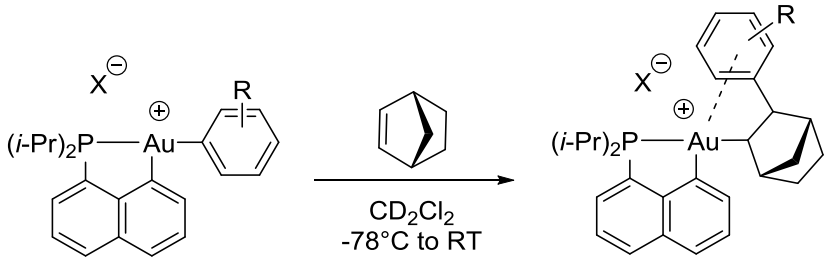

Scheme 2.5 Insertion of norbornene into Au(III)-Csp^2 bond leading to η^2-arene gold(III) complexes.

1.2.3 β-Hydride Elimination Reaction

The β-hydride elimination reaction from a metal alkyl complex is the microscopic reverse of an olefin insertion into a metal-hydride bond. This reaction occurs by the migratory de-insertion of olefins and the formation of metal hydride species (Scheme 2.6).

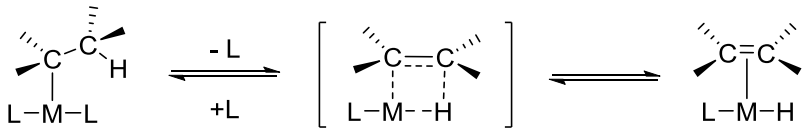

Scheme 2.6 β-H elimination from a metal alkyl complex.

During metal mediated catalysis, β-hydride elimination can be a key step or an undesired side reaction. For example, in the Mizoroki-Heck coupling, the products are released *via* β-hydride elimination reactions, whereas in the preparation of linear polyethylene by coordination insertion polymerization, undesired β-hydride elimination results in lower yields and formation of side products. In contrast to other transition metals, reports on β-hydride elimination at gold complexes are very rare and its reluctance to undergo this transformation is even designated as a distinctive feature of gold in catalysis.

A joint experimental and computational study devoted to β-hydride elimination of ethylene from an (NHC)ethylgold(I) complex was reported recently by Hashmi and Köppel.[29] DFT calculations predicted a high barrier (49.7 kcal/mol) for the β-hydride elimination reaction, and experimentally, this complex was shown to decompose around 180°C, but not *via* the elimination of ethylene. The absence of reactivity was attributed to the filled 5d orbital of gold(I) complexes, preventing the necessary C-H agostic interaction required for the elimination to take place. However, as suggested by Hashmi et *al.*, these interactions may occur in the case of gold(III) complexes for which empty 5d shells are available.

As mentioned earlier, our team has already performed the migratory insertion of olefins in the Au(III)-C bond and provided clear evidence for a C-H agostic interaction with a well defined bidentate gold(III) complex. The next step was to investigate the feasibility of the reverse of the migratory insertion reaction, *i.e* β-hydride elimination. To start with, a tricoordinated

cationic gold(III) *n*-butyl complex was generated at low temperature by iodide abstraction with silver bis(trifluoromethanesulfonyl)imide (Scheme 2.7). Increasing the temperature above 0°C resulted in the quick formation of a cationic bis(cyclometallated) gold(III) complex along with the formation of 2-butene (*cis* and *trans* isomers) and butane in a quantitative manner, indicating that β-H elimination (and bimolecular reductive elimination) has occurred.[30]

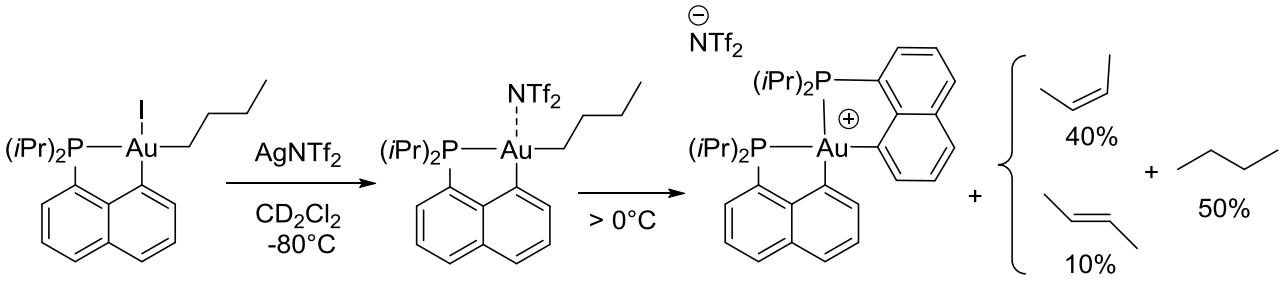

Scheme 2.7 β-H elimination from the cationic gold(III) butyl complex.

The formation of the internal alkene from the gold(III) *n*-butyl complex indicates that the olefin isomerization takes place after β-H elimination since no trace of 1-butene was detected. These results suggest that the highly reactive gold(III) hydride intermediate (generated after the β-H elimination) readily inserts olefins. Moreover, a bimolecular reaction between the cationic gold(III) complex and the corresponding hydride species can explain the formation of butane. The feasibility of the β-H elimination was demonstrated as well with different gold(III) alkyl complexes. Finally, although the β-hydride elimination is not favored with gold(I) complexes, it appears as a very favorable and rapid process for the bidentate (P,C) gold(III) species.

1.3 Bidentate or Tridentate Ligands for the Characterization of Gold Intermediates

Similar to the bidentate (P,C) ligand used in our group, the use of bidentate (N,C) or tridentate (C,N,C) ligands was shown to play a key role in isolating or in characterizing gold(III) intermediates. Some of these literature examples will be presented in this section.

In 2013, the group of Bochmann investigated the reactivity of a gold(III) complex featuring a tridentate (C,N,C) ligand towards various olefins (cyclopentene, norbornene and ethylene).[31] In fact, starting from this gold(III) pincer complex and in the presence of $B(C_6F_5)_3$ and an olefin at -40°C, they isolated and characterized by NMR spectroscopy three gold(III)-olefin complexes (Scheme 1.8).

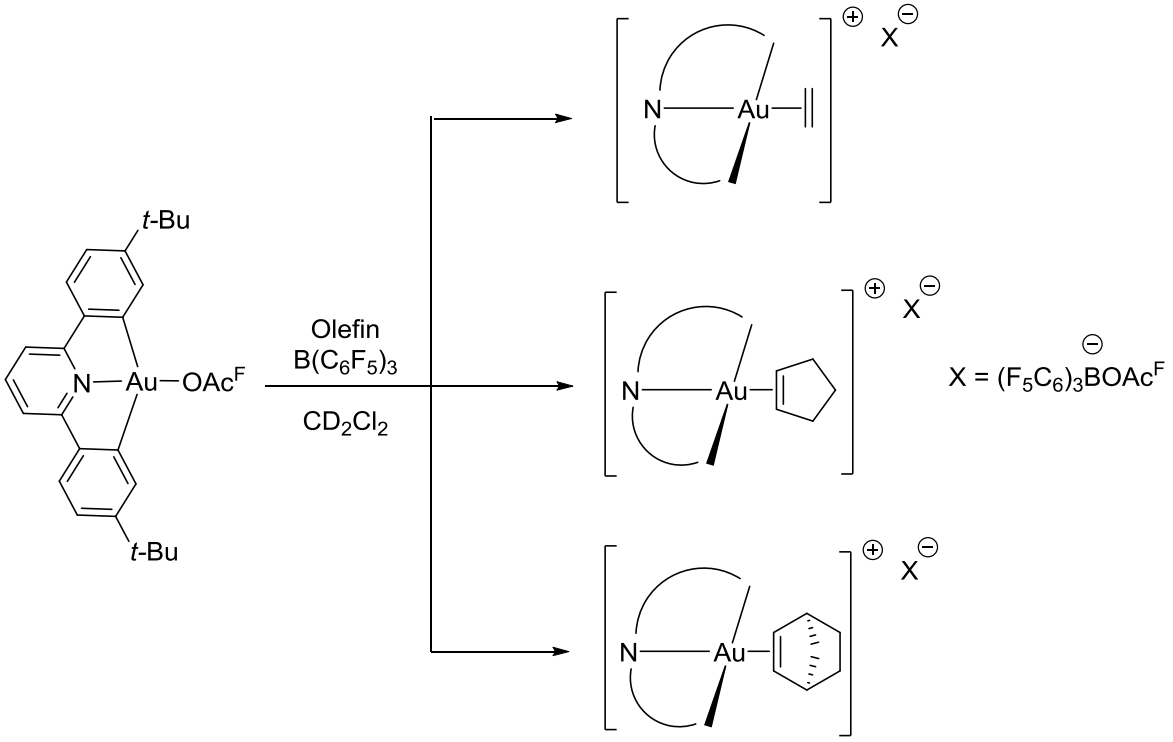

Scheme 1.8 Synthesis of gold(III)-olefin complexes with a tridentate (C,N,C) ligand.

Only the (C,N,C) gold(III)-norbornene complex was stable in solution at room temperature, but once isolated, the three complexes were stable in the solid state for hours at room temperature and in air with minimal degradation. For the authors, the tridentate ligand plays a major role in stabilizing the gold(III)-olefin complexes by preventing the reductive elimination reaction.

Using the same rigid tridentate (C,N,C) ligand, Bochmann *et al.* reported the synthesis of a thermally stable gold(III) hydride complex.[32] The reaction of the [(C,N,C)AuOH] complex with $LiHBEt_3$ at -78°C afforded the [(C,N,C)AuH] complex (Scheme 1.9).

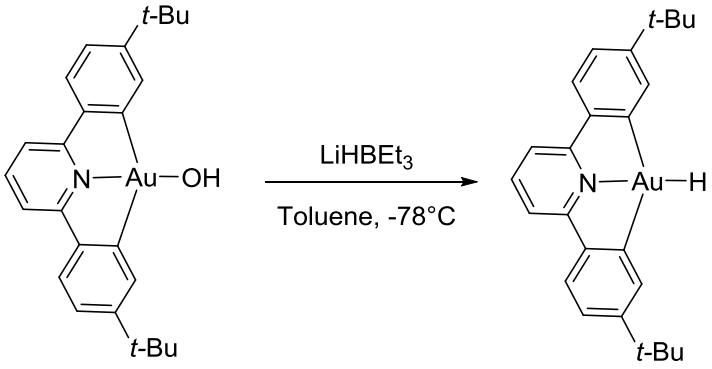

Scheme 1.9 Synthesis of gold(III)-hydride complex with a tridentate (C,N,C) ligand.

The structure of the gold(III)-hydride complex was confirmed by NMR spectroscopy as well as by X-ray diffraction analysis. Interestingly, in the solid state, this hydride was stable to air and moisture at room temperature and showed no sign of decomposition. This is most probably due to the high rigidity of the tridentate ligand, preventing the decomposition of the complex *via* reductive elimination.

Another example highlighting the key role of multidentate ligands in stabilizing reactive gold species was reported recently by Nevado and coworkers. Using a bidentate (C,N) ligand, they presented the synthesis of a stable monomeric bis-fluoride gold(III) complex.[33] The reaction

between a bis-chloro gold(III) complex, featuring a 2-phenylpyridine based ligand, and silver fluoride in dichloromethane at room temperature afforded the desired [(C,N)AuF_2] complex in excellent yields (Scheme 1.10).

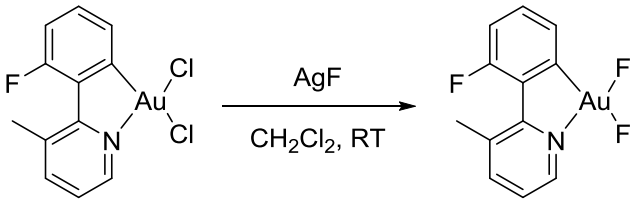

Scheme 1.10 Synthesis of a bis-fluoride gold(III) complex with a bidentate (C,N) ligand.

Gold(III) fluorine complexes have been invoked as key partners for boron species toward the formation of new C-C bonds, but such intermediates remained elusive due to their highly unstable character. However, the gold(III)-fluoride complexes reported by Nevado *et al.* were stable even at room temperature, and no sign of decomposition was observed. The authors associated the stability observed to the ability of the bidentate (C,N) ligands to stabilize electron-deprived gold(III) species.

To sum up, the judicious choice of multidentate ligands to control the coordination sphere of the gold center allowed the synthesis, the characterization and the isolation of highly unstable gold(III)-olefin, gold(III)-hydride and gold(III)-fluoride species. The above-mentioned examples clearly point out the key role of bidentate or tridentate ligands in stabilizing reactive intermediates, thus providing more insight into the reactivity of gold.

1.4 Gold Catalysis with Bidentate Gold Complexes

As mentioned before, the vast majority of catalytic transformations in the field of homogeneous gold catalysis are based on the typical π-activation of unsaturated substrates by gold species. However, this is not the only approach and by a judicious choice of the ligand, gold-catalyzed reactions that are not based on π-bond activation were developed and some examples will be presented in this section.

1.4.1 (P,P) Bidentate Ligand

In 2005, the group of Sawamura reported the gold-catalyzed dehydrogenative silylation of alcohols using a Xantphos gold(I) catalyst.[34] The reaction afforded silyl ethers under mild conditions (50°C, 2.5 h) and was proposed to involve gold-hydride species intermediates (Scheme 1.11).

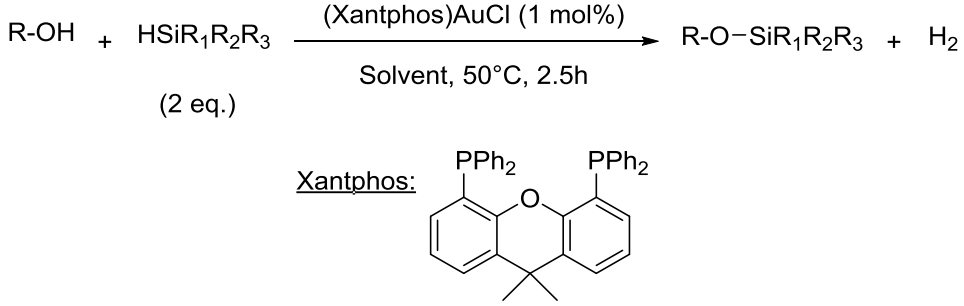

Scheme 1.11 (Xantphos)AuCl-catalyzed dehydrogenative silylation of alcohols.

The reaction displayed unprecedentedly high chemoselectivity and solvent tolerance. In fact, the gold catalyst was found to be selective for the silylation of hydroxy groups even in the presence of other functional groups (alkenes, alkynes, alkyl halides, aldehydes, ketones, esters...), and no dehydrogenative silylation catalyst compatible with such a large range of

functional group has been reported. Few transition metal catalysts are active in polar solvents or coordinating ones, but in this case, the catalysis was effective in a broad range of solvents (acetone, DMF, DMSO, $CHCl_3$, $CF_3C_6H_5$, PhMe, PhCN...). The authors screened as well a series of gold(I) catalysts prepared by mixing $(SMe_2)AuCl$ with phosphines. The Xantphos ligand performed better than the other ligands and only traces of the desired product was detected with other monodentate and bidentate phosphine-based ligands. This highlights the crucial role of the employed ligand in triggering and controlling the reactivity of gold.

Sawamura and coworkers proposed a plausible mechanism for the dehydrogenative silylation of alcohols (Scheme 1.12). The reaction of the starting gold(I) complex (A) with hydrosilane generates a gold(I) hydride complex (B). This species reacts with an alcohol through σ-bond metathesis involving the transition state (C) to afford the alkoxygold(I) complex (D) and dihydrogen. A σ-bond activation step between the hydrosilane and the alkoxygold(I) (E) affords the silyl ether, and the gold(I) hydride species is regenerated to close the catalytic cycle. Although the authors didn't provide clear explanations for the superiority of the Xantphos ligand *vs.* other monodentate and bidentate phosphine-based ligands, one could imagine its crucial role in stabilizing the key reactive gold(I) hydride intermediate (B).

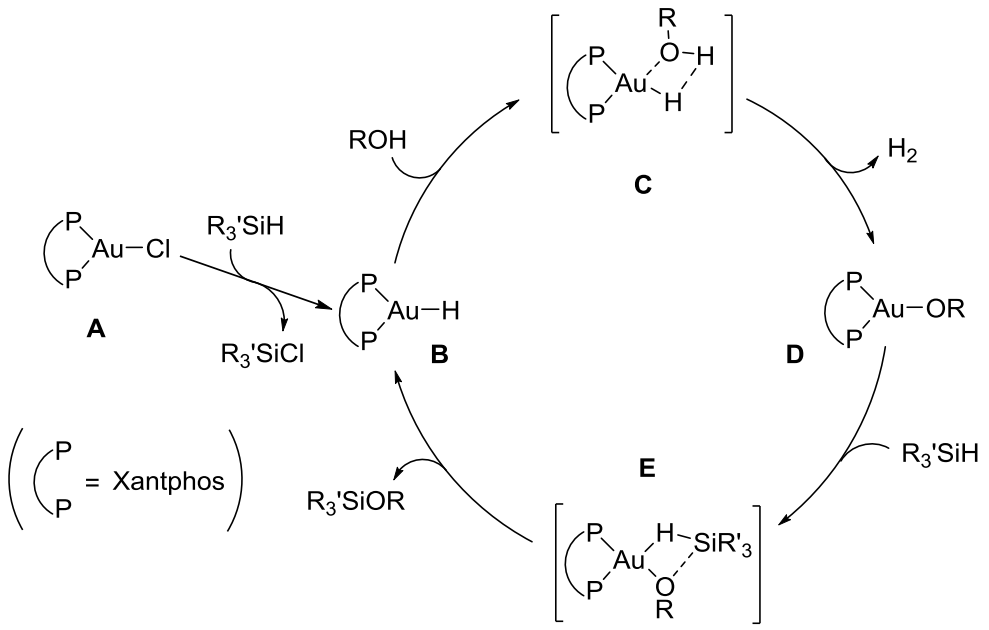

Scheme 1.12 Proposed mechanism for (Xantphos)AuCl-catalyzed dehydrogenative silylation.

In 2012, J.-L. Zhang and coworkers investigated the hydrodefluorination of activated aryl fluorides with hydrosilanes catalyzed by Xantphos-based gold(I) complexes (Scheme 1.13).[35] The authors performed a ligand screening and once again the bidentate Xantphos outperformed other ligands including NHC, monophosphine and bidentate arylphosphine ligands. This example illustrates as well the key role of the coordination sphere around gold in triggering its reactivity. The reaction conditions were optimized and it was found that the addition of catalytic amount of (i) Xantphos prevents the decomposition of the catalyst and (ii) acetic acid affords the desired product in good yields and with high regioselectivity for the *p*-C-F bond of the aryl fluoride.

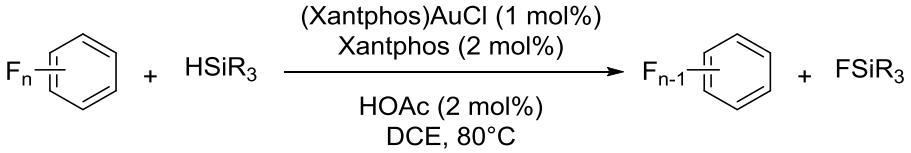

Scheme 1.13 (Xantphos)AuCl-catalyzed hydrodefluorination of aryl fluorides with hydrosilanes.

The hydrodefluorination of aryl fluorides reaction exhibited high functional group tolerance (ketone, ester, carboxylate, alkynyl, alkenyl and amide groups) which suggests its potential applications in late stage chemoselective C-F bond activation. Furthermore, several mechanistic pathways were examined by computational means. The authors ruled out the involvement of a gold(I) hydride species as an active intermediate for the transfer of hydride to replace the fluorine atom of the C-F bond. Thus, J.-L. Zhang *et al.* proposed a mechanism (Scheme 1.14) involving first an oxidative addition step of the C-F bond of the aryl fluoride (step A) with subsequent concerted C-H and Si-F bond formation (step B). The high regioselectivity observed experimentally was rationalized by the activation barrier computed for the oxidative addition of the *p*-C-F bond of pentafluoropyridine (30.4 kcal/mol), which is lower than the value for the corresponding *o*-C-F activation (34.6 kcal/mol).

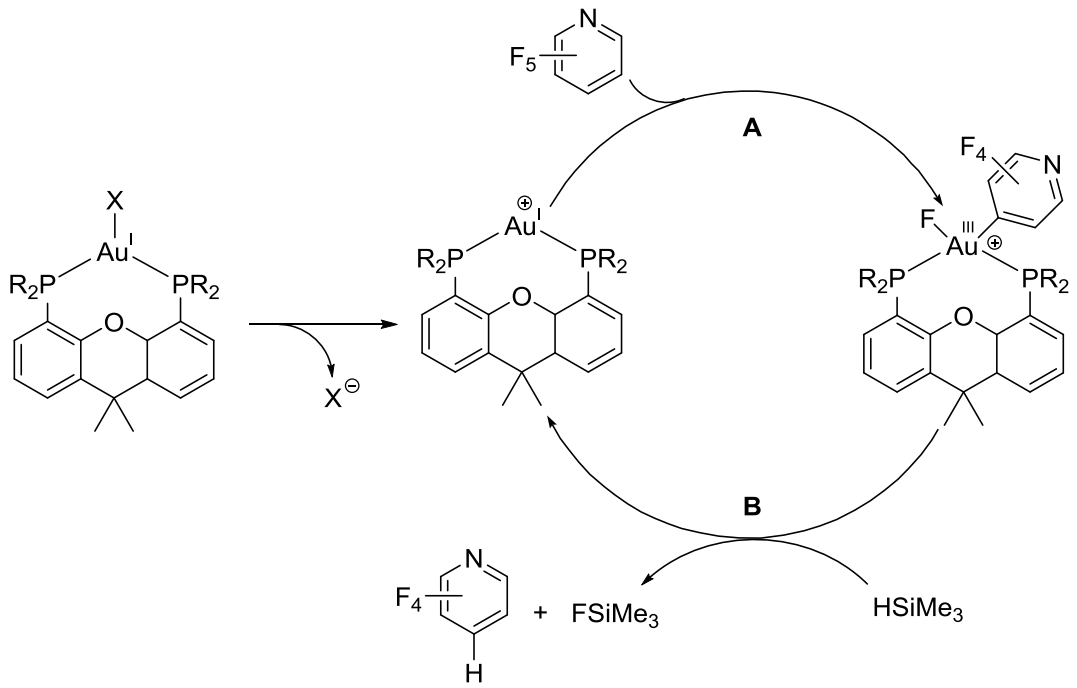

Scheme 1.14 Proposed mechanism for the Au-catalyzed hydrodefluorination of aryl fluorides with hydrosilanes.

1.4.2 (C,C) Bidentate Ligand

Recently, the group of Toste reported an original pathway to access gold(III) complexes. Taking advantage of the strained C-C bond, the oxidative addition of biphenylene to a cationic (NHC)gold(I) complex was performed under very mild conditions in contrast to the relatively harsh conditions often required for other transition metals (such as Rh, Ir, Ni, Ru and Fe).[36] The resulting cationic gold(III) species was trapped with tetrabutylammonium chloride to afford the more stable tetracoordinated gold(III) complex (Scheme 1.15). After oxidative addition, the biphenyl moiety can be considered as a bidentate ligand featuring two strong Au-C bonds, explaining the stability of this gold(III) species.

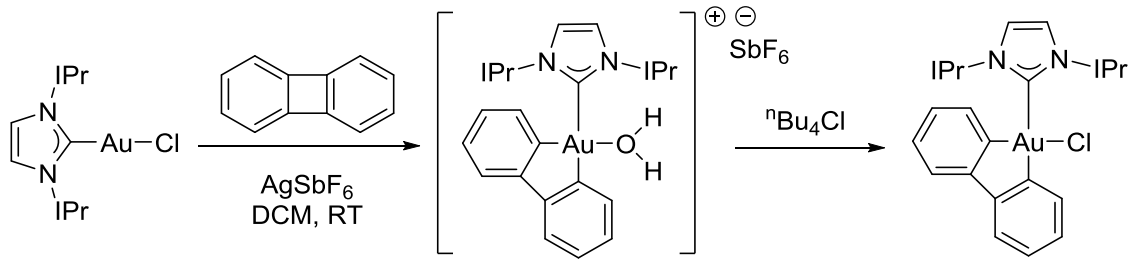

Scheme 1.15 Synthesis of stable gold(III) complexes *via* oxidative addition of biphenylene.

The gold(III) complex can also be trapped and stabilized by adding polar solvents like DMF to generate the tetracoordinated gold(III) species *via* coordination of a lone pair of electrons on the carbonyl oxygen to the gold center. These observations suggest that this gold(III) complex exhibits a hard oxophilic Lewis acid character, complementary to the soft carbophilic character of gold(I) complexes. Toste and coworkers took advantage of this hard Lewis acid character in catalysis. In fact, this gold(III) complex was shown to be an efficient catalyst for addition reactions to α,β-unsaturated carbonyl compounds, affording the desired products in good yields and with excellent selectivities. The Mukaiyama-Michael addition reactions to α,β-unsaturated aldehydes catalyzed by Lewis acids afford generally 1,2-addition

products and all the systems leading to 1,4-addition require stoichiometric amounts of the Lewis acid. However, the cyclometallated chloro-gold(III) complex, in the presence of AgOTf as halide scavenger, catalyzed the addition reaction with cinnamaldehyde and ketene silyl acetal or silyl nitronate to afford selectively the 1,4-addition products (Scheme 1.16).

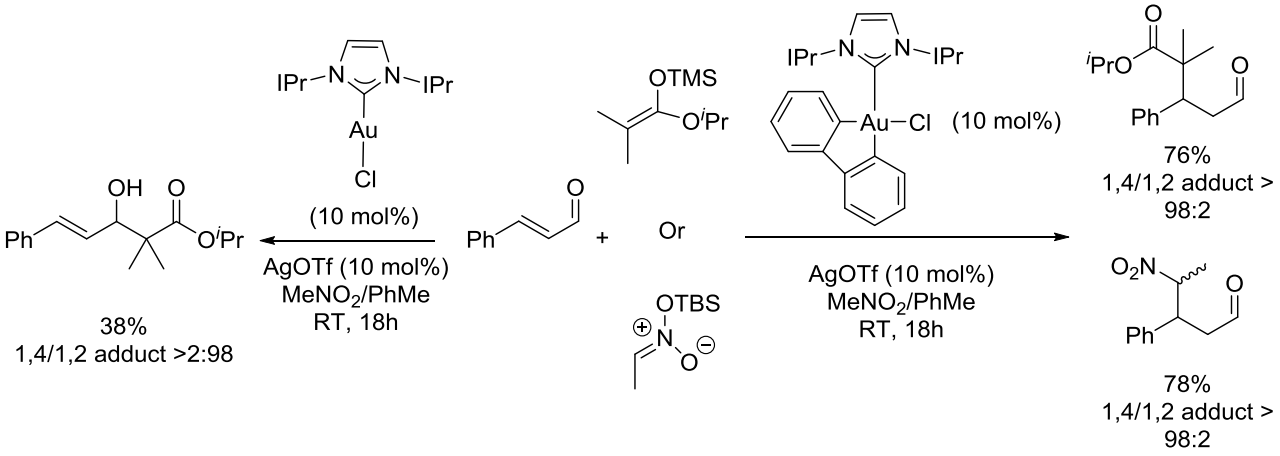

Scheme 1.16 Examples of selective Au(III)-catalyzed 1,4-additions (right) and comparison with gold(I) (left).

Moreover, taking profit of the soft/hard character of gold(I)/gold(III) complexes, one-pot tandem reactions in which two distinct reactions with catalysts of different oxidation states originating from the same precursor were conducted. First the (NHC)gold(I) complex catalyzed the Meyer-Schuster rearrangement of propargyl alcohol to afford the α,β-unsaturated aldehyde, followed by the gold(III)-catalyzed Mukaiyama-Michael reaction after oxidative addition of biphenylene (Scheme 1.17).

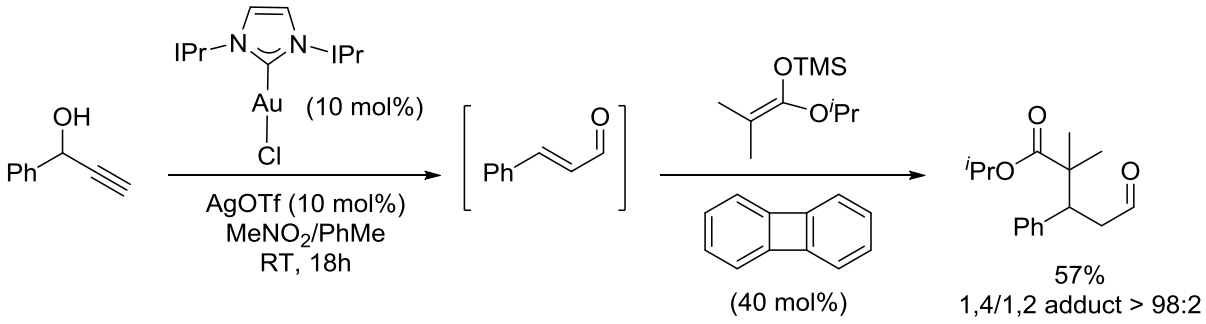

Scheme 1.17 One-pot tandem Au(I)/Au(III)-catalyzed reaction.

This high selectivity was also extended to α,β,γ,δ-diunsaturated aldehydes for thiol addition reactions and for Diels-Alder reactions, with γ,δ-selectivity rather than the classically observed α,β selectivity (Scheme 1.18).

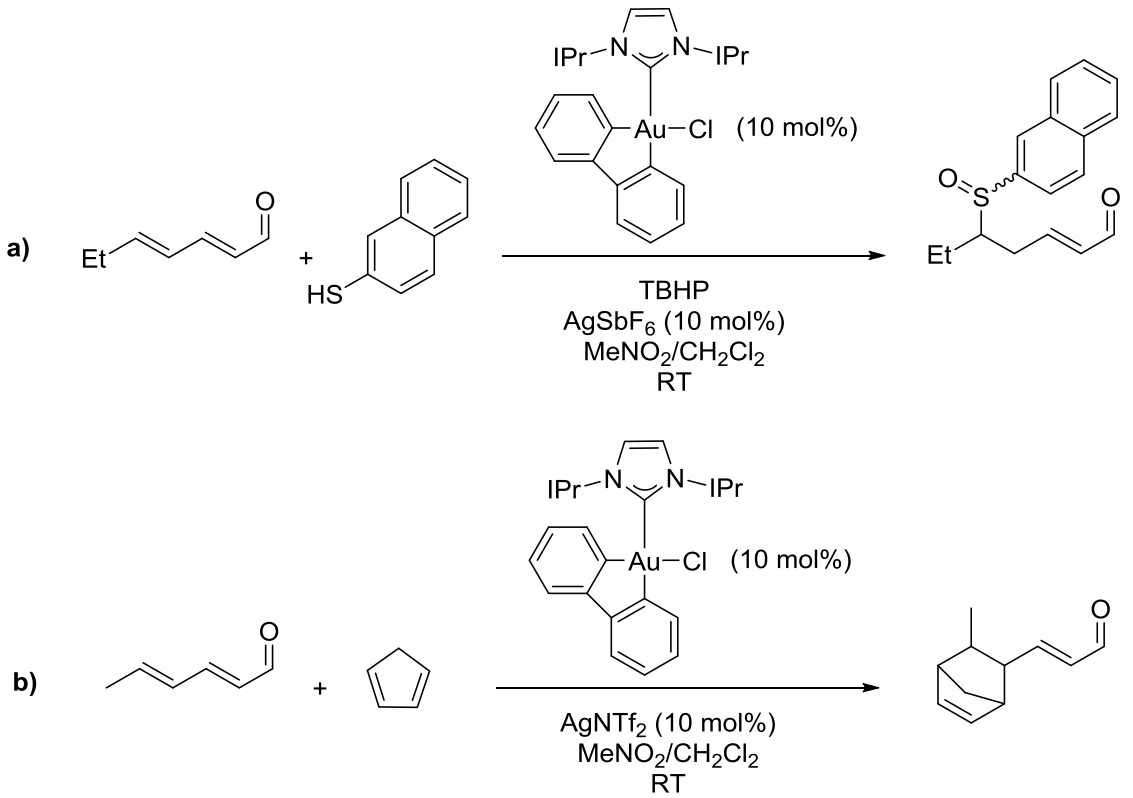

Scheme 1.18 δ-selective thiol addition reaction (a) and γ,δ-selective Diels-Alder reaction (b) catalyzed by gold(III).

Finally, the [2+2] intramolecular cycloadditions of α,β-unsaturated aldehyde-allene compounds was realized with this gold(III) complex to afford the cyclic product in good yields and with high selectivity (Scheme 1.19). This result is remarkable since no other Lewis acid (gold(I) complexes, organocatalysts or metallic salts) allowed this transformation.

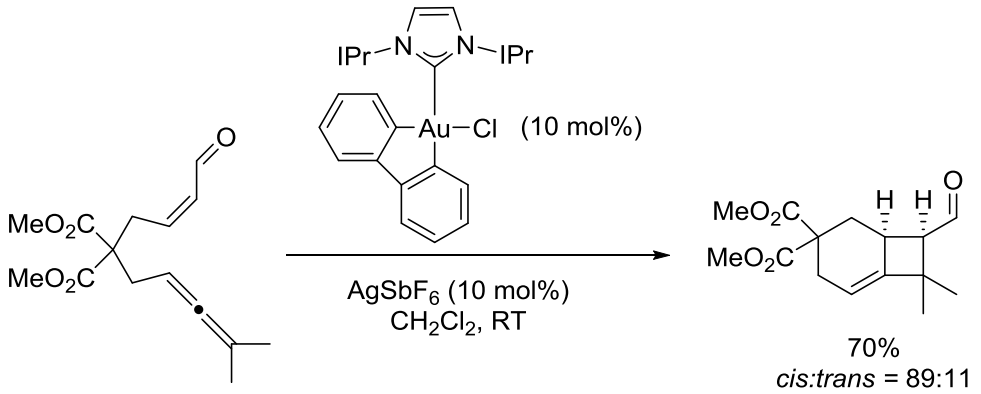

Scheme 1.19 Au(III)-catalyzed [2+2] cycloaddition of an allene-aldehyde.

The key intermediate for all these reactions is a gold(III) complex [IPrAu(biphenyl)(η^1-cinnamaldehyde)][SbF_6], which was isolated and characterized by X-ray diffraction analysis (Figure 1.1). This complex displays a distorted square planar geometry with η^1 coordination of the oxygen atom of the cinnamaldehyde. The excellent selectivities observed with this catalyst are explained by the steric pocket created by the NHC and the biphenyl ligands, shielding the carbonyl moiety from nucleophilic attacks.

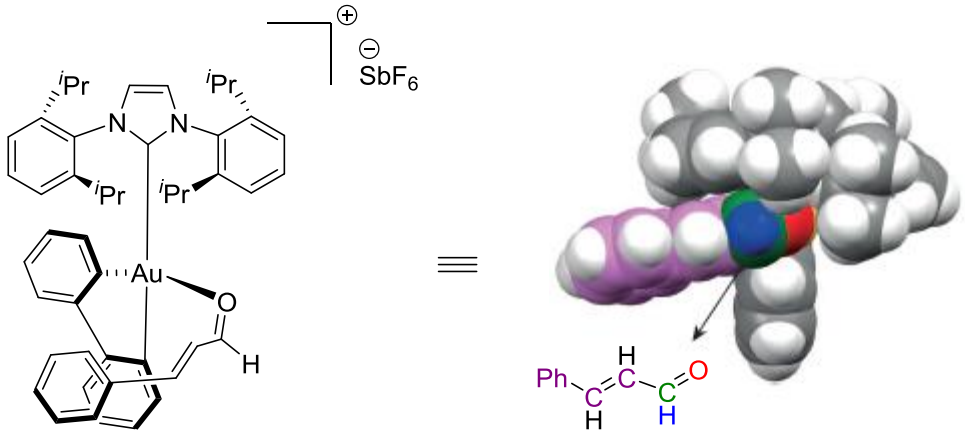

Figure 1.1 X-ray structure of the [IPrAu(biphenyl)(η^1-cinnamaldehyde)][SbF_6] with emphasis of the pocket generated by the ligands.

1.4.3 (C,O) Bidentate Ligand

Very recently, Wong and coworkers reported unprecedented stable 1,1'-bi-2-napthol gold(III) complexes adopting a novel (C,O) chelation mode, instead of the conventional (O,O) chelation.[37] Since phenolate ligands are strong reductants, and in order to prevent decomposition, their strategy was based on the replacement of the two chloride atoms of a robust cyclometallated gold(III) dichloride complex by a BINOL ligand. Thus, treatment of an oxazoline-based gold(III) dichloride complex with the commercially available *(S)*-BINOL in the presence of cesium carbonate in methanol afforded an air and moisture stable complex (Scheme 1.20). The reaction with *(S)*-BINOL and (*R*)-BINOL ligands gave exclusively the (*R*)-gold(III) and the (*S*)-gold(III) complexes, respectively, with an axial-to-central chirality transfer.

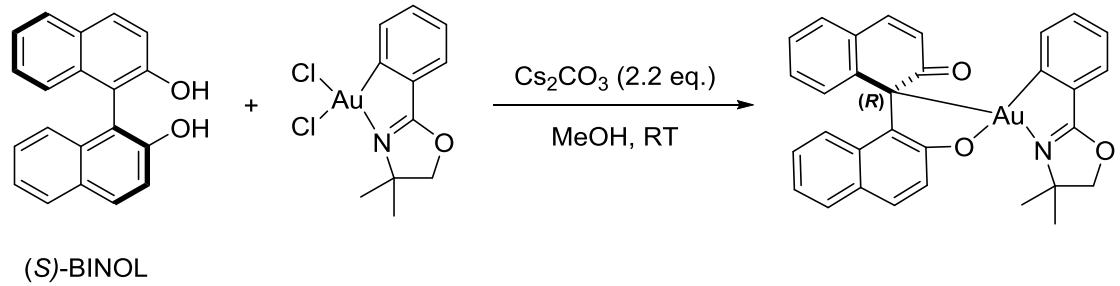

Scheme 1.20 Synthesis of (*R*)-gold(III)-BINOL complex with unusual (C,O) chelation.

This unusual (C,O) binding mode was proposed to occur *via* the tautomerization of BINOL in the presence of Cs_2CO_3, but the authors didn't provide a clear explanation for its occurrence. One could imagine that, due to steric or geometric constraints, the formation of a 5-membered ring is more favorable than the 7-membered ring. Noteworthy, that this (C,O) binding mode is impressive, since gold(III) complexes are known to be oxophilic species.

The racemic gold(III) complex was also synthesized starting from *rac*-BINOL, and its reactivity towards the carboalkoxylation of *ortho*-ethynylbenzaldehydes with trialkyl orthoformates was investigated. The reaction conditions were optimized, and they found that using catalytic amount of the *rac*-gold(III) complex and camphorsulfonic acid in dichloroethane affords the desired products in good yields (Scheme 1.21).

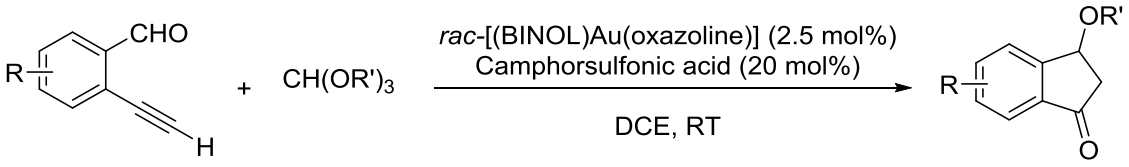

Scheme 1.21 Gold(III)-catalyzed carboalkoxylation reaction.

Substrates with electron-withdrawing groups, electron-donating groups, as well as two substituents on the aryl ring were tolerated. Interestingly, no carboalkoxylation product was

obtained when monophosphine gold(I) or other cyclometallated gold(III) complexes were used.

1.4.4 (P,N) Bidentate Ligand

In 2010, Stradiotto *et al*. investigated the gold-catalyzed stereoselective hydroamination of internal aryl alkynes with dialkylamines. Various monodentate and bidentate ligands were tested, and it was found that the most efficient gold(I) complex for this transformation was supported by a (P,N) bidentate ligand, affording the desired *E*-enamines in good yields (Scheme 1.22).[38]

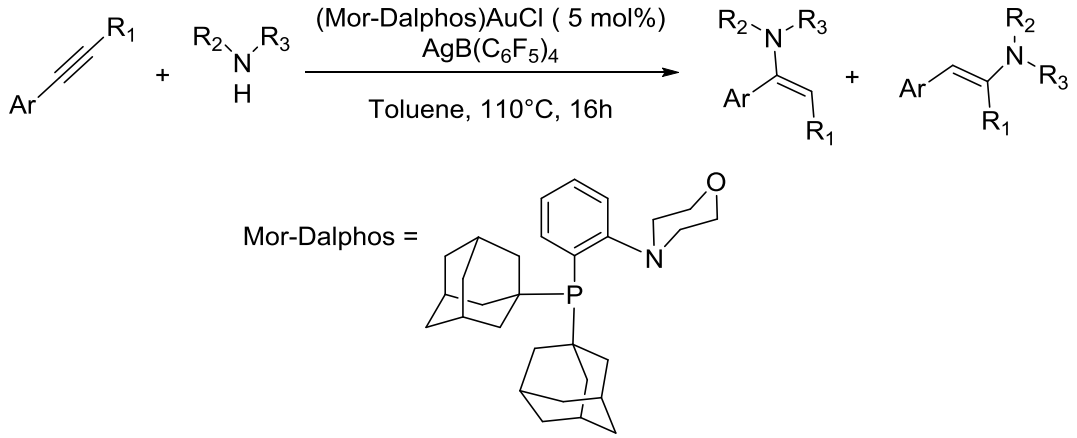

Scheme 1.22 Gold-catalyzed hydroamination of unsymmetrical internal alkynes with dialkylamines.

With the (Mor-Dalphos)AuCl catalyst, the hydroamination of unsymmetrically substituted internal aryl alkynes with dialalkylamines proceeded with complete stereoselectivity and in good yields and regioselectivity. Moreover, the reaction was shown to be general and various alkynes and dialkylamines underwent this transformation. Under the same reaction conditions, monodentate (R_3P or NHC) gold(I) complexes were used, and the yield dropped

dramatically. The nitrogen position of the (P,N) ligand was also shown to be crucial. In fact, positioning the nitrogen donor in the *para* position (respect to the phosphorus atom) decreased the yield as well. Based on stoichiometric tests and the stereo- and regioselectivity observed, Stradiotto and coworkers proposed an inner-sphere mechanism for this transformation. However, four years later, the group of Maier investigated in details the gold(I)-catalyzed hydroamination of alkynes.[39] They provided more insight about the reaction's mechanism, and confirmed that this transformation occurs *via* an outer-sphere mechanism.

The important role of the nitrogen atom in the Mor-Dalphos ligand was also identified by the group of L. Zhang during their study of the gold-catalyzed [3+2] annulation reaction between terminal alkynes and carboxamides for the formation of 2,4-disubstituted oxazoles.[39] This example will be discussed in chapter 2.

All the above mentioned gold-catalyzed reactions point out the key role of bidentate ligands. In fact, the reactivity of gold is governed and controlled by coordination sphere around it, and thus new reactivities and new catalytic transformations have been reported with gold complexes thanks to the use of well defined multidentate ligands.

1.5 Research Objectives and Thesis Outline

Despite the progress achieved over the past few years, the precise understanding of the reactivity of gold still lags behind when compared to other transition metals. Moreover, as briefly described above, the use of multidentate ligands in the reactivity of gold complexes has been shown to offer promising opportunities in terms of stabilization and reactivity. Therefore, the aim of the research projects presented in this manuscript was to gain further knowledge on the impact of the ligands on the reactivity of gold towards the intermolecular oxidative addition of aryl halides in a first part and also on the stabilization of highly reactive gold(I) intermediates.

Oxidative addition *via* the concerted activation of σ-bonds is of high fundamental interest and very unusual with gold. After achieving the intramolecular oxidative addition at a gold(I) center, we became more interested to investigate this reactivity but in an intermolecular manner. Thus, we defined geometrical and electronic requirements for the redox-activity of gold(I) and for the stability of the gold(III) complexes stemming from oxidative addition. Two different strategies have been elaborated. The first one consists in the use of an *o*-carborane diphosphine ligand that forces a bent geometry around gold, whereas the second strategy involves a hemi-labile bidentate ligand bearing a soft and a hard donor group. Both strategies were found to be fruitful, and the gold(III) complexes generated from intermolecular oxidative addition reactions were isolated and fully characterized. Having in hands two gold(I) complexes that undergo the oxidative addition reaction, we wanted to go beyond this elementary step. We constructed a new Au(I)/Au(III) catalytic cycle involving a sequence of Csp^2-X oxidative addition, Csp^2-H auration and reductive elimination, allowing the first example of gold-catalyzed direct arylation of arenes with aryl halides.

The bidentate diphosphine ligand was also employed to isolate reactive gold(I) complexes such as α-oxo gold(I) carbenes. These highly reactive species are proposed in many catalytic transformations as key intermediates. However, to our knowledge, this α-oxo gold carbene has never been isolated or characterized (in solution or in solid state) due to its high electrophilic character. Therefore, we were eager to attempt to isolate this reactive species and investigate its reactivity. The use of an *o*-carborane-based diphosphine gold(I) complex and ethyl diazoacetate derivatives allowed the quick formation of the α-oxo gold(I) carbene at low temperature. The gold(I) carbene was completely characterized for the first time by means of multinuclear NMR spectroscopy, X-ray diffraction analysis and high resolution mass spectroscopy (ESI+). The electronic properties of the diphosphine gold moiety allowed the back-donation from the gold center to the carbene, which explains its stability at low temperature. We then tested the reactivity of the α-oxo gold(I) carbene towards insertion reactions (with phenol and phosphine borane), and the classical cyclopropanation reaction with styrene. Interestingly, the reactivity of the generated gold(I) carbenes can be modulated depending on the electronic properties of the aryl ethyl diazoacetate used.

One common motivation behind these two different research topics was to improve our knowledge of gold's reactivity. The experimental work was supported by theoretical studies conducted by the group of Dr. Karinne Miqueu (University of Pau). These computational analyses were extremely helpful and insightful, regarding the bonding properties, the ligand influence and the reaction mechanisms.

1.6 References

(1) Gimeno, M. C. *Modern Supramolecular Gold Chemistry*; Laguna, A., Ed.; Wiley-VCH Verlag GmbH & Co. KGaA, 2008; 1–63.

(2) Heinze, K. *Angew. Chem. Int. Ed.* 10.1002/anie.201708349

(3) Pyykko, P.; Desclaux, J. P. *Acc. Chem. Res.* **1979**, *12*, 276.

(4) Pyykkö, P. *Angew. Chem. Int. Ed.* **2004**, *43*, 4412.

(5) Mohr, F. *Gold Chemistry: Applications and Future Directions in the Life Sciences*, Wiley-VCH, Weinheim, **2009**.

(6) Gorin, D. J.; Toste, F. D. *Nature* **2007**, *446*, 395.

(7) Barrett, J. *Structure and Bonding*, Royal Chemical Society of Chemistry, Cambridge, **2001**.

(8) Cordero, B.; Gomez, V.; Platero-Prats, A.E.; Revés, M.; Echeverria, J.; Cremades, E.; Barragan, F.; Alvarez, S. *Dalton Trans.* **2008**, 2832

(9) Schwerdtfeger, P. *J. Am. Chem. Soc.* **1989**, *111*, 7261.

(10) Allred, A. L. *J. Inorg. Nucl. Chem.* **1961**, *17*, 215.

(11) Teles, J. H.; Brode, S.; Chabanas, M. *Angew. Chem. Int.Ed.* **1998**, *37*, 1415.

(12) Hashmi, A. S. K. *Chem. Rev.* **2007**, *107*, 3180.

(13) Hashmi, A. S. K. *Angew. Chem. Int. Ed.* **2010**, *49*, 5232.

(14) Liu, L.-P.; Hammond, G. B. *Chem. Soc. Rev.* **2012**, *41*, 3129.

(15) Wong, B. Y.-W.; Wong, H.-L.; Wong, Y.-C.; Au, V. K.-M.; Chan, M.-Y.; Yam, V. W.-W. *Chem. Sci.* **2017**, *8*, 6936.

(16) Fung, S. K.; Zou, T.; Cao, B.; Lee, P.-Y.; Fung, Y. M. E.; Hu, D.; Lok, C.-N.; Che, C.-M. *Angew. Chem. Int. Ed.* **2017**, *56*, 3892.

(17) Chung, C. Y.-S.; Fung, S.-K.; Tong, K.-C.; Wan, P.-K.; Lok, C.-N.; Huang, Y.; Chen, T.; Che, C.-M. *Chem. Sci.* **2017**, *8*, 1942.

(18) Johnson, M. W.; DiPasquale, A. G.; Bergman, R. G.; Toste, F. D. *Organometallics* **2014**, *33*, 4169.

(19) Chambrier, I.; Roşca, D.-A.; Fernandez-Cestau, J.; Hughes, D. L.; Budzelaar, P. H. M.; Bochmann, M. *Organometallics* **2017**, *36*, 1358.

(20) Kumar, R.; Linden, A.; Nevado, C. *Angew. Chem. Int. Ed.* **2015**, *54*, 14287.

(21) Gualco, P.; Amgoune, A.; Miqueu, K.; Ladeira, S.; Bourissou, D. *J. Am. Chem. Soc.* **2011**, *133*, 4257.

(22) Gualco, P.; Ladeira, S.; Miqueu, K.; Amgoune, A.; Bourissou, D. *Angew. Chem. Int. Ed.* **2011**, *50*, 8320.

(23) Joost, M.; Gualco, P.; Coppel, Y.; Miqueu, K.; Kefalidis, C. E.; Maron, L.; Amgoune, A.; Bourissou, D. *Angew. Chem. Int. Ed.* **2014**, *53*, 747.

(24) Joost, M.; Gualco, P.; Mallet-Ladeira, S.; Amgoune, A.; Bourissou, D. *Angew. Chem. Int. Ed.* **2013**, *52*, 7160.

(25) Rekhroukh, F.; Estevez, L.; Bijani, C.; Miqueu, K.; Amgoune, A.; Bourissou, D. *Organometallics* **2016**, *35*, 995.

(26) Rekhroukh, F.; Brousses, R.; Amgoune, A.; Bourissou, D. *Angew. Chem. Int. Ed.* **2015**, *54*, 1266.

(27) Rekhroukh, F.; Estévez, L.; Bijani, C.; Miqueu, K.; Amgoune, A.; Bourissou, D. *Angew. Chem. Int. Ed.* **2016**, *55*, 3414.

(28) Rekhroukh, F.; Blons, C.; Estévez, L.; Mallet-Ladeira, S.; Miqueu, K.; Amgoune, A.; Bourissou, D. *Chem. Sci.* **2017**, *8*, 4539.

(29) Klatt, G.; Xu, R.; Pernpointner, M.; Molinari, L.; Quang Hung, T.; Rominger, F.; Hashmi, A. S. K.; Köppel, H. *Chem. Eur. J.* **2013**, *19*, 3954.

(30) Rekhroukh, F.; Estevez, L.; Mallet-Ladeira, S.; Miqueu, K.; Amgoune, A.; Bourissou, D. *J. Am. Chem. Soc.* **2016**, *138*, 11920.

(31) Savjani, N.; Roşca, D.-A.; Schormann, M.; Bochmann, M. *Angew. Chem. Int. Ed.* **2013**, *52*, 874.

(32) Roşca, D.-A.; Smith, D. A.; Hughes, D. L.; Bochmann, M. *Angew. Chem. Int. Ed.* **2012**, *51*, 10643.

(33) Kumar, R.; Linden, A.; Nevado, C. *J. Am. Chem. Soc.* **2016**, *138*, 13790.

(34) Ito, H.; Takagi, K.; Miyahara, T.; Sawamura, M. *Org. Lett.* **2005**, *7*, 3001.

(35) Zhan, J.-H.; Lv, H.; Yu, Y.; Zhang, J.-L. *Adv. Synth. Catal.* **2012**, *354*, 1529.

(36) Wu, C.-Y.; Horibe, T.; Jacobsen, C. B.; Toste, F. D. *Nature* **2015**, *517*, 449.

(37) Cui, J.-F.; Ko, H.-M.; Shing, K.-P.; Deng, J.-R.; Lai, N. C.-H.; Wong, M.-K. *Angew. Chem. Int. Ed.* **2017**, *56*, 3074.

(38) Hesp, K. D.; Stradiotto, M. *J. Am. Chem. Soc.* **2010**, *132*, 18026.

(39) Zhdanko, A.; Maier, M. E. *Angew. Chem. Int. Ed.* **2014**, *53*, 7760.

(40) Luo, Y.; Ji, K.; Li, Y.; Zhang, L. *J. Am. Chem. Soc.* **2012**, *134*, 17412.

2 Ligand Design to Trigger the Oxidative Addition to Gold(I)

2.1 Historical Background

Despite the availability and stability of +I, +II and +III oxidation states, gold has earned the reputation of a redox-neutral metal. This general doctrine is mainly based on gold's high redox potential compared to that of its close neighbors palladium and platinum (E_0: Au^{3+}/ Au^{+} = 1.41 V, Pd^{2+}/ Pd = 0.91 V, and Pt^{2+}/ Pt = 1.18V).[1]

The term oxidative addition generally refers to reactions that lead to an increase in the oxidation state, in the number of valence electrons of the metal center by two units, and an increase in the coordination number of the complex by one or two.[2] This term doesn't point out the mechanism by which the oxidative addition occurs. In fact, depending on the employed reagent, two main pathways can be envisioned: S_N2-type mechanism vs. concerted mechanism. From a historical point of view, the oxidative addition *via* an S_N2 mechanism with dihalogens and alkyl halides to gold(I) has been established as early as 1940 (Scheme 2.1).[3-5] Since then, the reactivity of dihalogen and alkyl halide towards gold(I) complexes has been exploited and studied to access the corresponding gold(III) complexes.

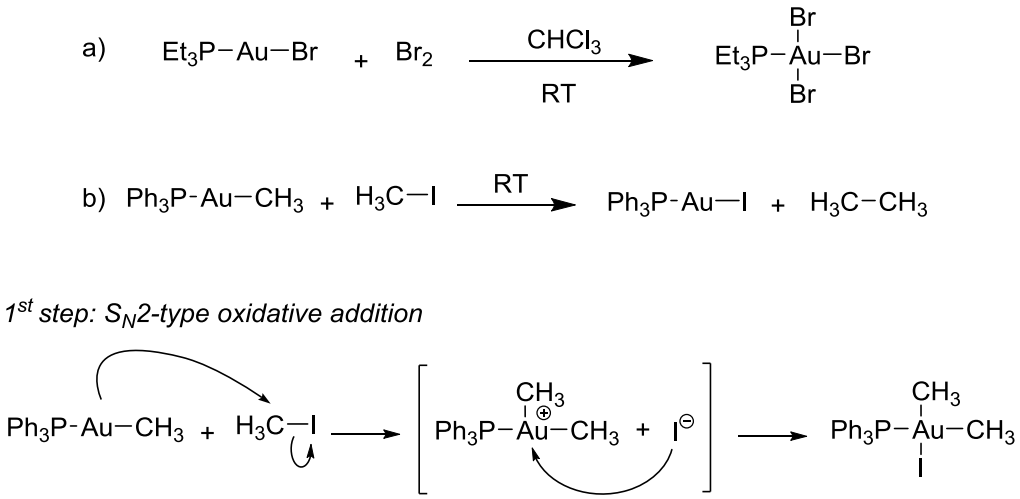

Scheme 2.1 a) Addition of dibromine to gold(I) reported by Mann and Purdie (1940). b) Reaction of methyl iodide with gold(I) reported independently by Kochi and Schmidbaur (1972).

Even though the above-cited reactions prove the feasibility of the transition from the oxidation state of +I to +III for organogold, the oxidative addition *via* a concerted mechanism remained a debatable subject for a long time. In fact, the oxidative addition of less polar substrates (for which S_N2-like mechanisms are ruled-out) to gold(I) complexes was unexplored until the beginning of this decade.

The reaction of aryl halides with gold not only remained a challenge but provoked a lively debate in the organometallic community. In fact, in 2007, Corma and coworkers reported the Sonogashira cross coupling reaction between iodobenzene and phenyl acetylene catalyzed by Au(I) (Scheme 2.2).[6] By analogy with that observed with Pd catalysts, the oxidative addition of PhI to gold(I) was proposed as the first step of the reaction.

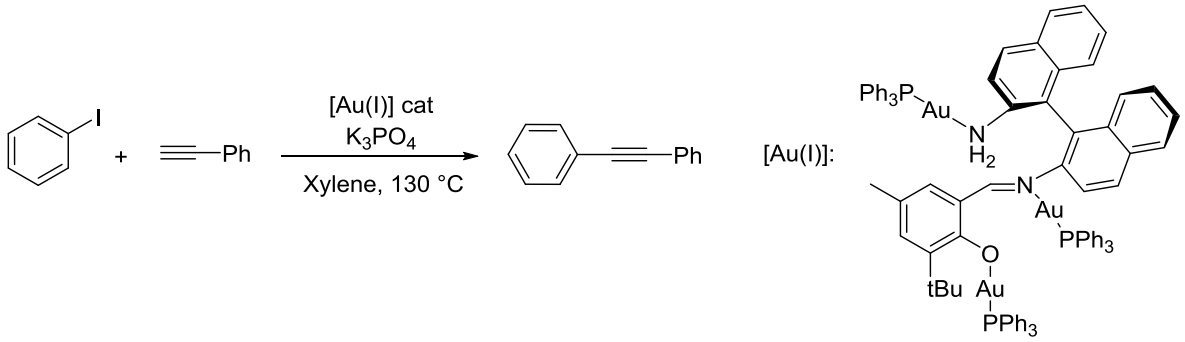

Scheme 2.2 Sonogoshira cross coupling catalyzed by a gold (I) Schiff-base complex reported by Corma *et al.*

Three years later, Echavarren *et al.* failed to reproduce the results obtained by the Corma group and proposed that the reaction is in fact catalyzed by palladium impurities.[7] The authors concluded that gold(I) species can not be catalytically active for this cross coupling due to the incapacity of gold(I) to undergo the key oxidative addition of PhI. After this comeback, and in the same year, Corma analyzed his own results more carefully and concluded that indeed the reaction does not occur at gold(I) but on gold nanoparticles generated *in situ* from the decomposition of the Schiff-base catalyst.[8]

In the course of this debate concerning the ability of gold(I) complexes to undergo the oxidative addition of aryl halides, O'Hair and coworkers explored the reaction of iodobenzene with phosphine gold(I) complexes and small gold clusters in the gas phase. While cationic diphosphine gold(I) complexes proved to be inert, the monoligated cationic phosphine complexes were shown to activate the C_{sp2}-I bond: iodobenzene and phosphine gold(I) complexes formed adducts, as indicated by detection of the corresponding cations by mass spectrometry.[9] These adducts were shown to fragment to the respective phenyl phosphonium ions and gold iodide (Scheme 2.3). The overall process can be explained by an oxidative addition reaction of iodobenzene at gold(I), followed by a reductive elimination to form the phosphorus-carbon bond.

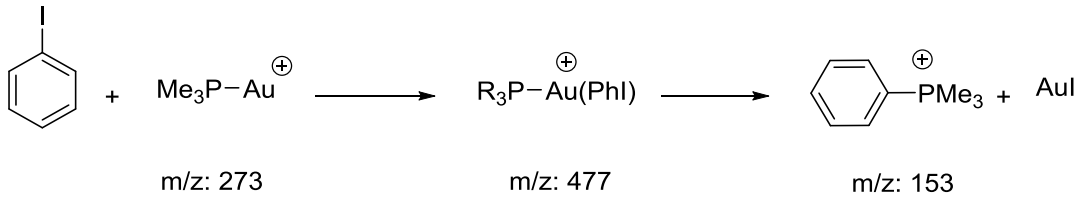

Scheme 2.3 Reaction of a cationic phosphine gold(I) complex with PhI in the gas phase.

The results of the DFT calculations were consistent with the experimental observations. The oxidative addition of iodobenzene to bis(trimethylphenylphosphine) gold(I) was predicted to be an endothermic process by 5.9 kcal/mol, whereas the same reaction with the monoligated cationic gold(I) features an accessible activation barrier (24.7 kcal/mol), and both the formation of gold(III) and the subsequent P-C reductive elimination reaction were shown to be exothermic.

As mentioned in the first chapter, our group studied the oxidative addition of non-polar Si-Si and Sn-Sn bonds to gold(I) both experimentally and computationally, and it was found to proceed *via* a concerted pathway.[10-12] Using the same chelate assistance strategy, the feasibility of oxidative addition of aryl halides to gold(I) was shown by our group. The rigid naphthylphosphine backbone allowed the intramolecular oxidative addition of aryl halides to a single gold(I) metal center.[13] With this chelate-assisted strategy, Csp^2-I bond was activated at room temperature while the more challenging Csp^2-Br bond required higher temperatures. (Scheme 2.4)

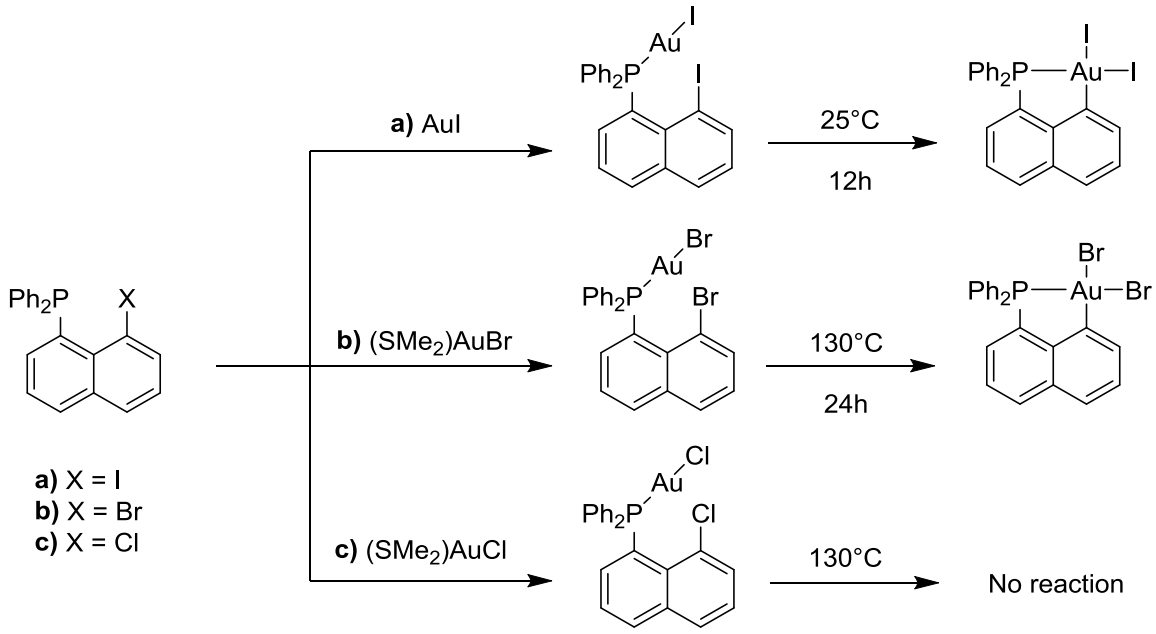

Scheme 2.4 Intramolecular oxidative addition of C_{sp2}-I and C_{sp2}-Br bonds at Au(I).

A similar chelate-assisted approach was revealed to be an efficient methodology to access original gold(III) "PCP" pincer complexes. Indeed, a bis(phosphine) aryl bromide reacts cleanly with [(Me_2S)AuBr] to afford the cyclometalated bis(phosphine) gold(III) bromide complex (Scheme 2.5).[13] While the chelate system facilitates the oxidative addition reaction

of Csp^2-Br (reaction proceeds at 60°C vs. 130°C with the napthylphosphine backbone), Csp^2-Cl bond activation remained a challenge.

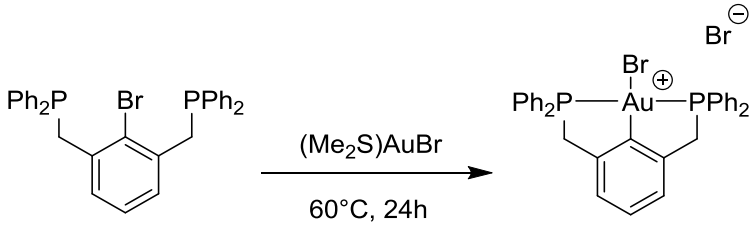

Scheme 2.5 Synthesis of a gold(III) pincer complex *via* oxidative addition of Csp^2-Br.

The ligand design was shown to be crucial to perform the intramolecular oxidative addition of aryl halides. Indeed, the rigidity of the backbone or the presence of a second phosphine arms were proven to be essential parameters to trigger the reactivity of gold towards the activation of Csp^2-X bonds. This was illustrated in the examples reported independently by the groups of Hashmi and Echavarren (Scheme 2.6).[14,15] In both cases, the monodentate gold(I) complexes were unreactive towards an adjacent Csp^2-X bonds even after prolonged periods (several days). DFT calculations reported by Echavarren and coworkers indicated that a high-lying transition state prevents the formation of a thermodynamically favorable five-membered metallacycle. The origin of the elevated barrier was suggested to be linked to the high deformation energy of the linear gold(I) complex necessary to achieve the square-planar geometry of the gold(III) product.

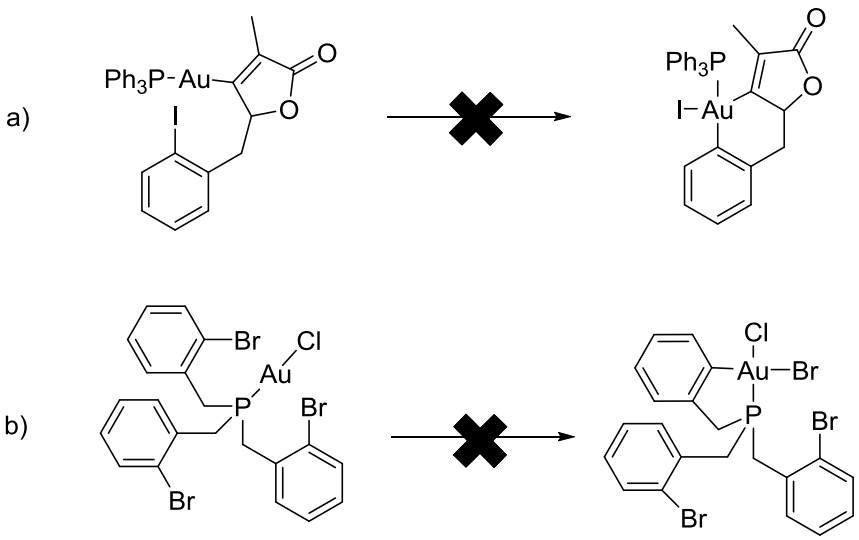

Scheme 2.6 Attempted intramolecular oxidative addition of Csp^2-X bonds.

Recently, the group of Ribas, inspired by the chelate strategy, performed the intramolecular oxidative addition of 10-iodobenzo[h]quinolone to gold iodide to yield the cyclometallated Au(III) complex (Scheme 2.7).[16] The oxidative addition was possible in this case due to the rigidity of the backbone as well, but the reaction conditions are relatively harsh compared to the intramolecular oxidative addition reported by our group.

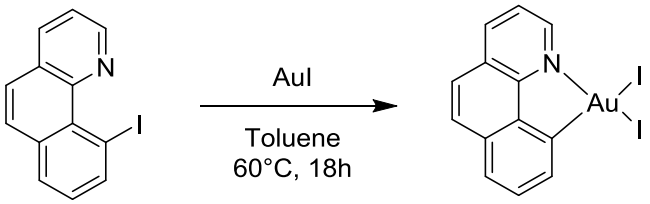

Scheme 2.7 Intramolecular oxidative addition of Csp^2-I bond to gold(I).

As shown above in this section, gold(I) complexes can undergo not only the oxidative addition of polar bonds, but also the intramolecular oxidative addition of non-polar bonds and aryl halides *via* a concerted mechanism. These results not only raise questions on the

feasibility of the intermolecular oxidative addition of aryl halides to gold(I), but also on the parameters that allow this key elementary step.

2.2 Intermolecular Oxidative Addition: Design Principles

After achieving the intramolecular oxidative addition to gold(I), we started to investigate if this transformation can also proceed in an intermolecular manner. Actually, the study of the intermolecular oxidative addition to gold(I) is valuable not only from a fundamental point of view, but also from a synthetic point of view as it will pave the way for subsequent transformations since the oxidative addition is the entry point to many catalytic cycles.

Based on our previous results and the different observations regarding the reactivity between gold and iodobenzene, we sought to learn more about the key geometric and electronic parameters that govern the reactivity of Au(I) complexes towards the oxidative addition reaction. The major requirement is the geometry around the gold center. The first tests carried out in our group for the intermolecular σ-bond activation, consisted in the use of monocoordinated cationic Au(I) complexes. Even though this strategy was fruitful for the activation of σ-SiSi, the resulting three-coordinated gold(III) complexes exhibited low thermal stability.[11] A tetracoordinated, square planar environment is generally required to impart stability to gold(III) complexes. On the other hand, dicoordinated gold(I) complexes, either neutral such as $(R_3P)AuCl$, or cationic such as $[Au(PR_3)_2]^+X^-$, showed to be unreactive towards oxidative addition even at high temperatures. These two coordinated complexes are linear, by far the most common geometry for gold(I).[17]

It is well established for linear dicoordinated palladium(0) and platinum(0) complexes that in order to reach the transition state of an oxidative addition reaction, bending of the L-M-L angle has to occur.[2] This bending is mandatory because in a linear ML_2 complex the orbital

interactions with the σ-bond to be cleaved are unfavorable (Figure 2.1). This situation is well manifested in the Walsh diagram below for a PtL_2 complex.[18,19]

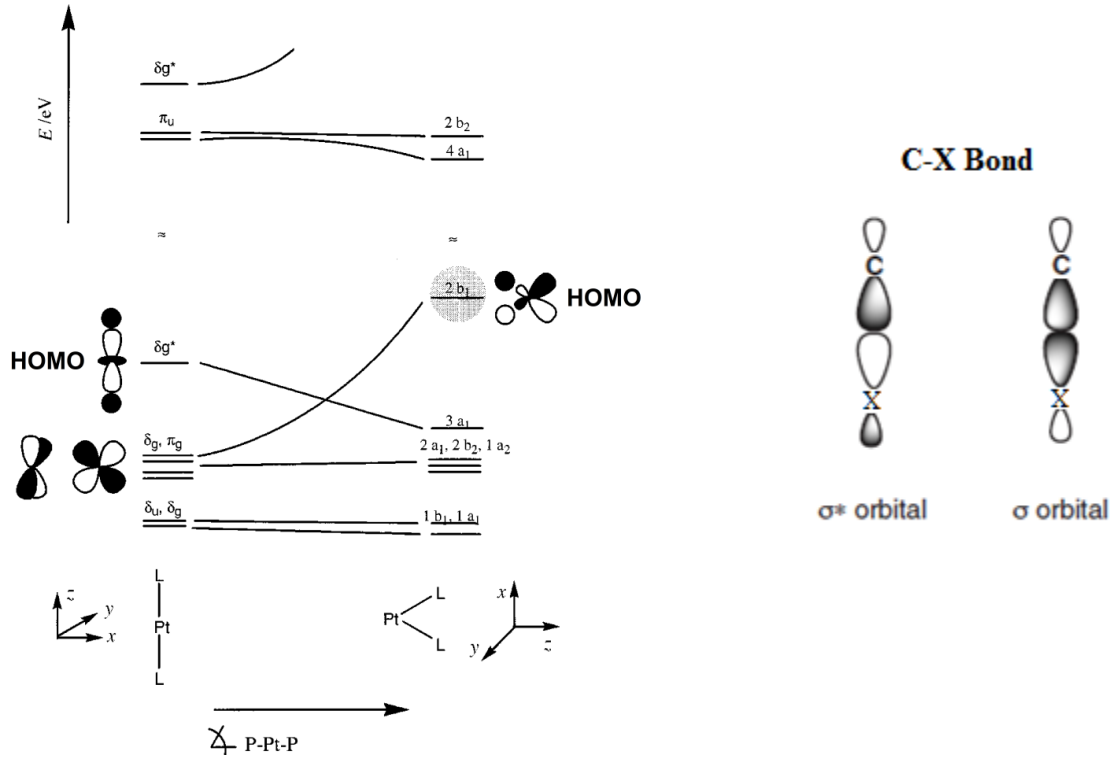

Figure 2.1 Walsh diagram for PtL_2 complexes (left) [19] and schematic illustration of σ and σ* orbitals of a C-X bond (right).

On the left side, for the linear platinum complex, the HOMO (δ_g*) doesn't exhibit matching symmetry for interaction with the antibonding orbital of the σ-bond to be activated. But, in the case of a smaller bite angle (right side of the figure), the frontier orbital energies changes: the δ_g* orbital lowers in energy, while the $2b_1$ orbital rises in energy and becomes the HOMO, with a symmetry more suitable for interaction with the σ* orbital.

As Pt(0) and Au(I) are isoelectronic, the same analysis and conclusions also apply to dicoordinate gold(I) complexes.[20] Accordingly, we hypothesized that the high deformation

energy of the ligand sphere around gold, in order to reach the transition state, was behind the absence of reactivity of linear dicoordinated gold(I) complexes towards oxidative addition.

Therefore, a small L-Au-L bite angle forced by the ligand framework is expected to destabilize the ground state of the gold(I) complex and as a direct consequence should decrease the activation barrier for oxidative addition.

Taking into consideration these geometric and electronic requirements, and in order to realize the intermolecular oxidative addition of aryl halides, we decided to start from a gold(I) complex, in which the ligand will pre-organize the geometry of the metal fragment, and in which the gold(I) center will still features a free coordination site to allow for an interaction with a σ-bond (Scheme 2.8).

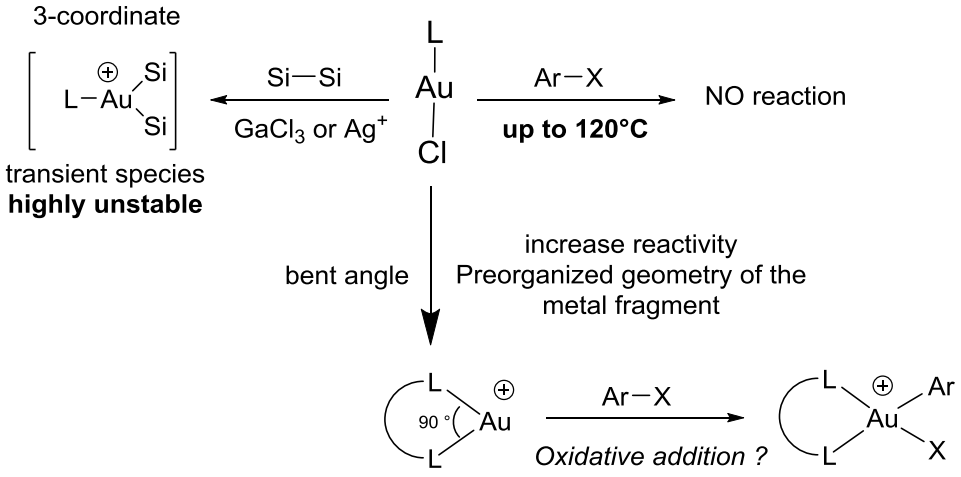

Scheme 2.8 The design principles that we established to trigger the reactivity of gold(I) towards the oxidative addition reaction.

Starting from a trigonal gold(I) complex featuring a chelating ligand L_2 with a small bite angle (close to 90°) and one anionic X ligand (preferably an halide) will allow to access a bent 14-electron $[L_2Au(I)]^+$ complex with an open coordination site after abstraction of the halide. But as mentioned earlier, such ligand environment is highly unusual for gold(I) due to

its high preference for linear geometry. In fact, many dicoordinating L_2 ligands that are employed with other transition metals to form chelating structures, form dinuclear species with gold(I) in order to preserve the linear geometry. These dinuclear complexes are thermodynamically favored due to the formation of aurophilic interactions (Scheme 2.9).

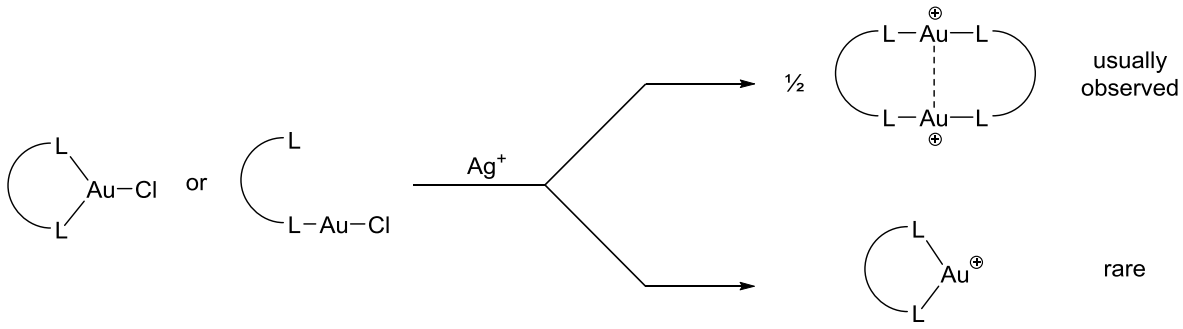

Scheme 2.9 Usual behavior of gold (I) complexes with chelating ligands.

A broad search in the literature revealed that the choice of suitable ligands that satisfy the previously-mentioned criteria is rather limited.[21] Among the rare examples, a gold(I) complex reported by Laguna and coworkers attracted our attention. This cationic (1,2-bis(diphenylphosphino)-1,2-dicarba-*closo*-dodecarborane-χ^2P,P')(triphenylphosphine) gold(I) complex displays a P-Au-P angle of 90.2(1)° according to the reported X-ray structure.[22] Moreover, this reported gold(I) complex was prepared from chloro-[1,2-bis(diphenylphosphino)-1,2-dicarba-*closo*-dodecarborane-χ^2P,P'] gold(I) *via* chloride abstraction and subsequent addition of triphenylphosphine (Scheme 2.10). This indicates that the chloride abstraction is a feasible strategy to generate the cationic dicoordinate gold(I) complex.

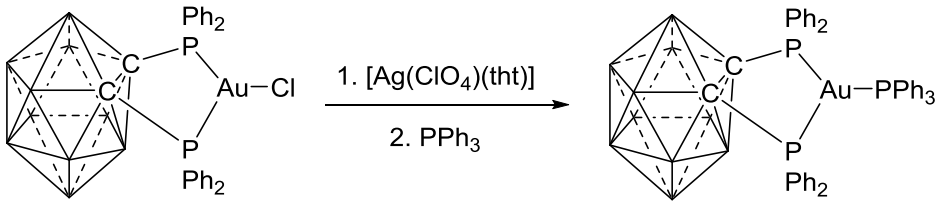

Scheme 2.10 Reported synthesis for the *o*-carborane gold(I) phosphine complex.

2.3 Synthesis and Reactivity of (P,P) Au(I) Complex

2.3.1 Synthesis of Diphosphine-*o*-carborane Gold(I) Complexes

The results discussed in section 2.3 are mainly the results of Dr. Maximilian Joost. I contributed to these results when I arrived in the lab for my master.

Dicarba-*closo*-dodecarboranes (shortened carboranes) are icosahedral clusters based on the parent dodecarborate, with two BH-vertices replaced by CH units. Carboranes are occasionally denoted as "three-dimensional analogues of benzene" based on the similarities. The size of a carborane resembles approximately to a rotating benzene molecule. Moreover, carboranes exhibit a delocalized molecular orbital system involving 3-center 2-electron bonding (except for the *exo*-icosahedral CH and BH bonds which are classical Lewis bonds), that acidifies the two CH protons (pKa for o-carborane: 22.0), and thus allow for functionalization of the CH units *via* deprotenation / nucleophilic trapping reactions.[23,24] Besides the electronic properties, the long CC bond (ca. 1.7 Å *vs.*1.4 Å in benzene) and the rigidity of the carborane cluster permit the chelation of a metal center.

Based on these considerations, our group focused on the synthesis of 1,2-bis(diphenylphosphino)-1,2-dicarba-*closo*-dodecarborane, the 1,2-bis(diisopropylphosphino)-1,2-dicarba-*closo*-dodecarborane, as well as the more electron donating ligand the 1,2-bis(diaminophosphino)-1,2-dicarba-*closo*-dodecarborane.[25-27] Gold(I) chloride complexes **1**,

2 and **3** were prepared by reacting the corresponding ligand with [(SMe_2)AuCl] (Scheme 2.11).

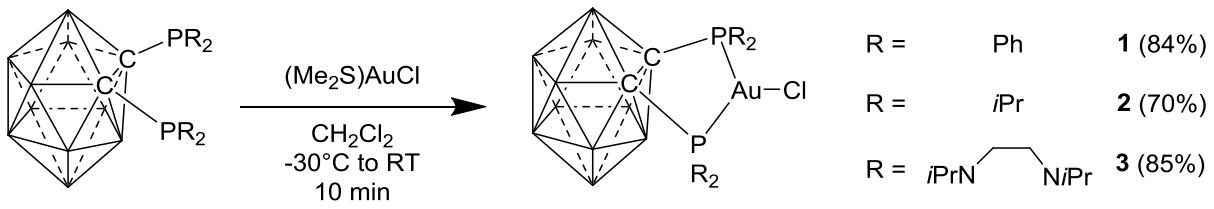

Scheme 2.11 Synthesis of *o*-carborane gold(I) chloride complexes.

All complexes were isolated and fully characterized by multinuclear NMR spectroscopy. Complex **2** was also characterized by X-ray diffraction analysis. In the solid state, only one phosphorus arm is involved in the coordination to gold, the second arm being pendant. The coordination environment around the gold center is almost linear with a P1-Au-Cl angle of 175.52(6)°. The second phosphorus arm is rather far from the metal center (AuP2 = 3.083(2) Å), but still below the sum of Van der Waals radii (r_{VdW} = 4.05 Å).[28] Moreover, the lone pair of the pendant phosphine is oriented in the direction of the gold atom. In solution, complex **2** exhibits a single $^{31}P\{^1H\}$ NMR resonance at δ = 35.9 ppm, which indicates either a rapid exchange of the phosphines on the metal center, or a symmetric coordination of both phosphorus arms in solution. Thus, the trigonal planar structures will be used instead of the dicoordinate linear one to describe these complexes.

2.3.2 Influence of Phosphorus Substituents on the Oxidative Addition Reaction

With complexes **1**, **2** and **3** in hands, our team investigated first the reactivity of complex **1** towards the oxidative addition of iodobenzene. To generate the bent two-coordinate cationic

gold(I) complexes, gallium trichloride was chosen first as the halide scavenger (Scheme 2.12).

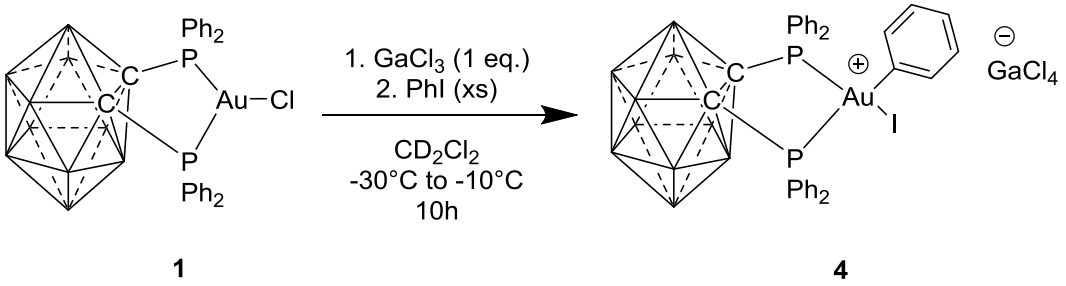

1 **4**

Scheme 2.12 Synthesis of gold(III) complex **4** by oxidative addition of iodobenzene.

The addition of phenyl iodide at low temperature caused a rapid change of color to bright yellow. Taking advantage of the phosphorus probe, the reaction was monitored by $^{31}P\{^{1}H\}$ NMR spectroscopy. The NMR's spectra revealed the presence of a new phosphorus-containing compound: two associated doublet resonance at δ = 61.8 pm and δ = 44.6 ppm with a coupling constant J_{PP} of 29.1 Hz. These two doublets are indicative of the desymmetrization of the ligand framework by oxidative addition of iodobenzene. Besides the $^{31}P\{^{1}H\}$ NMR, the ^{13}C NMR data displayed a doublet resonance at δ = 144.8 ppm with a large C-P coupling constant (J_{CP} = 122.0 Hz), in the range of a *trans* carbon – phosphorus coupling. These spectroscopic data for complex **4** are in agreement with a gold(III) complex generated by oxidative addition of iodobenzene.[29]

Unfortunately, complex **4** is thermally unstable and decomposes rapidly at room temperature to gold metal and unidentified products. Even at temperatures as low as -80°C, the complex is not stable and decomposes over days.

The same reaction was run again using complex **2**. In this case, the reaction was very fast (fast color change to bright orange-yellow) indicating a possible gold(I) to gold(III) transition. But

once again, the oxidative addition of iodobenzene resulted in the formation of an unstable complex that decomposed rapidly to unidentified products.

In the objective of increasing the thermal stability of the gold(III) complexes generated from the oxidative addition, complex **3** was tested. This complex features a chelating ligand with strong donation properties due to the electron-rich substituents on phosphorus and offers it displays significant steric bulk that may help stabilizing the gold(III) complexes. Once again, gallium trichloride was used as the halide scavenger to generate the cationic electrophilic species, followed by the addition of iodobenzene (Scheme 2.13).

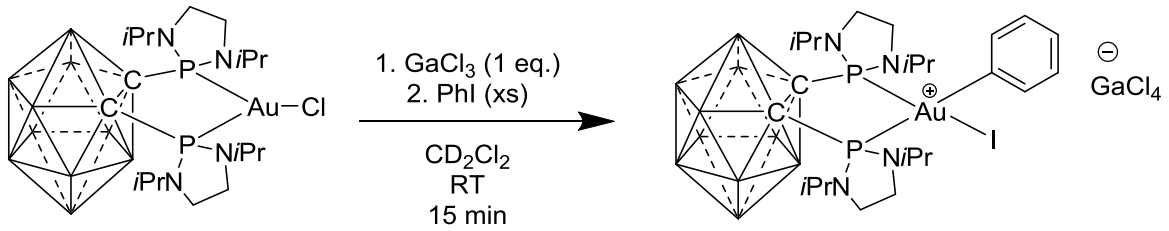

3 **5**

Scheme 2.13 Synthesis of gold(III) complex **5** by oxidative addition of iodobenzene.

We were pleased to see that the generated gold(III) complex **5** displayed increased stability compared to complex **4**. In fact, this complex can be prepared and handled for short time in solution even at room temperature but after few hours, significant decomposition was observed. Complex **5** was completely characterized in solution and solid state thanks to its increased thermal stability.[29]

Despite the gain in stability of the gold(III) complex bearing the diamino substituents on phosphorus (compared to complex **4**), we decided to vary another parameter to further increase the stability of the gold(III) species. For this purpose, a study regarding the influence of the counteranion was realized.

2.3.3 Influence of the Counter anion on the Oxidative Addition Reaction

The stability of the gold(III) center may also depend on the association strength and the nature of the counter anion. Indeed, the tetrachlorogallate anion can be a possible chloride source: nucleophilic attack of Cl^- or other side reactions may cause the decomposition of the formed gold(III) complex.

Halide abstraction is not limited to gallium trichloride. Chloride can be abstracted as well by salt elimination with sodium or silver salts bearing different anions with distinct properties (weakly coordinating or non-coordinating anions). Sodium tetrakis((3,5-trifluoromethyl)phenyl)borate, silver trifluoromethanesulfonate and silver bis(trifluoromethane)sulfonamide were all able to activate the gold(I) complex for oxidative addition of iodobenzene. However, the bis(trifluoromethane)sulfonamide (NTf_2^-) counter anion offered a good compromise between reactivity and stability of the generated cationic gold(I) complex. This capacity of the NTf_2^- anion to bind and stabilize gold was already observed in Gagosz's catalyst.[30]

In order to verify if the NTf_2^- anion would provide a beneficial impact on the stability of our gold(III) species, complex **3** was first reacted with one equivalent of $AgNTf_2$ to yield the corresponding triflimidate complex **6**. The advantages of using bis(trifluoromethane)sulfonamide as a counter anion were directly observed since the gold(I) complex can be isolated, handled and stored at room temperature (Scheme 2.14).

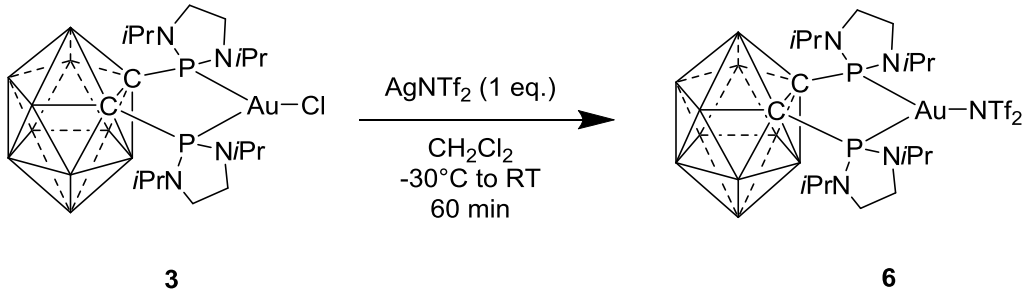

3 **6**

Scheme 2.14 Synthesis of gold(I) triflimidate complex **6**.

Complex **6** was fully characterized. One single resonance (δ = 138.3 ppm) was observed by $^{31}P\{^{1}H\}$ NMR, indicating once again a symmetric environment around gold. The molecular structure of **6** in the solid state was determined by single X-ray diffraction analysis which confirmed the tricoordinate environment around the gold. The PAuP bite angle is 100.73(2)° which is not far from the 90° for an ideal square planar geometry in a gold (III) complex.

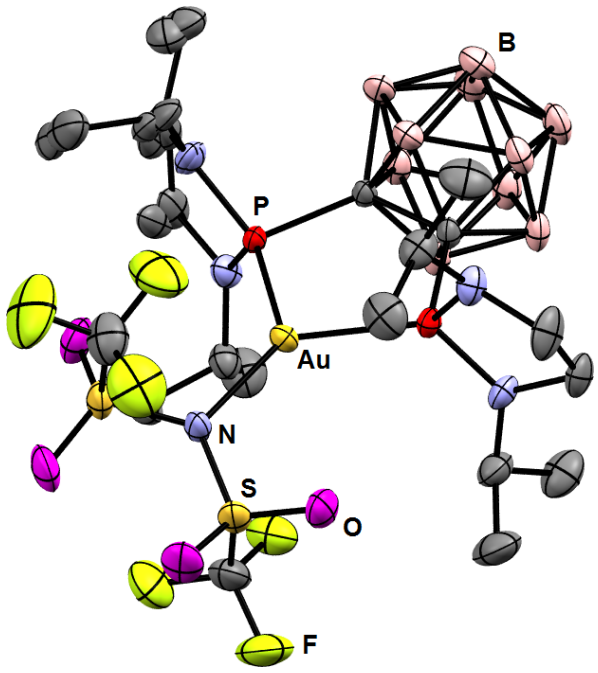

Figure 2.2 Molecular structure of complex **6** determined by single X-ray crystallography. Solvent molecules and hydrogen atoms were omitted for clarity. Selected bond lengths [Å] and angles [°]: P1Au 2.3215(5), P2Au 2.3172(5), AuN 2.221(2), P1AuP2 100.73(2).

The triflimidate ion is tightly bound to the metal center as indicated by the short Au-N distance (2.221(1) Å) but longer than the Au-N in Gagosz's catalyst ([PPh_3]$AuNTf_2$) (2.102(3) Å).[30] And, since the triphenylphosphine gold(I) triflimidate is an active catalyst in solution, we hypothesized that NTf_2^- will also behave as a labile counter anion in our case and will allow the oxidative addition of aryl halides.

After observing the positive impact of the triflimidate anion on the stability of the gold(I) complex, the oxidative addition of iodobenzene was tested to examine the impact of NTf_2^- on the gold(III) complex. One equivalent of iodobenzene was added at room temperature to a dichloromethane-d^2 solution of complex **6** (Scheme 2.15).

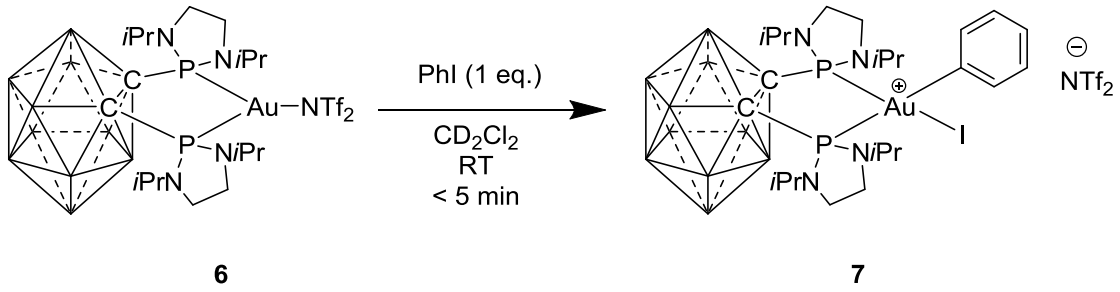

6 **7**

Scheme 2.15 Synthesis of gold(III) complex **7** by oxidative addition of iodobenzene.

The addition of iodobenzene resulted in a quick color change to bright yellow, indicating the formation of the complex **7** by oxidative addition of phenyl iodide. Gratifyingly, complex **7** displayed a reasonable stability and can be handled for a certain period of time in solution at room temperature without excessive decomposition. The formation of complex **7** was confirmed by multinuclear NMR spectroscopy.[29]

The use of 1,2-bis(diaminophosphino)-1,2-dicarba-*closo*-dodecarborane as a ligand and bis(trifluoromethane)sulfonamide as a counteranion, allowed the synthesis of a stable bent

cationic gold(I) complex that undergo the oxidative addition of phenyl iodide to afford relatively stable gold(III) complex.

2.3.4 Oxidative Addition to Complex 6: Scope and Limitations

2.3.4.1 Oxidative Addition of Aryl Iodides

As mentioned above, the bent gold(I) triflimidate complex **6** reacts spontaneously and rapidly with iodobenzene at room temperature: complete conversion was achieved within less than five minutes. Furthermore, the oxidative addition reaction is general and a variety of aryl iodides were activated. The reaction shows good functional group compatibility (*p*-OMe, *p*-NHAc, *p*-F, *p*-CN and *p*-NO_2 substituted iodobenzenes). It works with 1-iodonaphthalene as well as heterocyclic substrates such as 2-iodothiophene and 2-iodopyridine (Scheme 2.16).

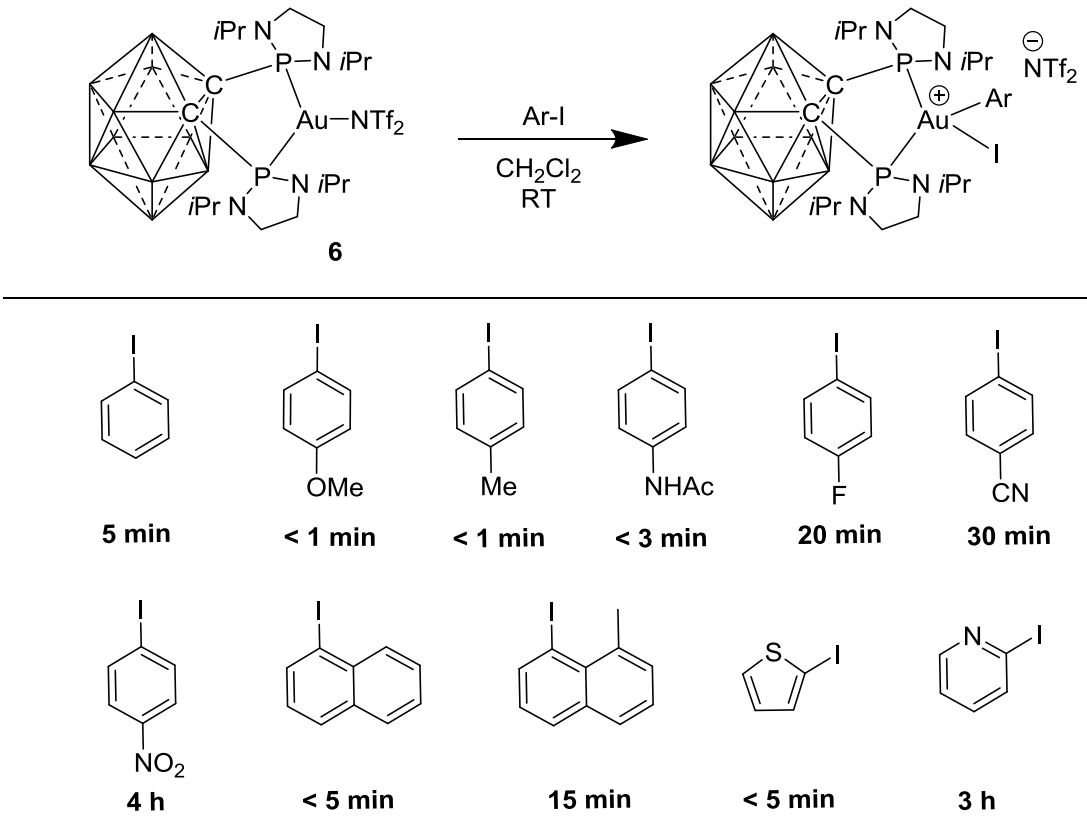

Scheme 2.16 Scope of the oxidative addition of aryl iodides with complex **6**.

Using NMR spectroscopy along with high resolution mass spectrometry, the products of the oxidative addition of the C-I bonds were identified at room temperature. Nevertheless, these complexes displayed low stability and decomposition was observed: the rate of degradation was dependent on the aryl moiety bounded to the gold(III) center. For example, further increase of the stability was accomplished with the use of 1-iodo-8-methyl naphthalene: the gold(III) complex generated from the oxidative addition of this substrate can be isolated (93% yield). No sign of decomposition was observed even after weeks in the solid state, and only little decomposition was detected in solution after several days.

Surprisingly, oxidative addition of *p*-substituted iodobenzenes proceeds faster with electron-donating group than with electron-withdrawing substituents. For example, 4-iodotoluene reacted immediately (< 1 min) at room temperature, while the oxidative addition of 1-iodo-4-nitrobenzene required 4h to reach full conversion. This reactivity trend is opposite to that encountered upon oxidative addition of aryl halides to $L_2Pd(0)$ complexes.[31] It is possible that the rate-enhancement effect of electron-donating substituents is related to the formation of π-intermediates.

To gain more insight into the mechanism of the oxidative addition of aryl iodides to complex **6**, DFT calculations were carried out in collaboration with the group of Dr. Karinne Miqueu. The starting point of the reaction is the displacement of the weakly coordinated NTf_2^- counter anion by phenyl iodide to form the π-complex **6'**, which is slightly uphill in energy (ΔE = 3.0 kcal/mol and ΔG = 12.5 kcal/mol) (Figure 2.3). The phenyl iodide is coordinated to the cationic gold (I) center in a η^2 fashion ($d(AuC_{ipso})$ = 2.876 Å and $d(AuC_{ortho})$ = 2.612 Å). It is important to mention that another minimum was located on the potential energy surface corresponding to the iodine adduct (d(AuI) = 2.800 Å) which is placed 2.3 kcal/mol higher in energy than the π-complex **6'** and may also be implicated in the oxidative addition process.

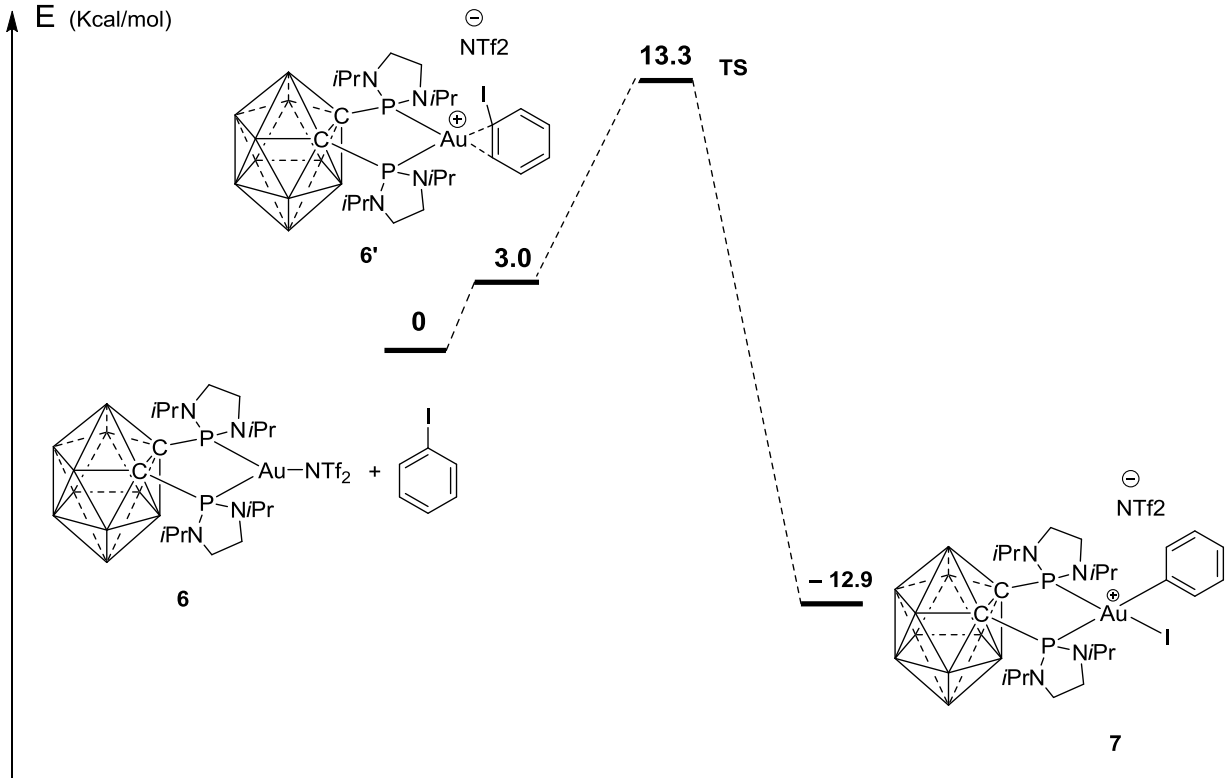

Figure 2.3 Energy profile (electronic energy including ZPE correction, in kcal/mol) computed at the B97D/SDD+f(Au),SDD(I),6.31G+**(other atoms) level of theory for the oxidative addition of phenyl iodide to complex **6**, taking into account solvent effects (SMD model: dichloromethane).

The reaction proceed *via* a concerted transition state with a remarkably low activation barrier ($\Delta E^{\ddagger}$ = 10.3 kcal/mol and $\Delta G^{\ddagger}$ = 10.7 kcal/mol from complex **6'**), in agreement with the mild conditions in which the reaction occurs experimentally. A shortening in the C_{ipso}-gold distance ($d(AuC_{ipso})$ = 2.34 Å) is observed in the transition state along with an elongation of the C-I bond (by 0.26 Å) and its bending out of the Ph plane (by 35.6 °). This TS collapses into the square-planar cationic gold(III) complex **7,** and the overall process is thermodynamically favorable.

In order to examine the impact of the bending on the oxidative addition process, the transition state was analyzed using the activation strain model.[32,33] The activation energy $\Delta E^{\ddagger}$ is decomposed into different components: the strain energy ($\Delta E^{\ddagger}_{strain} = \Delta E^{\ddagger}_{dist\text{-}Au} + \Delta E^{\ddagger}_{dist\text{-}PhI}$)

and the interaction energy ($\Delta E^{\ddagger}_{int}$). In our case, most of the strain energy associated with the TS arises from the distortion energy of phenyl iodide (11.7 kcal/mol), while the distortion of the gold fragment requires only 6.3 kcal/mol thanks to the carborane framework that preorganizes the coordination sphere. The interaction energy between the distorted fragments is large (-34.8 kcal/mol), resulting overall in a small activation barrier. For the sake of comparison, the same strain model was also applied to the linear [$(Me_3P)_2Au^+$] complex. A higher $\Delta E^{\ddagger}_{dist\text{-}PhI}$ (18.5 kcal/mol) and relatively lower $\Delta E^{\ddagger}_{int}$ (-28.6 kcal/mol) are found for the reaction of iodobenzene with this linear gold(I) complex. But the main difference comes from the $\Delta E^{\ddagger}_{dist\text{-}Au}$ component (24.4 kcal/mol) which is almost four times higher than for the [carborane-Au^+]. These data highlight that the large difference of reactivity between the two systems originates essentially from the bent *vs.* linear geometry of the dicoordinated cationic gold(I) complex.

After achieving the oxidative addition of aryl iodides, the reactivity of complex **6** towards the activation of more challenging bonds (Csp^2-Br and Csp^2-Cl) was then investigated. Sadly, the oxidative addition of aryl bromides and chlorides remained a challenge since no sign of activation of the Csp^2-halogen bond was observed and prolonged heating resulted only in the decomposition of complex **6**.

In order to enlarge the scope of the intermolecular oxidative addition and to explore further the potential of this bending strategy, we extended our investigation to other σ-bonds.

2.3.4.2 Oxidative Addition of Biphenylene

Transition metal mediated σ-CC bond activation (in stoichiometric or catalytic manner) represents an interesting reaction for the transformation of organic molecules.[34,35] Nevertheless, it has been achieved only for a handful of substrates and only a few efficient complexes (with late transition metals) have been described to undergo the oxidative addition of CC bonds.

This transformation is considered to be one of the most challenging reactions in the field of organometallic chemistry.[36] This statement is based on (i) the strength of a σ-CC bond (high bond dissociation energy of 83 kcal/mol), and (ii) the high directionality of the σ-orbital of the CC bond that restricts the interaction with a metal center (Figure 2.4).[37]

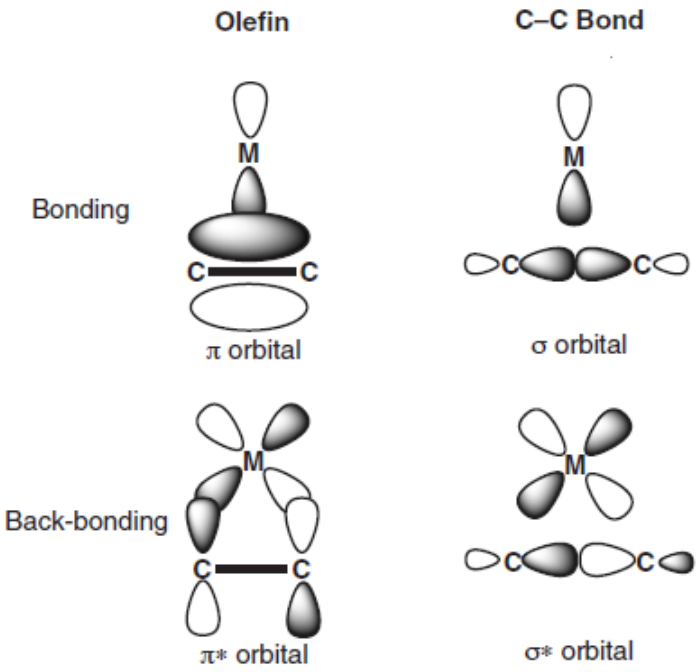

Figure 2.4 Schematic bonding for the interaction of CC multiple bonds (left) and single bonds (right) to transition metals, illustrating the unfavorable overlap of the orbitals engaged in the activation process of σ-CC bonds.[37]

Several strategies can be employed to overcome the above-mentioned obstacles concerning the cleavage of CC bonds. One of the strategies is to increase the energy state of the starting material by using strained carbocycles that possess weakened CC bonds. The release of ring strain during the CC bond cleavage can make this process thermodynamically feasible.

Based on that, our group focused on the activation of biphenylene, since it is considered as a prototypical substrate for CC bond activation at transition metals due to the relatively weak CC bond (65.4 kcal/mol) linking the aromatic rings.[38]

The reactivity of gold(I) chloride **2** towards biphenylene was tested. Again, using gallium trichloride as the chloride scavenger with subsequent addition of biphenylene (5 equivalents) in dichloromethane and heating to 120°C resulted in a quick color change to bright yellow, indicative of the formation of a new product. Complete conversion is achieved after five hours and complex **8** was isolated in 95% yield (Scheme 2.17).[39]

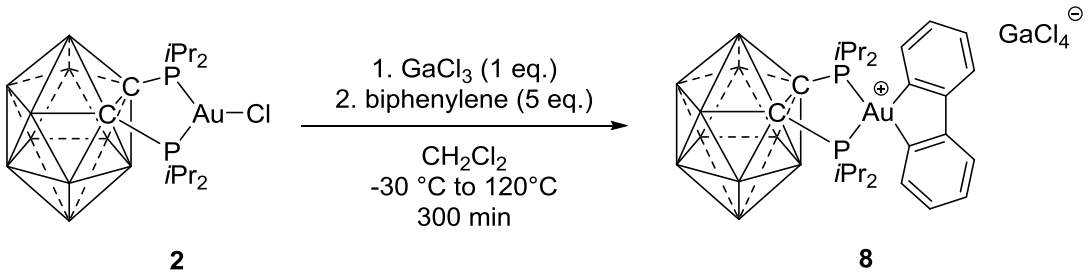

2 **8**

Scheme 2.17 Synthesis of the dibenzoaurole **8** by oxidative addition of biphenylene to gold(I).

The spectroscopic data are in accordance with the dibenzoaurole structure. In the $^{13}C\{^{1}H\}$ NMR spectrum, a doublet of doublets is observed at low field (δ = 165.6 ppm) that turns into a singlet in the corresponding $^{13}C\{^{1}H, ^{31}P\}$ spectrum. This multiplet features two different C-P coupling constants of 114.3 Hz and 9.7 Hz which are typical of a *trans* and *cis* coupling to phosphorus. The complete ^{13}C NMR spectroscopic data and high resolution mass

spectroscopy (ESI+) confirms that biphenylene underwent oxidative addition to the cationic gold(I) complex.

It's worth mentioning that at the same time, Toste and coworkers reported the intermolecular oxidative addition to gold(I). Using a combination of [1,3-bis(2,6-diisopropylphenyl)imidazol-2-ylidenel] gold(I) chloride and silver hexafluoroantimonate as halide scavenger, the oxidative addition of biphenylene was realized and afforded a stable Au(III) complex after chloride trapping (Scheme 2.18).[40]

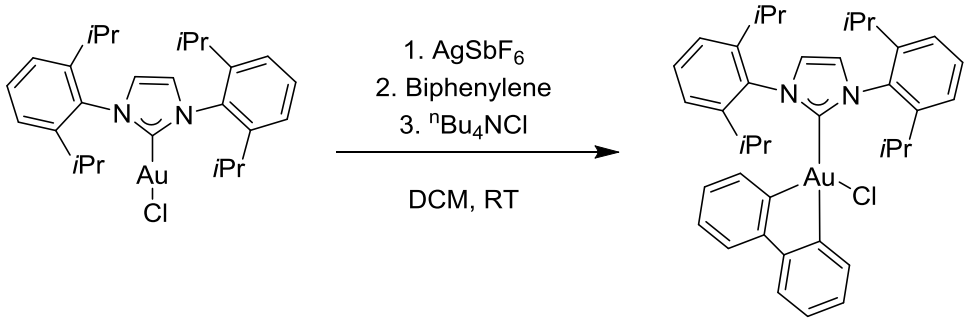

Scheme 2.18 Oxidative addition of CC bond to gold(I).

We have seen that the bending of dicoordinate gold(I) complexes is an efficient strategy to trigger the reactivity of gold for the oxidative addition of aryl iodides and CC bonds under mild conditions. However, the relative low stability of these new gold(III) complexes can be problematic for catalytic perspectives. In addition, the scope of bidentate ligands that can induce a bent dicoordinated geometry around gold is considerably limited. That's why, in order to expand the scope of active Au(I) complexes for the oxidative addition reaction, we turned to another ligand design.

2.4 From (P,P) -Ligand to Simpler Hemi-Labile (P,L) Ligands

2.4.1 Design Principles

As mentioned in section 2, cationic gold(I) complexes featuring monodentate ligands (L = R_3P or NHC) can undergo oxidative addition, but the resulting three-coordinate gold(III) species are highly unstable and difficult to exploit in further reactivity. Thus, we speculated that hemi-labile bidentate ligands might provide an appropriate balance between reactivity and stability of the key species. Taking advantage of the soft/hard character of Au(I)/Au(III), we envisioned to use (P,L) bidentate ligands (with L being a hard donor group, L = N,O). In addition of being an NMR probe and a soft donor group, the coordination of a mono-phosphine to the soft Au(I) center would grant a reactive cationic complex. And upon oxidative addition, the pendant hard donor group (L) would coordinate the resulting hard Au(III) center to form a stable square-planar tetra-coordinated complex (Scheme 2.19).

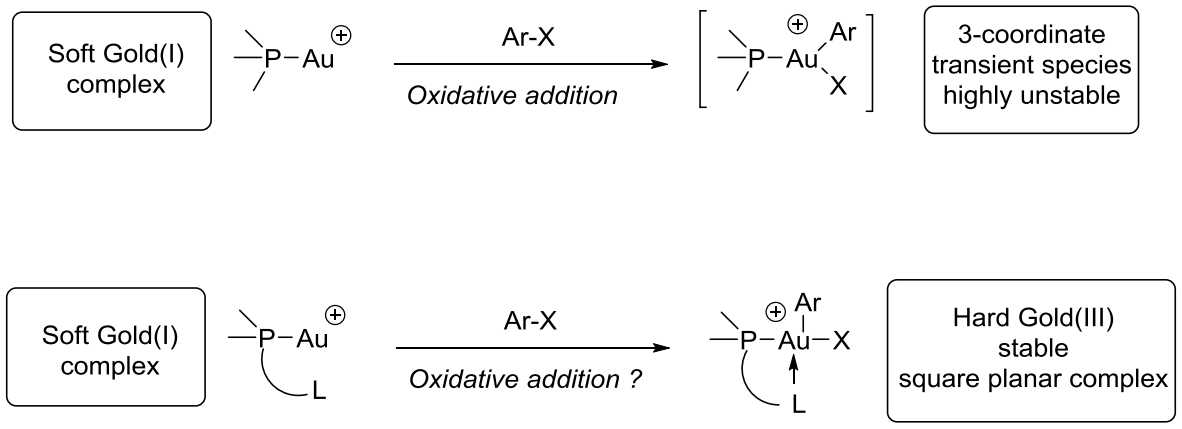

Scheme 2.19 Design principle for the oxidative addition to mono-coordinated Au(I) complexes.

2.4.2 Preliminary Results with Different (P,N) Ligands

In order to explore this hypothesis, we first studied the reactivity of two gold (I) complexes featuring commercially available ligands such as Mor-Dalphos and Me-Dalphos

(Scheme 2.20). The two selected ligands possess a soft electron rich phosphine and a hard pendant nitrogen atom.[41]

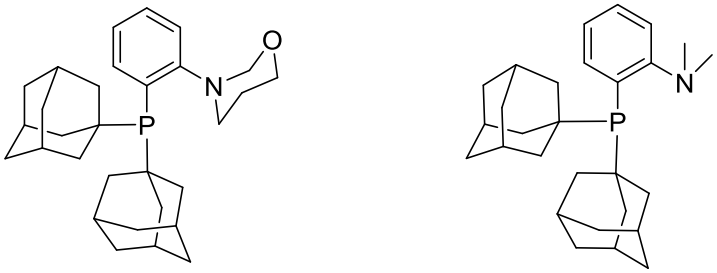

MorDalphos **MeDalphos**

Scheme 2.20 Commercially available (P,N) ligands selected for OA tests.

The use of these (P,N) ligands has been reported to play a key role in the generation and reactivity of α-oxo gold carbene intermediates in oxidative gold catalysis. Zhang and coworkers employed the corresponding gold(I) complexes as catalysts for the [3+2] annulation reaction between a terminal alkyne and a carboxamides for the formation of 2,4-disubstituted oxazoles.[42] In this study, Zhang suspects the role of nitrogen in stabilizing the α-oxo gold(I) carbene, a highly electrophilic intermediate postulated for this transformation (Scheme 2.21).

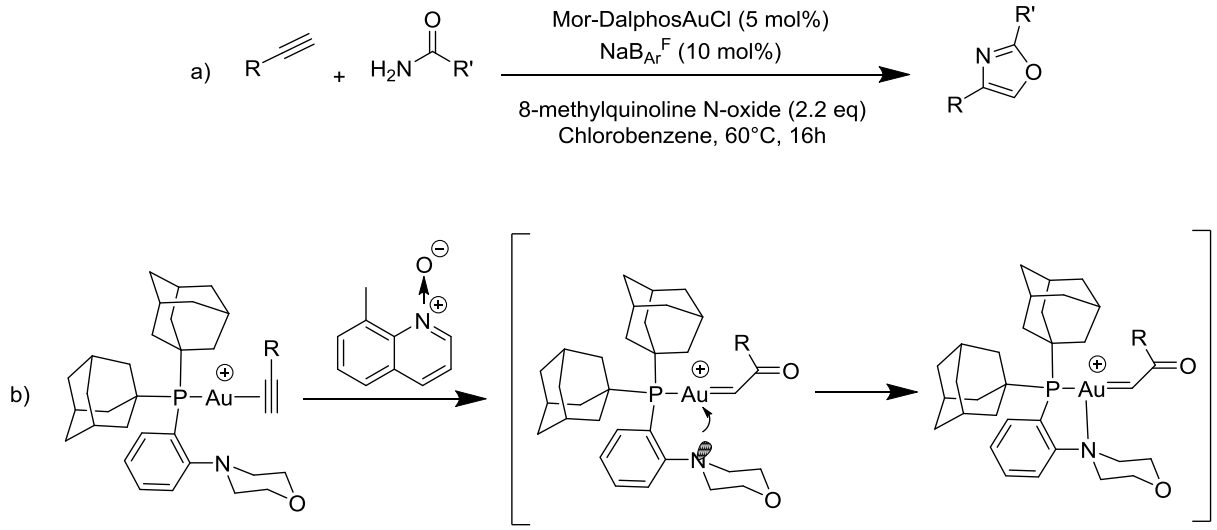

Scheme 2.21 a) Synthesis of 2,4-disubstituted oxazoles via [3+2] annulations. b) Rational for the role of Mor-Dalphos in the stabilization of α-oxo gold(I) carbene.

In the beginning, to explain the effectiveness of these gold(I) catalysts and the role of the neighboring nitrogen atom, Zhang thought that H-bonding may be at play. However, inspection of the X-ray structure of the (MorDalphos) gold(I) complex showed that the nitrogen atom, with its lone pair pointing to the gold center is too congested for H-bonding. Moreover, to rule out the participation of the ortho nitrogen atom *via* H-bonding, Zhang and coworkers synthesized the related (P,S) bidentate gold(I) complexes and tested their reactivity in catalysis. The (P,S) based catalysts promoted the oxazole formation with efficiencies close to those of (P,N) catalysts. Thus, the role of these bidentate ligands was ascribed to the stabilization of the highly electrophilic gold carbene intermediate by the nitrogen or the sulfur moiety allowing more chemoselective reactions with nucleophiles.

Having this in mind, we tested first the reactivity of the MorDalphos and MeDalphos gold(I) chloride complexes towards the oxidative addition of iodobenzene. After witnessing the positive impact of NTf_2 anion on the reactivity and stability of the carborane gold(I)

complexes, silver bis(trifluoromethane)sulfonamide was chosen as the halide scavenger to generate the mono-coordinate cationic gold(I) complexes (Scheme 2.22).

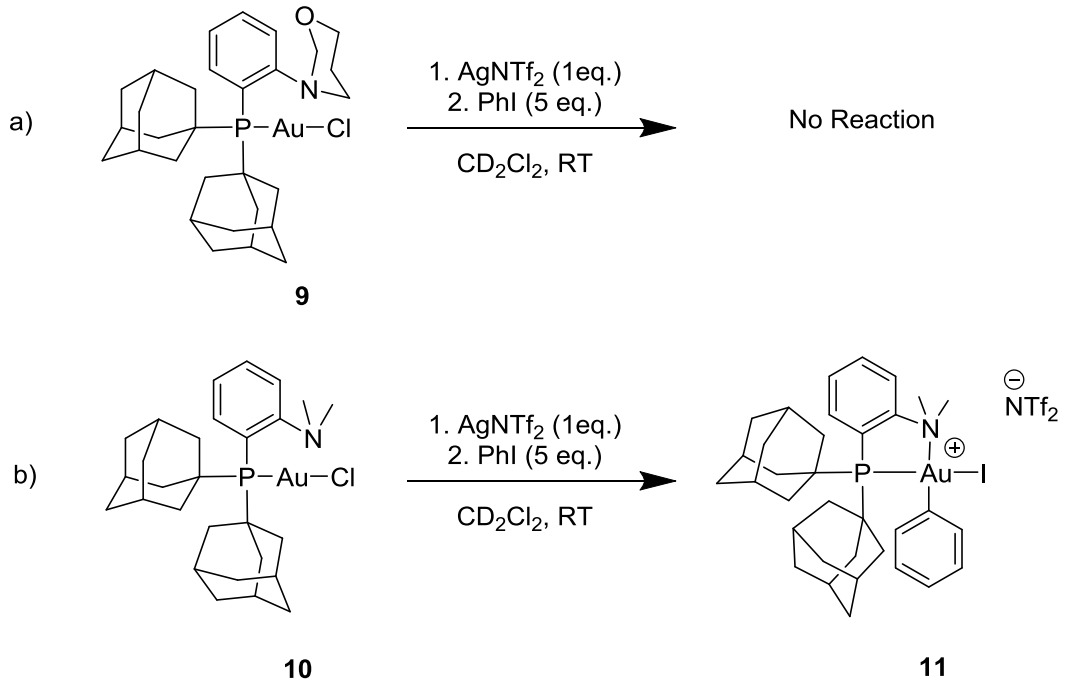

Scheme 2.22 Oxidative addition attempts of iodobenzene to complex **9** and **10**.

Taking advantage of the phosphine probe, the reactions were monitored by $^{31}P\{^{1}H\}$ NMR spectroscopy. No reaction was observed after the addition of iodobenzene on complex **9** even after days. The absence of oxidative addition can be due to the steric hindrance induced by the morpholine moiety and therefore preventing the interaction between the gold center and iodobenzene.

Gratifyingly, controlling the reaction between complex **10** and iodobenzene by ^{31}P NMR indicated gradual formation of the (MeDalphos)gold(III)-aryl complex **11** (δ 74.1 ppm) as the major phosphorus-containing compound, along with a small amount of unidentified species. After 48 hours at room temperature, the reaction is complete, and complex **11** is formed in 92% (spectroscopic) yield. Most diagnostic in NMR is the downfield shift of the ^{13}C NMR

signal for the quaternary carbon atom, from 92.6 ppm in iodobenzene to 127.7 ppm in complex **11**. This signal appears as a broad singlet (no C-P coupling constant) suggesting that the phenyl group sits in *cis* position to phosphorus (Figure 2.5). Besides the ^{31}P and ^{13}C NMR, the ^{1}H NMR indicates as well the formation of complex **11** *via* oxidative addition. In fact, the downfield shift of the resonance signal for the -N(CH_3)$_2$ substituent, from 2.5 ppm in complex **10** to 3.5 ppm in complex **11**, indicates the coordination of nitrogen to the gold(III) center (Figure 2.6).

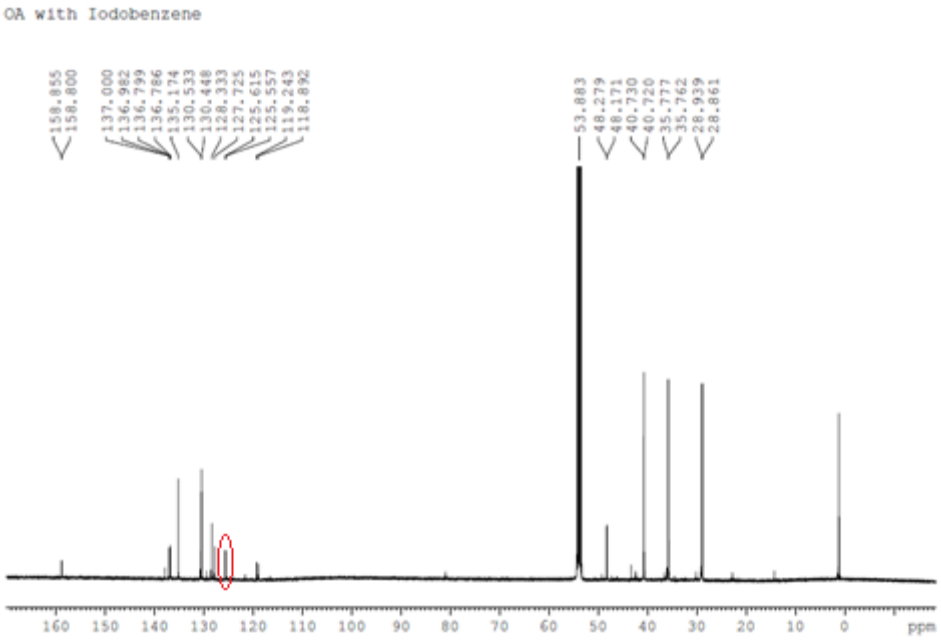

Figure 2.5 $^{13}C\{^{1}H\}$ NMR spectrum of complex **11** in CD_2Cl_2.

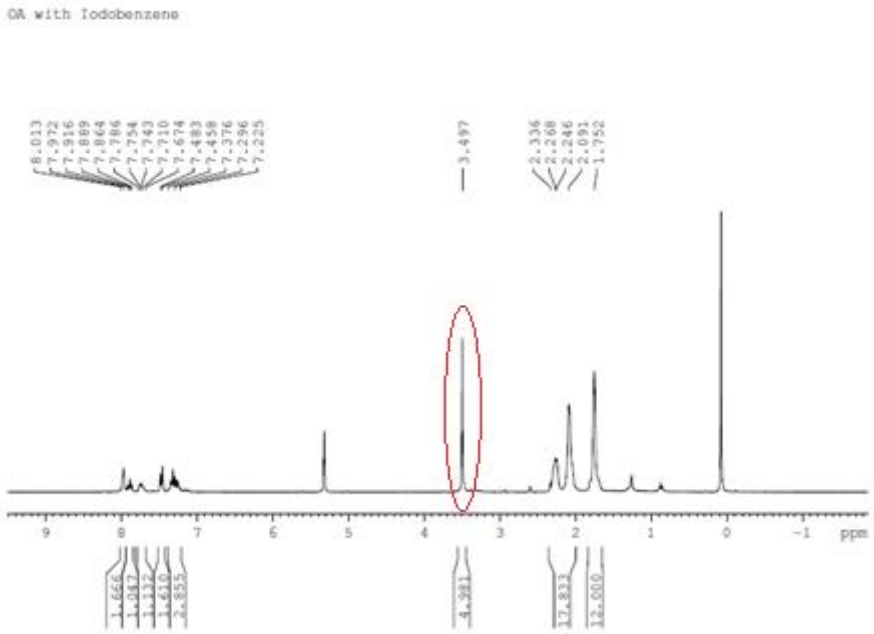

Figure 2.6 ^{1}H NMR spectrum of complex **11** in CD_2Cl_2.

Complex **11** can be handled conveniently at room temperature and no sign of decomposition was detected after one week in solution. The molecular structure of **11** in the solid state was determined by single X-ray diffraction analysis which confirmed the bidentate character of the MeDalphos ligand (Figure 2.7).

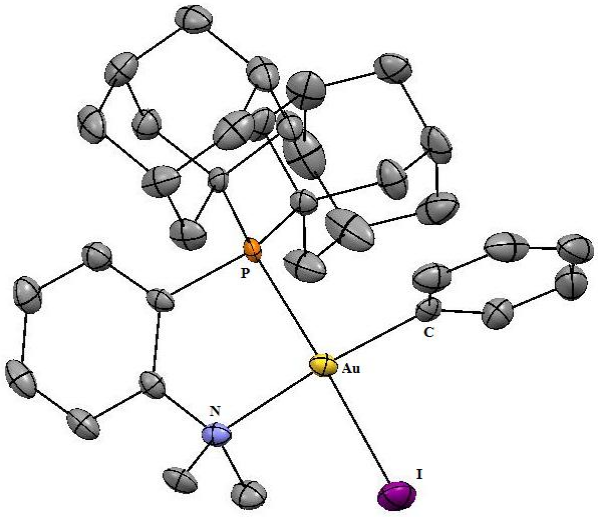

Figure 2.7 Molecular structure of complex **11** determined by single X-ray crystallography. Hydrogen atoms and the NTf_2 counter anion were omitted for clarity. Selected bond lengths [Å] and angles [°]: AuN 2.214(5), AuP 2.369(2), AuC 2.064(6), PAuN 84.62(13).

In complex **11**, the gold center is tetra-coordinate and adopts a square-planar geometry. The phenyl ring sits indeed in *cis* position to phosphorus in agreement with that observed in solution.

After achieving the oxidative addition of iodobenzene with the (MeDalphos) gold(I) complex, and before advancing to more detailed studies concerning (P,N) bidentate ligands, we were intrigued to test the reactivity of the (P,S) gold(I) complex. Although sulfur is known to be a soft donor, the curiosity to study the behavior of a (P,S) gold complex towards the oxidative addition was amplified by the results reported by Zhang's group: the (P,S) gold complex exhibited similar catalytic behavior to the (P,N) analogue for the oxazole formation. This would suggest that the sulfur lone pair might be able of coordinating and stabilizing the gold metal center.

To verify this hypothesis, chloro [(2-methylthio)phenyl]diphenylphosphine gold(I) and chloro [2-(*tert*-butylthio)phenyl]diphenylphosphino gold(I) complexes were synthesized. Once again, the subsequent addition of a halide scavenger and iodobenzene was realized (Scheme 2.23).

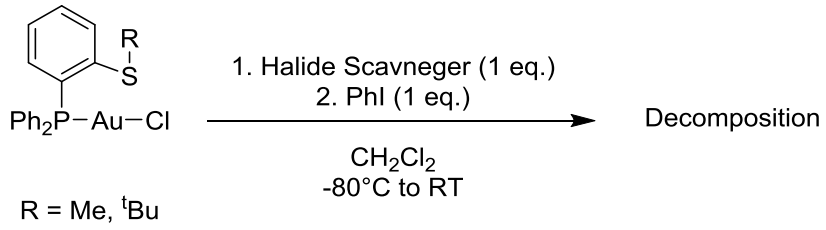

Scheme 2.23 Oxidative addition attempts of iodobenzene to (P,S) gold (I) complexes.

By NMR spectroscopy, no product of oxidative addition could be detected in both cases. The cationic gold (I) complexes decomposes instantaneously to give metallic gold and the four-

coordinate complex $[(P,S)_2Au]^+$ as indicated by high resolution mass spectrometry (ESI+). This highlights the necessity to have a hard donor group to stabilize the hard gold(III) center.

Noteworthingly, during the course of this work, bidentate ligands with a hemi-labile nitrogen based donor have been shown to stabilize gold(III) species as well (Scheme 2.24). Hashmi and coworkers, using the 8-(diphenylphosphino)quinoline ligand realized the addition of aryldiazonium salts to gold(I) upon irradiation with a blue LED.[43] Using a similar approach, Glorius *et al.* reported the straightforward access to (C,N)-cyclometallted gold(III) complex *via* addition of aryl diazonium salts to gold(I) under visible-light photoredox conditions.[44] Also, the group of Bertrand reported recently the synthesis gold(I) complexes bearing hemi-labile cyclic (alkyl)(amino) carbenes that promote the oxidative addition of biphenylene.[45]

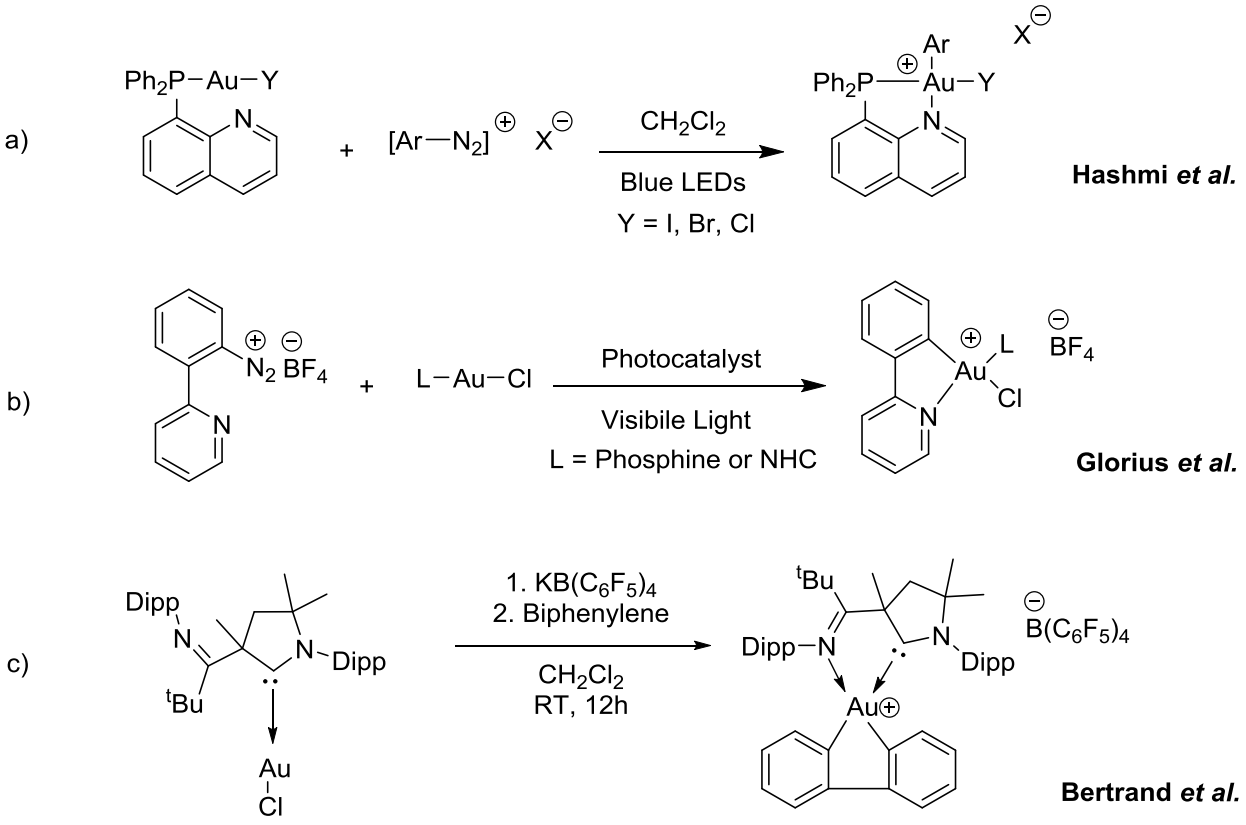

Scheme 2.24 Reported syntheses of well defined gold(III) complexes.

2.4.3 (P,N) Ligands Screening

The successful oxidative addition reaction of iodobenzene to the (MeDalphos) gold(I) complex confirmed that the use of hemi-labile (P,N) ligands is an efficient strategy to access gold(III)-aryl complexes.

In order to expand the scope of (P,N) bidentate ligands that trigger the reactivity of gold towards oxidative addition, a ligand screening was carried out. Three additional gold(I) complexes were tested (Scheme 2.25).

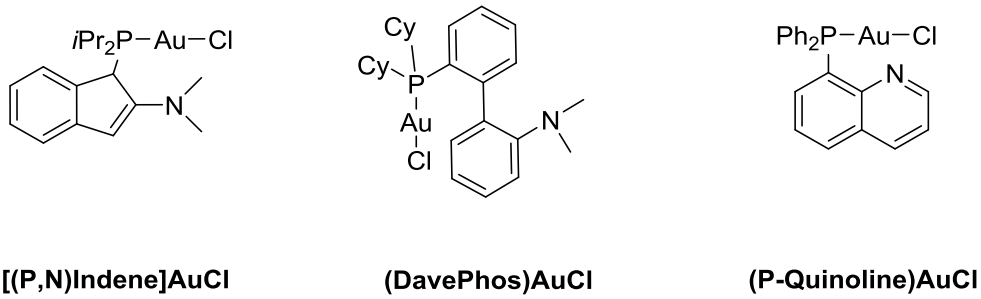

Scheme 2.25 Selected (P,N) gold(I) complexes for OA tests.

The oxidative addition tests were performed following the standard conditions: addition of one equivalent of a halide scavenger to generate the cationic gold(I) complex, followed by the addition of five equivalents of iodobenzene. With the [(P,N)Indene]AuCl, the oxidative addition of iodobenzene didn't occur and the cationic complex decomposes overtime. The same result was obtained with different halide abstractors.

With the commercially available DavePhos ligand, on the other hand, instantaneous decomposition of the gold complex was observed (gold mirror) even with NTf_2^- as the counter anion. This demonstrates the importance of the nitrogen position with respect to gold and the necessity of a rigid backbone.

Instantaneous color change to bright yellow was observed upon addition of the halide scavenger and iodobenzene to the (P-Quinoline)AuCl complex, indicating a possible Au(I) → Au(III) transition. Unfortunately, the gold(III) complex stemming from the oxidative addition of phenyl iodide was not unambiguously detected due to the formation of side products.

With the above-selected ligands, the oxidative addition of iodobenzene was not feasible or the resulting gold(III) complexes were highly unstable at room temperature.

2.4.4 Influence of the Counter Anion on the Oxidative Addition Reaction

To this extent, we have in hands a readily available (P,N) gold(I) complex capable of activating the C-I bond of iodobenzene at room temperature. With NTf_2^- as counter anion, the reaction is complete after 48h at room temperature.

In the objective of increasing the rate of the oxidative addition process while maintaining mild conditions, non-coordinating counter anions were then tested. Interestingly, we found that silver hexafluoroantimonate influences significantly the reaction rate. With SbF_6^-, which is less coordinating than NTf_2^-, oxidative addition of iodobenzene (1 eq.) occurs instantaneously, and the gold(III) complex **12** is obtained as sole product (Scheme 2.26). This result suggests that the first step of the oxidative addition process is the displacement of the counter anion by iodobenzene to form an adduct with the gold center.

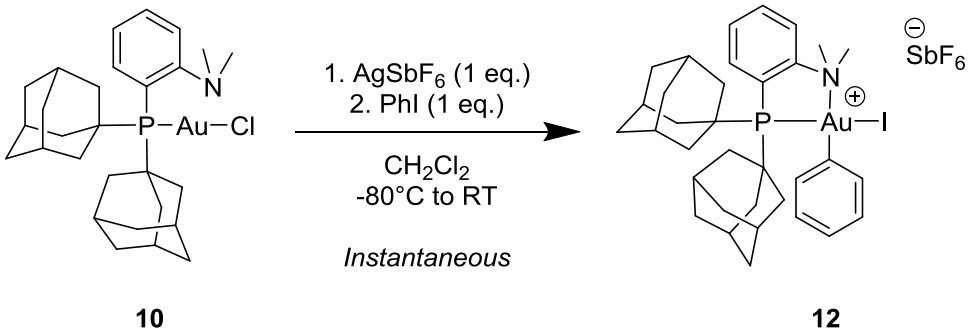

Scheme 2.26 Synthesis of gold(III) complex **12** by oxidative addition of iodobenzene.

The mechanism of the reaction was examined computationally to understand better the impact of the counter anion and the key role of the MeDalphos ligand on the oxidative addition process. In collaboration with the group of Dr. Karinne Miqueu, DFT calculations were carried out with the real complex **10** taking into account the counter anion and solvent effects (dichloromethane). The first step of the reaction is the displacement of the weakly coordinating counter anion SbF_6^- by iodobenzene to form the linear two-coordinate I-adduct (no coordination of nitrogen to gold d_{Au-N} = 2.863 Å) which is slightly downhill in energy (ΔG = -3.0 kcal/mol). The oxidative addition then proceeds with a low activation barrier ($\Delta G^{\ddagger}$ = 11.2 kcal/mol) *via* the 3-center transition state, in agreement with the mild conditions under which the reaction occurs experimentally. The geometric features of $\mathbf{TS_1}$ indicate a short C_{ipso} to gold distance (2.489 Å *vs.* 3.414 Å in the corresponding I-adduct) with an elongation of the C-I bond (2.438 Å *vs.* 2.184 Å in the corresponding I-adduct). The nitrogen atom of the ligand gets closer to the gold center (d_{Au-N} = 2.670 Å). The process is thermodynamically favorable ($\Delta G_{10\text{-}SbF6 \rightarrow 12}$ = -8.9 kcal/mol or $\Delta G_{I\text{-}adduct \rightarrow 12}$ = -5.9 kcal/mol) and leads to the four-coordinate gold(III) complex **12** we obtained experimentally (Figure 2.8).

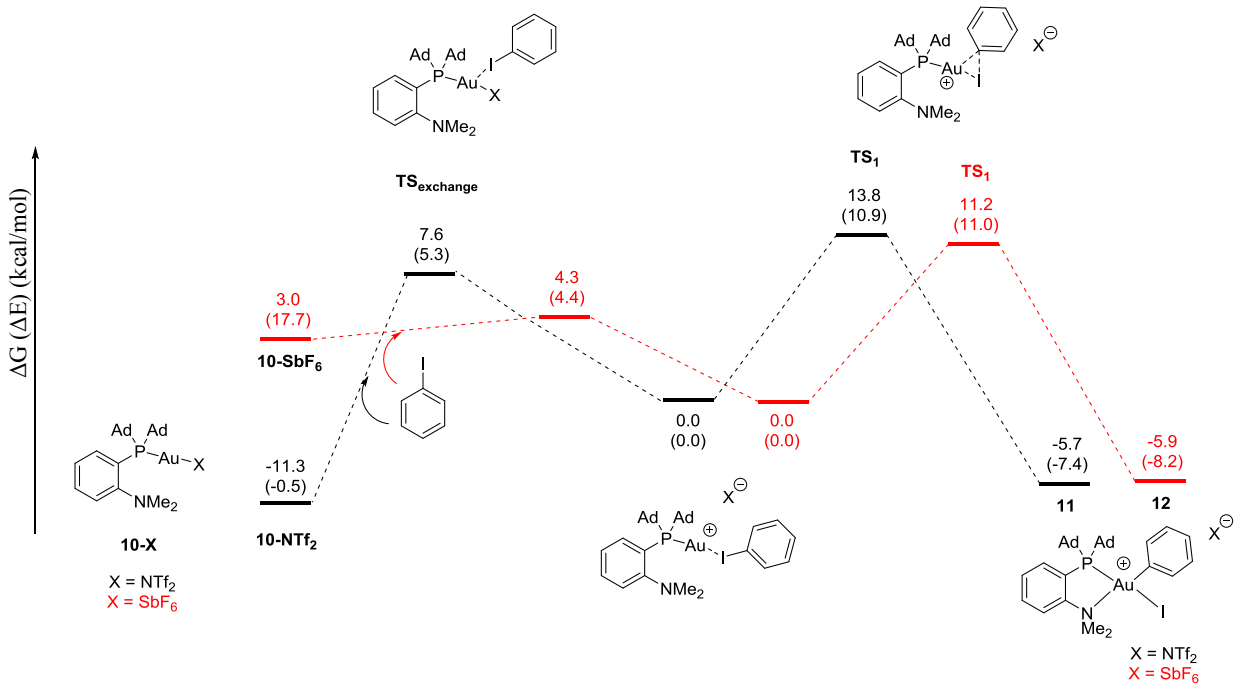

Figure 2.8 Energy profile computed in solvent (SMD model: dichloromethane) at the B97D(SMD-DCM)/SDD+f(Au),SDD(I,Sb),6.31G** (other atoms) level of theory for the oxidative addition of PhI to complex **10-NTf$_2$** (profile in black) and **10-SbF$_6$** (profile in red). Electronic energy (ΔE) including ZPE correction into brackets and Gibbs free energy (ΔG) in kcal/mol. All energies referred to the I-adduct.

In comparison, NTf_2^- coordinates more strongly the gold(I) center ($\Delta G_{10\text{-}NTf2 \rightarrow I\text{-adduct}}$ = 11.3 kcal/mol). Its displacement by iodobenzene requires an activation barrier ($\Delta G^{\ddagger}$ = 18.9 kcal/mol) which is even higher than that of the oxidative addition step ($\Delta G^{\ddagger}$ = 13.8 kcal/mol). This explains perfectly the strong counter anion effect observed experimentally (the reaction rate is significantly slower with NTf_2^- than SbF_6^-). It is noteworthy that the formation of the other gold(III) diasteromer with the phenyl ring in *cis* position to nitrogen was also investigated theoretically: the reaction is less favored thermodynamically and requires a higher activation barrier.

Finally, to further analyze the impact of the adjacent nitrogen atom, the reaction profile for the oxidative addition of iodobenzene to bis(1-adamantyl)phenyl phosphine gold(I) chloride was computed (Figure 2.9). The transformation is still kinetically feasible, but the activation barrier is twice as large. On the other hand, as expected, the reaction without the adjacent

NMe_2 group is not favored thermodynamically due to the formation of a high-energy three-coordinate gold(III) complex. This comparison highlights the crucial role of the hemi-labile MeDalphos ligand that not only lowers the activation barrier for oxidative addition but also stabilizes the resulting gold(III) specie by nitrogen coordination.

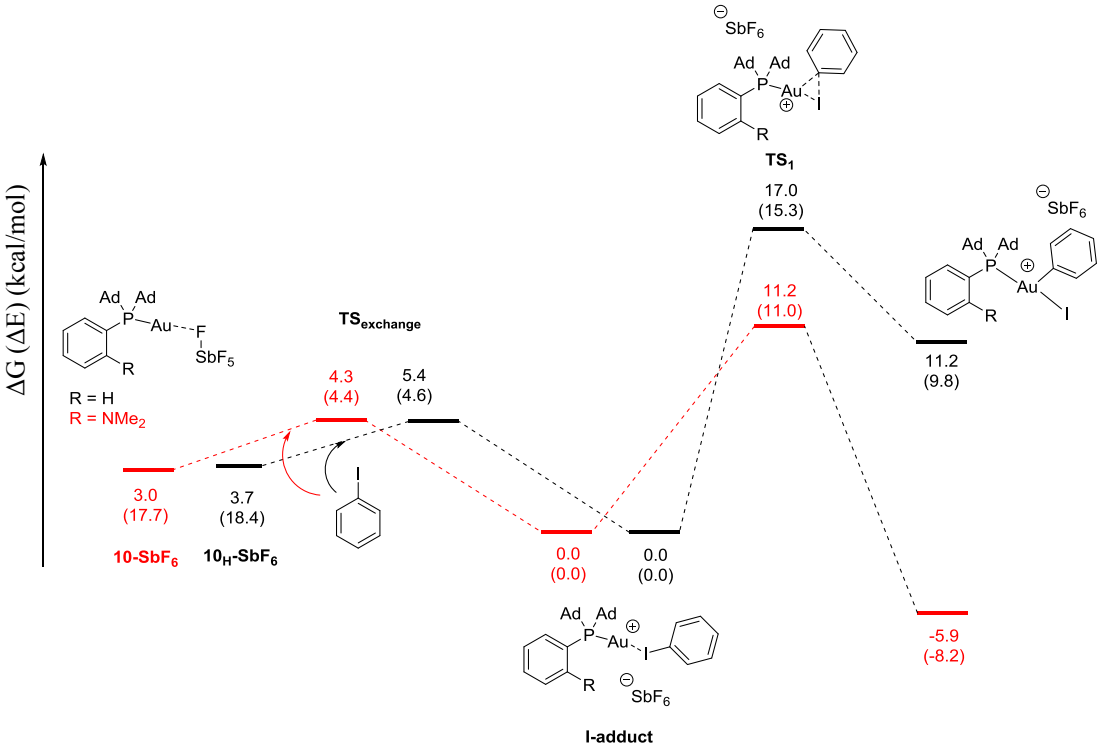

Figure 2.9 Energy profile computed in solvent (SMD model: dichloromethane) at the B97D(SMD-DCM)/SDD+f(Au),SDD(I,Sb),6.31G** (other atoms) level of theory for the oxidative addition of PhI to the model complex **10-H** devoid of NMe_2 group (profile in black) and **10-SbF$_6$** (profile in red) for comparison. Electronic energy (ΔE) including ZPE correction into brackets and Gibbs free energy (ΔG) in kcal/mol. All energies referred to the I-adduct.

2.4.5 Influence of Phosphorus Substituents on the Oxidative Addition Reaction

After improving the reaction rate of the oxidative addition with the use of SbF_6^- as counter anion, we investigated the influence of the substitution pattern of the phosphorus donor arm while maintaining the *o*-dimethylaniline backbone.

In addition to gold(I) chloride complex **10** featuring adamantyl substituents at the phosphorus atom, two other members of this series were prepared: complex **13** with phenyl substituents

and complex **14** with isopropyl substituents. With these two complexes in hands, oxidative addition of iodobenzene after chloride abstraction with $AgSbF_6$ was tested (Scheme 2.27).

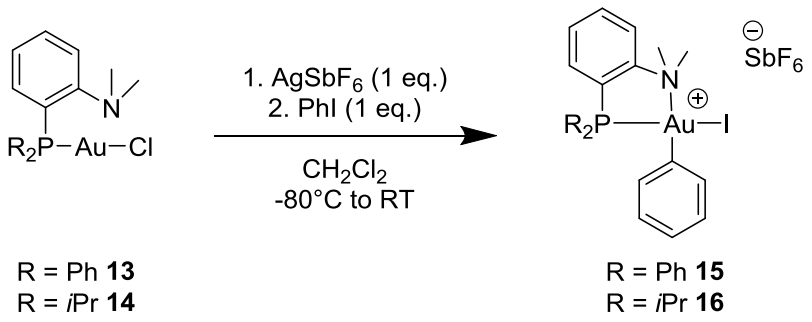

R = Ph **13**
R = *i*Pr **14**

R = Ph **15**
R = *i*Pr **16**

Scheme 2.27 Oxidative addition of iodobenzene with complexes **13** and **14**.

The addition of iodobenzene to complex **13** resulted in a quick color change to bright yellow suggesting a possible Au(I)/Au(III) transition. Unfortunately, the gold(III) complex **15** was not unambiguously detected by NMR spectroscopy due to the instability of the desired species, and rapid decomposition at room temperature to unidentified products. Changing the phosphorus substituents from phenyl to the more electron-donating isopropyl groups had a strong impact on the oxidative addition reaction. This time, with complex **14**, the oxidative addition of iodobenzene resulted in the formation of the stable gold(III) complex **16** that was identified by $^{31}P\{^1H\}$ and ^1H NMR. Moreover, full conversion was achieved after 45 minutes at room temperature.

These results are in line with the electron-donating properties of the ligands. With the more electron-donating adamantyl substituents on phosphorus, the oxidative addition of iodobenzene is instantaneous whereas with the less donating isopropyl substituents the reaction is complete after 45 minutes. And the impact of phosphorus substituents on the stability of the formed gold(III) complexes is very pronounced: with phenyl substituents, very fast decomposition was observed at room temperature, whereas with adamantyl and even

isopropyl substituents, the gold(III) complexes stemming from oxidative addition of phenyl iodide were found to be highly stable at room temperature.

2.4.6 Oxidative Addition to Complex 10: Scope and Limitations

2.4.6.1 Characterization of Au(III) Species Stemming From the Oxidative Addition of Aryl Iodides

After inspecting the impact of the counter anion and phosphorus substituents on the oxidative addition of iodobenzene with complex **10**, we were interested to study the behavior of (MeDalphos)AuCl towards aryl iodides bearing electron-donating or electron-withdrawing groups. So in addition to iodobenzene, the oxidative addition of 4-iodoanisole and 1-iodo-4-nitrobenzene was tested (Scheme 2.28).

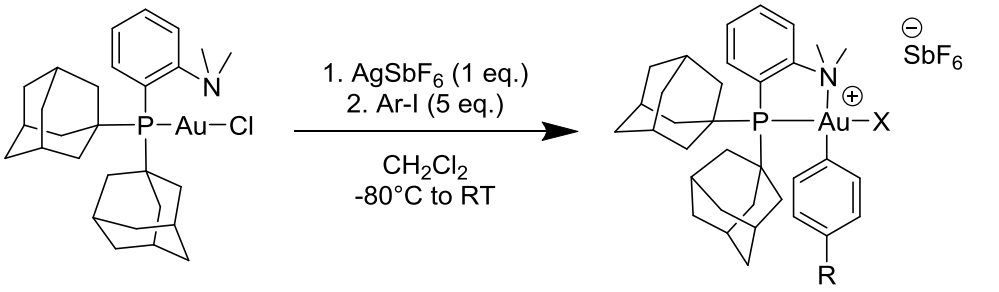

10

Scheme 2.28 Synthesis of gold(III) complexes **17** and **18** *via* oxidative addition.

Instantaneous reactions were observed with *p*-methoxy and *p*-nitro iodobenzenes. Moreover, on the basis of $^{31}P\{^{1}H\}$ NMR, full conversion was achieved for both substrates: **17** and **18** feature a singlet resonance at δ 75.1 and δ 79.7 ppm, respectively. The coordination of nitrogen to the gold(III) center is indicated by the downfield shift of the ^{1}H NMR signal for

the -N(CH_3)$_2$ substituents (from 2.5 ppm to 3.5 ppm). Surprisingly, high resolution mass spectrometry (ESI+) of aliquots taken directly from both reaction media revealed the presence of the expected gold(III)-aryl iodide complex, but also of the corresponding gold(III)-aryl chloride complexes. In fact, after oxidative addition, the iodide was probably replaced by a chloride coming from the solvent (dichloromethane) or the silver salts (AgCl) generated during the reaction. This halogen exchange was also confirmed in the solid state by means of single X-ray diffraction (Figure 2.10 – 2.11).

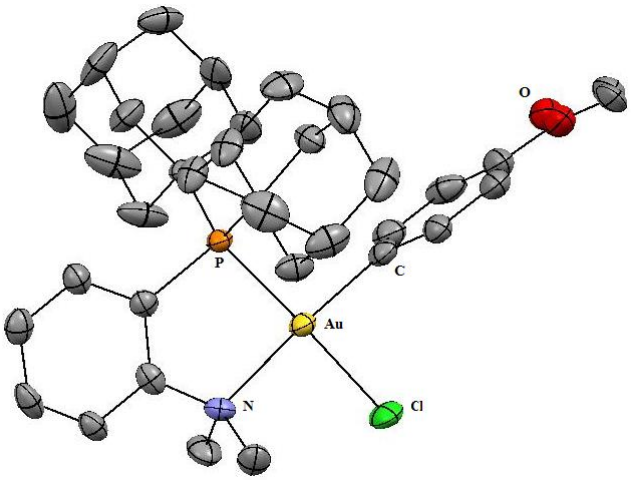

Figure 2.10 Molecular structure of complex **17'** determined by single X-ray crystallography. Hydrogen atoms and the SbF_6 counter anion were omitted for clarity. Selected bond lengths [Å] and angles [°]: AuN 2.190(5), AuP 2.3159(16), AuC 2.3333(16), PAuN 85.80(14).

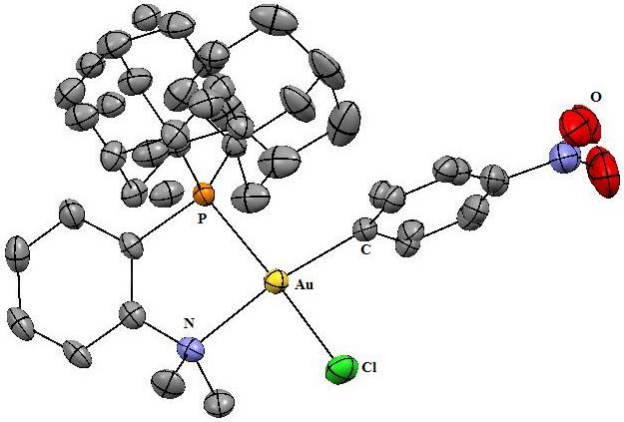

Figure 2.11 Molecular structure of complex **18'** determined by single X-ray crystallography. Hydrogen atoms and the SbF_6 counter anion were omitted for clarity. Selected bond lengths [Å] and angles [°]: AuN 2.187(5), AuP 2.3174(16), AuC 2.030(6), PAuN 86.18(14).

This halogen exchange after oxidative addition is undetectable by NMR (one signal in ^{31}P NMR despite the presence of the two complexes) suggesting a fast swap between iodide and chloride in solution or that both halogens have the same electronic impact on the phosphorus atom in *trans* position in our case.

Facile exchange of iodide for chloride at gold(III) was also reported recently by the group of Toste during the study of the reductive elimination step from different gold(III) complexes.(46) In fact, thermodynamic studies performed by Toste *et al.* revealed that the Au(III)-X bond strength increases in the order X = I < Br < Cl (the Au(III)-I bond is roughly 33 kcal/mol weaker than the Au(III)-Cl for the same complex).

Several tests were carried out in order to avoid the halogen exchange reaction and to determine the chloride source. But unfortunately, the high resolution mass spectrometry revealed every time the presence of both gold(III)-I and gold(III)-Cl species.

So, in order to characterize the gold(III)-I species, one equivalent of tetrabutylammonium iodide was added at room temperature after the oxidative addition of iodobenzene (Scheme 2.29).

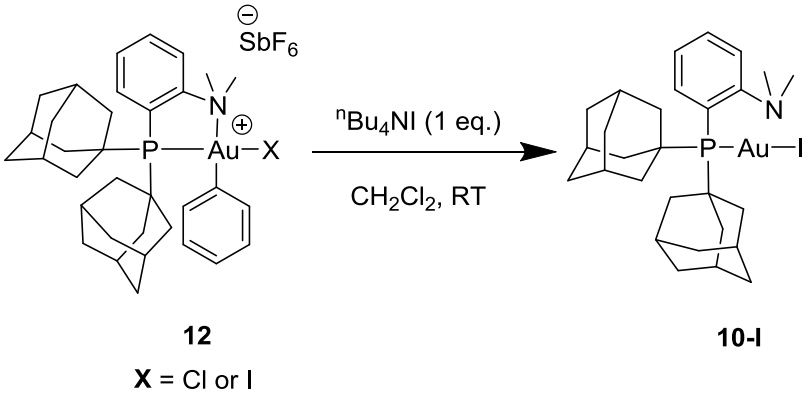

Scheme 2.29 Reductive elimination from Au(III) complex **12** triggered by $^{n}Bu_4NI$.

Surprisingly, after the addition of $^{n}Bu_4NI$, a color change was observed (from bright yellow to colorless) and the $^{31}P\{^{1}H\}$ NMR showed one singlet (δ 59.4 ppm) in the zone of gold(I) complexes. The ^{1}H NMR confirmed the formation of the Au(I) complex **10-I** (upfield shift from 3.5 ppm to 2.5 ppm for the -N(CH_3)$_2$ substituents). The nature of the halogen

coordinated to this gold(I) complex was confirmed by HRMS (ESI+). The formation of complex **10-I** can be explained by a fast and quantitative reductive elimination reaction triggered by the addition of $^{n}Bu_4NI$.

After this result, we then turned to characterize the Au(III)-Cl complex. One equivalent of tetrabutylammonium chloride was added at room temperature to completely convert complex **12** in the corresponding gold(III)-chloride which was isolated in 80% yield and was fully characterized. High resolution mass spectrometry (ESI+) confirmed the conversion of all the Au(III)-I to the desired Au(III)-Cl species. This complex exhibited high stability in solution and no sign of reductive elimination was observed over time.

2.4.6.2 Oxidative Addition of Aryl Halides

Although we are aware of this halogen exchange process after oxidative addition, the presentation of gold(III) complexes with an iodide coordinated to gold will be used in this manuscript to avoid confusions. Moreover, even though the addition of tetrabutylammonium chloride is an efficient method to obtain exclusively the gold(III)-Cl species, this strategy was only applied for the iodobenzene substrate.

Complex **10** was found to readily react with a series of aryl iodides (Scheme 2.30). Instantaneous reactions were observed with *p*-substituted iodobenzenes featuring electron-donating as well as electron-withdrawing substituents. More sterically hindered *ortho*-substituted substrates such as iodonaphthalene and 2-iodo-5-nitrotoluene were also efficiently activated, although complete conversion requires one hour in those cases. In addition, the scope of aryl iodides was extended to very electron-poor substrates such as iodopentafluorobenzene and the oxidative addition is complete and quantitative after three hours and a half at room temperature. Iodoheteroarenes such as 2-iodopyridine were also

compatible with the oxidative addition reaction. Competitive nitrogen coordination to the cationic gold(I) complex after chloride abstraction was observed and resulted in slowing the process: complete conversion was reached after three days at room temperature.

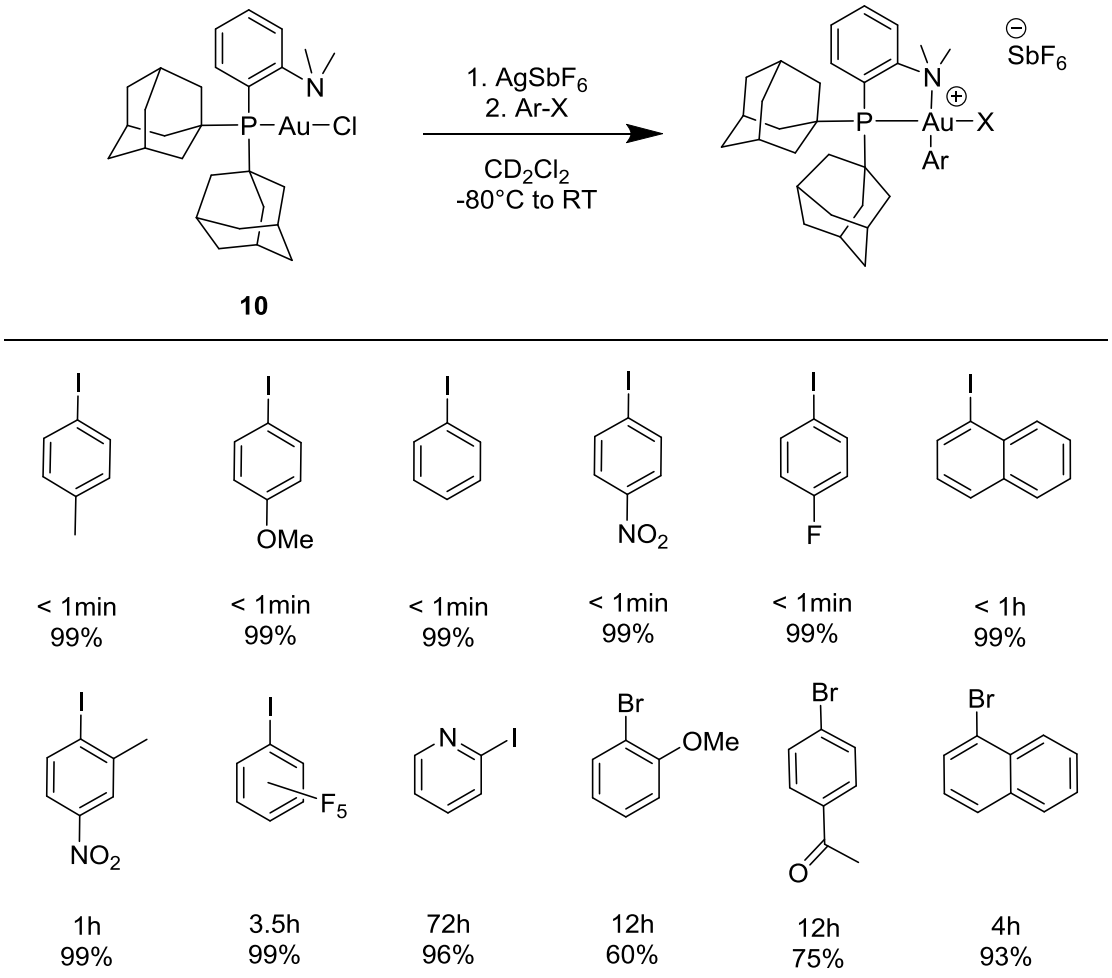

Scheme 2.30 Oxidative addition of aryl halides to complex **10** (with reaction time to reach complete conversion and spectroscopic yields based on ^{31}P NMR).

Remarkably, oxidative addition of aryl bromides was also demonstrated for the first time with gold thanks to the (MeDalphos) ligand. The activation of the more challenging Csp^2-Br bond works well with both electron-rich and electron-poor substrates as demonstrated by the *p*-acetyl and *o*-methoxy bromobenzenes. With extended reaction times (4 to 12h), good to high yields (60 to 93%) were obtained for aryl bromides. DFT calculations were also carried out

for the oxidative addition of aryl bromides and were in agreement with the experimental observations. The activation of Csp^2-Br bond proceeds with slightly higher activation barriers but the overall process remains thermodynamically favorable. All the gold(III)-aryl complexes demonstrated high stability in solution and in the solid state which allowed us to characterize these complexes by ^1H and ^{31}P NMR spectroscopy at room temperature (some of the complexes were also characterized by ^{13}C and X-ray diffraction analysis) and high resolution mass spectroscopy (ESI+). Unfortunately, under the same reaction conditions and with several aryl chlorides, the oxidative addition of Csp^2-Cl bond was not achieved and remained a challenge for gold chemistry.

2.4.6.3 Oxidative Addition of Biphenylene

After having achieved the activation of Csp^2-I and Csp^2-Br bonds, the C-C bond oxidative addition of biphenylene to complex **10** was tested. (MeDalphos)AuCl was reacted with silver hexafluoroantimonate at low temperature in order to generate a free coordination site and to increase the electrophilicity at the metal center, and biphenylene was added in dichloromethane (Scheme 2.31).

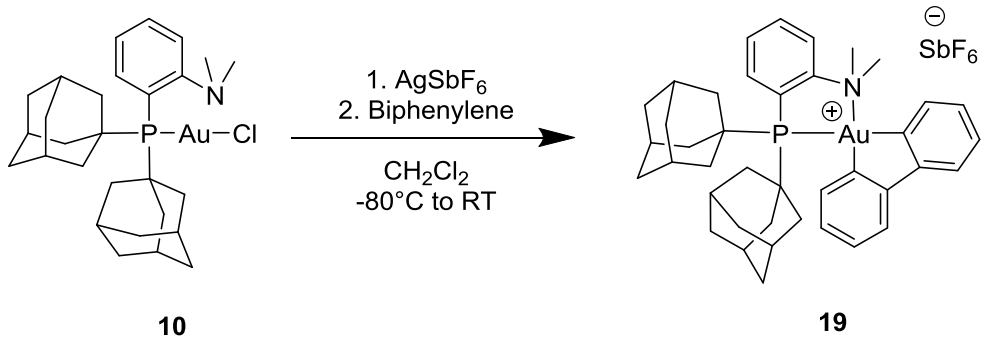

10 **19**

Scheme 2.31 Synthesis of dibenzoaurole **19** by oxidative addition of biphenylene to gold(I).

After two hours at room temperature, the ^{31}P NMR monitoring of the reaction indicated full conversion of complex **10** into the desired complex **19**. Unlike the (P,P) ligand, desymmetrization of the dibenzoaurole was observed with the (P,N) ligand. Indeed, the $^{13}C\{^{1}H\}$ NMR spectroscopy revealed the presence of two doublets at δ 172.6 and 154.4 ppm with coupling constants of 116.3 and 3.6 Hz respectively, which are typical of *trans* and *cis* coupling to phosphorus. Moreover, using the hydrogen atoms of -N(CH_3)$_2$ substituents as a probe for the oxidation state of the gold center, the ^{1}H NMR indicated the presence of one Au(III) species (downfield shift from 2.5 ppm to 3.7 ppm). The proposed structure is further corroborated by HRMS (ESI+) and X-ray diffraction analysis (Figure 2.12).

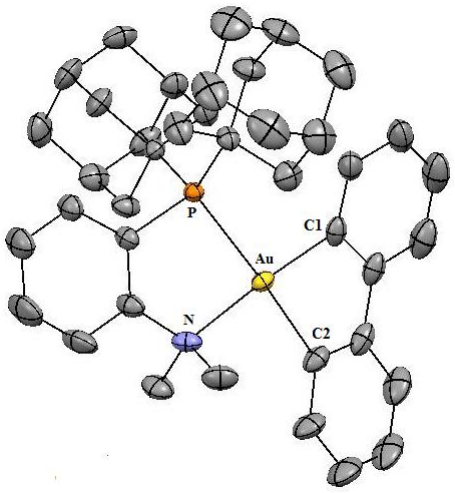

Figure 2.12 Molecular structure of complex **19** determined by single X-ray crystallography. Solvent molecules and hydrogen atoms were omitted for clarity. Selected bond lengths [Å] and angles [°]:AuN 2.207(2), AuP 2.4188(6), AuC1 2.048(3), AuC2 2.101(3), PAuN 82.96(6).

Besides generalizing this transformation to simpler and readily available gold(I) species, the MeDalphos complex **10** also displays an enhanced reactivity compared to the *o*-carborane complex **6**. As previously mentioned, the oxidative addition of biphenylene to the (P,P) complex **6** is possible but requires five hours at 120°C whereas with complex **10** the reaction is complete within two hours at room temperature.

2.5 Conclusion

In conclusion, the results presented in this chapter provide unambiguous evidence for the oxidative addition of σ-Csp^2-I, σ-Csp^2-Br and σ-CC bonds to gold and prove that the intermolecular oxidative addition proceeding *via* concerted pathway is not excluded for gold(I) complexes. Thanks to a rational ligand design, we have in hands two gold(I) complexes that perform the oxidative addition reaction: an *o*-carborane based diphosphine complex with a small bite angle and a gold(I) complex featuring an hemi-labile (P,N) ligand.

Even though both complexes can undergo the oxidative addition, the (MeDalphos) gold chloride displayed enhanced reactivity. Moreover, a strong counter anion effect was observed on the reaction rate of the oxidative addition of aryl halides with complex **10**, whereas in the case of the *o*-carborane complex, the nature of the counter anion had little impact.

The *o*-carborane gold(I) complex activates the Csp^2-I bond easily and under mild conditions, but substrates bearing EWG required prolonged reaction time compared to the MeDalphos complex (for example, the reaction with 1-iodo-4-nitrobenzene is instantaneous with complex **10** whereas it takes 4 hours at room temperature to achieve full conversion with complex **6**). Moreover, with electron-poor substrates (like iodopentafluorobenzene), no reaction occurred with the carborane-based complex whereas with (MeDalphos)AuCl the reaction is complete after three hours and a half at room temperature.

Furthermore, the activation of Csp^2-Br bonds remained a challenge for complex **6**, but remarkably the intermolecular oxidative addition of aryl bromides was feasible for the first time with gold using complex **10**. The enhanced reactivity of MeDalphos complex was particularly striking for the oxidative addition of biphenylene as well.

Gold(III) complexes stemming from the oxidative addition with complex **10** displayed much higher stability compared to the carborane-based gold(III) complexes, which will allow us to inspect their reactivity and go beyond the oxidative addition step.

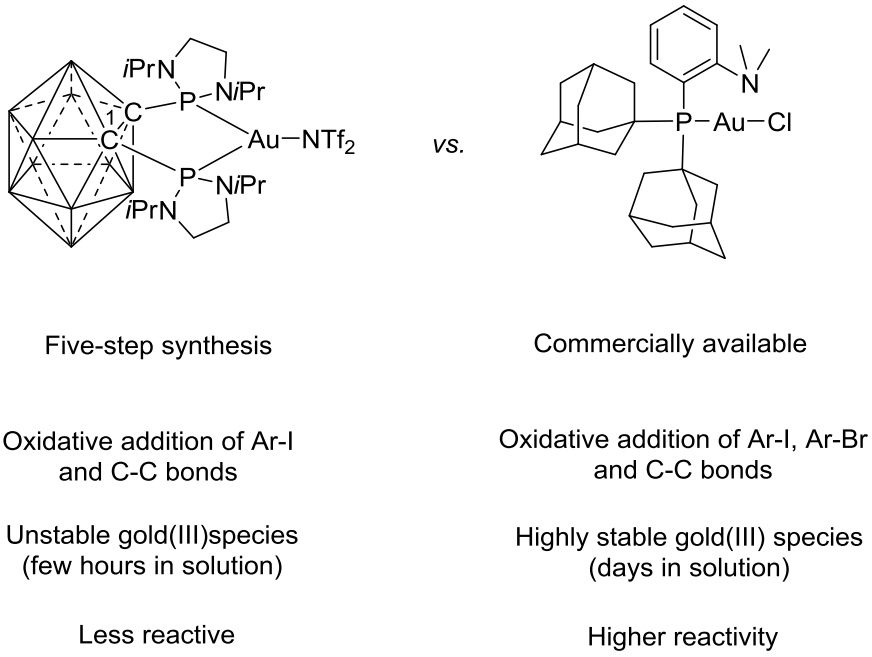

Scheme 2.32 Comparison between *o*-carborane diphosphine gold(I) and (MeDalphos)gold(I) complexes.

2.6 Experimental Part

2.6.1 General Remarks

(P,N)Indene, DavePhos and MorDalphos ligands are commercially available and were bought from Sigma Aldrich.

Dilithio-1,2-dicarba-closo-dodecarborane,[47] 2-chloro-1,3-diisopropyl-1,3,2-diazaphospholidine,[48] (P,N)Quinoline,[49],[(2 methylthio)phenyl]diphenylphosphine,[50,51] [2-(*tert*-butylthio)phenyl]diphenylphosphino,[50,51] 2-(diisopropylphosphanyl)-N,N-dimethyl amine,[52] and 2-(diphenylphosphanyl)-N,N-dimethyl amine[52] were prepared according to reported procedures.

2.6.2 Synthesis of 1,2-bis(diaminophosphino)-1,2-dicarba-*closo*-dodecarborane

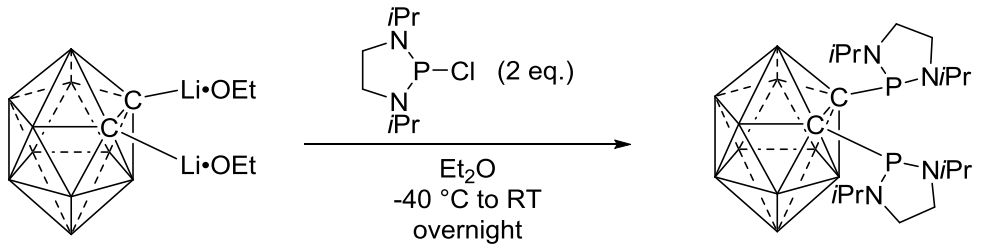

A solution of 2-chloro-1,3-diisopropyl-1,3,2-diazaphospholidine (140.5 mg, 0.67 mmol, 1 eq.) in diethyl ether (2 mL) was added to a solution of 1,2-dilithio-1,2-dicarba-*closo*-dodecaborane (102.5 mg, 0.33 mmol, 1 eq.)in diethyl ether (2 mL) at -40 °C *via* cannula transfer. The cannula was rinsed with additional diethyl ether (2 mL). The reaction mixture was stirred overnight and allowed to warm up to room temperature. Volatiles were removed *in vacuo*. The residue was redissolved in toluene and the resulting dispersion was filtered over celite. Volatiles were removed under vacuum. Yield: 120 mg (75 %).

Mp: 127–129 °C; **^{1}H NMR** (300 MHz, $CDCl_3$): δ 3.60 (m, 4H, C*H*$(CH_3)_2$), 3.32 (mbr, 4H, N(C*H*$_2$)$_2$N), 3.06 (mbr, 4H, N(C*H*$_2$)$_2$N), 1.20 (d, $^{3}J_{HH}$ = 6.6 Hz, 12H, CH(C*H*$_3$)$_2$), 1.10 (d, $^{3}J_{HH}$ = 6.5 Hz, 12H, CH(C*H*$_3$)$_2$), 1.4–3.4 (vbr, 10H, H_{BH}); **^{31}P{^{1}H} NMR** (121 MHz, $CDCl_3$): δ 114.2 (s); **^{11}B{^{1}H}** NMR (96 MHz, $CDCl_3$): δ -2.2, -7.7, -10.1, -12.5; **^{13}C{^{1}H}** NMR (100 MHz, $CDCl_3$): δ 89.9 (*pseudo* t, J_{CP} = 59.4 Hz, C_1), 50.0 (*pseudo* t, J_{CP} = 17.0 Hz, *C*H$(CH_3)_2$), 45.2 (*pseudo* t, J_{CP} = 3.5 Hz, N(*C*H$_2$)$_2$N), 22.5 (*pseudo* t, J_{CP} = 4.6 Hz, CH(*C*H$_3$)$_2$), 21.5 (*pseudo* t, J_{CP} = 2.1 Hz, CH(*C*H$_3$)$_2$); **HRMS (ESI+)**: calculated for $[M]^+ = C_{18}H_{47}B_{10}N_4P_2^+$: 489.4288. Found: 489.4278.

2.6.3 Synthesis of Complex 3

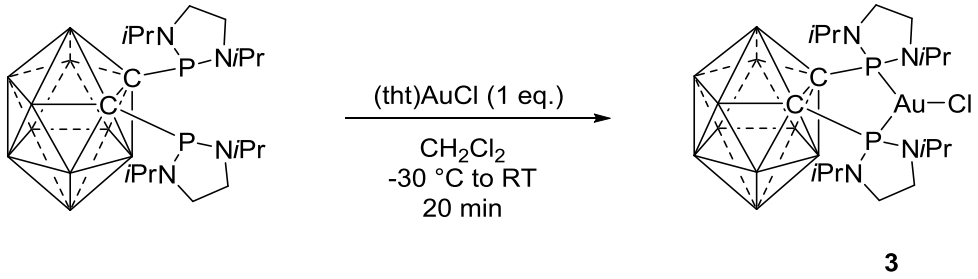

3

A solution of 1,2-bis(diaminophosphino)-1,2-dicarba-*closo*-dodecarborane (100 mg, 0.20 mmol) in dichloromethane (4 mL) was added to a solution of (THT)AuCl (65.6 mg, 0.20 mmol, 1 eq) in dichloromethane (4 mL) at -20 °C, stirred at this temperature for 5 minutes. After warming up to room temperature, volatiles were removed *in vacuo*. Yield: 127 mg (88 %).

Mp: 112–113 °C; **^{1}H NMR** (300 MHz, $CDCl_3$): δ 3.91 (sept, $^{3}J_{HH}$ = 6.6 Hz, 4H, C*H*$(CH_3)_2$), 3.26 (mbr, 4H, N(C*H*$_2$)$_2$N), 3.19 (mbr, 4H, N(C*H*$_2$)$_2$N), 1.23 (d, $^{3}J_{HH}$ = 6.6 Hz, 12H, CH(C*H*$_3$)$_2$), 1.19 (d, $^{3}J_{HH}$ = 6.6 Hz, 12H, CH(C*H*$_3$)$_2$), 1.6–3.7 (vbr, 10H, H_{BH}); **^{31}P{^{1}H} NMR** (121 MHz, $CDCl_3$): δ 116.6 (s); **^{11}B{^{1}H}** NMR (96 MHz, $CDCl_3$): δ -1.5, -6.8, -10.4; **^{13}C{^{1}H}** NMR (75 MHz, $CDCl_3$): δ 89.9 (*pseudo* t, $^{1}J_{CP}$ =28.2 Hz, C_1), 49.9 (*pseudo* t, $^{2}J_{CP}$ = 12.8 Hz, *C*H$(CH_3)_2$), 42.7 (s, N(*C*H$_2$)$_2$N), 21.6 (*pseudo* t, $^{3}J_{CP}$ = 3.7 Hz, CH(*C*H$_3$)$_2$), 20.7 (s, CH(*C*H$_3$)$_2$); **HRMS (ESI+)**: calculated for $[M]^+$ = $C_{18}H_{46}B_{10}N_4P_2Au^+$: 685.3875. Found: 685.3885.

2.6.4 Synthesis of Complex 6

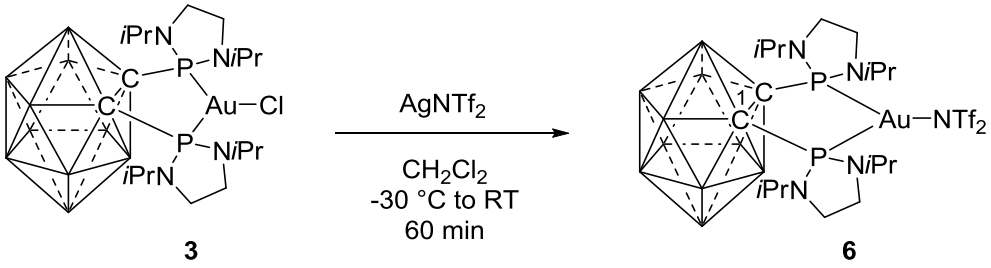

A solution of **3** (500 mg, 0.69 mmol) in dichloromethane (10 mL) was added to a dispersion of $AgNTf_2$ (269.1 mg, 0.69 mmol, 1 eq) in dichloromethane (5 mL) at -20 °C and stirred for 60 minutes under protection from light while slowly warming up to room temperature. The reaction mixture was filtered over a pad of celite to give a clear yellow filtrate. The filter frit was rinsed with dichloromethane (3 × 5 mL). Volatiles were removed *in vacuo*. The residue is washed with pentane (3 × 3 mL) and dried under vacuum to give **6** as a yellow powder that was of sufficient quality to be used without further purification. Yield: 600 mg (90 %). Crystals suitable for X-ray diffraction were obtained at -30 °C from a concentrated solution of **6** in dichloromethane layered with pentane.

Mp: 119–121 °C (decomposition); **^{1}H NMR** (300 MHz, $CDCl_3$): δ 3.90 (sept, $^{3}J_{HH}$ = 6.5 Hz, 4H, C*H*$(CH_3)_2$), 3.39 (mbr, 4H, N(C*H*$_2$)$_2$N), 3.23 (mbr, 4H, N(C*H*$_2$)$_2$N), 1.22 (d, $^{3}J_{HH}$ = 6.5 Hz, 12H, CH(C*H*$_3$)$_2$), 1.14 (d, $^{3}J_{HH}$ = 6.5 Hz, 12H, CH(C*H*$_3$)$_2$), 1.3–4.0 (vbr, 10H, H_{BH}); **^{31}P{^{1}H} NMR** (121 MHz, $CDCl_3$): δ 138.3 (s); **^{11}B{^{1}H}** NMR (96 MHz, $CDCl_3$): δ -2.3, -4.1, -10.3, -15.3; **^{13}C{^{1}H} NMR** (75 MHz, $CDCl_3$) δ 119.8 (q, $^{1}J_{CF}$ = 321.8 Hz, CF_3), 95.3 (*pseudo* t, $^{1}J_{CP}$ =24.7 Hz, C_1), 49.7 (*pseudo* t, $^{2}J_{CP}$ = 11.1 Hz, *C*H$(CH_3)_2$), 43.5 (m, N(*C*H$_2$)$_2$N), 42.6 (m, N(*C*H$_2$)$_2$N), 21.5 (sbr, CH(*C*H$_3$)$_2$), 20.9 (s, CH(*C*H$_3$)$_2$), 20.3 (s, CH(*C*H$_3$)$_2$), 20.0 (s, CH(*C*H$_3$)$_2$); **HRMS (ESI+)**: calculated for $[M]^+$ = $C_{18}H_{46}B_{10}N_4P_2Au^+$: 685.3875. Found: 685.3892.

2.6.5 Oxidative Addition with Complex 6

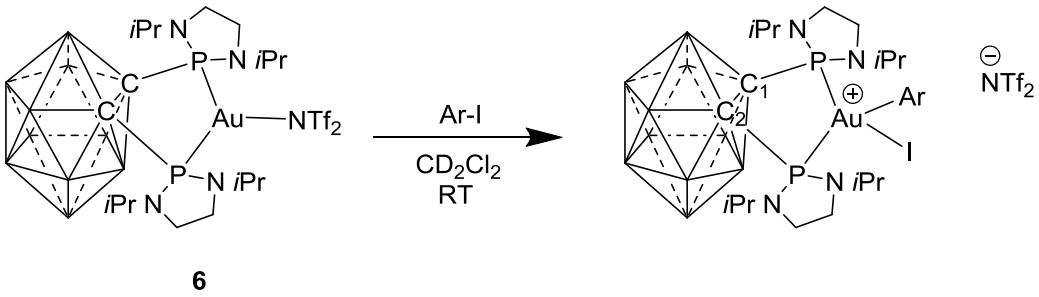

6

General Procedure for the Oxidative Addition of Aryl Iodides with Complex 6

In a glovebox, 15 mg of complex **5** (0.016 mmol, 1 eq.) was transferred into an NMR tube and solubilized with dichloromethane-d2 (0.6 mL), followed by addition of the aryl iodide (0.080 mmol, 5 eq.). The reaction was left to proceed until completion as monitored by 31P{1H}NMR. After complete conversion was reached, the formation of the gold(III) complex was further confirmed by ^{1}H NMR analysis and high resolution mass spectrometry (Electrospray ionization, positive ion mode).

Reaction of Complex 6 with Iodobenzene

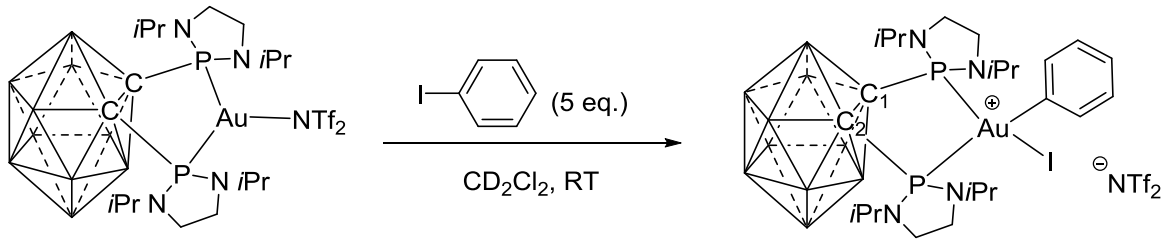

6

^{1}H NMR (300 MHz, CD_2Cl_2): δ 7.64–7.61 (m, H_4), 7.29–7.23 (m, H_6), 7.06–7.00 (m, H_5), 3.76–3.17 (m, 12H, N(C*H*$_2$)$_2$N, C*H*(CH$_3$)$_2$), 2.90–1.82 (m, 10H, H_{BH}), 1.48 (d, $^{3}J_{HH}$ = 6.6 Hz, 3H, CH(C*H*$_3$)$_2$), 1.37–1.10 (m, 18H, CH(C*H*$_3$)$_2$), 0.8 (d, $^{3}J_{HH}$ = 6.3 Hz, 3H, CH(C*H*$_3$)$_2$); **^{31}P{^{1}H} NMR** (121 MHz, CD_2Cl_2): δ 123.0 (d, $^{2}J_{PP}$ = 22.1 Hz, 1P), 82.2 (d, $^{2}J_{PP}$ = 22.1 Hz, 1P); **HRMS (ESI+)**: calculated for $[M]^+ = C_{24}H_{51}B_{10}N_4P_2IAu^+$: 890.3285. Found: 890.3317.

Reaction of Complex 6 with 4-Methoxyiodobenzene

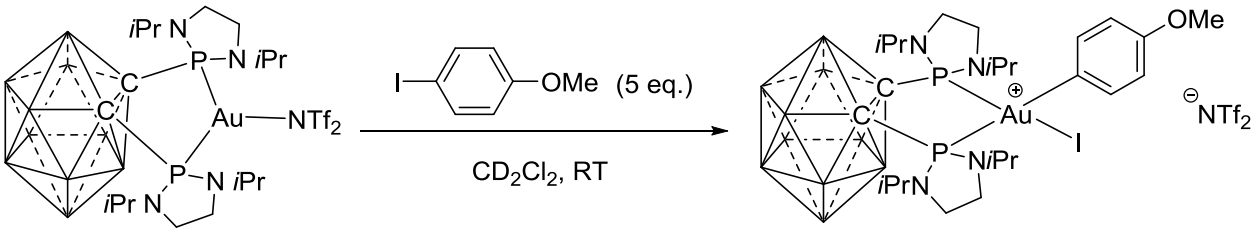

6

^{1}H NMR (300 MHz, CD_2Cl_2) : δ 7.35-7.29 (m, H_{ar}), 7.19-7.09 (m, H_{ar}), 7.00-6.82 (m, H_{ar}), 6.86-6.81 (m, H_{ar}), 3.70-3.28 (m, N(C*H*$_2$)$_2$N, C*H*(CH$_3$)$_2$, OC*H*$_3$), 3.05-1.67 (m, H_{BH}), 1.48 (d, $^{3}J_{HH}$ = 6.3 Hz, CH(C*H*$_3$)$_2$), 1.35-0.99 (m, CH(C*H*$_3$)$_2$), 0.83 (d, $^{3}J_{HH}$ = 6.3 Hz,CH(C*H*$_3$)$_2$); **^{31}P{^{1}H} NMR** (121 MHz, CD_2Cl_2): δ 123.7 (d, $^{2}J_{PP}$ = 21.7 Hz, 1P), 82.5 (d, $^{2}J_{PP}$ = 21.7 Hz, 1P); **HRMS (ESI+)**: calculated for $[M]^+ = C_{25}H_{53}B_{10}N_4OP_2IAu^+$: 919.34200. Found: 919.3442.

Reaction of Complex 6 with 4-Methyliodobenzene

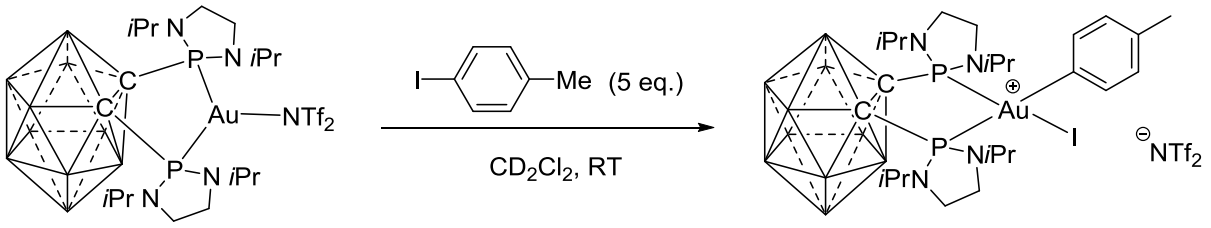

6

^{1}H NMR (300 MHz, CD_2Cl_2): δ 7.08 (d, J_{HH} = 8.4 Hz, 2H, H_{ar}), 6.90–6.82 (m, H_{ar}), 3.89–3.13 (m, 12H, N(CH_2)$_2$N, CH(CH$_3$)$_2$), 2.95–2.01 (m, 10H, H_{BH}), 2.24 (s, 3H, $H_{Ph\text{-}CH_3}$), 1.47 (d, $^{3}J_{HH}$ = 6.6 Hz, 3H, CH(CH_3)$_2$), 1.40–1.11 (m, 12H, CH(CH_3)$_2$), 0.80 (d, $^{3}J_{HH}$ = 6.6 Hz, 3H, CH(CH_3)$_2$); **^{31}P{^{1}H} NMR** (121 MHz, CD_2Cl_2): δ 123.8 (d, $^{2}J_{PP}$ = 22.4 Hz, 1P), 82.5 ($^{2}J_{PP}$ = 22.4 Hz, 1P). **HRMS (ESI+)**: calculated for $[M]^+$ = $C_{25}H_{53}B_{10}N_4P_2IAu^+$: 904.3442. Found: 904.3469.

Reaction of Complex 6 with 4- Iodoacetanilide

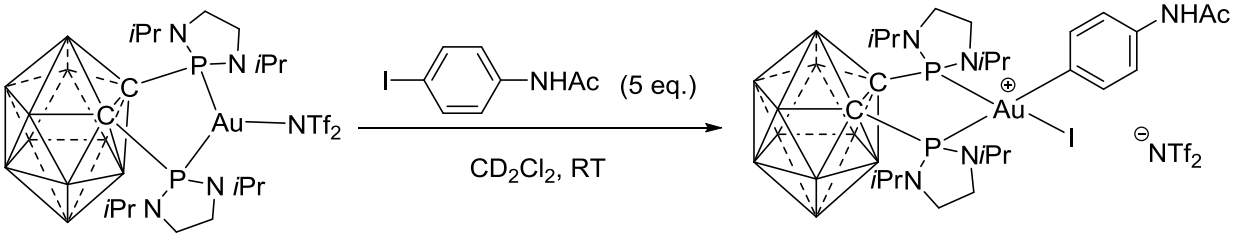

6

^{1}H NMR (300 MHz, CD_2Cl_2) : δ 8.08–7.82 (m, H_{ar}), 7.38–6.98 (m, H_{ar}), 7.19–7.09 (m, H_{ar}), 4.10–3.19 (m, N(CH_2)$_2$N, CH(CH$_3$)$_2$), 3.10–2.23 (m, H_{BH}), 2.77–2.07 (m, CO(CH_3)), 1.50 (d, $^{3}J_{HH}$ = 6.3 Hz, CH(CH_3)$_2$), 1.38–1.00 (m, CH(CH_3)$_2$), 0.85 (d, $^{3}J_{HH}$ = 6.3 Hz, CH(CH_3)$_2$); **^{31}P{^{1}H} NMR** (121 MHz, CD_2Cl_2): δ 123.2 (d, $^{2}J_{PP}$ = 21.8 Hz, 1P), 82.2 (d, $^{2}J_{PP}$ = 21.8 Hz, 1P); **HRMS (ESI+)**: calculated for $[M]^+$ = $C_{26}H_{54}B_{10}N_5P_2IOAu^+$: 947.3501. Found: 947.3513.

Reaction of Complex 6 with 4- Fluoroiodobenzene

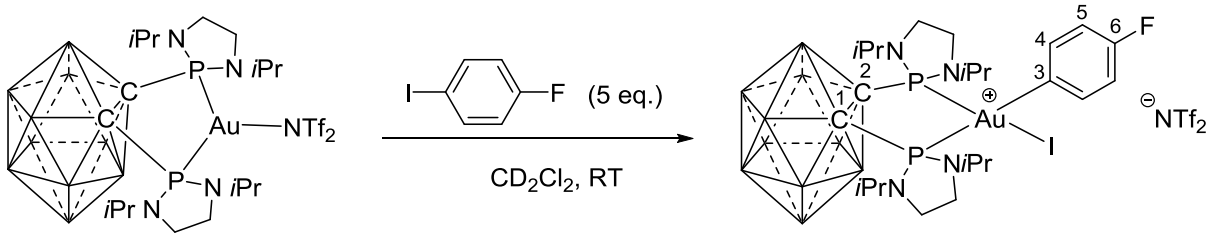

6

Alternatively to the general procedure in an NMR tube, this complex was synthesized and isolated according to the following procedure: 4-fluoroiodobenzene (7.7 mL, 0.067 mmol, 1 eq.) was added to a solution of **6** (65 mg, 0.067 mmol, 1 eq) in dichloromethane (4 mL) at room temperature. After stirring for 45 minutes at room temperature, the reaction mixture was concentrated *in vacuo* to a volume of about 1 mL. Upon addition of pentane (10 mL) a dark-yellow solid precipitates that was separated by cannula filtration. The residue was washed with pentane (3 x 2 mL) and dried under vacuum to give the desired product as a yellow powder. Yield: 76 mg (96 %).

^{1}H NMR (400 MHz, CD_2Cl_2, 253 K): δ 7.35 (m, $^{5}J_{HP}$ = 2.8 Hz, 2H, H_5), 7.15 (m, $^{4}J_{HP}$ = 3.6 Hz 2H, H_4), 3.77–3.28 (m, 12H, $N(CH_2)_2N$ & $CH(CH_3)_2$), 1.55 (d, $^{3}J_{HH}$ = 6.3 Hz, 6H, $CH(CH_3)_2$), 1.42 (d, $^{3}J_{HH}$ = 6.8 Hz, 6H, $CH(CH_3)_2$), 1.41 (d, $^{3}J_{HH}$ = 6.5 Hz, 6H, $CH(CH_3)_2$), 0.89 (d, $^{3}J_{HH}$ = 6.3 Hz, 6H, $CH(CH_3)_2$), 1.6–3.2 (vbr, 10H, H_{BH}); **^{31}P{^{1}H} NMR** (161 MHz, CD_2Cl_2, 253 K): δ 122.2 (dd, $^{2}J_{PP}$ = 20.1 Hz, $^{6}J_{PF}$ =3.1 Hz, 1P), 81.7 (dd, $^{2}J_{PP}$ = 20.1 Hz, $^{6}J_{PF}$ = 1.3 Hz, 1P); **^{19}F{^{1}H} NMR** (282 MHz, CD_2Cl_2): δ -79.0 (s, 6F, CF_3), -114.4 (dd, $^{6}J_{FP\text{-}trans}$ = 3.1 Hz, $^{6}J_{FP\text{-}cis}$ = 1.3 Hz, 1F); **^{13}C{^{1}H} NMR** (100 MHz, CD_2Cl_2, 253 K): δ 162.5 (dd, $^{1}J_{CF}$ = 246.5 Hz, $^{5}J_{CP\text{-}trans}$ = 3.0 Hz, C_6), 138.5 (dbr, $^{2}J_{CP\text{-}trans}$ = 162.0 Hz, $^{4}J_{CF}$ not resolved, C_3), 136.0 (m, $^{3}J_{CF}$ = 6.9 Hz, $^{3}J_{CP\text{-}trans}$ not resolved, C_4), 119.8 (q, $^{1}J_{CF}$ = 321.3 Hz, $N(SO_2CF_3)_2$), 117.4 (dd, $^{2}J_{CF}$ = 20.3 Hz, $^{4}J_{CP\text{-}trans}$ = 14.3, C_5), 88.1 (*virtual* dd, *N* = 27.0 Hz, 13.1 Hz, C_1 or C_2), 84.3 (*virtual* d, *N* = 20.1 Hz, C_1 or C_2), 50.1 (d, $^{2}J_{CP}$ = 8.8 Hz, $CH(CH_3)_2$), 49.7 (d, $^{2}J_{CP}$ = 12.0 Hz, $CH(CH_3)_2$), 43.0 (d, $^{2}J_{CP}$ = 3.3 Hz, $N(CH_2)_2N$), 42.4 (s, $N(CH_2)_2N$), 22.0 (d, $^{3}J_{CP}$ = 3.2 Hz, $CH(CH_3)_2$), 21.7 (d, $^{3}J_{CP}$ = 4.1 Hz, $CH(CH_3)_2$), 21.5 (d, $^{3}J_{CP}$ = 4.7 Hz, $CH(CH_3)_2$), 20.9 (d, $^{3}J_{CP}$ = 3.7 Hz, $CH(CH_3)_2$); **HRMS (ESI+)**: calculated for $[M]^+ = C_{24}H_{50}B_{10}P_2N_4FIAu^+$: 908.3190. Found: 890.3217.

Reaction of Complex 6 with 4- Nitroiodobenzene

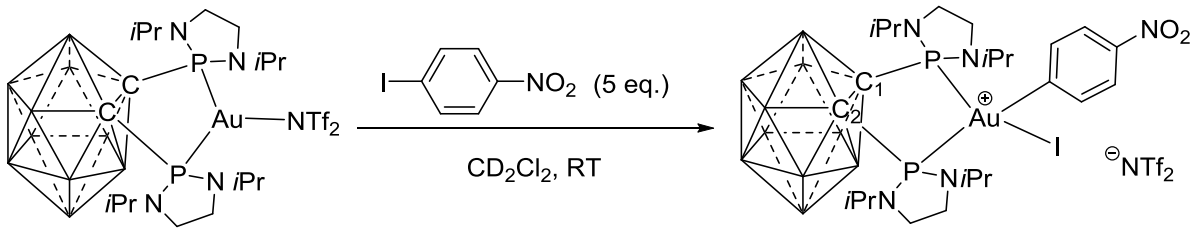

6

^{1}H NMR (500 MHz, CD_2Cl_2): δ 8.28-8.20 (m, 2H, H_{ar}), 7.66-7.60 (m, 2H, H_{ar}), 4.04-3.24 (m, 12H, N(CH_2)$_2$N, CH(CH$_3$)$_2$), 3.10-1.78 (m, 10H, H_{BH}), 1.61 (d, $^{3}J_{HH}$ = 6.5 Hz, 6H, CH(CH_3)$_2$), 1.50-1.45 (m, 12H, CH(CH_3)$_2$), 1.00 (d, $^{3}J_{HH}$ = 6.5 Hz, 6H, CH(CH_3)$_2$); **^{31}P{^{1}H} NMR** (121 MHz, CD_2Cl_2): δ 123.0 (d, $^{2}J_{PP}$ = 25.0 Hz, 1P), 87.0 (d, $^{2}J_{PP}$ = 25.0 Hz, 1P); **HRMS (ESI+)**: calculated for $[M]^+$ = $C_{24}H_{50}B_{10}N_5O_2P_2IAu^+$: 935.3136. Found: 935.3140.

Reaction of Complex 6 with 4-Cyanoiodobenzene

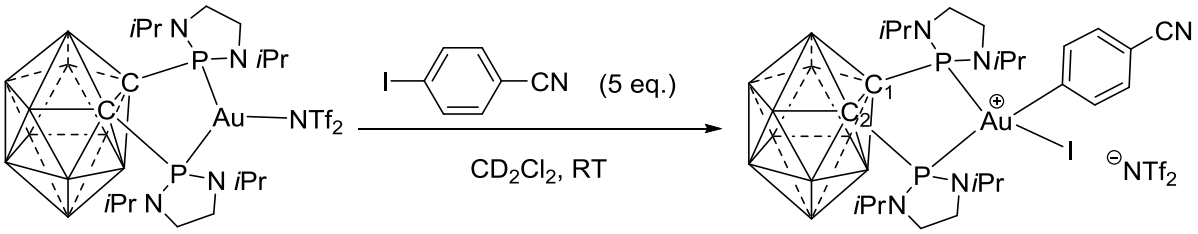

6

^{1}H NMR (300 MHz, CD_2Cl_2): δ 7.58-7.54 (m, 1H, H_{ar}), 7.46-7.38 (m, 1H, H_{ar}), 6.99-6.95 (m, 1H, H_{ar}), 3.91-3.17 (m, 12H, N(CH_2)$_2$N, CH(CH$_3$)$_2$), 2.98-1.65 (m, H_{BH}), 1.47 (d, $^{3}J_{HH}$ = 6.6 Hz, 3H, CH(CH_3)$_2$), 1.39-1.07 (m, 18H, CH(CH_3)$_2$), 0.85 (d, $^{3}J_{HH}$ = 6.6 Hz, 3H, CH(CH_3)$_2$); **^{31}P{^{1}H} NMR** (121 MHz, CD_2Cl_2): δ 118.6 (d, $^{2}J_{PP}$ = 18.7 Hz, 1P), 80.6 ($^{2}J_{PP}$ = 18.7 Hz, 1P); **HRMS (ESI+)**: calculated for $[M]^+$ = $C_{25}H_{50}B_{10}N_5P_2IAu^+$: 914.3267. Found: 914.3271.

Reaction of Complex 6 with 1-Iodonaphthalene

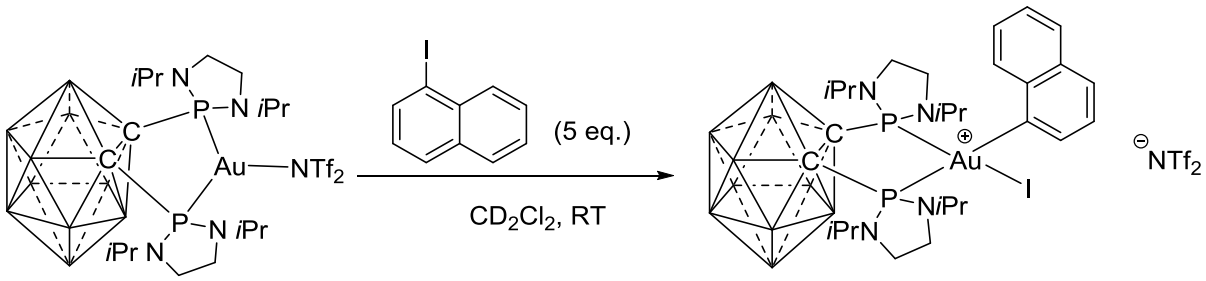

6

^{1}H NMR (300 MHz, CD_2Cl_2): δ 8.02–7.97 (m, H_{ar}), 7.80–7.67 (m, H_{ar}), 7.55–7.37 (m, H_{ar}), 7.14–7.06 (m, H_{ar}), 3.98–2.86 (m, 12H, $N(CH_2)_2N$, $CH(CH_3)_2$), 2.75–1.78 (m, 10H, H_{BH}), 1.64 (d, $^{3}J_{HH}$ = 6.6 Hz, 3H, $CH(CH_3)_2$), 1.58 (d, $^{3}J_{HH}$ = 6.3 Hz, 3H, $CH(CH_3)_2$), 1.52–1.40 (m, 9H, $CH(CH_3)_2$), 1.37–1.16 (m, 3H, $CH(CH_3)_2$), 0.99 (d, $^{3}J_{HH}$ = 6.3 Hz, 3H, $CH(CH_3)_2$), -0.71 (d, $^{3}J_{HH}$ = 6.3 Hz, 3H, $CH(CH_3)_2$); **^{31}P{^{1}H} NMR** (121 MHz, CD_2Cl_2): δ 122.7 (d, $^{2}J_{PP}$ = 24.0 Hz, 1P), 82.8 (d, $^{2}J_{PP}$ = 24.0 Hz, 1P); **HRMS (ESI+)**: calculated for $[M]^+ = C_{28}H_{53}B_{10}N_4P_2IAu^+$: 940.3444. Found: 940.3462

Reaction of Complex 6 with 1-Iodo-8-Methylnaphthalene

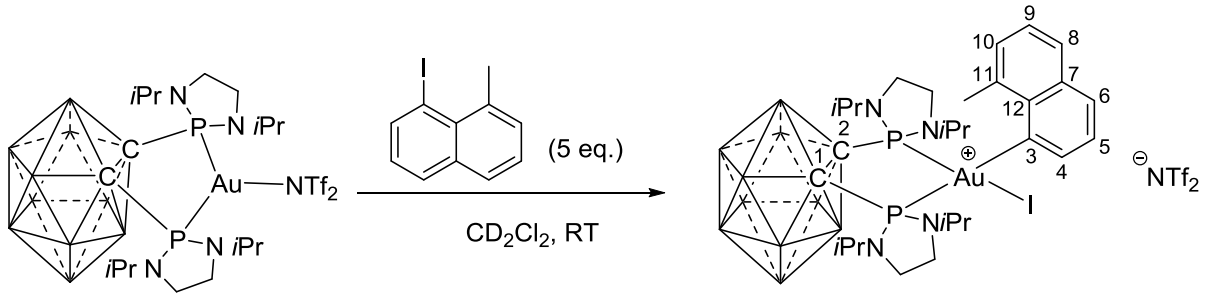

6

The gold(III) complex was synthesized and isolated according to the following procedure: A solution of 1-iodo-8-methylnaphthalene (8.3 mg, 0.03 mmol, 1 eq) in dichloromethane (2 mL) was slowly added to a solution of complex **6** (30 mg, 0.03 mmol) in dichloromethane (3 mL) at room temperature and stirred for 15 minutes. The reaction mixture turns immediately dark red. Volatiles were removed *in vacuo*. The residue was washed with pentane (3 x 2 mL) and dried under vacuum to give the desired product as a red solid. Yield: 34 mg (93 %).

Mp: 126–129 °C (decomposition); **^{1}H NMR** (500 MHz, CD_2Cl_2): δ 7.80 (d, J_{HH} = 7.9 Hz, 1H, H_{ar}), 7.72 (d, J_{HH} = 7.9 Hz, 1H, H_{ar}), 7.55–7.38 (m, 4H, H_{ar}), 4.05–2.95 (m, 8H, $N(CH_2)_2N$ & $CH(CH_3)_2$), 3.06 (s, 3H, naphthyl-CH_3), 1.69 (d, $^{3}J_{HH}$ = 10.4 Hz, 3H, $CH(CH_3)_2$), 1.64 (d, $^{3}J_{HH}$ = 10.4 Hz, 3H, $CH(CH_3)_2$), 1.63 (d, $^{3}J_{HH}$ = 10.4 Hz, 3H, $CH(CH_3)_2$), 1.58 (d, $^{3}J_{HH}$ = 6.3 Hz, 3H, $CH(CH_3)_2$), 1.52 (d, $^{3}J_{HH}$ = 6.3 Hz, 3H, $CH(CH_3)_2$), 1.50 (d, $^{3}J_{HH}$ = 6.3 Hz, 3H, $CH(CH_3)_2$), 1.14 (d, $^{3}J_{HH}$ = 6.6 Hz, 3H, $CH(CH_3)_2$),), 3.50–1.50 (vbr, 10H, H_{BH}), 1.50–1.25 (m, 8H, $N(CH_2)_2N$), -0.41 (d, $^{3}J_{HH}$ = 6.6 Hz, 3H, $CH(CH_3)_2$); **^{31}P{^{1}H} NMR** (121 MHz, CD_2Cl_2): δ 122.2 (d, $^{2}J_{PP}$ = 30.4 Hz, 1P), 81.7 (d, $^{2}J_{PP}$ = 30.4 Hz, 1P); **^{11}B{^{1}H} NMR** (96 MHz, CD_2Cl_2): δ -1.1, -9.4, -15.5; **^{13}C{^{1}H} NMR** (126 MHz, CD_2Cl_2): δ 137.9 (d, $^{3}J_{CP}$ = 11.6 Hz, C_{12}), 137.7 (d, $^{2}J_{CP\text{-}trans}$ = 157.0 Hz, C_3), 137.6 (d, $^{4}J_{CP}$ = 6.4 Hz, C_7 or C_{11}), 132.3 (d, $^{4}J_{CP}$ = 6.6 Hz, C_5), 131.7 (d, $^{4}J_{CP}$ = 4.6 Hz, C_7 or C_{11}), 130.5 (s, C_8 or C_9 or C_{10}), 129.8 (s, C_8 or C_9 or C_{10}), 129.1 (d, $^{5}J_{CP}$ = 2.3 Hz, C_6), 126.2 (s, C_8 or C_9 or C_{10}), 125.3 (d, $^{3}J_{CP}$ = 14.1 Hz, C_4), 120.0 (q, $^{1}J_{CF}$ = 319.8 Hz, $N(SO_2CF_3)_2$), 89.0 (*virtual* dd, *N* = 31.9 Hz, 9.5 Hz, C_1 or C_2), 85.6 (*virtual* dd, *N* = 17.2 Hz, 3.8 Hz, C_1 or C_2), 50.2 (d, $^{2}J_{CP}$ = 12.7 Hz, $CH(CH_3)_2$), 49.7 (d, $^{2}J_{CP}$ = 9.8 Hz, $CH(CH_3)_2$), 49.6 (d, $^{2}J_{CP}$ = 8.0 Hz, $CH(CH_3)_2$), 49.5 (d, $^{2}J_{CP}$ = 11.7 Hz, $CH(CH_3)_2$), 42.8 (d, $^{2}J_{CP}$ = 3.2 Hz, $N(CH_2)_2N$), 42.5 (s, $N(CH_2)_2N$), , 42.1 (s, $N(CH_2)_2N$), 40.7 (d, $^{2}J_{CP}$ = 2.5 Hz, $N(CH_2)_2N$), 29.9 (s, naphthyl-CH_3), 23.2 (d, $^{3}J_{CP}$ = 4.6 Hz, $CH(CH_3)_2$), 21.8 (d, $^{3}J_{CP}$ = 4.5 Hz, $CH(CH_3)_2$), 21.5 (d, $^{3}J_{CP}$ = 4.4 Hz, $CH(CH_3)_2$), 21.4 (d, $^{3}J_{CP}$ = 3.0 Hz, $CH(CH_3)_2$), 21.3 (d, $^{3}J_{CP}$ = 4.5 Hz, $CH(CH_3)_2$), 21.2 (d, $^{3}J_{CP}$ = 4.4 Hz, $CH(CH_3)_2$), 21.0 (d, $^{3}J_{CP}$ = 4.2 Hz, $CH(CH_3)_2$), 20.4 (d, $^{3}J_{CP}$ = 3.7 Hz, $CH(CH_3)_2$); **HRMS (ESI+)**: calculated for $[M]^+ = C_{29}H_{55}B_{10}P_2N_4IAu^+$: 954.3601. Found: 954.3621.

Reaction of Complex 6 with 2-Iodothiophene

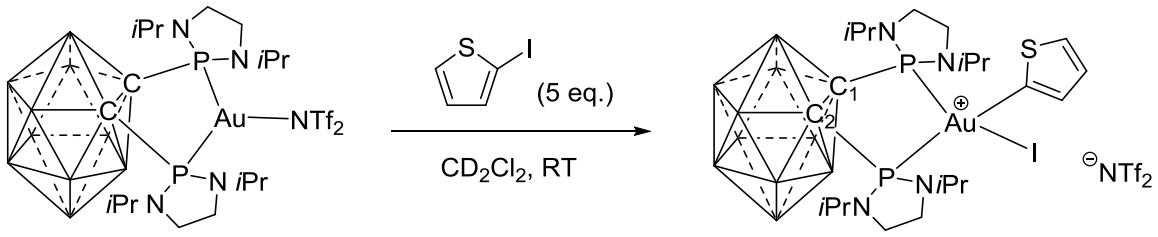

6

^{1}H NMR (300 MHz, CD_2Cl_2): δ 7.58-7.54 (m, H_{ar}), 7.35-7.27 (m, H_{ar}), 7.19-7.09 (m, H_{ar}), 7.04-6.94 (m, H_{ar}), 6.75-6.72 (m, H_{ar}), 3.67-3.35 (m, 12H, $N(CH_2)_2N$, $CH(CH_3)_2$), 3.20-1.68 (m, 10H, H_{BH}), 1.49 (d, $^{3}J_{HH}$ = 6.3 Hz, 6H, $CH(CH_3)_2$), 1.4-1.26 (m, 12H, $CH(CH_3)_2$), 0.82 (d, $^{3}J_{HH}$ = 6.3 Hz, 6H, $CH(CH_3)_2$); **^{31}P{^{1}H} NMR** (121 MHz, CD_2Cl_2): δ 116.3 (d, $^{2}J_{PP}$ = 13.5 Hz, 1P), 78.5 (d, $^{2}J_{PP}$ = 13.5 Hz, 1P); **HRMS (ESI+)**: calculated for $[M]^+ = C_{22}H_{49}B_{10}N_4P_2ISAu^+$: 896.2849. Found: 896.2867.

Reaction of Complex 6 with 2-Iodopyridine

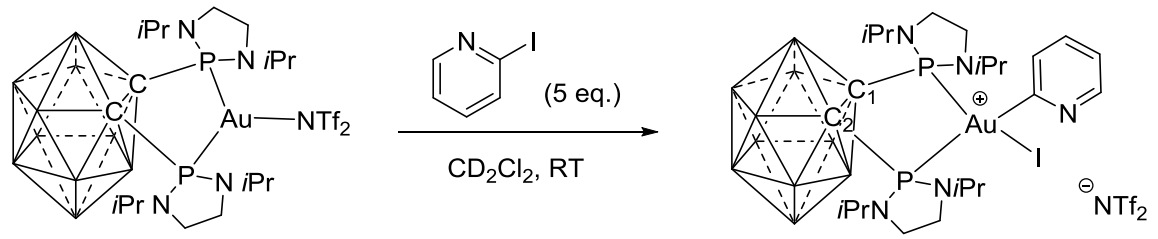

6

^{1}H NMR (300 MHz, CD_2Cl_2): 8.40-8.27 (m, H_{ar}), 7.72-7.50 (m, H_{ar}), 7.38-7.15 (m, H_{ar}), 6.75-6.72 (m, H_{ar}), 3.98-3.21 (m, $N(CH_2)_2N$, $CH(CH_3)_2$), 3.12-1.97 (m, H_{BH}), 1.50 (d, $^{3}J_{HH}$ = 6.3 Hz, $CH(CH_3)_2$), 1.39-1.04 (m, $CH(CH_3)_2$), 0.84 (d, $^{3}J_{HH}$ = 6.6 Hz, $CH(CH_3)_2$); **^{31}P{^{1}H} NMR** (121 MHz, CD_2Cl_2): δ 123.0 (d, $^{2}J_{PP}$ = 25.0 Hz, 1P), 87.0 (d, $^{2}J_{PP}$ = 25.0 Hz, 1P); **HRMS (ESI+)**: calculated for $[M]^+ = C_{23}H_{50}B_{10}N_5P_2IAu^+$: 890.3266. Found: 890.3286.

2.6.6 General Procedure for the Coordination of Au(I) to (P,L) Ligands

A solution of a (P,L) ligand (1eq.) in dichloromethane was added to a solution of $(Me_2S)AuCl$ (1 eq.) in dichloromethane at -20 °C, stirred at this temperature for 5 minutes. After warming up to room temperature, volatiles were removed *in vacuo* and the resulting solid was washed with pentane to yield the pure (P,L) gold(I) complex.

2.6.7 Synthesis of Complex 11

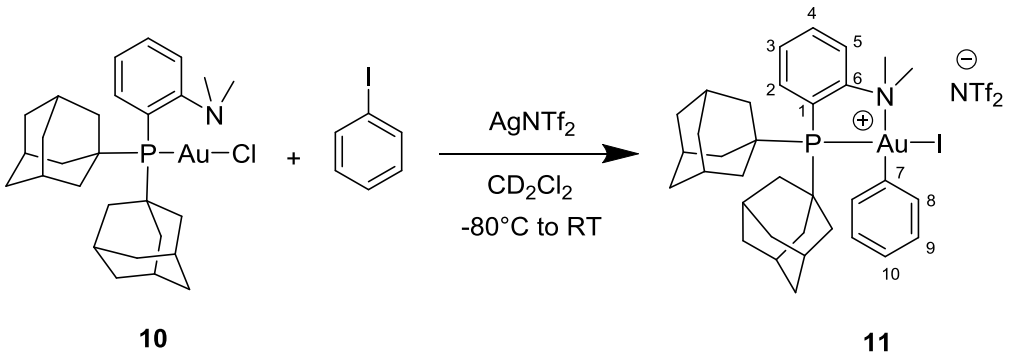

10 **11**

In a glovebox, a screw-cap NMR tube was charged with silver bis(trifluoromethanesulfonyl)imide (12.0 mg, 0.031 mmol) in dichloromethane-d^2 (0.3 mL). Complex **10** (20 mg, 0.031 mmol) was transferred into a small glass vial and dissolved in dichloromethane-d^2 (0.3 mL). The prepared solution was loaded into a plastic syringe equipped with stainless steel needle. Outside the glovebox, the NMR tube was cooled down to –80°C (Ethanol/N_2 cold bath). At this temperature, the solution of complex **10** was added to the $AgNTf_2$ solution. The tube was gently shaken and allowed to warm to RT. After formation of the cationic gold(I) complex **10/AgNTf$_2$**, iodobenzene (3.5 µL, 0.031 mmol) was added to the NMR tube at room temperature. The reaction was monitored by ^{31}P NMR spectroscopy. Complete conversion of **10/AgNTf$_2$** is observed after 48 h to give complex **11** (92 % NMR spectroscopic yield), along with unidentified species. Crystals suitable for X-ray diffraction were obtained directly from a concentrated solution of **11** in dichloromethane-d^2.

^{1}H NMR (300 MHz, CD_2Cl_2): δ 8.01-7.94 (m, 2H, H_{Ar}), 7.92-7.86 (m, 1H, H_{Ar}), 7.79-7.67 (m, 1H, H_{Ar}), 7.48-7.46 (m, 2H, H_{Ar}), 7.38-7.23 (m, 3H, H_{Ar}), 3.50 (s, 6H, N(C*H*$_3$)$_2$), 2.34-2.09 (m, 18H, H_{Ad}), 1.75 (s, 12H, H_{Ad}). **^{31}P{^{1}H} NMR** (121 MHz, CD_2Cl_2): δ 74.2 (s). **^{13}C{^{1}H} NMR** (126 MHz, CD_2Cl_2): δ 158.8 (d, J_{P-C} = 6.9 Hz, C_6), 137.0 (d, J_{P-C} = 2.3 Hz, C_5), 136.8 (d, J_{P-C} = 1.6 Hz, C_4), 135.2 (s, C_9), 130.5 (s, C_3), 130.4 (s, C_8), 128.3 (s, C_{10}), 127.7 (s, C_7), 125.6 (d, J_{P-C} = 7.3 Hz, C_2), 119.1 (d, J_{P-C} = 44.0 Hz, C_1), 53.9 (s, N(CH_3)$_2$), 48.2 (d, J_{P-C} = 13.6 Hz, C_{qtAd}), 40.7 (d, J_{P-C} = 1.3 Hz, CH_{2Ad}), 35.8 (d, J_{P-C} = 2.0 Hz, CH_{2Ad}), 28.9 (d, J_{P-C} = 9.8 Hz, CH_{Ad}). **HRMS (ESI+)**: calculated for [M^+] = $C_{34}H_{45}NPIAu^+$: 822.2000. Found: 822.2006. For [M'^+] = $C_{34}H_{45}NPClAu^+$: 730.2644. Found: 730.2657.

2.6.8 Synthesis of Complex 12

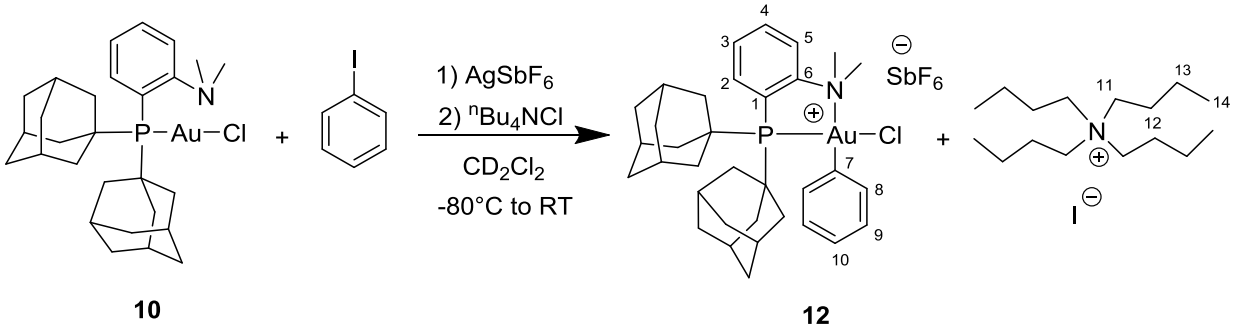

10 **12**

In a glovebox, a screw-cap NMR tube was charged with silver hexafluoroantimonate (10.7 mg, 0.031 mmol) in dichloromethane-d^2 (0.3 mL). Complex **10** (20 mg, 0.031 mmol) was transferred into a small glass vial and dissolved in dichloromethane-d^2 (0.3 mL). Iodobenzene (3.5 µL, 0.031 mmol) was added to the solution of complex **10**. The prepared solution was loaded into a plastic syringe equipped with stainless steel needle. The syringe was closed by blocking the needle with a septum. Outside the glovebox, the NMR tube was cooled down to –80°C (Ethanol/N_2 cold bath). At this temperature, the solution of complex **10** and iodobenzene was added to the $AgSbF_6$ solution. The tube was gently shaken and allowed to warm to room temperature. After complete conversion (as indicated by ^{31}P NMR monitoring), the tube was reintroduced in the glovebox, and tetrabutylammonium chloride (8.6 mg, 0.031 mmol) was added at room temperature to completely convert complex 1**2** into the corresponding aryl gold(III)–chloride complex, which was isolated in 80 % yield.

^{1}H NMR (500 MHz, CD_2Cl_2): δ 8.34 (dd, $^3J_{H\text{-}H}$ = 4.0 Hz, $^3J_{P\text{-}H}$ = 8.2 Hz, 1H, H_2), 8.02-7.99 (m, 1H, H_5), 7.90-7.87 (pseudo t, 1H, H_4), 7.75-7.72 (m, 1H, H_3), 7.50-7.48 (m, 2H, H_9), 7.31 (t, $^3J_{H\text{-}H}$ = 7.5 Hz, 2H, H_8), 7.25-7.22 (m, 1H, H_{10}), 3.56 (s, 6H, N(C*H*$_3$)$_2$), 3.24-3.20 (m, 8H, H_{11}), 2.31-2.02 (m, 18H, H_{Ad}), 1.79-1.60 (m, 20H, H_{Ad} & H_{12}), 1.42 (sextuplet, $^3J_{H\text{-}H}$ = 7.4 Hz, 8H, H_{13}), 1.00 (t, $^3J_{H\text{-}H}$ = 7.3 Hz, 12H, H_{14}). **^{31}P{^{1}H} NMR** (121 MHz, CD_2Cl_2): δ 74.4 (s). **^{13}C{^{1}H}** (126 MHz, CD_2Cl_2): δ 159.2 (d, $J_{P\text{-}C}$ = 6.8 Hz, C_6), 137.2 (d, $J_{P\text{-}C}$ = 2.2 Hz, C_5), 136.7 (d, $J_{P\text{-}C}$ = 1.8 Hz, C_4), 135.4 (s, C_9), 130.5 (s, C_3), 130.4 (s, C_8), 128.3 (s, C_{10}), 128.0 (s, C_7), 126.5 (d, $J_{P\text{-}C}$ = 7.3 Hz, C_2), 118.9 (d, $J_{P\text{-}C}$ = 44.5 Hz, C_1), 58.9 (s, C_{11}), 54.1 (s, N(CH_3)$_2$), 48.3 (d, $J_{P\text{-}C}$ = 13.8 Hz, C_{qtAd}), 40.8 (d, $J_{P\text{-}C}$ = 1.1 Hz, CH_{2Ad}), 35.9 (d, $J_{P\text{-}C}$ = 1.7 Hz, CH_{2Ad}), 29.1 (d, $J_{P\text{-}C}$ = 9.8 Hz, CH_{Ad}), 24.4 (s, C_{12}), 20.2 (s, C_{13}), 13.9 (s, C_{14}). **HRMS (ESI+)**: calculated for [M^+] = $C_{34}H_{45}NPClAu^+$: 730.2644. Found: 730.2633.

2.6.9 Synthesis of Complex 16

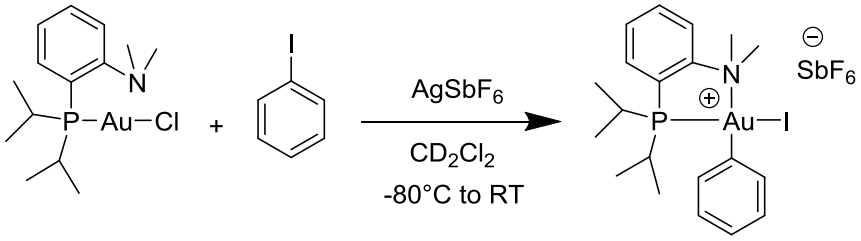

14 **16**

In a glovebox, a screw-cap NMR tube was charged with silver hexafluoroantimonate (8.0 mg, 0.023 mmol) in dichloromethane-d^2 (0.3 mL). Complex **14** (11 mg, 0.023 mmol) was transferred into a small glass vial and dissolved in dichloromethane-d^2 (0.3 mL Iodobenzene (13.0 µL, 0.115 mmol) was added to the solution of complex **14**. The prepared solution was loaded into a plastic syringe equipped with stainless steel needle. The syringe was closed by blocking the needle with a septum. Outside the glovebox, the NMR tube was cooled down to -80°C (Ethanol/N_2 cold bath). At this temperature, the solution of complex **14** and iodobenzene was added. The tube was gently shaken and allowed to warm to RT. The reaction was left to proceed until completion as monitored by $^{31}P\{^1H\}$ NMR. The formation of the gold(III) complexes was confirmed by ^1H and ^{31}P NMR spectroscopy.

^{1}H NMR (300 MHz, CD_2Cl_2): δ 8.05-7.89 (m, 3H, H_{Ar}), 7.67-7.61 (m, 1H, H_{Ar}), 3.47 (s, 6H, N(C*H*$_3$)$_2$), 3.00 (m, 2H, C*H*(CH$_3$)$_2$), 1.38 (d, J_{HH} = 6.9 Hz, 3H, CH(C*H*$_3$)$_2$), 1.32 (d, J_{HH} = 6.9 Hz, 3H, CH(C*H*$_3$)$_2$), 1.05 (d, J_{HH} = 7.0 Hz, 3H, CH(C*H*$_3$)$_2$), 0.98 (d, J_{HH} = 7.0 Hz, 3H, CH(C*H*$_3$)$_2$). **$^{31}P\{^1H\}$ NMR** (121 MHz, CD_2Cl_2): δ 69.3 (s).

2.6.10 Synthesis of Complex 10-I

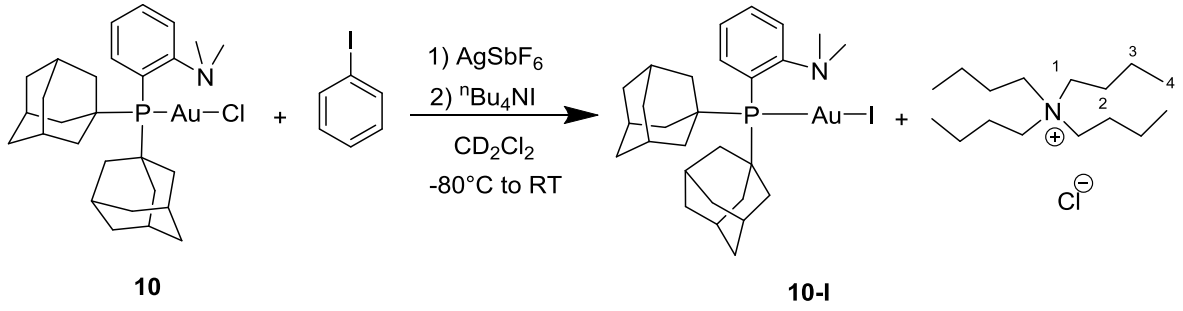

10 **10-I**

In a glovebox, a screw-cap NMR tube was charged with silver hexafluoroantimonate (10.7 mg, 0.031 mmol) in dichloromethane-d^2 (0.3 mL). Complex **10** (20 mg, 0.031 mmol) was transferred into a small glass vial and dissolved in dichloromethane-d^2 (0.3 mL). Iodobenzene (3.5 µL, 0.031 mmol) was added to the solution of complex **10**. The prepared solution was loaded into a plastic syringe equipped with stainless steel needle. The syringe was closed by blocking the needle with a septum. Outside the glovebox, the NMR tube was cooled down to –80°C (Ethanol/N_2 cold bath). At this temperature, the solution of complex **10** and iodobenzene was added to the $AgSbF_6$ solution. The tube was gently shaken and allowed to warm to room temperature. After complete conversion (as indicated by ^{31}P NMR monitoring), the tube was reintroduced in the glovebox, and tetrabutylammonium iodide (11.5 mg, 0.031 mmol) was added at room temperature.

^{1}H NMR (300 MHz, CD_2Cl_2): δ 7.78-7.67 (m, 1H, H_{Ar}), 7.59-7.50 (m, 1H, H_{Ar}), 7.37-7.27 (m, 1H, H_{Ar}), 7.11 (t, $^3J_{H-H}$ = 7.7 Hz, 1H, H_{Ar}), 3.28-3.18 (m, 8H, H_1), 2.55 (s, 6H, N(C*H*$_3$)$_2$), 2.29-1.94 (m, 18H, H_{Ad}), 1.74-1.58 (m, 20H, H_{Ad} & H_2), 1.42 (sextuplet, $^3J_{H-H}$ = 7.4 Hz, 8H, H_3), 1.00 (t, $^3J_{H-H}$ = 7.4 Hz, 12H, H_4). **^{31}P{^{1}H} NMR** (121 MHz, CD_2Cl_2): δ 59.4 (s). **HRMS (ESI+)**: calculated for $[M + H]^+ = C_{28}H_{41}NPIAu^+$: 746.1687. Found: 746.1680.

2.6.11 Oxidative Addition with Complex 10

General Procedure for the Oxidative Addition of Aryl Iodides with Complex 10

In a glovebox, a screw-cap NMR tube was charged with silver hexafluoroantimonate (8.0 mg, 0.023 mmol) in dichloromethane-d^2 (0.3 mL). Complex **10** (15 mg, 0.023 mmol) was transferred into a small glass vial and dissolved in dichloromethane-d^2 (0.3 mL). The aryl iodide (0.115 mmol) was added to the solution of **10**. The prepared solution was loaded into a plastic syringe equipped with stainless steel needle. The syringe was closed by blocking the needle with a septum. Outside the glovebox, the NMR tube was cooled down to -80°C (Ethanol/N_2 cold bath). At this temperature, the solution of complex **10** and aryl iodide was added. The tube was gently shaken and allowed to warm to RT. The reaction was left to proceed until completion as monitored by $^{31}P\{^1H\}$ NMR. The formation of the gold(III) complexes was confirmed by ^1H and ^{31}P NMR spectroscopy and high-resolution mass spectrometry (Electrospray ionization, positive mode). Halide exchange reaction from aryl gold(III) complexes was systematically observed with all substrates. In the following examples, only the mass peak corresponding to the aryl gold(III) chloride derivatives is indicated.

Reaction of Complex 10 with 4-Methoxyiodobenzene (17)

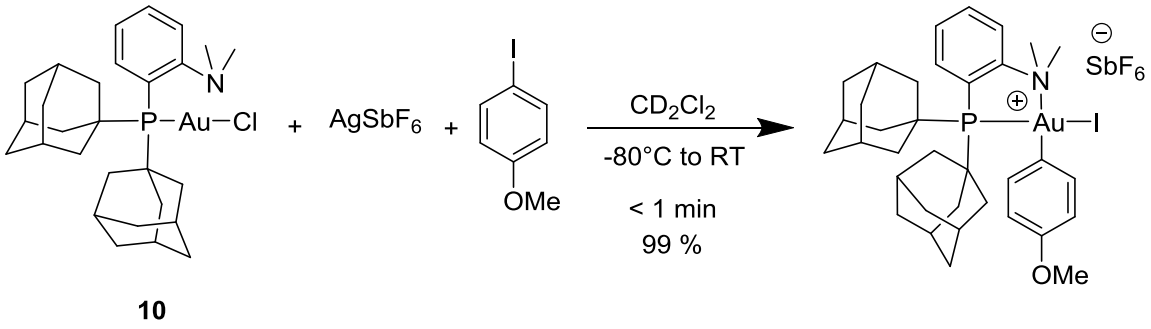

10

^{1}H NMR (300 MHz, CD_2Cl_2): δ 8.00-7.87 (m, 3H, H_{Ar}), 7.80-7.71 (m, 1H, H_{Ar}), 7.36-7.33 (d, J_{HH} = 8.9 Hz, 2H, H_{Ar}), 6.94-6.91 (d, J_{HH} = 8.9 Hz, 2H, H_{Ar}), 3.83 (s, 3H, OMe), 3.49 (s, 6H, $N(CH_3)_2$), 2.30-2.01 (m, 18H, H_{Ad}), 1.76 (bs, 12H, H_{Ad}). **^{31}P{^{1}H} NMR** (121 MHz, CD_2Cl_2): δ 75.1 (s). **HRMS (ESI+)**: calculated for $[M^+]$ = $C_{35}H_{47}NOPClAu^+$: 760.2749. Found: 760.2756.

Reaction of Complex 10 with 4-Methyliodobenzene

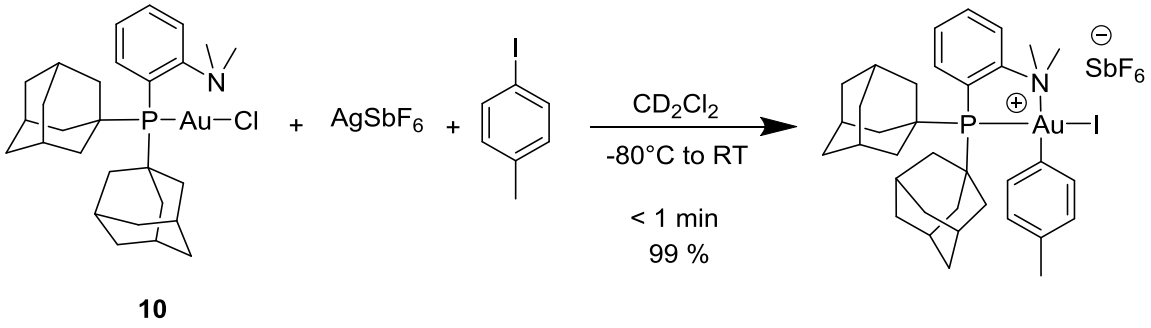

10

^{1}H NMR (300 MHz, CD_2Cl_2): δ 8.02-7.88 (m, 3H, H_{Ar}), 7.79-7.71 (m, 1H, H_{Ar}), 7.35-7.31 (m, 2H, H_{Ar}), 7.16-7.13 (m, 2H, H_{Ar}), 3.49 (s, 6H, $N(CH_3)_2$), 2.38 (s, 3H, CH_3), 2.30-2.05 (m, 30H, H_{Ad} and $CH_{3excess}$), 1.76 (bs, 12H, H_{Ad}). **^{31}P{^{1}H} NMR** (121 MHz, CD_2Cl_2) : δ 74.2 (s). **HRMS (ESI+)**: calculated for $[M^+]$ = $C_{35}H_{47}NPClAu^+$: 744.2800. Found: 744.2799.

Reaction of Complex 10 with 4-Fluoroiodobenzene

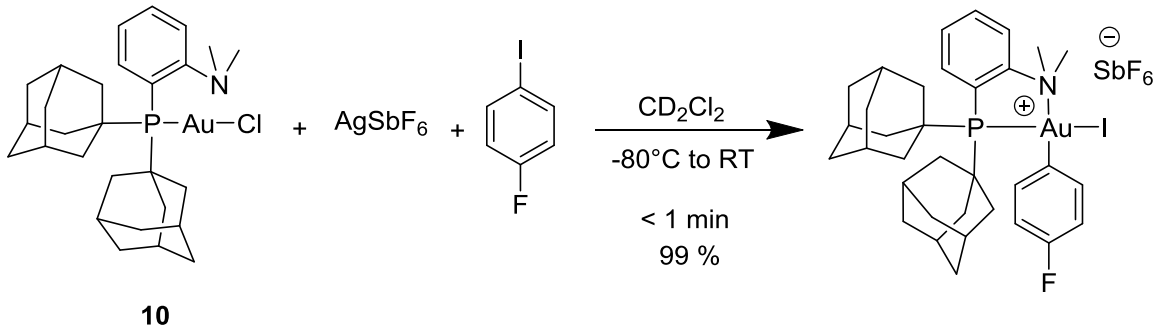

10

^{1}H NMR (300 MHz, CD_2Cl_2): δ 8.02-7.88 (m, 3H, H_{Ar}), 7.78-7.72 (m, 1H, H_{Ar}), 7.51-7.46 (m, 2H, H_{Ar}), 7.14 (t, J_{HH} = 8.7 Hz, 2H, H_{Ar}), 3.52 (s, 6H, $N(CH_3)_2$), 2.42-2.04 (m, 18H, H_{Ad}), 1.76 (s, 12H, H_{Ad}). **^{31}P{^{1}H} NMR** (121 MHz, CD_2Cl_2): δ 76.03 (s). **HRMS (ESI+)**: calculated for $[M^+] = C_{34}H_{44}NPClFAu^+$: 748.2549. Found: 748.2562.

Reaction of Complex 10 with 4-Nitroiodobenzene (18)

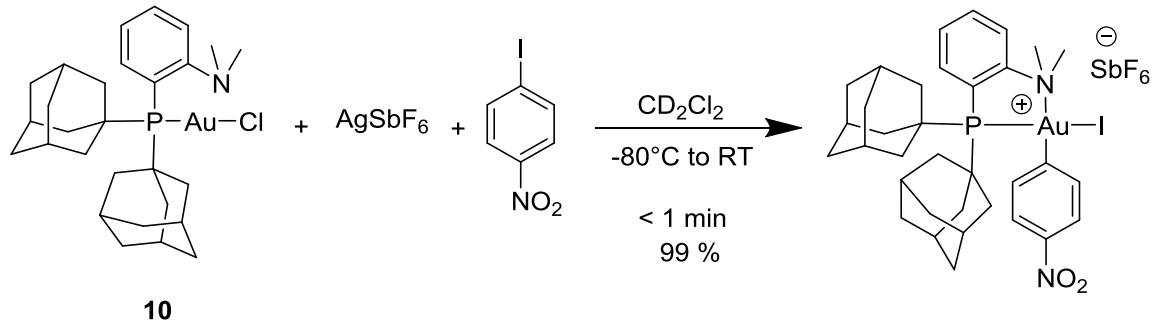

10

^{1}H NMR (300 MHz, CD_2Cl_2): δ 8.21-8.16 (m, H_{Ar}), 8.03-7.98 (m, H_{Ar}), 7.97-7.88 (m, H_{Ar}), 7.81-7.74 (m, H_{Ar}), 3.56 (s, 6H, $N(CH_3)_2$), 2.38-2.02 (m, 18H, H_{Ad}), 1.77 (s, 12H, H_{Ad}). **^{31}P{^{1}H} NMR** (121 MHz, CD_2Cl_2): δ 79.7 (s). **HRMS (ESI+)**: calculated for $[M^+] = C_{34}H_{44}N_2O_2PClAu^+$: 775.2494. Found: 775.2482.

Reaction of Complex 10 with Iodopentafluorobenzene

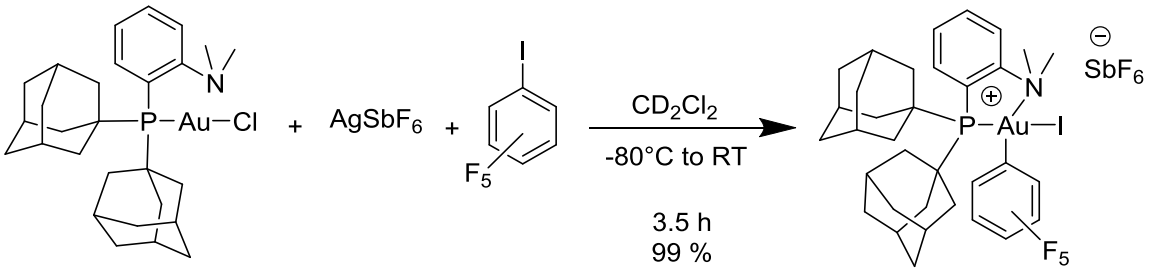

10

^{1}H NMR (300 MHz, CD_2Cl_2): δ 8.09-7.95 (m, 3H, H_{Ar}), 7.85-7.81 (m, 1H, H_{Ar}), 7.89-7.85 (m, 6H, H_{Ar}), 3.68 (s, 6H, N(CH_3)$_2$), 2.39-1.97 (m, 18H, H_{Ad}), 1.77 (s, 12H, H_{Ad}). **^{31}P{^{1}H} NMR** (121 MHz, CD_2Cl_2): δ 102.3 (s). **HRMS (ESI+)**: calculated for [M^+] = $C_{34}H_{40}NF_5PClAu^+$: 820.2174. Found: 820.2182.

Reaction of Complex 10 with 1-Iodonaphthalene

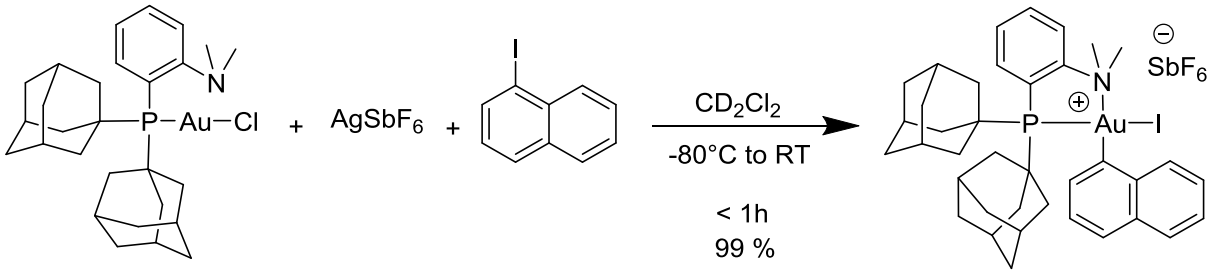

10

^{1}H NMR (300 MHz, CD_2Cl_2): δ 8.11-8.04 (m, 8H, H_{Ar}), 7.99-7.92 (m, 3H, H_{Ar}), 7.89-7.85 (m, 6H, H_{Ar}), 7.82-7.74 (m, 7H, H_{Ar}), 7.62-7.48 (m, 10H, H_{Ar}), 7.44-7.39 (t, J_{H-H} = 7.8 Hz, 1H, H_{Ar}), 7.23-7.18 (m, 4H, H_{Ar}), 3.59 (d, J_{HH} = 6.2 Hz, 6H, N(CH_3)$_2$), 2.45-1.27 (m, 30H, H_{Ad}). **^{31}P{^{1}H} NMR** (121 MHz, CD_2Cl_2) : δ 79.7 (s). **HRMS (ESI+)**: calculated for [M^+] = $C_{38}H_{47}NPClAu^+$: 780.2820. Found: 780.2810.

Reaction of Complex 10 with 2-Iodo-5-nitrotoluene

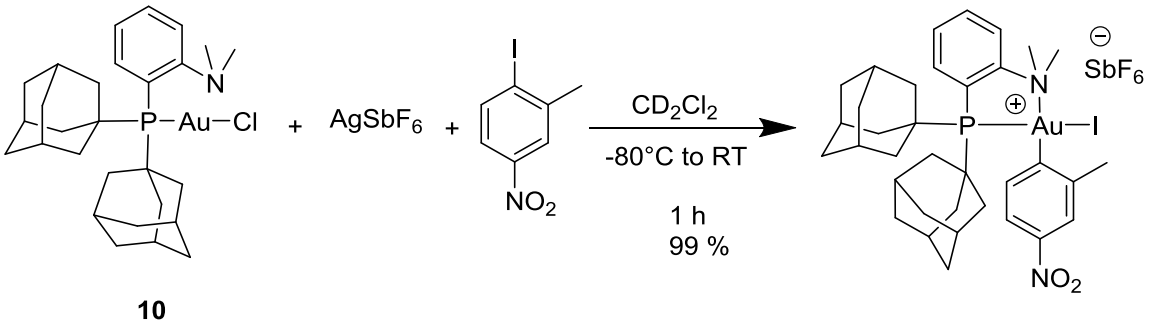

10

^{1}H NMR (300 MHz, CD_2Cl_2): δ 8.07-8.00 (m, 13H, H_{Ar}), 7.80-7.76 (m, 2H, H_{Ar}), 7.72-7.71 (m, 2H, H_{Ar}), 7.70-7.68 (m, 2H, H_{Ar}), 3.55 (d, J_{HH} = 15.0 Hz, 6H, N(CH_3)$_2$), 2.39 (s, 3H, CH_3), 2.39-1.59 (m, 30H, H_{Ad}). **^{31}P{^{1}H} NMR** (121 MHz, CD_2Cl_2): δ 80.8 (s). **HRMS (ESI+)**: calculated for [M^+] = $C_{35}H_{46}N_2O_2PClAu^+$: 789.2651. Found: 789.2650

Reaction of Complex 10 with 2-Iodopyridine

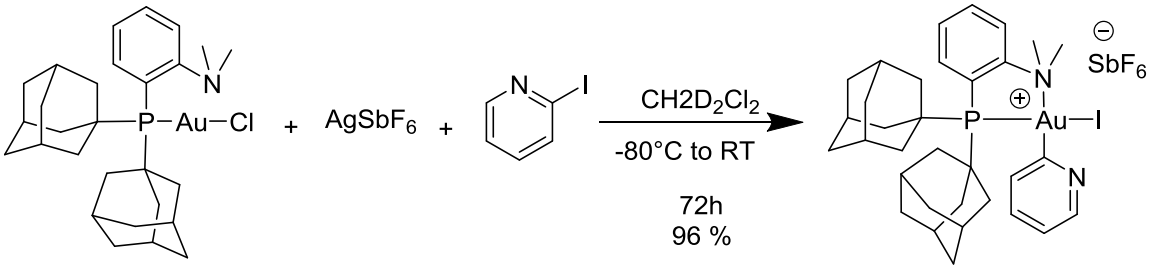

10

^{1}H NMR (300 MHz, CD_2Cl_2): δ 8.48-8.46 (m, 1H, H_{Ar}), 8.37-8.32 (m, 4H, H_{Ar}), 7.98-7.87 (m, 3H, H_{Ar}), 7.76-7.74 (m, 5H, H_{Ar}), 7.63-7.62 (m, 1H, H_{Ar}), 7.48-7.46 (m, 1H, H_{Ar}), 7.40 – 7.28 (m, 8H, H_{Ar}), 7.22-7.19 (m, 1H, H_{Ar}), 3.45 (s, 6H, N(CH_3)$_2$), 2.38-1.97 (m, 18H, H_{Ad}), 1.75 (s, 12H, H_{Ad}). **^{31}P{^{1}H} NMR** (121 MHz, CD_2Cl_2): δ 70.0 (s). **HRMS (ESI+)**: calculated for [M^+] = $C_{33}H_{44}N_2PClAu^+$: 731.2596. Found: 731.2590.

General procedure for the reaction of Complex 1 with aryl bromides

In a glovebox, a flame dried Schlenk equipped with a magnetic stirrer bar was charged with silver hexafluoroantimonate (32.0 mg, 0.092 mmol) in dichloromethane (3 mL). Complex **10** (60 mg, 0.092 mmol) was transferred into a small glass vial and dissolved in dichloromethane (2 mL). Aryl bromide (0.46 mmol, 5eq.) was added to the solution of complex **10**. The prepared solution was loaded into a plastic syringe equipped with stainless steel needle. The syringe was closed by blocking the needle with a septum. Outside the glovebox, the NMR tube was cooled down to – 80°C (Ethanol/N_2 cold bath). At this temperature, the solution of complex **1** and aryl bromide was added to the $AgSbF_6$ solution. The reaction mixture was then stirred at room temperature overnight (12h). The reaction mixture was then filtered to give a clear solution. Volatiles were removed *in vaccuo*. The residue was washed with pentane (3 x 3 mL) and dried under vacuum to give a solid powder. The formation of the gold(III) complex was confirmed by ^{1}H and ^{31}P NMR analysis and high-resolution mass spectrometry (Electrospray ionization, positive mode).

Reaction of Complex 10 with 2-bromoanisole

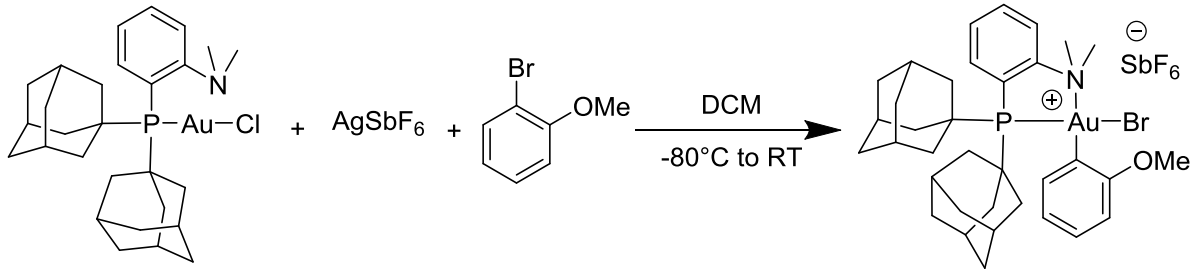

10

Yield 75 %. Mp: 211°C (decomposition). **^{1}H NMR** (300 MHz, CD_2Cl_2): δ 8.00-7.90 (m, 3H, H_{Ar}), 7.74 (t, J_{HH} = 7.8 Hz, 1H, H_{Ar}), 7.42 (d, J_{HH} = 7.9 Hz, 1H, H_{Ar}), 7.33-7.28 (m, 1H, H_{Ar}), 6.99 (t, J_{HH} = 7.8 Hz, 1H, $H_{Ar,}$), 6.85 (d, J_{HH} = 7.9 Hz, 1H, $H_{Ar,}$), 3.92 (s, 3H, O(C*H*$_3$)), 3.51 (d, J_{HH} = 10.9 Hz, N(C*H*$_3$)$_2$), 2.37-1.63 (m, 30H, H_{Ad}). **^{31}P{^{1}H} NMR** (121 MHz, CD_2Cl_2): δ 78.0 (s). **HRMS (ESI+)**: calculated for [M^+] = $C_{35}H_{47}NOPClAu^+$: 760.2749. Found: 760.2748. For [M'$^+$] = $C_{35}H_{47}NOPBrAu^+$: 804.2244. Found: 804.2238.

Reaction of Complex 10 with 4'-bromoacetophenone

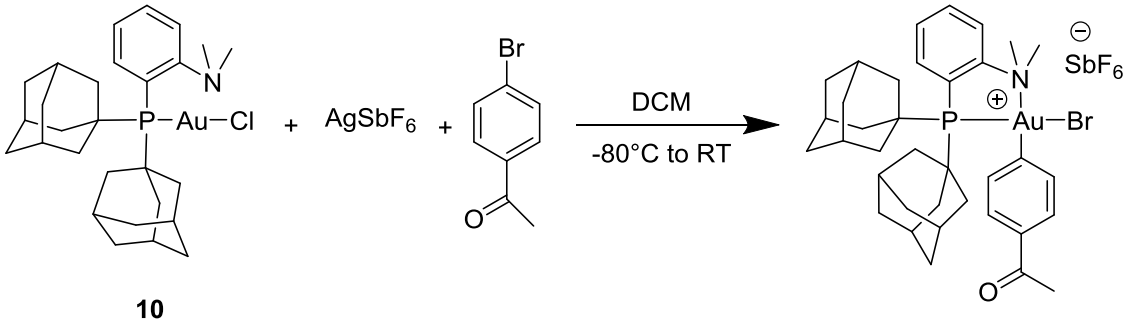

10

Yield 60 %. Mp: 201°C (decomposition). **^{1}H NMR** (300 MHz, CD_2Cl_2): δ 7.96-7.91 (m, 2H, H_{Ar}), 7.83 (d, J_{HH} = 8.7 Hz, 2H, H_{Ar}), 7.78-7.67 (m, 2H, H_{Ar}), 7.59 (d, J_{HH} = 8.7 Hz, 2H, $H_{Ar,}$), 3.47 (s, N(C*H*$_3$)$_2$), 2.56 (s, OC(C*H*$_3$)), 2.28-1.99 (m, 18H, H_{Ad}), 1.71 (br.s, 12H, H_{Ad}). **^{31}P{^{1}H} NMR** (121 MHz, CD_2Cl_2): δ 77.0 (s). **HRMS (ESI+)**: calculated for [M^+] = $C_{36}H_{47}NOPClAu^+$: 772.2749. Found: 772.2755. For [M'$^+$] = $C_{36}H_{47}NOPBrAu^+$: 816.2244. Found: 816.2233.

Reaction of Complex 10 with 1-Bromonaphthalene

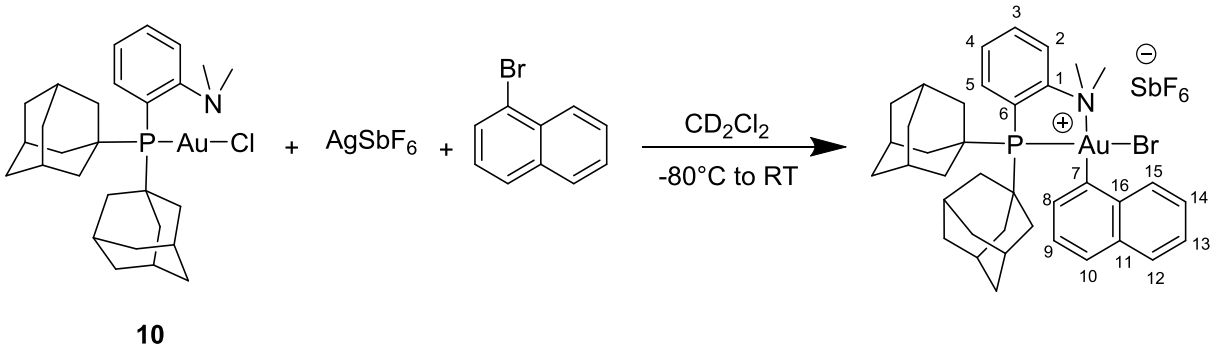

10

In a glovebox, a screw-cap NMR tube was charged with silver hexafluoroantimonate (10.7 mg, 0.031 mmol) in dichloromethane-d^2 (0.3 mL). Complex **10** (20 mg, 0.031 mmol) was transferred into a small glass vial and dissolved in dichloromethane-d^2 (0.3 mL). 1-Bromonaphthalene (4.3 µL, 0.031 mmol) was added to the solution of complex **10**. The prepared solution was loaded into a plastic syringe equipped with stainless steel needle. The syringe was closed by blocking the needle with a septum. Outside the glovebox, the NMR tube was cooled down to -80°C (Ethanol/N_2 cold bath). At this temperature, the solution of complex **1** and bromonaphthalene was added to the $AgSbF_6$ solution. The tube was gently shaken and allowed to warm to room temperature. Complete conversion to the desired gold(III) complex (93 % spectroscopic yield) and a minor unidentified species was observed after 4 h. This complex was spectroscopically characterized at room temperature from the reaction mixture.

^{1}H NMR (500 MHz, CD_2Cl_2): 8.07-8.02 (m, 3H, H_3, H_4 & H_{15}), 7.93-7.88 (m, 2H, H_2 & H_{12}), 7.83-7.80 (m, 2H, H_5 & H_8), 7.78-7.70 (m, 2H, H_{10} & H_{14}), 7.60-7.53 (m, 1H, H_{13}), 7.44 (t, $J_{H\text{-}H}$ = 7.7 Hz, 1H, H_9), 3.60 (d, J_{CP} = 8.5 Hz, 6H, N(CH_3)$_2$), 2.37-1.41 (m, 30H, H_{Ad}). **^{31}P{^{1}H} NMR** (121 MHz, CD_2Cl_2): δ 76.8 (s). **^{13}C{^{1}H}** (126 MHz, CD_2Cl_2): δ 158.2 (d, $J_{P\text{-}C}$ = 7.1 Hz, C_1), 137.0 (d, $J_{P\text{-}C}$ = 2.3 Hz, C_3), 136.6 (s, C_{16}), 136.4 (d, $J_{P\text{-}C}$ = 1.7 Hz, C_2), 136.1 (s, C_{11}), 132.4 (s, C_8), 131.2 (s, C_{15}), 130.8 (d, $J_{P\text{-}C}$ = 7.3 Hz, C_5), 129.1 (s, C_{10} & C_{12}), 128.9 (s, C_7), 127.3 (s, C_{14}), 127.0 (s, C_{13}), 126.3 (s, C_9), 125.6 (d, $J_{P\text{-}C}$ = 7.2 Hz, C_4), 119.7 (d, $J_{P\text{-}C}$ = 44.1 Hz, C_6), 54.0 (s, N($\underline{C}H_3$)$_2$) , 53.5 (s, N($\underline{C}H_3$)$_2$), 47.9 (d, $J_{P\text{-}C}$ = 13.8 Hz, C_{qtAd}), 41.1 (d, $J_{P\text{-}C}$ = 1.4 Hz, CH_{2Ad}), 39.5 (d, $J_{P\text{-}C}$ = 1.4 Hz, CH_{2Ad}), 35.9 (d, $J_{P\text{-}C}$ = 1.7 Hz, CH_{2Ad}), 35.3 (d, $J_{P\text{-}C}$ = 1.8 Hz, CH_{2Ad}), 29.1 (d, $J_{P\text{-}C}$ = 9.8 Hz, CH_{Ad}), 28.7 (d, $J_{P\text{-}C}$ = 9.8 Hz, CH_{Ad}). **HRMS (ESI +)**: calculated for [M^+] = $C_{38}H_{47}NPBrAu^+$: 824.2295. Found: 824.2297. For [M'^+] = $C_{38}H_{47}NPClAu^+$: 780.2800. Found: 780.2802.

Oxidative addition of biphenylene to complex 10 in the presence of $AgSbF_6$

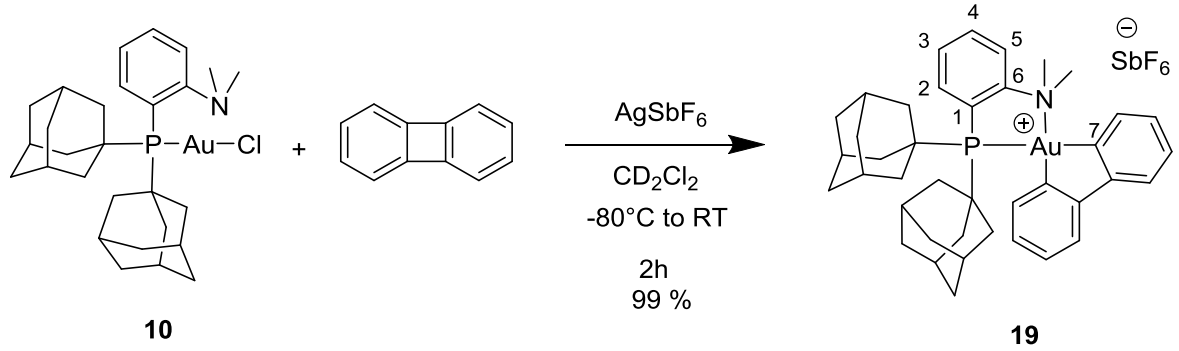

10 **19**

In a glovebox, a screw-cap NMR tube was charged with silver hexafluoroantimonate (8.0 mg, 0.023mmol) in dichloromethane-d^2 (0.3 mL). Complex **10** (15 mg, 0.023 mmol) was transferred into a small glass vial and dissolved in dichloromethane-d^2 (0.3 mL). Biphenylene (35.0 mg, 0.230 mmol) was added to the solution of complex **10**. The prepared solution was loaded into a plastic syringe equipped with stainless steel needle. The syringe was closed by blocking the needle with a septum. Outside the glovebox, the NMR tube was cooled down to -80°C (Ethanol/N_2 cold bath). At this temperature, the solution of complex **1** and biphenylene was added to the $AgSbF_6$ solution. The tube was gently shaken and allowed to warm to RT. Crystals suitable for X-ray diffraction were obtained from a concentrated solution of **19**.

^{1}H NMR (300 MHz, CD_2Cl_2): δ 8.21 (d, J_{HH} = 7.6 Hz, 1H, H_{Ar}), 8.01 (t, J_{HH} = 7.0 Hz, 1H, H_{Ar}), 7.91-7.85 (m, 2H, H_{Ar}), 7.67-7.44 (m, 4H, H_{Ar}), 7.37-7.29 (m, 3H, H_{Ar}), 7.03-6.98 (m, 1H, H_{Ar}), 3.72 (s, 6H, N(C*H*$_3$)$_2$), 2.35-2.09 (m, 18H, H_{Ad}), 1.77-1.65 (m, 12H, H_{Ad}). **^{31}P{^{1}H} NMR** (121 MHz, CD_2Cl_2): δ 76.7 (s). **^{13}C{^{1}H}** (126 MHz, CD_2Cl_2): δ 172.6 (d, J_{CP} = 116.3 Hz, C7), 163.5 (d, J_{CP} = 11.6 Hz, C6), 154.4 (d, J_{CP} = 3.6 Hz, $C_{biphenyl}$), 153.5 (d, J_{CP} = 1.6 Hz, $C_{biphenyl}$), 150.3 (d, J_{CP} = 5.0 Hz, $C_{biphenyl}$), 142.3 (d, J_{CP} = 6.8 Hz, $CH_{biphenyl}$), 137.5 (s, C4 or C5), 136.3 (s, C4 or C5), 131.3 (d, J_{CP} = 4.7 Hz, C3), 126.6 (d, J_{CP} = 2.5 Hz, $CH_{biphenyl}$), 125.9 (s, $CH_{biphenyl}$), 125.1 (d, J_{CP} = 7.2 Hz, C2), 123.9 (s, $CH_{biphenyl}$), 123.1 (d, J_{CP} = 5.5 Hz, $CH_{biphenyl}$), 120.0 (d, J_{CP} = 38.1 Hz, C1), 55.70 (s, N(CH_3)$_2$), 46.6 (d, J_{CP} = 6.9 Hz, C_{qtAd}), 42.60 (s, CH_{2Ad}), 36.10 (s, CH_{2Ad}), 29.6 (d, J_{CP} = 9.3 Hz, CH_{Ad}). **HRMS (ESI+):** calculated for [M+] = $C_{40}H_{48}NPAu^+$: 770.3190. Found: 770.319.

2.7 Computational Details

DFT studies reported have been performed with B97D Grimme's functional including dispersion,[53] as implemented in Gaussian 09.[54] Gold, iodine or bromide and antimony atoms were described with the relativistic electron core potential SDD and the associated basis set.[55] The gold atom has been augmented by a set of f polarization functions.[56] 6-31G** basis set was employed for all other atoms. All stationary points involved were fully optimized. Frequency calculations were undertaken to confirm the nature of the stationary points, yielding one imaginary frequency for transition states (TS), corresponding to the expected process, and zero for *minima*. The connectivity of the transition states and their adjacent *minima* was confirmed by intrinsic reaction coordinate (IRC)[57] calculations. All total energies and Gibbs free energies have been zero-point energy (ZPE) and temperature corrected using unscaled density functional frequencies. Solvent effects (dichloromethane) were taken into account. Optimization have been carried out in solvent using SMD implicit solvation model.[58] Single point calculations were carried out, on fully optimized geometries in solution as mentioned above, by means of the SMD model at the B97D/SDD+f(Au), SDD(I),6-31+G**(other atoms) level of theory in order to obtain accurate energy values.

2.8 References

(1) Bratsch, S.G., *J. Phys. Chem. Ref. Data.* **1989**, *18*, 1.

(2) Hatrwig, J.F. *Oganotransition Metal Chemistry: From Bonding to Catalysis*, University Science Books, Sausalito, **2009**.

(3) Mann, F. G.; Purdie, D. *J. Chem. Soc.* **1940**, *0*, 1235.

(4)Tamaki, A.; Kochi, J.K. *J. Organomet. Chem.* **1972**, *40*, C81.

(5) Shiotani, A.; Schmidbaur, H. *J. Organomet. Chem.* **1972**, *37*, C24.

(6) González-Arellano, C.; Abad, A.; Corma, A.; García, H.; Iglesias, M.; Sánchez, F. *Angew. Chem. Int. Ed.* **2007**, *46*, 1536.

(7) Lauterbach, T.; Livendahl, M.; Rosellón, A.; Espinet, P.; Echavarren, A. M. *Org. Lett.* **2010**, *12*, 3006.

(8) Corma, A.; Juarez, R.; Boronat, M.; Sanchez, F.; Iglesias, M.; Garcia, H. *Chem. Commun.* **2011**, *47*, 1446.

(9) Robinson, P. S. D.; Khairallah, G. N.; da Silva, G.; Lioe, H.; O'Hair, R. A. J. *Angew. Chem. Int. Ed.* **2012**, *51*, 3812.

(10) Gualco, P.; Ladeira, S.; Miqueu, K.; Amgoune, A.; Bourissou, D. *Angew. Chem. Int. Ed.* **2011**, *50*, 8320.

(11) Joost, M.; Gualco, P.; Coppel, Y.; Miqueu, K.; Kefalidis, C. E.; Maron, L.; Amgoune, A.; Bourissou, D. *Angew .Chem. Int. Ed.* **2014**, *53*, 747.

(12) Lassauque, N.; Gualco, P.; Mallet-Ladeira, S.; Miqueu, K.; Amgoune, A.; Bourissou, D. *J. Am. Chem. Soc.* **2013**, *135*, 13827.

(13) Guenther, J.; Mallet-Ladeira, S.; Estevez, L.; Miqueu, K.; Amgoune, A.; Bourissou, D. *J. Am. Chem. Soc.* **2014**, *136*, 1778.

(14) Hashmi, A. S. K.; Lothschütz, C.; Döpp, R.; Ackermann, M.; De Buck Becker, J.; Rudolph, M.; Scholz, C.; Rominger, F. *Adv. Synth. Catal.* **2012**, *354*, 133.

(15) Livendahl, M.; Goehry, C.; Maseras, F.; Echavarren, A. M. *Chem. Commun.* **2014**, *50*, 1533.

(16) Serra, J.; Parella, T.; Ribas, X. *Chem. Sci.* **2017**, *8*, 946.

(17) Carvajal, M. A.; Novoa, J. J.; Alvarez, S. *J. Am. Chem. Soc.* **2004**, *126*, 1465.

(18) Otsuka, S. *J. Organomet. Chem.* **1980**, *200*, 191.

(19) Dierkes, P.; van Leeuwen, P. W. N. M. *J. Chem. Soc., Dalton Trans.* **1999**, *10*, 1519.

(20) Hoffmann, R. *Front. Chem.* (Ed.: K.J. Laidler), Pergamon Press, New-York, **1982**, 247

(21) Gimeno, M. C.; Laguna, A. *Chem. Rev.* **1997**, *97*, 511.

(22) Crespo, O.; Gimeno, M. C.; Laguna, A.; Jones, P. G. *J. Chem. Soc., Dalton Trans.* **1992**, *0*, 1601.

(23) Valliant, J. F.; Guenther, K. J.; King, A. S.; Morel, P.; Schaffer, P.; Sogbein, O. O.; Stephenson, K. A. *Coord. Chem. Rev.* **2002**, *232*, 173.

(24) Kang, S. O.; Ko, J. *Adv. Organomet. Chem.*, **2001**, *47*, 61.

(25) Nakamura, H. ; Kamakura, T.; Onagi, S. *Org. Lett.* **2006**, *8*, 2095.

(26) Alexander, R. P.; Schroeder, H. *Inorg. Chem.* **1963**, *2*, 1107.

(27) Teixidor, F.; Viñas, C.; Mar Abad, M.; Nuñez, R.; Kivekäs, R.; Sillanpää, R. *J. Organomet. Chem.* **1995**, *503*, 193.

(28) Batsanov, S. S. *Inorg. Mater.* **2001**, *37*, 871.

(29) Joost, M.; Zeineddine, A.; Estévez, L.; Mallet−Ladeira, S.; Miqueu, K.; Amgoune, A.; Bourissou, D. *J. Am. Chem. Soc.* **2014**, *136*, 14654.

(30) Mézailles, N.; Ricard, L.; Gagosz, F. *Org. Lett.* **2005**, *7*, 4133.

(31) Lewis, A. K.; Caddick, S.; Cloke, F. G.; Billingham, N. C.; Hitchcock, P. B.; Leonard, J. *J. Am. Chem. Soc.* **2003**, *125*, 10066.

(32) Fernandez, I.; Bickelhaupt, F. M. *Chem. Soc. Rev.* **2014**, *43*, 4953.

(33) van Zeist, W. J.; Bickelhaupt, F. M. *Org. Biomol. Chem*. **2010**, *8*, 3118.

(34) Jun, C.-H. *Chem. Soc. Rev.* **2004**, *33*, 610.

(35) Murakami, M.; Matsuda, T. *Chem. Commun.* **2011**, *47*, 1100.

(36) Ruhland, K. *Eur. J. Org. Chem.* **2012**, *2012*, 2683.

(37) Murakami, M.; Ito, Y. *Act. Unreactive Bonds Org. Synth.* (Eds.: P.S. Murai, H. Alper, R.A. Gossage, V.V. Grushin, M. Hidai, Y. Ito, W.D. Jones, F. Kakiuchi, G. van Koten, Y.-S. Lin, *et al*.), Springer, Heidelberg, **1999**, 97.

(38) Perthuisot, C.; Edelbach, B. L.; Zubris, D. L.; Simhai, N.; Iverson, C. N.; Müller, C.; Satoh, T.; Jones, W. D. *J. Mol. Catal. Chem.* **2002**, *189*, 157.

(39) Joost, M.; Estévez, L.; Miqueu, K.; Amgoune, A.; Bourissou, D. *Angew. Chem. Int. Ed.* **2015**, *54*, 5236.

(40) Wu, C.-Y.; Horibe, T.; Jacobsen, C. B.; Toste, F. D. *Nature* **2015**, *517*, 449.

(41) Hesp, K. D.; Stradiotto, M. *J. Am. Chem. Soc.* **2010**, *132*, 18026.

(42) Luo, Y.; Ji, K.; Li, Y.; Zhang, L. *J. Am. Chem. Soc.* **2012**, *134*, 17412.

(43) Huang, L.; Rominger, F.; Rudolph, M.; Hashmi, A. S. K. *Chem. Commun.* **2016**, *52*, 6435.

(44) Tlahuext-Aca, A.; Hopkinson, M. N.; Daniliuc, C. G.; Glorius, F. *Chem. Eur. J.* **2016**, *22*, 11587.

(45) Chu, J.; Munz, D.; Jazzar, R.; Melaimi, M.; Bertrand, G. *J. Am. Chem. Soc.* **2016**, *138*, 7884.

(46) Winston, M. S.; Wolf, W. J.; Toste, F. D. *J. Am. Chem. Soc.* **2015**, *137*, 7921.

(47) Wrackmeyer, B.; Klimkina, E. V.; Milius, W. *Appl. Organomet. Chem.* **2010**, *24*, 25.

(48) Krysiak, J.; Lyon, C.; Baceiredo, A.; Gornitzka, H.; Mikolajczyk, M.; Bertrand, G. *Chem. Eur. J.* **2004**, *10*, 1982.

(49) Huang, L.; Rominger, F.; Rudolph, M.; Hashmi, A. S. K. *Chem. Commun.* **2016**, *52*, 6435.

(50) Harkins, S. B.; Peters, J. C. *J. Am. Chem. Soc.* **2004**, *126*, 2885.

(51) Kim, Y.; Zhao, H.; Gabbaï, F. P. *Angew. Chem. Int. Ed.* **2009**, *48*, 4957.

(52) Lundgren, R. J.; Stradiotto, M. *Chem. Eur. J.* **2008**, *14*, 10388.

(53) Grimme, S. *J. Comput. Chem.* **2006**, *27*, 1787.

(54) Gaussian 09, Revision D.01, Frisch, M. J.; Trucks, G. W.; Schlegel, H. B.; Scuseria, G. E.; Robb, M. A.; Cheeseman, J. R.; Scalmani, G.; Barone, V.; Mennucci, B.; Petersson, G. A.; Nakatsuji, H.; Caricato, M.; Li, X.; Hratchian, H. P.; Izmaylov, A. F.; Bloino, J.; Zheng, G.; Sonnenberg, J. L.; Hada, M.; Ehara, M.; Toyota, K.; Fukuda, R.; Hasegawa, J.; Ishida, M.; Nakajima, T.; Honda, Y.; Kitao, O.; Nakai, H.; Vreven, T.; Montgomery, J. A., Jr. ; Peralta, J. E.; Ogliaro, F.; Bearpark, M.; Heyd, J. J.; Brothers, E.; Kudin, K. N.; Staroverov, V. N.; Kobayashi, R.; Normand, J.; Raghavachari, K.; Rendell, A.; Burant, J. C.; Iyengar, S. S.; Tomasi, J.; Cossi, M.; Rega, N.; Millam, J. M.; Klene, M.; Knox, J. E.; Cross, J. B.; Bakken, V.; Adamo, C.; Jaramillo, J.; Gomperts, R.; Stratmann, R. E.; Yazyev, O.; Austin, A. J.; Cammi, R.; Pomelli, C.; Ochterski, J. W.; Martin, R. L.; Morokuma, K.; Zakrzewski, V. G.; Voth, G. A.; Salvador, P.; Dannenberg, J. J.; Dapprich, S.; Daniels, A. D.; Farkas, O .; Foresman, J. B.; Ortiz, J. V.; Cioslowski, J.; Fox, D. J. Gaussian 09; Gaussian, Inc., Wallingford, CT, **2009**.

(55) Andrae, D.; Häussermann, U.; Dolg, M.; Stoll, H.; Preuss, H. *Theor. Chim. Acta.* **1990**, *77*, 123.

(56) Ehlers, A.W.; Biihme, M.; Dapprich, S.; Gobbi, A.; Hijllwarth, A.; Jonas, V.; Kiihler, K.F.; Stegmann, R.; Veldkamp, A.; Frenking, G. *Chem. Phys. Chem.* **1993**, *208*, 111.

(57) a) Fukui, K. *Acc. Chem. Res.* **1981**, *14*, 363. (b) Hratchian, H. P.; Schlegel, H. B. Finding minima, transition states, and following reaction pathways on ab initio potential energy surfaces. In *Theory and Applications of Computational Chemistry: The First 40 Years*; Dykstra, C. E., Frenking, G., Kim, K. S., Scuseria, G., Eds.; Elsevier: Amsterdam, **2005**, 195.

(58) Marenich, A. V.; Cramer, C. J.; Truhlar, D. G., *J. Phys. Chem. B*, **2009**, *113*, 6378.

3 Development of C-C Cross Coupling Reactions with Ar-X

3.1 State of the Art of Cross Coupling with Gold

The importance of organic molecules maybe hinted at by considering their omnipresence in the world around us. Not only they compose the building blocks of living organisms but they are also found in pharmaceuticals, agrochemicals, fuels, polymers and a vast number of other widely varied areas. Methods to synthesize these sophisticated molecules are in high-demand, since the construction of these compounds usually requires multi-step processes involving the assembly of fragments and addition of new functionalities at sites possessing high chemical reactivity (*e.g.* multiple bonds, halogen, heteroatom...) to create new carbon-carbon bonds.

Over the last few decades, homo- and cross-coupling reactions catalyzed by transition metals under homogeneous conditions have emerged as powerful tools for the mild and selective coupling of a range of functionalized organic compounds. These types of reactions are well known with about all mid and late transition metals. In particular, palladium-catalyzed processes such as the Mizoroki-Heck, Negishi, and Suzuki-Miyaura reactions have revolutionized the way chemists approach synthetic challenges and were recognized with the 2010 Nobel Prize in Chemistry. The mechanism of the various cross-coupling reactions (with the exception of the Heck reaction), includes three stages: oxidative addition of aryl halides, transmetallation (with organoboron, organozinc, or organomagnesium reagents obtained from the prefunctionalization of the corresponding hydrocarbons), followed by reductive elimination to liberate the desired product and regenerate the catalyst.

Along with the requirement of green chemistry for atom-economy and step-economy transformations in modern chemistry for constructing new chemical bonds, more efforts were devoted to develop novel synthetic methodology by directly using hydrocarbons as the

nucleophiles to achieve C-H functionalizations. This class of reactions, which avoids the need for pre-installing functional groups in order to perform the desired transformation, holds a great potential for shorter and less wasteful routes to both bulk and fine chemicals. Furthermore, the ability to selectively functionalize any given C-H bond in a complex molecule would allow facile late-stage functionalization thus speeding up the development of new pharmaceutical and agrochemicals.

Although many metals have been studied, gold is often overlooked in the C-H functionalization field. This is even more surprising when considering the mild conditions under which gold can functionalize C-H bonds. In fact, gold(III) salts have been recognized early on to readily perform Csp^2-H bond activation. The functionalization of aryl C-H bonds by gold(III) was first reported by Kharasch and Isbell in 1931.[(1)] Adding gold(III) chloride to benzene at room temperature led to the evolution of gaseous hydrogen chloride followed by the precipitation of gold(I) chloride indicating the formation of chlorobenzene. Kharasch and Isbell proposed a mechanism involving an electrophilic aromatic substitution step onto $AuCl_3$ leading to phenyl gold(III) species that undergoes a C-Cl reductive elimination step to form chlorobenzene and AuCl (Scheme 3.1).

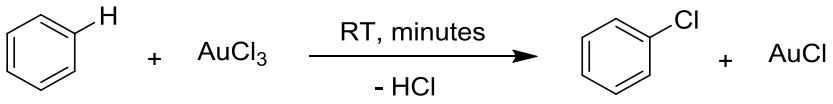

Scheme 3.1 Chlorination of benzene with $AuCl_3$.

But for the true potential of gold-mediated C-H functionalization to be realized, the process must be made catalytic. For this to occur, the gold(I) species formed upon reductive elimination must be re-oxidized to the electrophilic gold(III) at some stage in the catalytic cycle. Unlike for other late transition metals, this elementary step is considered to be

unfavorable with gold (see Chapter 2). Recent studies have shown that this limitation can be overcome by using (i) strong external oxidants or (ii) strong electrophiles under thermal or photochemical conditions which give access to the gold(III) oxidation state. Although aware of the existence of other gold-catalyzed cross-coupling reactions (C-N, C-O, C-S, C-X, C-P, Csp^2-Csp, Csp^2-Csp^3 and Csp-Csp),[2-7] only Au(I)/Au(III)-mediated Csp^2-Csp^2 bond formation will be discussed in this section.

3.1.1 Cross Coupling with External Oxidants

The first gold-catalyzed intermolecular aryl-aryl bond-forming reactions from Csp^2-H bonds were homocouplings. Tse and Beller reported in 2008 the formation of biaryls through oxidative coupling (dimerization) of electron-rich arenes.[8,9] In this reaction, $PhI(OAc)_2$ is used as the stoichiometric oxidant, $HAuCl_4$ as the catalyst and a large excess of the arenes in acetic acid (Scheme 3.2). Under these conditions, a variety of simple arenes could be homocoupled. Only limited mechanistic insight was provided by Tse and coworkers: the oxidative coupling was proposed to proceed *via* double C-H activation, most likely at a gold(III) species, followed by a reductive elimination to release the homocoupling products. They also attempted to achieve the cross- coupling but the selectivity was poor even when one of the arenes was used in large excess.

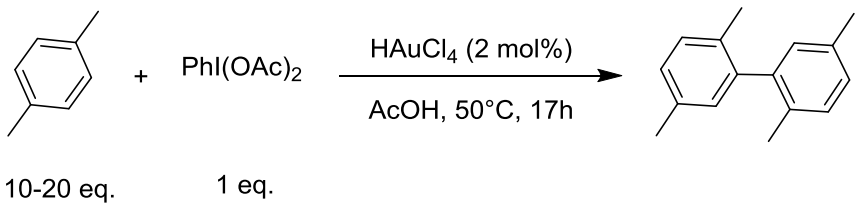

Scheme 3.2 Oxidative homocoupling of arenes by Tse *et al.*

A solution to this selectivity issue was provided in 2012 by Lloyd-Jones and Russel who proposed the use of a trimethylsilyl group on one of the coupling partners, and thus replacing one C-H functionalization step by the activation of a Csp^2-Si bond.[10] The improved efficiency is remarkable: now, instead of using a large excess of one of the coupling partners, they can be both used in equimolar amounts and the arenes are now the limiting reagents. The cross-coupled biaryls are obtained in high yields at room temperature using [(PPh_3)Au(OTs)] as a catalyst and $PhI(OAc)_2$ as the external oxidant (Scheme 3.3).

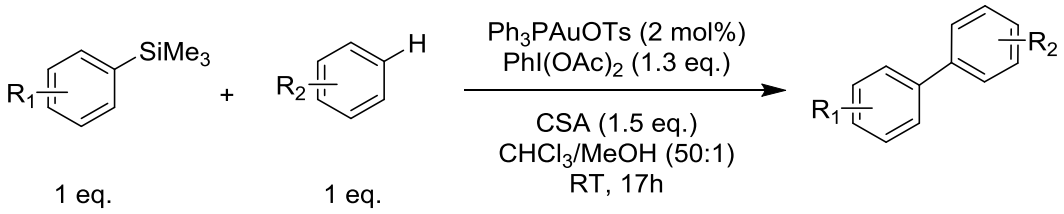

Scheme 3.3 Gold-catalyzed direct arylation.

The mechanism of this reaction was meticulously studied by means of kinetic analyses and a detailed catalytic cycle was established.[11] It was shown that the gold catalyst was phosphine-free (*i.e.* coordinated by methanol, camphorsulfonic acid and the respective conjugate bases) and that the electrophilic C-Si auration (step A) takes place before the C-H auration (step B). Competition experiments and Hammett plots showed that electron-donating groups on arylsilanes and arenes accelerate the auration steps which is more consistent with an electrophilic aromatic substitution pathway than σ-bond metathesis. Then the diarylgold(III) complex undergoes reductive elimination (step C) to release the cross-coupled product and re-oxidation of the gold(I) species by the external oxidant regenerates the catalyst (step D). A simplified catalytic cycle is represented in Scheme 3.4.

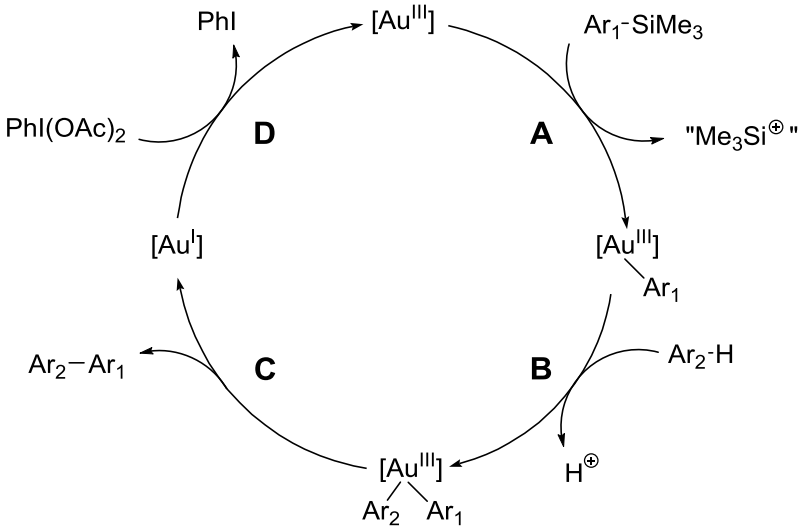

Scheme 3.4 Simplified catalytic cycle for the gold-catalyzed direct arylation.

In 2015, Itami and coworkers, using the same strategy to achieve high selectivity of cross-coupling, proposed the C-H functionalization of heterocycles with arylsilanes.[12] The authors showed that this reaction was more efficient with strong electron-donating ligands such as PyC (3,5-bis(2,6-dimethylphenyl)-1-mesityl-2pyridylidene) (Scheme3.5).

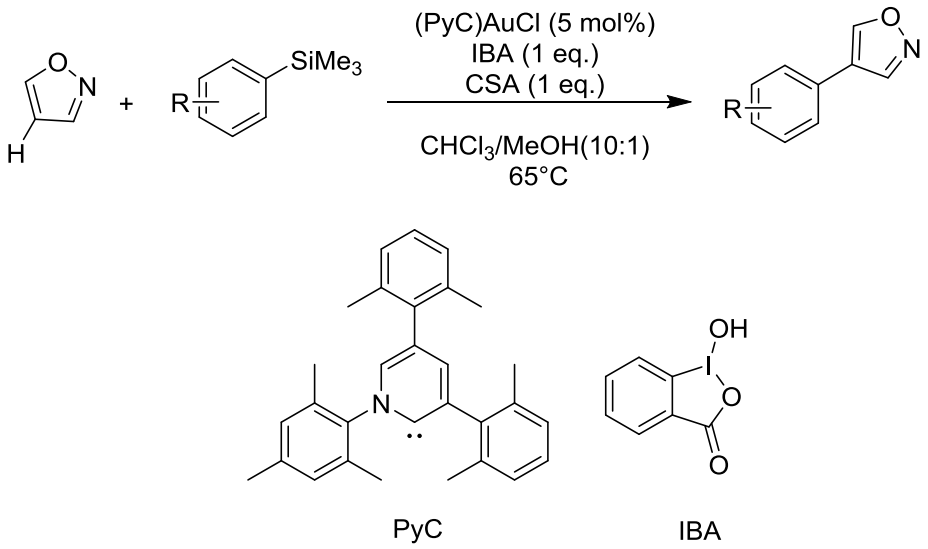

Scheme 3.5 Gold-catalyzed oxidative C-H arylation of heterocycles facilitated by PyC ligand.

They claim that this non-classical N-heterocyclic carbene ligand facilitates the oxidation of gold(I) and stabilizes more efficiently the resulting gold(III) species (*vs.* triphenylphosphine and classical N-heterocyclic carbenes), thereby facilitating the oxidative coupling reaction. The reaction mechanism was proposed to proceed first *via* C-Si auration at gold(III), followed by the electrophilic metalation of the heteroarene. The reductive elimination from the bis(arylated)gold(III) species releases the desired product and re-oxidation of the gold(I) specie regenerates the catalyst.

Another highly selective catalytic aryl-aryl cross-coupling reaction was recently reported by Larrosa and coworkers.[13] Based on the orthogonal reactivity of Au(I)/Au(III) complexes towards C-H activation of electron-poor/electron-rich arenes respectively, an oxidative cross coupling protocol was developed. While gold(I) auration (in the presence of a base) proceeds through a concerted metalation-deprotonation pathway, gold(III) follows an electrophilic aromatic substitution pathway, hence selectively functionalizing the electron-rich arene (the least acidic). The reactions are performed with the electron-rich arene as the limiting reagent, five equivalents of the electron-poor arene and 1.5 equivalents of PBX (1-pivaloyloxy-1,2-benziodoxol-3(1*H*)one) as the external oxidant (Scheme 3.6).

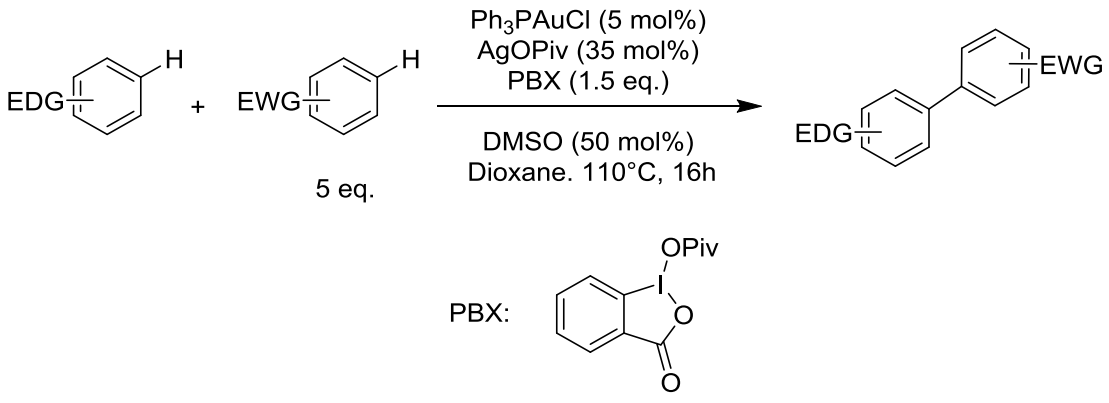

Scheme 3.6 Cross-coupling *via* double C-H activation by Larrosa *et al.*

Besides from displaying excellent cross-coupling selectivity, the reactions are also highly regioselective with only one regioisomer observed in most cases. Larrosa *et al.* proposed a catalytic cycle that starts with a gold(I) species that metalates the arene which contains the most acidic C-H bond (Scheme 3.7, step A). The generated arylgold(I) intermediate is then oxidized to generate the electrophilic arylgold(III) complex (step B). Selective C-H activation of the electron-rich arene was then proposed to give the bis(aryl)gold(III) complex (step C), which undergoes rapid reductive elimination step to afford the biaryl product and close the catalytic cycle (step D).

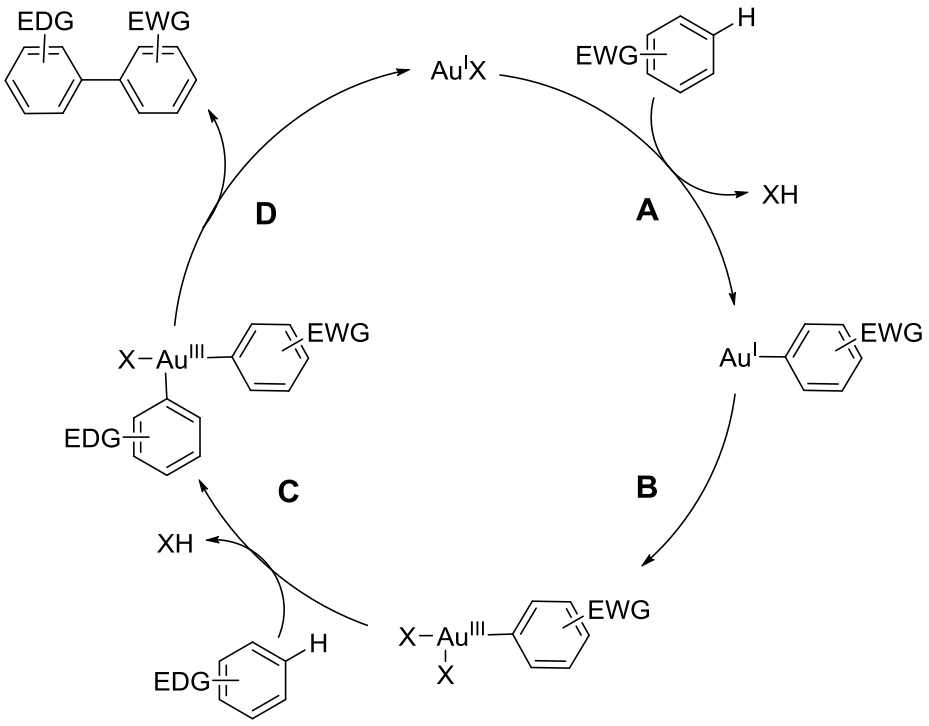

Scheme 3.7 Proposed catalytic cycle for the gold-catalyzed cross-coupling *via* double C-H activation.

Another example, illustrating the orthogonal reactivity of Au(I)/Au(III) complexes, was published very recently by Nevado and coworkers. This time the selectivity is achieved by the activation of strong electron-deficient aryl boronates with a neutral gold(I) complex followed by the activation of arenes after oxidation of the catalyst with a sacrificial oxidant.[(14)] The

reactions are performed in 1,2-dichloroethane, with the electron-poor aryl boronic ester as the limiting reagent, two equivalents of the rich arene and 1.2 equivalents of $PhI(OAc)_2$ as the external oxidant. A gold(I) catalyst bearing an acetato ligand as an internal base was selected to facilitate the B/Au(I) transmetallation step (Scheme 3.8).

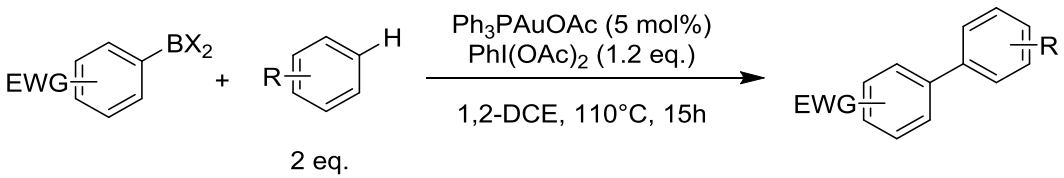

Scheme 3.8 Gold-catalyzed oxidative arylation with boron coupling partners.

In order to maintain high selectivity, the scope with respect to the boronic esters is limited, and only perfluorinted substrates were coupled. As for the arene coupling partner, the scope is broader and a series of simple arenes (different xylenes, anisoles, toluene and benzene) was shown to undergo the C-H activation reaction. The reaction is proposed to be initiated by a selective B/Au(I) transmetalation of $Ph_3PAuOAc$ with the electron-deficient boronic ester to form an arylgold(I) complex (Scheme 3.9, step A). This intermediate is oxidized by $PhI(OAc)_2$ to form the bis(acetate)aryl gold(III) species (step B). Activation of the arene by an electrophilic aromatic substitution process is suggested to form the bis(aryl)gold(III) complex (step C). Subsequent reductive elimination produces the Csp^2-Csp^2 coupling product and regenerates the gold(I) catalyst (step D).

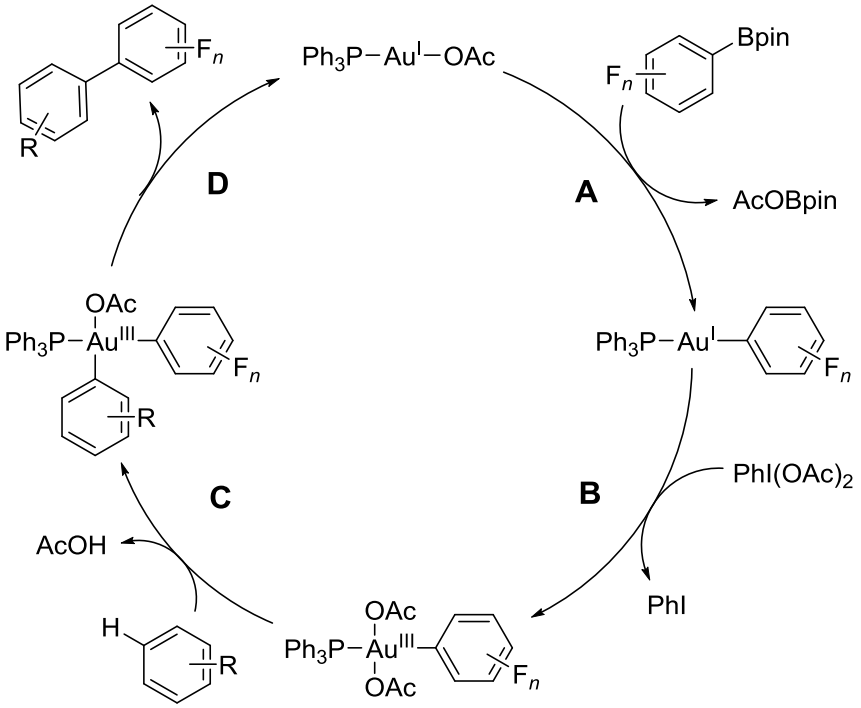

Scheme 3.9 Proposed catalytic cycle for the gold-catalyzed oxidative arylation with boron coupling partners.

J. You and coworkers provided a detailed experimental and mechanistic study for gold(III)-catalyzed oxidative cross-coupling between arylboronic acids and arenes.[15] Taking advantage of chelation-assisted C-H bond activation, well-defined gold(III) complexes were prepared and their reactivity towards arylboronic acids was investigated (Scheme 3.10). A series of *meta*- and *para*- phenylboronic acids bearing either electron-donating or electron-withdrawing substituents delivered the desired coupling products, whereas *ortho*-substituted arylboronic resulted in low yields probably due to steric effect. Other biaryls containing *N*-heteroarenes also underwent the cross-coupling reactions with arylboronic acids.

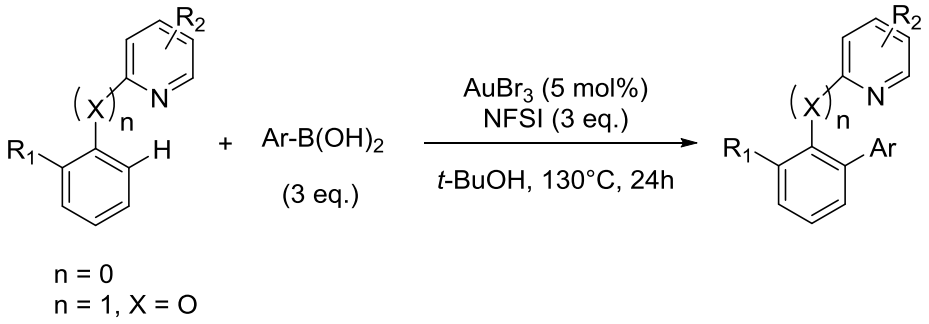

Scheme 3.10 Gold-catalyzed directed C-H arylation of arenes with arylboronic acids.

N-fluorobenzenesulfonimide (NFSI) was used as an external oxidant to access the +III oxidation state of gold, and to generate Au-F species that were shown to assist the C-B bond cleavage during the transmetallation step. Moreover, stoichiometric tests and HRMS (ESI+) analyses indicated that the transmetallation occurs in this case from boronic acid to gold(III) and not to gold(I). Based on these observations, the authors proposed a plausible mechanistic pathway for this cross coupling reaction (Scheme 3.11). The first step is the fast coordination of a gold(III) species to the *N*-heterocyclic biaryl (step A), followed by a C-H bond auration to give the cyclometallated species (step B). Then this gold(III) complex undergoes a transmetallation reaction with the arylboronic acid (step C) to afford the biaryl gold(III) intermediate. The reductive elimination reaction generates the desired biaryl product along with a gold(I) species (step D). Finally, the gold(I) complex is reoxidized by NFSI to complete the catalytic cycle (step E).

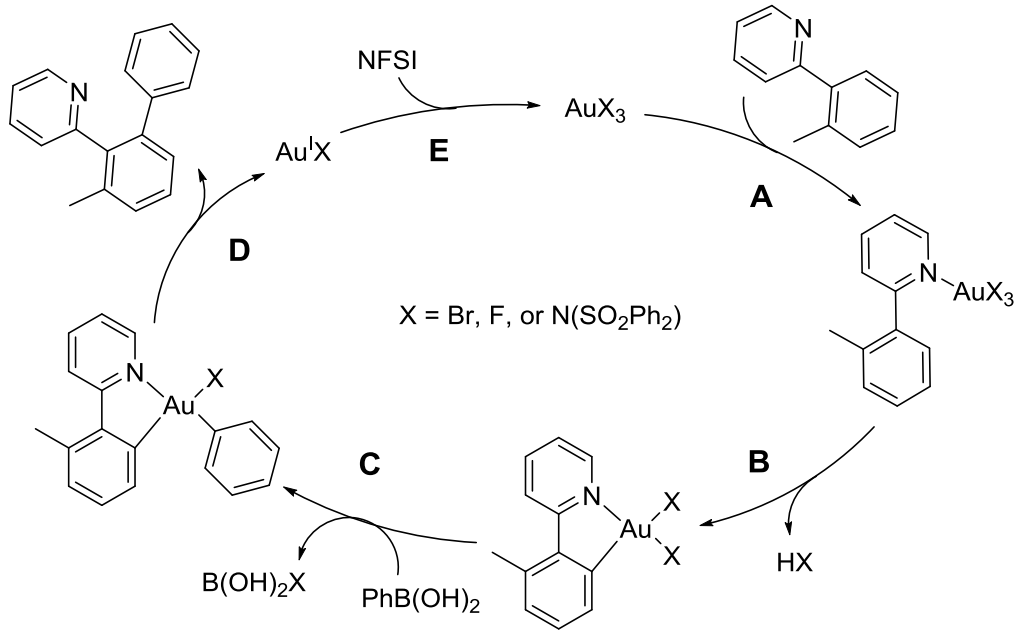

Scheme 3.11 Proposed catalytic cycle for the gold-catalyzed directed C-H arylation of arenes with arylboronic acids.

The above-mentioned transformations describe efficient and selective Csp^2-Csp^2 cross-coupling reactions. However, the necessity to use stoichiometric amount of an external oxidant to promote the Au(I)/Au(III) transition is a major drawback. In fact, due to their strong oxidizing properties, several functional groups are incompatible with these sacrificial oxidants and thereby the reaction scope is somehow limited. These conditions diminish the attractive features of gold catalysis which are mild reaction conditions and excellent functional group tolerance. In order to circumvent these harsh conditions, some other strategies have been reported to perform the Csp^2-Csp^2 cross-coupling *via* a Au(I)/Au(III) redox cycle.

3.1.2 Cross-Coupling with Strong Electrophiles

To get rid of the strong sacrificial oxidant, the use of strong electrophiles (aryldiazonium or diaryliodonium salts) emerged as an efficient strategy to access the gold(III) oxidation state. The oxidation of gold(I) with strong electrophiles is regularly assisted by a photoredox catalyst or by visible light.

A.-L. Lee and coworkers reported a dual gold photoredox biaryl coupling reaction under visible light conditions.[16] With $Ph_3PAuNTf_2$ as the gold(I) catalyst and $[Ru(bpy)_3](PF_6)_2$ as the photocatalyst, they successfully coupled a wide scope of aryldiazonium salts with aryl boronic acids (Scheme 3.12). The reaction was found to be tolerant to a range of different functional groups. For the arylboronic acids, higher yields were obtained with electron-donating groups, whereas for the aryldiazonium salts, the opposite was observed. This trend allowed good yields to be achieved by the judicious choice of coupling partners.

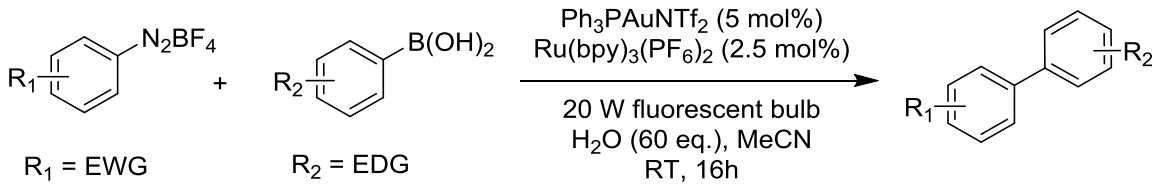

Scheme 3.12 Dual gold/photoredox Csp^2-Csp^2 coupling.

The authors suggested that the reaction proceeds through two different mechanisms depending on the nature of the gold(I) catalyst. In the case of $Ph_3PAuNTf_2$, the cationic gold(I) complex undergoes first transmetallation with the arylboronic acid to form the corresponding arylgold(I) species prior to the addition of the arene radical and oxidation to Au(II). But, in the case of the neutral Ph_3PAuCl complex, the oxidation of the Au(I) species to Au(II) occurs before the B/Au transmetallation. In both cases, after the addition of the radical,

a single electron transfer (SET) from the photocatalyst to the gold(II) species will afford bis(aryl)gold(III) complexes that undergoes then reductive elimination to release the products. The postulated catalytic cycle for the cationic gold(I) complex is represented in Scheme 3.13.

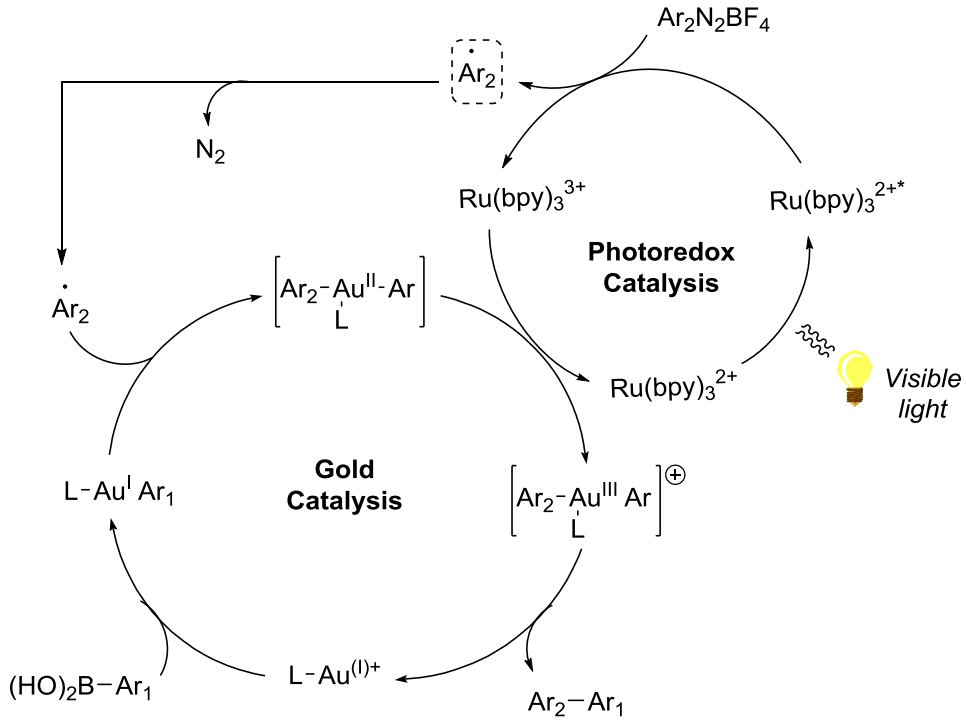

Scheme 3.13 Proposed catalytic cycle for the dual gold/photoredox cross coupling.

The cross-coupling reaction between aryl boronic acids and aryldiazonium salts was found to be an efficient method to access biaryl compounds and was further improved. Indeed, X. Shi and coworkers showed that this Csp^2-Csp^2 coupling is still working without the use of a photocatalyst (Scheme 3.14).[17] In fact, during their control experiments, almost identical kinetics and yields were obtained under either standard or dark conditions in the absence of the photocatalyst, which contradicted the involvement of a photocatalytic process. This result implies that the aryldiazonium salt alone, in this reaction, might be capable of oxidizing the gold(I) species into gold(III). The addition of catalytic amounts of 2,2'-bipyridine (bpy) to the

reaction media helps to achieve full conversion and the authors suggested that bpy acts as an ancillary ligand assisting dinitrogen extrusion from aryldiazonium salts.

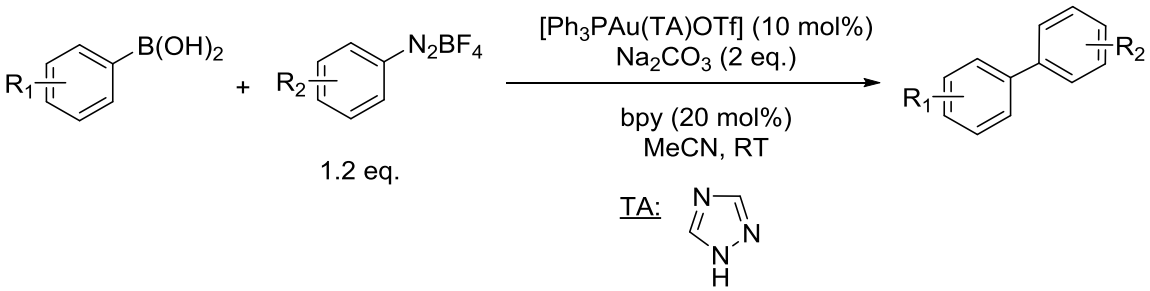

Scheme 3.14 Gold-catalyzed cross-coupling with aryldiazonium salts without a photocatalyst.

Under these reaction conditions, various substituted aryl boronic acids and diazonium salts bearing electron-donating or electron-withdrawing afforded the cross coupling products in good yields. The proposed catalytic cycle (Scheme 3.15) involves first a transmetallation from boron to the cationic gold(I) species (step A). The formed arylgold(I) complex undergoes oxidation with aryldiazonium salts (step B) affording a bis(aryl)gold(III) species and the N_2 extrusion is assisted by 2,2'-bipyridine (step C). After reductive elimination, the biaryl compound is formed and the initial gold(I) species is regenerated (step D).

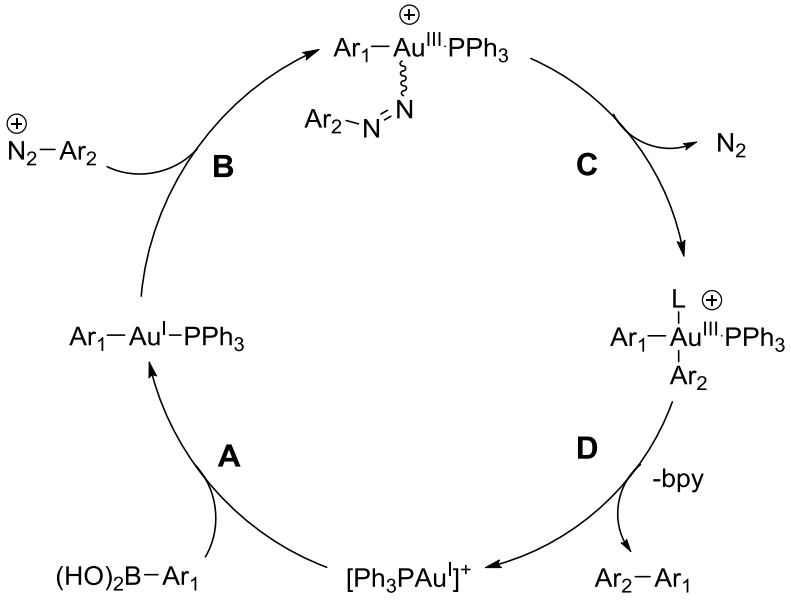

Scheme 3.15 Proposed catalytic cycle for the gold-catalyzed cross-coupling without a photocatalyst (L = bpy).

Even though in the above-mentioned reaction, X. Shi and coworkers got rid of the expensive Ru(II) photocatalyst, the addition of a base and an ancillary ligand is required to reach full conversion.

In a very recent report, Hashmi *et al.* improved further the Csp^2-Csp^2 cross-coupling between boronic acids and diazonium salts. This time, the two partners are coupled together under visible light irradiation and without the use of a photocatalyst or a base.[18] The reactions are performed in methanol with a neutral gold(I) complex bearing an electron-poor phosphine ($[4\text{-}CF_3\text{-}C_6H_4]_3P$) and under blue LEDs irradiation (Scheme 3.16). Under these conditions, the reaction provides various biaryls in good yields under very mild conditions.

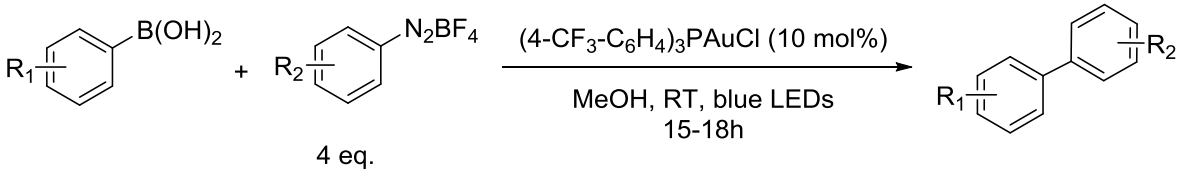

Scheme 3.16 Gold-catalyzed cross-coupling with aryldiazonium salts without a photocatalyst or base.

A possible reaction mechanism for the cross-coupling was proposed by the authors (Scheme 3.17). As mentioned above, with a neutral gold(I) complex, the oxidation of the Au(I) species by the diazonium salt occurs before the transmetallation of the aryl moiety from B to Au. Accordingly, the reaction is possibly initiated by a gold-induced single electron transfer to the aryldiazonium salt, generating an aryldiazo radical and gold(II) species (step A). Then, the aryl radical oxidizes the gold(II) to a gold(III) complex (step B) followed by the elimination of N_2 with the assistance of light (step C). The transmetallation of the *in situ* activated aryl boronic acid affords the bis(aryl)gold(III) complex (step D), that undergoes a fast reductive elimination to deliver the biaryl and completes the catalytic cycle (step E).

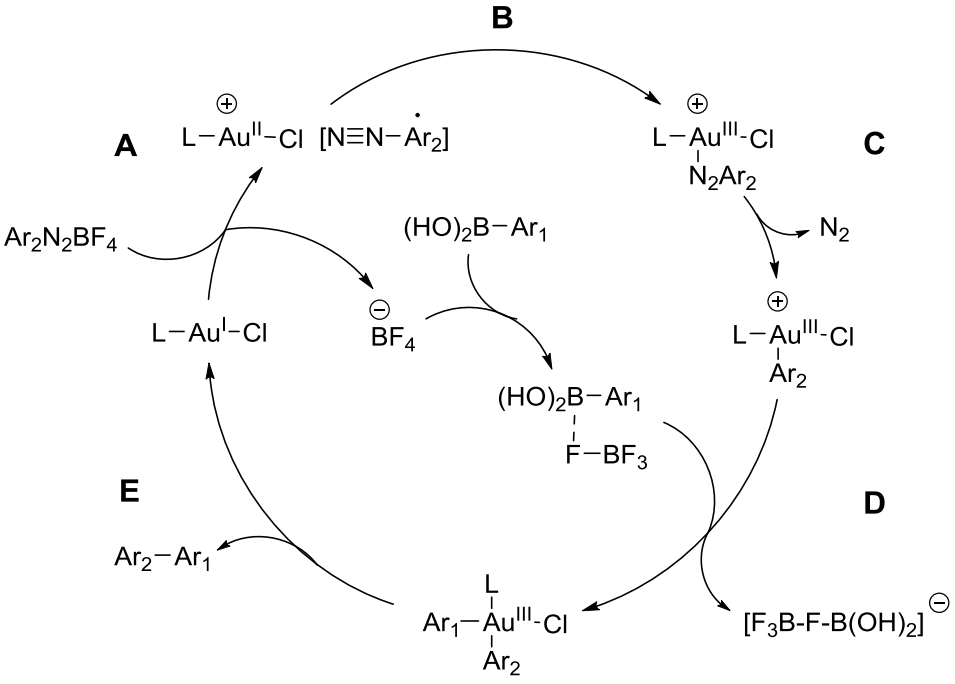

Scheme 3.17 Proposed reaction mechanism for the cross-coupling reaction without a photocatalyst or a base.

In a recent report by Lee and coworkers, the aryl-aryl cross-coupling *via* Csp^2-H activation using dual gold and photoredox catalysis was demonstrated for the first time.[19] With PPh_3AuNTf_2 as the gold(I) catalyst and $[Ru(bpy)_3](PF_6)_2$ as the photocatalyst, they

successfully coupled a wide scope of aryldiazonium salts with arenes at room temperature under blue LED irradiation (Scheme 3.18). However, under these conditions, the reaction was shown to have some electronic restrictions. In fact, electron-rich aryldiazonium salts reacted more sluggishly and electron-poor arenes afforded lower yields.

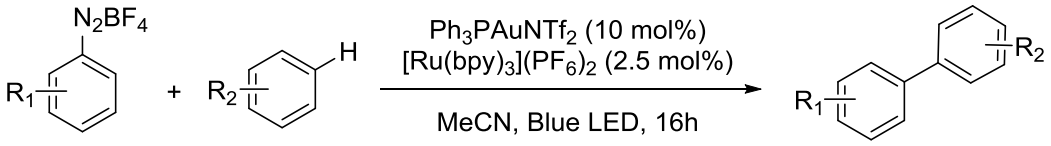

Scheme 3.18 Dual gold and photoredox catalyzed C-H activation of arenes for Csp^2-Csp^2 coupling.

The authors proposed a plausible reaction mechanism for the cross-coupling reaction. The first step is the oxidation of the gold(I) catalyst by an aryl radical, followed by a single electron transfer to form the gold(III) aryl species and to regenerate the photocatalyst. Then, the arene undergoes an electrophilic auration with the gold(III) complex to give the bi(aryl) gold(III) intermediate. Subsequent reductive elimination reaction produces the Csp^2-Csp^2 coupling product and close the catalytic cycle.

The use of strong electrophiles such as aryldiazonium salts is indeed an elegant strategy to circumvent the use of strong external oxidants and access the +III oxidation state of gold. Despite it's fast improvement (no photocatalyst or base), this methodology is hindered by the hazardous nature of aryldiazonium substrates due to the highly energetic diazo moiety and thus potential of explosion. Consequently these reactions are usually advised to be performed in small scales. Moreover, the aryldiazonium substrates are not readily available (in most cases) and have to be prepared unlike "traditional" electrophiles (aryl halides).

In this section, some examples of gold-catalyzed Csp^2-Csp^2 cross coupling reactions were presented. However, these reactions require an external oxidant or a strong electrophile to

achieve the Au(I)/Au(III) redox cycle, and high selectivity for cross-coupling (*vs.* homocoupling) necessitates usually electronically different coupling partners (one electron-rich and one electron-poor aryl ring). Nonetheless, these contributions highlights the ability of gold species for Csp^2-H bond activation or transmetallation and the easiness of Csp^2-Csp^2 reductive elimination at gold.[20,21]

3.2 Rational Construction of a Csp^2-Csp^2 Catalytic Cycle

Having substantiated that oxidative addition of aryl halides to gold(I) occurs readily with the *o*-carborane complex **6** and with the MeDalphos complex **10**, we then sought to go beyond this elementary step. Due to the known ability of gold(III) complexes for (i) Csp^2-H bond activation of arenes and heteroarenes *via* electrophilic aromatic substitution and for (ii) fast Csp^2-Csp^2 reductive elimination from bi(aryl)gold(III) complexes, it was very appealing to investigate the reactivity of our arylgold(III) complexes for direct arylation processes. We thus envisioned to construct a catalytic cycle where the first step would be the oxidative addition of aryl halides to generate the arylgold(III) complex (step A), followed by the electrophilic C-H activation of a rich arene (step B). Reductive elimination from the bis(aryl)gold(III) species (step C) would then close the cycle with the formation of the biaryl compound and regeneration of the initial gold(I) species (Scheme 3.19).

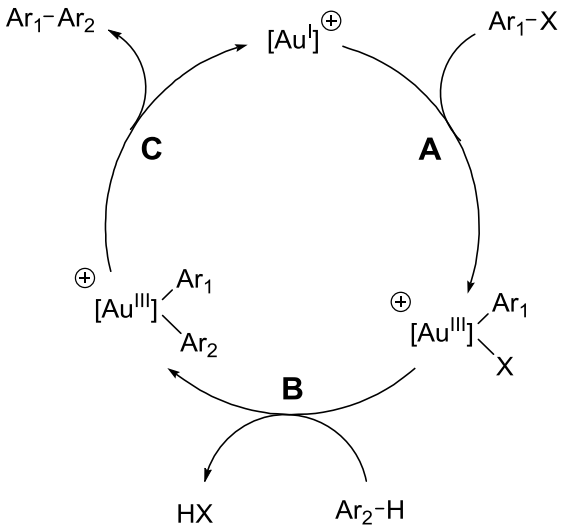

Scheme 3.19 Hypothetical Au(I)/Au(III) catalytic cycle for CC coupling of aryl halides and arenes.

3.2.1 Model Stoichiometric Reactions

Since the oxidative addition of aryl iodides to complex **10** affords stable gold(III) complexes (*vs. o*-carborane bis(phosphine) gold(III) complex **7**), we first evaluated the coupling between iodobenzene and 1,3,5-trimethoxbenzene (TMB) with complex **10**. The transformation was first performed under stoichiometric conditions, by reacting the arylgold(III) complex stemming from the oxidative addition of PhI with one equivalent of TMB at room temperature. Under these conditions, GC-MS analysis of aliquots taken from the reaction media revealed the presence of an organic fragment with the same molecular weight as the desired cross-coupling product, but being formed very slowly. However, addition of one equivalent of silver hexafluoroantimonate increased dramatically the reaction rate. This is most likely due to the increase of the electrophilicity of the gold(III) center after abstracting the iodine from complex **12** with $AgSbF_6$. After twelve hours of reaction, a classical work-up afforded the desired biaryl product in 90% isolated yield (Scheme 3.20).

The ^{1}H NMR confirmed the formation of the desired product, 2,4,6-trimethoxy-1,1'-biphenyl, and it is consistent with that previously reported in the literature.

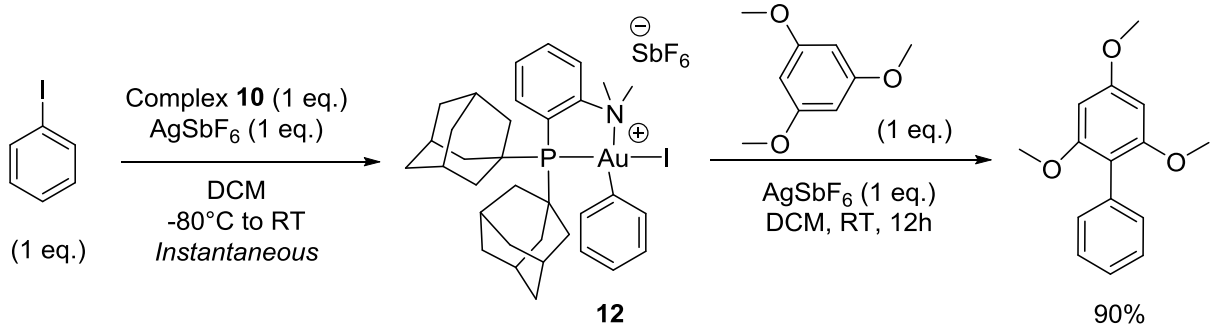

Scheme 3.20 Cross-coupling of PhI and TMB with complex **10** under sequential conditions.

Stimulated by this preliminary result, we tested the same reaction in a one-step manner since our goal is to develop a catalytic cycle. To do so, a solution of iodobenzene (1 eq.), 1,3,5-trimethoxybenzene (1 eq.) and complex **10** in dichloromethane was added to a solution of $AgSbF_6$ (2 eq.) at room temperature. Encouragingly, the coupling reaction proceeded equally well (Scheme 3.21).

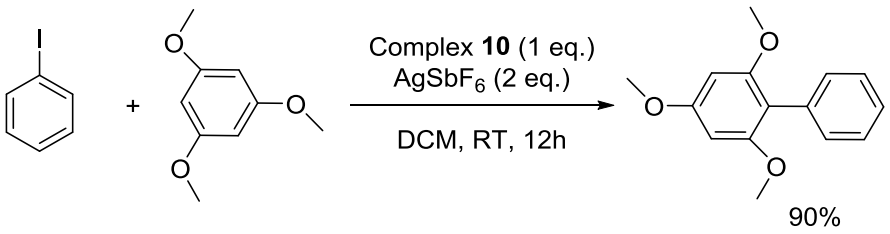

Scheme 3.21 Cross-coupling of PhI and TMB with complex **10** in one-pot manner.

This reaction was monitored by $^{31}P\{^{1}H\}$ NMR and it revealed the formation of a new species at δ 76.7 ppm. This phosphorus-containing complex could not been characterized, and was

gradually converted to a new complex with a chemical shift at δ 51.2 ppm. Crystals suitable for X-Ray diffraction spectroscopy were obtained from the reaction media and were analyzed. The species at δ 51.2 ppm was the starting gold(I) complex but with a molecule of water coordinated to gold instead of chloride. This result confirms that, at the end of the reaction, a mono-nuclear gold(I) complex is formed, which is encouraging for the catalytic version of this reaction.

At this stage, we decided to start optimizing the reaction conditions and several parameters (phosphorus substituents, halide scavenger, solvent and co-solvent) were thus examined. In order to carry out this optimization study, the GC-MS was calibrated with the isolated 2,4,6-trimethoxy-1,1'-biphenyl *vs. n*-dodecane as an internal standard.

The effect of the phosphorus substituents on the direct arylation reaction was the first parameter we examined. The oxidative addition of iodobenzene with the chloro[(diphenyl)-2-dimethylaminophenylphosphine]gold(I) complex **13** and the chloro[(diisopropyl)-2-dimethylaminophenylphosphine]gold(I) complex **14** was already tested (see 2.4.5). Like with complex **10**, the reactivity of these two gold(I) species was assessed towards the coupling of PhI and TMB under the same reaction conditions (Scheme 3.22). After five hours at room temperature with complex **13**, GC-MS analysis confirmed the formation of the biaryl compound in 21% yield. This result proved that the oxidative addition of iodobenzene to complex **13** was feasible, and the low yield is most likely caused by the instability of the corresponding arylgold(III) species. On the other hand, after five hours at room temperature, complex **14** and complex **10** afforded the coupling product in 44% and 50% yields, respectively, as indicated by GC-MS. Even though the oxidative addition of iodobenzene with complex **14** requires 45 minutes to reach full conversion (*vs*. instantaneous with complex **10**), the reactivity of both complexes for the cross-coupling reaction is quite similar.

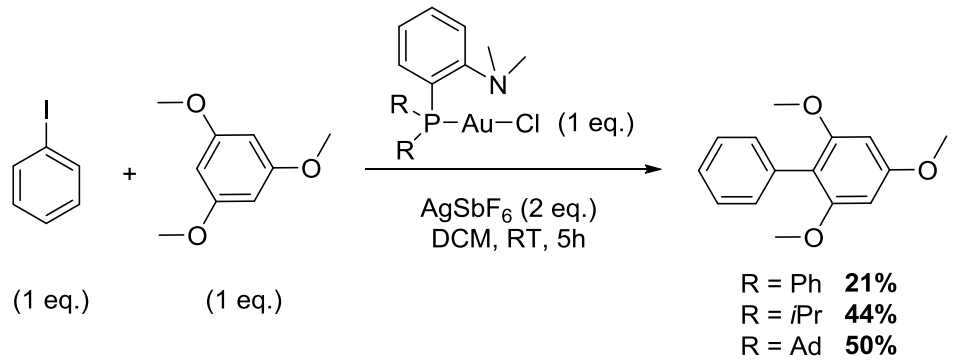

Scheme 3.22 Effect of the phosphorus substituents on the cross-coupling of PhI and TMB.

After verifying that complex **10** exhibits higher reactivity for the cross-coupling transformation, different halide scavengers, solvents and additives were then tested to try to improve the efficiency and the rate of this reaction (Table 3.1). The influence of different silver salts was first investigated (entry 1-4). With silver oxide (Ag_2O) and silver camphorsulfonate (AgCSA), the coupling product was not detected by GC-MS even after twelve hours at room temperature. This can be explained by the strong coordination of CSA^- or AgO^- anions to the gold(I) center after chloride abstraction, thus preventing the oxidative addition reaction. When tetrafluoroborate is used as a weakly coordinated counter anion, the cross-coupling reaction occurs but the desired compound is formed in only 10% yield. This is probably due to undesired side reactions between the gold(I) center and the tetrafluoroborate anion. After this small screening, silver hexafluoroantimonate was the most suited chloride scavenger for the cross coupling reaction.

We then studied the effect of the solvent on the reaction. As a result of the poor solubility of complex **10** in dimethyl sulfoxide and dimethylformamide, the cross-coupling product could not be detected by GC-MS after five hours (entry 5-6). On the other hand, in trifluoroacetic acid, no solubility issue was observed, but the desired reaction didn't occur as well, probably due to the coordination of the solvent or $CF_3CO_2^-$ to the gold(I) center after chloride

abstraction (entry 7). When 1,2-dichloroethane was used as the solvent (entry 8), the reaction worked pretty well (44% yield) but better result was achieved with dichloromethane.

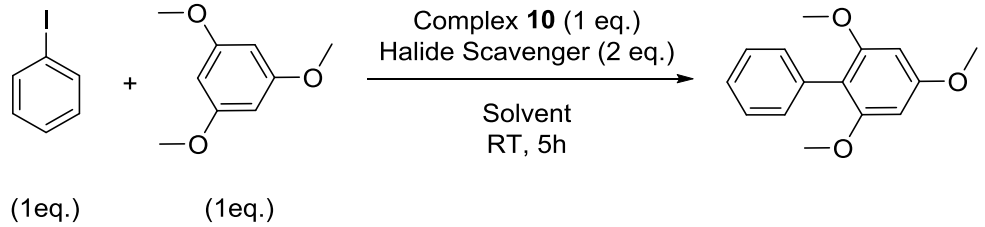

Table 3.1 Optimization of reaction conditions with iodobenzene and 1,3,5-trimethoxybenzene (screening of solvents and halide scavengers)

Entry	Halide Scavenger	Solvent	Yield (%)[a]
1	$AgSbF_6$	DCM	50%
2	Ag_2O	DCM	0%
3	AgCSA	DCM	0%
4	$AgBF_4$	DCM	10%
5	$AgSbF_6$	DMSO	0%
6	$AgSbF_6$	DMF	0%
7	$AgSbF_6$	TFA	0%
8	$AgSbF_6$	DCE	44%

[a] Yields determined using calibrated GC-MS analysis *vs. n*-dodecane as internal standard.

Finally, the influence of co-solvents on the rate of the Csp^2-Csp^2 cross-coupling reaction was investigated. In the above-mentioned examples of cross-coupling reactions with gold(I) complexes (see 3.1)[(10-12)], addition of co-solvents in small quantity improved the rate of the reactions. There is no clear evidence for their exact role, but polar additives probably help the dissociation of ion pairs in solution and thus increase the reaction rate. Based on that, we tested DMSO, TFA and methanol as co-solvents (Table 3.2). Regardless of the quantity of DMSO used (entry 2-3), the coupling product was not detected, which suggests that dimethyl sulfoxide coordinates tightly to gold(I) and prevents the reaction to occur. A very low yield

(8%) was obtained when working in dichloromethane with a small quantity of TFA (50:1) (entry 4). The most significant positive impact on the reaction rate was obtained when performing the reaction in dichloromethane with small amount of methanol (50:1) (entry 5). Under these conditions, after five hours at room temperature, a 97% yield of the coupling product could be achieved. Interestingly, increasing (entry 6-7) or decreasing (entry 8) the amount of methanol in dichloromethane resulted in lower yields.

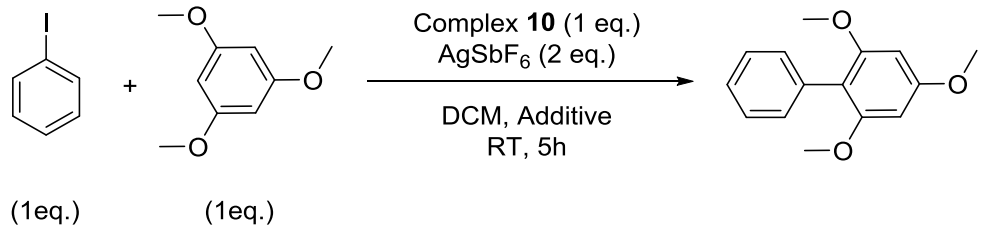

Table 3.2 Optimization of reaction conditions with iodobenzene and 1,3,5-trimethoxybenzene (co-solvent)

Entry	Co-solvent	Yield (%)[a]
1	DCM	50%
2	DCM/DMSO (50mol%)	0%
3	DCM/DMSO (50:1)	0%
4	DCM/TFA (50:1)	8%
5	DCM/MeOH (50:1)	97%
6	DCM/MeOH (1:1)	40%
7	DCM/MeOH (1:3)	30%
8	DCM/MeOH (120:1)	74%

[a] Yields determined using calibrated GC-MS analysis *vs. n*-dodecane as internal standard.

Having in hands another gold(I) complex that undergoes the oxidative addition of iodobenzene, we tested the reactivity of complex **6** towards the cross-coupling of PhI and TMB as well. The newly optimized reaction conditions were applied (dichloromethane with a small portion of methanol (50:1) was used as the solvent) except for the nature of the silver salt, since we already found that the bis(trifluoromethane)sulfonamide anion grants a good

compromise between reactivity and stability for the *o*-carborane bis(phosphine) gold(I) complex. Consequently, a solution of iodobenzene, trimethoxybenzene and one equivalent of $AgNTf_2$ was added at room temperature on a solution of the cationic gold(I) triflimidate complex **6** (Scheme 3.23).

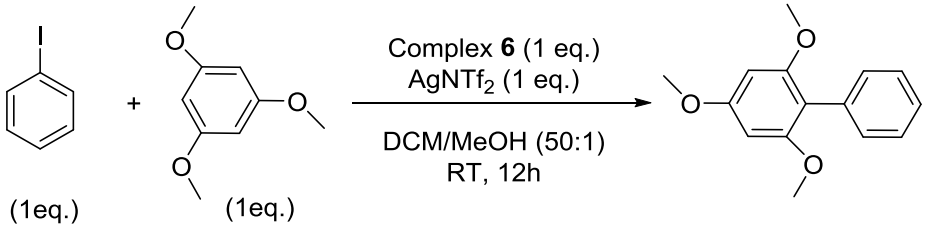

Scheme 3.23 One-pot cross coupling of PhI and TMB with complex **6**.

Unfortunately, even after twelve hours, only traces of the cross coupling product was detected by GC-MS, and this is probably due to the instability of the *o*-carborane diphosphine arylgold(III) complex.

3.2.2 Towards Catalysis

As mentioned above, monitoring the benchmark cross-coupling reaction of iodobenzene and 1,3,5-trimethoxybenzene with complex **10** by $^{31}P\{^{1}H\}$ NMR revealed the formation of a new phosphorus containing species (δ = 51.2 ppm) at the end of the reaction. Although this new complex could not be fully identified by NMR spectroscopy, the X-ray diffraction analysis confirmed the formation of a gold(I) species, which is quite promising for the envisioned catalytic reaction.

3.2.2.1 Experimental Conditions and Optimization

The next step was to translate the cross-coupling reaction of iodobenzene and 1,3,5-trimethoxybenzene with complex **10** from stoichiometric to catalytic conditions. To do so, a solution of PhI, TMB and 20 mol% of the gold complex **10** were added to a solution of 1.2 equivalents of $AgSbF_6$ in dichloromethane at room temperature. As indicated by GC-MS analysis, 2,4,6-trimethoxy-1,1'-biphenyl was obtained in 30% yield after 21 hours. Although the yield is low, this reaction demonstrated the feasibility of the catalytic transformation. Based on this promising result, we surveyed the influence of different parameters: the temperature, the catalytic loading, the ratio of the coupling partners, the halide scavenger and the presence of a base.

The first parameter we inspected was the temperature (Table 3.3). Giving the low boiling point of dichloromethane, 1,2-dichlorobenzene (DCB) was chosen as the solvent since it possesses a high boiling point (180°C) and complex **10** is perfectly soluble in it. The reaction with 20 mol% of the gold complex, one equivalent of each coupling partners and 1.2 equivalents of $AgSbF_6$ was performed at 50°C, 75°C and 100°C (entry 2-4). After 21 hours, 37% yield of the coupling product was obtained when the reaction was run at 50°C indicating that increasing the temperature improves the efficiency of the coupling reaction. Gratifyingly, at 75°C the yield was further increased to 82%, but this trend is not linear since the yield dropped to 61% when the reaction was run at 100°C. With this encouraging result, the catalytic loading of gold complex **10** was lowered and the reaction was tested at 75°C (entry 5-6). With 10 mol% of gold, a 69% yield was obtained, and even when the amount of gold was further decreased to 5 mol%, the reaction was still relatively efficient (46% yield).

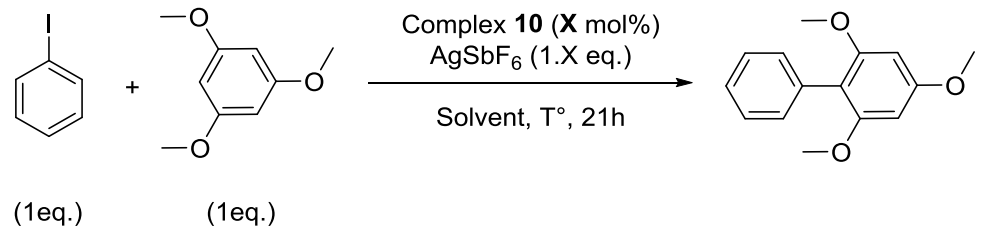

Table 3.3 Optimization of reaction conditions with iodobenzene and 1,3,5-trimethoxybenzene (T°C and [Au] loading).

Entry	[Au] loading (mol%)	Temperature (°C)	Solvent	Yield (%)[a]
1	20	25	DCM	30%
2	20	50	DCB	37%
3	20	75	DCB	82%
4	20	100	DCB	61%
5	10	75	DCB	69%
6	5	75	DCB	46%

[a] Yields determined using calibrated GC-MS analysis *vs. n*-dodecane as internal standard.

A large excess (10 equivalents) of 1,3,5-trimethoxybenzene was used in order to further increase the yield and the reaction rate. Indeed, with 5 mol% of gold and with $AgSbF_6$ as halide scavenger, the yield of the coupling product was increased from 46% in 21 hours to 88% in just 14 hours (Table 3.4 entry 1). Next, halide scavengers were screened using 10 equivalents of TMB. Coordinating counter-anions were tested again since the optimal temperature for the cross-coupling reaction is now 75°C, and at this temperature, the counter anion may dissociate more easily from the gold(I) center for the oxidative addition to occur. With sodium tetrakis[3,5-bis(trifluoromethyl)phenyl]borate ($NaBar^F$) and silver pivalate (AgOPiv), the cross coupling reaction didn't occur at 75°C (entry 2-3). On the other hand, with silver bis(trifluoromethylsulfonyl)imide (entry 4) and silver trifluoromethylsulfonate (entry 5), the reaction afforded decent yields after 21 hours (41% and 62%, respectively), but the best result was obtained with $AgSbF_6$.

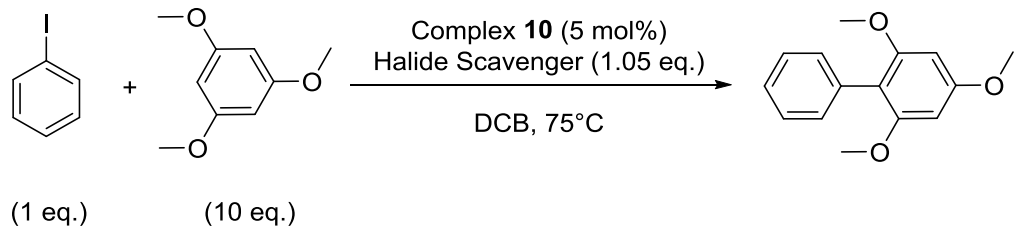

Table 3.4 Optimization of reaction conditions with iodobenzene and 1,3,5-trimethoxybenzene (halide scavenger)

Entry	Halide Scavenger	Time (h)	Yield (%)[a]
1	$AgSbF_6$	14	88%
2	$NaBar^F$	21	0%
3	AgOPiv	21	0%
4	$AgNTf_2$	21	41%
5	AgOTf	21	62%

[a] Yields determined using calibrated GC-MS analysis *vs.* *n*-dodecane as internal standard.

It is important to note that the cross-coupling reaction was tested with catalytic amounts of $AgSbF_6$ (20 or 50 mol%), but only traces of the coupling product were detected by GC-MS.

Although the yield was improved to 88%, ten equivalents of TMB are needed. The addition of precise amount of methanol in dichloromethane enhanced the stoichiometric coupling of iodobenzene and trimethoxybenzene. That's why, in the objective of decreasing the number of equivalents of TMB used, the influence of methanol on the catalytic cross coupling reaction was then assessed. With 5 mol% of complex **10** and 1.05 equivalents of $AgSbF_6$ in DCM/MeOH (50:1), the coupling reaction was conducted with different ratios of 1,3,5-trimethoxybenzene (Table 3.5). The effect of methanol on the yield and the reaction rate was remarkable. In fact, with 10, 5 and 2 equivalents of TMB, a 99% yield was obtained in just two hours at 75°C (entry 1-3) and even with one equivalent of trimethoxybenzene, the reaction was efficient (73% yield after two hours, entry 4).

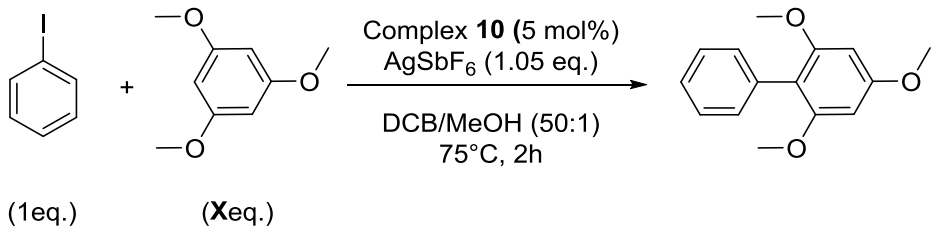

Table 3.5 Optimization of reaction conditions with iodobenzene and 1,3,5-trimethoxybenzene (TMB eq.)

Entry	TMB (X eq.)	Yield (%)[a]
1	10	99%
2	5	99%
3	2	99%
4	1	73%

[a] Yields determined using calibrated GC-MS analysis *vs. n*-dodecane as internal standard.

Before performing a wide substrate screening, 4-fluoroiodobenzene was tested to check if these new conditions can be applied to other substrates for the cross-coupling reaction without further optimization. So, the mixture of 5 mol% of complex **10**, one equivalent of 4-fluoroidobenzene and two equivalents of TMB was added to a solution of 1.05 equivalents of $AgSbF_6$ in DCM/MeOH (50:1). After two hours at 75°C, GC-MS analysis confirmed the formation of 4'-fluoro-2,4,6-trimethoxy-1,1'-biphenyl but in moderate yield (59%).

Knowing that the C-H activation process generates protons in the reaction media that can cause side reactions, we thought that the addition of a base to trap these protons may be beneficial. Since with iodobenzene, we already achieved full conversion, the base screening was realized with 4-fluoroiodobenzene (Table 3.6). Three equivalents of cesium carbonate (Cs_2CO_3) were added to the reaction media, but no impact on the yield was observed (entry 2). Cesium pivalate (CsOPiv) on the other hand quenched the cross-coupling reaction and no conversion was observed even after hours at 75°C (entry 3). This is presumably due to the strong coordination of the pivalate moiety to gold(I). With three equivalents of sodium acetate

(entry 4), the yield of the reaction was slightly improved from 59% to 62%, but potassium phosphate tribasic (K_3PO_4) afforded a higher yield (entry 5). K_3PO_4 allows for a good compromise between basicity and solubility. In fact, potassium phosphate tribasic is a quite soluble base in dichlorobenzene and its basicity allows to capture the protons released in the reaction media. Interestingly, when one equivalent of K_3PO_4 was used instead of three, a 90% yield in two hours was reached (entry 6), indicating probably the occurrence of side reactions caused by the excess of base. Moreover, 95% yield was attained with one equivalent of potassium phosphate and one equivalent of trimethoxybenzene (entry 7). Note that under these conditions, it is possible to lower the catalytic loading of gold to 1 mol% and reach 90% yield after 12 hours at 75°C (entry 8)

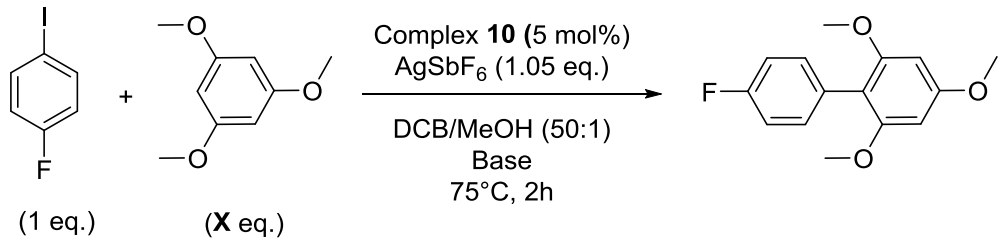

Table 3.6 Optimization of reaction conditions with 4-fluoroiodobenzene and 1,3,5-trimethoxybenzene (base).

Entry	TMB (Xeq.)	Base	Yield (%)[a]
1	2	-	59%
2	2	Cs_2CO_3 (3eq.)	58%
3	2	CsOPiv (3eq.)	0%
4	2	NaOAc (3eq.)	62%
5	2	K_3PO_4 (3eq.)	75%
6	2	K_3PO_4 (1eq.)	90%
7	1	K_3PO_4 (1eq.)	95%
8[b]	1	K_3PO_4 (1eq.)	90%

[a] Yields determined using calibrated GC-MS analysis *vs. n*-dodecane as internal standard. [b] Reaction conditions: 1mol% [Au] loading, 12h.

Although *o*-carborane bis(phosphine) gold(I) complexes couldn't undergo the stoichiometric Csp^2-Csp^2 cross coupling reaction, we decided to test them again for the catalytic version since we established new reaction conditions. The arylation of 1,3,5-trimethoxybenzene with 4-fluoroiodobenzene was thus tested with 1,2-bis(diisopropylphosphino)-1,2-dicarba-*closo*-dodecarborane (complex **2**) and with 1,2-bis(diaminophosphino)-1,2-dicarba-*closo*-dodecarborane (complex **6**) (Scheme 3.24).

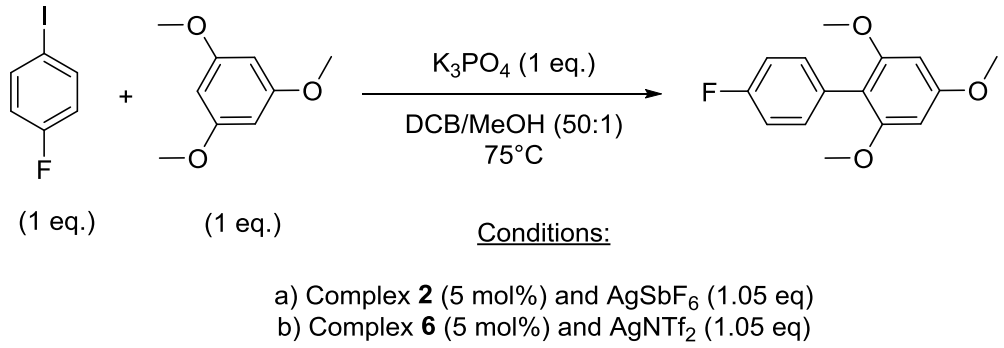

Scheme 3.24 Cross coupling of 4-fluoroiodobenzene and TMB with complexes a) **2** and b) **6**.

Both reactions were monitored by GC-MS, but sadly the coupling product was not detected even after twelve hours at 75°C. Once again, the instability of the arylgold(III) complexes stemming from the oxidative addition of the aryl iodide, especially after iodine abstraction, may explain the inability of *o*-carborane diphosphine gold(I) complexes to achieve the Au(I)/Au(III) catalytic cycle.

3.2.2.2 Csp^2-Csp^2 Cross-Coupling with Complex 10: Scope and Limitations

Having set good reaction conditions for the catalytic cross-coupling reaction of iodobenzene and 1,3,5-trimethoxybenzene with complex **10**, we screened the scope of aryl halides (Scheme 3.25). The direct arylation of TMB proceeded well with diverse iodobenzenes and

the corresponding biaryl products were obtained in good to excellent yields under mild conditions (75°C, 2h). In fact, the cross-coupling reaction tolerates electron-withdrawing (*p*-nitro and *p*-fluoro iodobenzenes) and electron-donating (*p*-methoxy and *p*-methyl iodobenzenes) aryl iodides as well as *ortho* substituted substrates such as 8-iodonaphthalene. The arylation of TMB was tested with aryl bromides since complex **10** was shown to activate the Csp^2-Br bond as well. To keep mild reaction conditions and reasonably short reaction times, the cross-coupling of aryl bromides and 1,3,5-trimethoxybenzene was performed with 10 mol% of gold and five equivalents of the aryl bromide. Under these conditions, the biaryl products were also obtained in good yields after a couple of hours at 75°C. Besides the advantage of avoiding the use of external oxidants or strong electrophiles, this aryl halide/arene coupling strategy has no electronic restraints for the coupling partners. This is illustrated in the coupling of the *para*- and *ortho*-methoxy substituted aryl halides substrates with trimethoxybenzene, which give access to biaryl compounds with electron-rich substituents on both aryl ring. With the oxidative coupling reactions developed recently (see 3.1), one of the coupling partners has to be be electron-deprived and thus electron-rich biaryls are inaccessible.

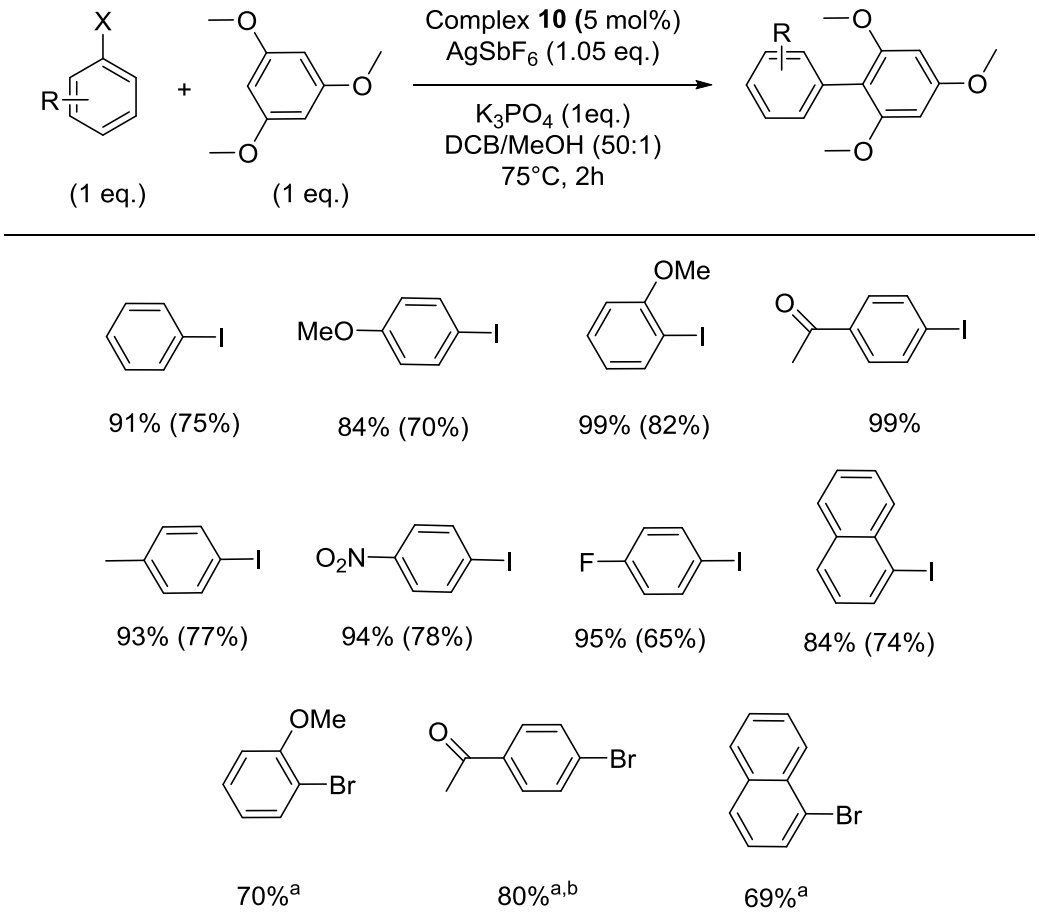

Scheme 3.25 Cross-coupling of aryl halides (X= I, Br) and TMB catalyzed by complex **10**. Yields determined using calibrated GC-MS *vs. n*-dodecane as internal standard, isolated yields in parentheses.
[a] Reaction conditions: [Au] 10 mol%, 5 eq. ArBr. [b] Reaction time: 12h.

1,3,5-trimethoxybenzene was tested first because it represents a model substrate for electron-rich arenes and to some extent heteroarenes. Similar to TMB, indoles are as well electron-rich heteroarenes, but whose function is very important, due to the presence of these motifs in different molecules (natural or designed) and find applications in pharmaceutical, agrochemical, and materials industries. Mainly, C2- and C3-arylindoles are ubiquitous substructures that can be found in many biologically active compounds. Thus there is great interest in synthesizing these arylated indoles as easily and efficiently possible.[(22)] Unlike the C2-selective arylation of unsubstituted indoles, few methodologies have been reported for the C3-selective coupling of indoles, and two examples will be presented hereafter.

In 2007, Fagnou and coworkers reported the catalytic cross-coupling of indoles and arene.[23] Using a palladium catalyst with a copper oxidant, catalytic amounts of cesium pivalate and 3-nitropyridine in pivalic acid, *N*-acetylindoles were successfully coupled with benzenes, affording the desired product in high yields and high regioselectivity (Scheme 3.26).

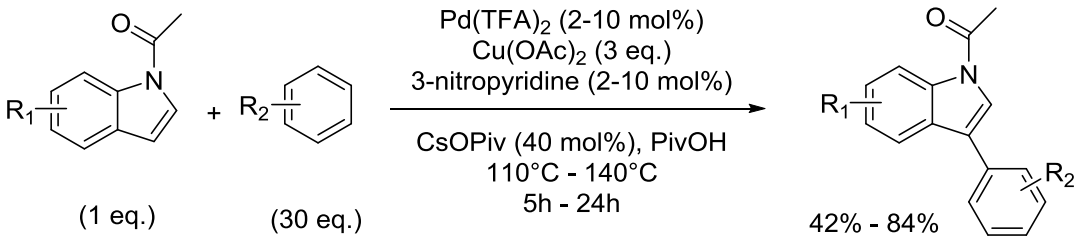

Scheme 3.26 Palladium-catalyzed cross-coupling of *N*-acetylindoles with arenes.

Cesium pivalate and 3–nitropyridine were found to increase the yield of the reaction. The authors proposed that the pyridine may stabilize the Pd(0) species before re-oxidation, and cesium pivalate may interact early in the reaction with $Pd(TFA)_2$ to generate palladium pivalate species. Moreover, only *N*-acetylindoles afforded the cross coupling product (indole did not react and with *N*-methylindole the homo-coupling product was observed), and thirty equivalents of the arene were found to be necessary. After prolonged heating, the C3-arylated indoles were obtained in moderate to good yields as the major products of the reaction.

Two years later, the group of Itami reported the C-H bond arylation of heteroarenes with iodoarenes.[24] The reactions are performed in *m*-xyelene with the commercially available Crabtree's catalyst ($[Ir(cod)(py)PCy_3]PF_6$) and silver carbonate (Scheme 3.27). After 18 hours at 160°C, the C3-arylated indoles were obtained in moderate yields.

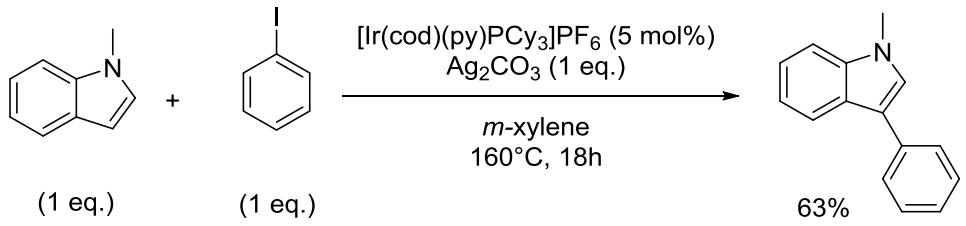

Scheme 3.27 Selected example for the Ir-catalyzed direct arylation reaction.

The authors proposed a plausible mechanism involving an Ir(I)/Ir(III) redox cycle. The catalysis is thought to be initiated by an oxidative addition reaction of the iodoarene to a cationic Ir(I) species. Abstraction of iodide from the Ir(III) complex generates an electrophilic species, followed by the C-H activation of the heteroarene. The resulting [Ar-Ir(III)-Het] undergoes a reductive elimination to deliver the biaryl product.

Since there is a great interest in developing new strategies to access C2- or C3-arylated indoles, and in the objective of showing that the gold-catalyzed arylation reaction is not restricted to 1,3,5-trimethoxybenzene, the direct arylation of indoles was investigated. Therefore, under the standard reaction conditions, the arylation of 1-methyl-1*H*-indole with iodobenzene was first tested. One regioisomer of the cross-coupling product was detected by GC-MS indicating a regioselective transformation, but only traces were formed. Even though $AgSbF_6$ is the most adapted halide scavenger for TMB arylation reaction, trifluoromethanesulfonate afforded the coupling product in good yields as well (see Table 3.4). Thus, the influence of AgOTf on the arylation of 1-methyl-1*H*-indole was examined. Gratifyingly, 99% yield of the coupling product was obtained after two hours at 75°C when silver trifluoromethanesulfonate was used with 5 mol% of gold, one equivalent of K_3PO_4 and two equivalents of the indole (Scheme 3.28).

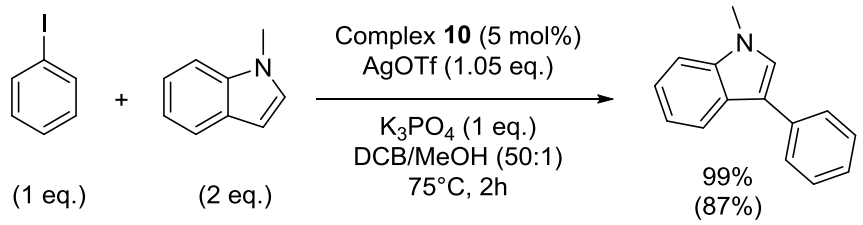

Scheme 3.28 Gold-catalyzed cross-coupling of iodobenzene and 1-methyl-1*H*-indole.

The coupling product was isolated in 87% yield (*via* column chromatography) and the ^{1}H NMR data confirmed the formation of 1-methyl-3-phenyl-1*H*-indole. The high C3 regioselectivity observed with complex **10** is typical for gold, and it's complementary to the C2 regioselectivity observed usually with other transition metals.[13,20,21] This result is in agreement with an electrophilic aromatic substitution mechanism since C3 position is the most nucleophilic position of indoles. With the right conditions in hands for the arylation of indoles, the scope of aryl halides was examined (Scheme 3.29). Like in the case of TMB, the reaction tolerates electron-deprived as well as electron-rich iodobenzenes and once again, the Ar-X/Ar-H strategy allows the electron-rich/electron-rich coupling thus expanding the scope of C3-arylated indoles. This arylation reaction is not restricted to 1-methyl-1*H*-indole. The cross-coupling of iodobenzene and 1-phenyl-1*H*-indole granted the desired product in an excellent yield of 95% after two hours at 75°C. Moreover, the more challenging 1*H*-indole substrate was arylated selectively at the C3 position with a 51% yield and the product stemming from *N*-arylation was not detected, indicating a selective transformation. Unfortunately, under these conditions, only traces of coupling products could be detected by GC-MS with aryl bromides, suggesting the need of further optimization.

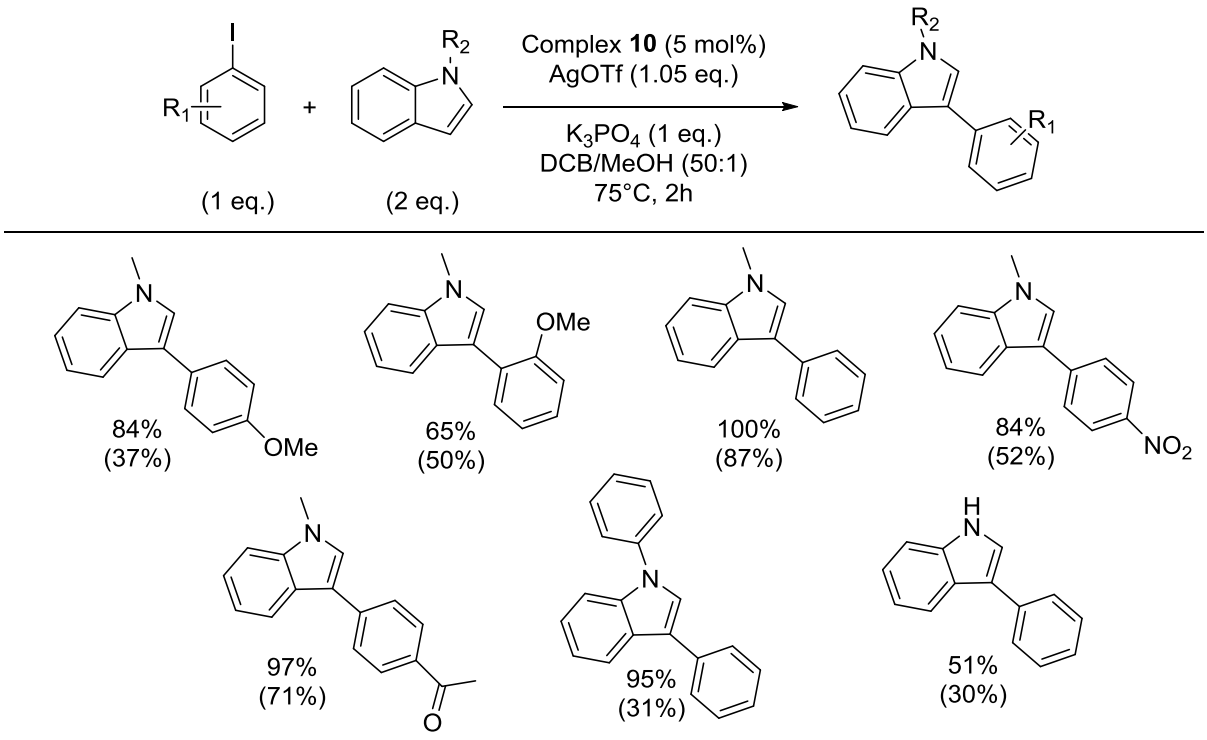

Scheme 3.29 Cross-coupling of aryl iodides and indoles catalyzed by complex **10**. Yields determined using calibrated GC-MS *vs. n*-dodecane as internal standard, isolated yields in parentheses.

The generality of this Csp^2-Csp^2 arylation was further demonstrated with other heteroarenes. Encouragingly, 1-phenyl-1*H*-pyrrole and iodobenzene were coupled using 5 mol% of complex **10** with 1 equivalent of $AgSbF_6$ under the standard mild conditions (Scheme 3.30). Without further optimization, the reaction gave a 61% isolated yield of a mixture of two isomers with high β-selectivity (β:α = 9/1). The two isomers were unambiguously identified by $^{13}C\{^1H\}$ NMR and their relative proportion was determined by ^1H NMR.

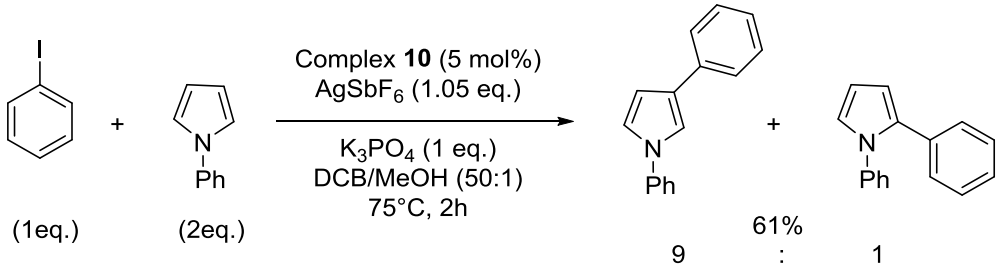

Scheme 3.30 Cross coupling of iodobenzene and 1-phenyl-1*H*-pyrrole with complex **10**.

Despite the progress and the development of methods in heterocyclic chemistry and C-C cross-coupling reactions, the current state-of-the art for the synthesis of β-arylpyrroles involves catalytic C-H borylation of pyrroles (usually with iridium catalyst), followed by palladium-catalyzed Suzuki-Miyaura cross-coupling.[25] In fact, transition metal-mediated arylation of pyrroles proceed preferentially at the α-position, making β-arylation processes rare and very appealing.[26,27] Recently, the group of Itami reported the first general β-selective arylation of pyrroles by using a rhodium catalyst (Scheme 3.31).[27]

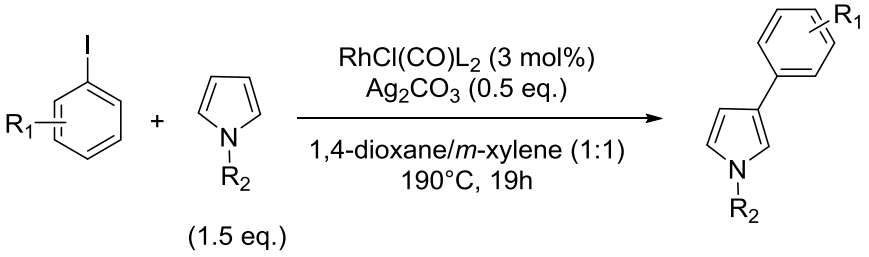

Scheme 3.31 β-selective arylation of pyrroles with rhodium catalyst.

A wide range of aryl iodides bearing electron-withdrawing or electron-donating groups were coupled to various pyrroles with high β-selectivity and in good yields. However, these rhodium-catalyzed reactions required harsher conditions (190°C, 19h) compared to our gold-catalyzed arylation of pyrroles (75°C, 2h).

The scope is not restricted to nitrogen-based heterocycles and can be expanded to oxygen-based substrates. Due to the low boiling point of furan (31°C), only traces of the desired coupling product were detected by GC-MS. Gratifyingly, the direct arylation of 2,3-dimethylfuran (bp = 87°C) with iodobenzene afforded the cross-coupling product in 71% yield after two hours at 75°C (Scheme 3.32). High regioselectivity was also observed and only the C2-arylated furan was formed as indicated by the ^{1}H NMR of the isolated product.

Once again, this result is in line with an electrophilic aromatic substitution pathway since C2 is the most nucleophilic position of furan.

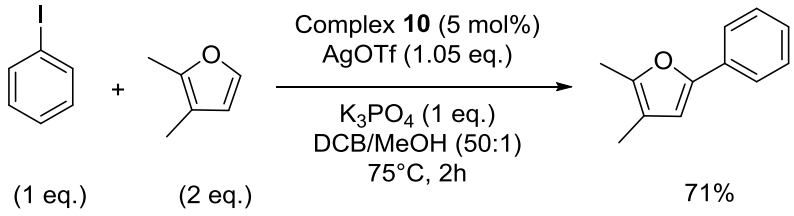

Scheme 3.32 Cross-coupling of iodobenzene and 2,3-dimethylfuran with complex **10**.

Under these mild reaction conditions, 1,3,5-trimethoxybenzene, indoles, 1-phenylpyrrole and 2,3-dimethylbenzene could be coupled to aryl halides. Other electron-rich arenes and heterocycles were also tested but the coupling products were not obtained (Scheme 3.33).

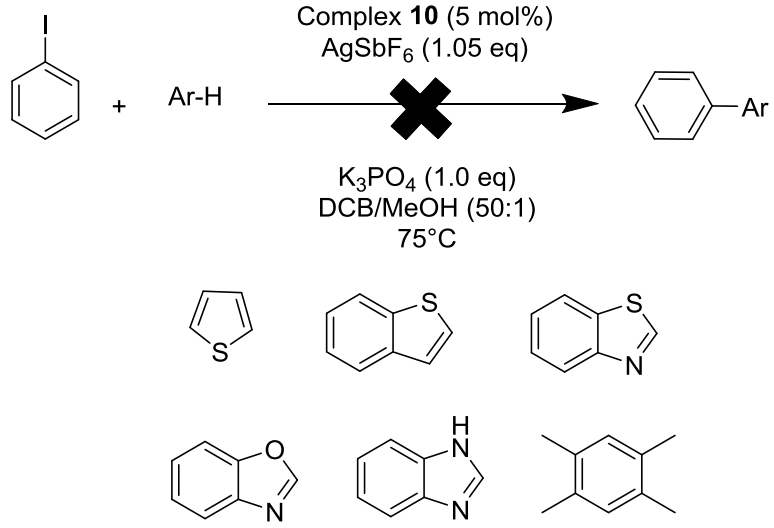

Scheme 3.33 Failed **c**ross-coupling attempts of iodobenzene and rich arenes with complex **10**.

The reluctance of the generated gold(III) complex to activate the C-H bonds of these substrates may be solved by optimizing the reaction conditions for each type of substrate.

3.2.2.3 Preliminary Mechanistic Investigations

Given that the oxidative addition of aryl halides to (MeDalphos)AuCl is very favorable, these cross-coupling reactions almost certainly operate *via* a 2-electron redox catalytic cycle. To further support this mechanistic proposition under catalytic conditions, some additional control experiments were carried out.

First, to rule out the possibility of a photo-induced catalytic cycle, the cross-coupling reaction of 4-fluoroiodobenzene and 1,3,5-trimethoxybenzene was carried out in parallel under day light and in the dark. After two hours at 75°C, aliquots from both reactions were submitted to GC-MS analysis, and in both cases the coupling product was formed in 95% yield. The same behavior of the reaction in the presence or absence of light contradicts the involvement of a photocatalytic process.

Next, to exclude the formation of gold nanoparticles under our standard reaction conditions, the coupling of 1-iodo-4-nitrobenzene and 1,3,5-trimethoxybenzene was realized with or without mercury (>2000 equivalents relative to the gold catalyst). Aliquots from both reaction media were analyzed by GC-MS every twenty minutes. After two hours, not only the same yield was obtained, but the kinetic of the two reactions was identical, which is in agreement with a homogeneous transformation (Scheme 3.34).

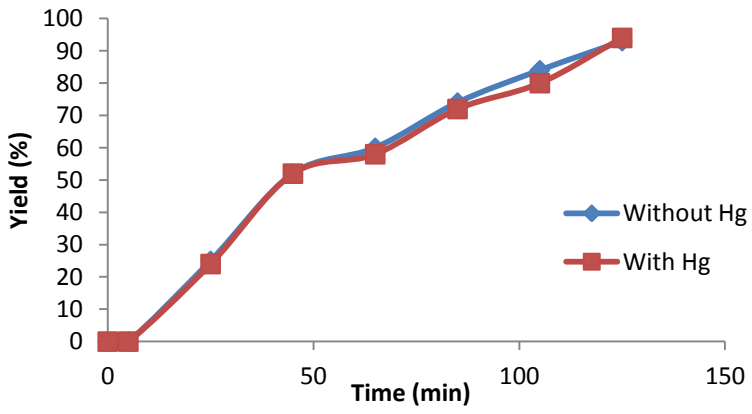

Figure 3.34 Monitoring of the *p*NO_2PhI / TMB coupling in the presence or not of Hg.

Finally, the Csp^2-Csp^2 coupling reaction of 1-iodo-4-nitrobenzene and 1,3,5 trimethoxybenzene was once again conducted in parallel but this time with or without the addition of galvinoxyl (a commercially available free radical trap) to eliminate the possibility of a radical pathway. GC-MS analysis of both reaction media revealed the formation of the desired product in 91% yield. The same behavior of the reaction in the presence or absence of a radical inhibitor contradicts a radical pathway (Scheme 3.35).

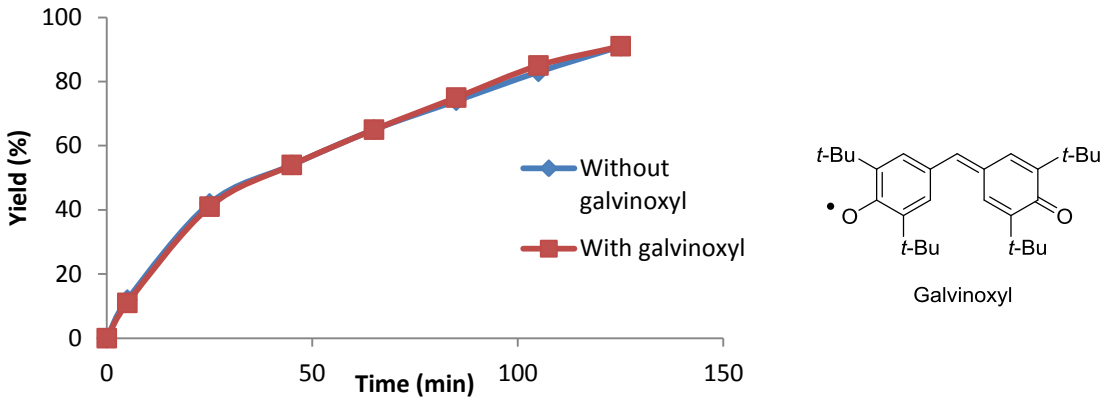

Figure 3.35 Monitoring of the *p*NO_2PhI / TMB coupling in the presence or not of galvinoxyl.

Since the kinetic and efficiency of the coupling reaction were not affected in all cases, then light-mediated, heterogeneous and radical paths are very unlikely and most probably these reactions occur *via* the 2-electron redox process envisioned initially (Scheme 3.19).

3.3 Conclusion

The *o*-carborane bis(phosphine) gold(I) complexes can undergo the oxidative addition of aryl iodides, but the cross-coupling reaction remained a challenge. In fact, the desired coupling product could not be obtained, and this is probably due to the decomposition of carborane bis(phosphine) gold(III) complexes in solution at room temperature. On the other hand, the first direct arylation process with gold made of Csp^2-X oxidative addition, Csp^2-H bond activation and reductive elimination was demonstrated with complex **10**. After the optimization of different reaction parameters (the catalytic loading, the ratio of coupling partners, the temperature, the halide scavenger, the solvent and the presence of a base), the one-pot stoichiometric reaction between aryl halides and rich arenes was transposed to a catalytic one. The gold-catalyzed cross-coupling reaction does not require an external oxidant or a strong electrophile and was realized under mild conditions compared to other transition metals (lower temperatures and reaction times). This transformation has a wide substrate scope: aryl halides bearing an electron-donating or an electron-withdrawing substituents were successfully coupled with electron-rich arenes (TMB) and heteroarenes (indoles, pyrroles and furans). Moreover, the preliminary mechanistic studies are in agreement with a 2-electron Au(I)/Au(III) redox catalytic cycle akin to that encountered with palladium complexes.

3.4 Experimental Part

3.4.1 Stoichiometric coupling of PhI and TMB with complex 10

In a glovebox, a flame dried Schlenk equipped with a magnetic stirrer bar was charged with silver hexafluoroantimonate (57 mg, 0.166 mmol) in dichloromethane (1.0 mL). Complex **10** (54 mg, 0.083 mmol) was transferred into a small glass vial and dissolved in dichloromethane (1.0 mL). Iodobenzene (9.3 µL, 0.083 mmol) and 1,3,5-trimethoxybenzene (14.0 mg, 0.083 mmol) were added to the gold complex solution. This solution was loaded into a plastic syringe equipped with stainless steel needle. The syringe was closed by blocking the needle with a septum. Outside the glovebox, the Schlenk was cooled down to –80°C (Ethanol/N_2 cold bath). At this temperature, the solution of complex **10**, iodobenzene and 1,3,5-trimethoxybenzene was added. The reaction mixture was then stirred at room temperature until complete conversion (12h). After filtration of the silver salts, the sample was purified by column chromatography (pentane/ethyl acetate 100:0 to 95:5). The fractions containing the biaryl product were then concentrated *in vaccuo* to yield the pure product as a white crystalline solid (18 mg, 0.074 mmol, 90% yield). Analytical data are consistent with those previously reported.[28]

^{1}H NMR (300 MHz, $CDCl_3$): δ 7.41-7.29 (m, 5H, H_{Ar}), 6.23 (s, 2H, H_{Ar}), 3.87 (s, 3H, OCH_3), 3.72 (s, 6H, OCH_3).

3.4.2 General procedure for the stoichiometric coupling of PhI and TMB

In a glovebox, a flame dried Schlenk equipped with a magnetic stirrer bar was charged with halide scavenger (0.046 mmol) in dichloromethane (0.5 mL). The gold complex (0.023 mmol) was transferred into a small glass vial and dissolved in dichloromethane (0.5 mL). Iodobenzene (2.6 µL, 0.023 mmol) and 1,3,5-trimethoxybenzene (4.0 mg, 0.023 mmol) were added to the gold complex solution. This solution was loaded into a plastic syringe equipped with stainless steel needle. The syringe was closed by blocking the needle with a septum. Outside the glovebox, the Schlenk was cooled down to –80°C (Ethanol/N_2 cold bath). At this temperature, the solution of gold, iodobenzene and 1,3,5-trimethoxybenzene was added. The reaction mixture was then stirred at room temperature. The yields were determined by GC-MS using *n*-dodecane as an internal standard.

Reaction of PhI and TMB with Complex 13

The general procedure described above was followed using the gold complex **13** (12.5 mg, 0.023 mmol) and $AgSbF_6$ (16.0 mg, 0.046 mmol) as a halide scavenger. Yield (5h): 21%.

Reaction of PhI and TMB with Complex 14

The general procedure described above was followed using the gold complex **14** (11.0 mg, 0.023 mmol) and $AgSbF_6$ (16.0 mg, 0.046 mmol) as a halide scavenger. Yield (5h): 44%.

Reaction of PhI and TMB with Complex 6

The general procedure described above was followed using the gold complex **6** (22.0 mg, 0.023 mmol) and $AgNTf_2$ (9.0 mg, 0.023 mmol) as a halide scavenger. Yield (5h): traces.

3.4.3 General procedure for gold-catalyzed direct arylation of 1,3,5-trimethoxybenzene with aryl iodides

In a glovebox, a flame dried Schlenk equipped with a magnetic stirrer bar was charged with silver hexafluoroantimonate (144 mg, 0.42 mmol) and potassium phosphate tribasic (85 mg, 0.40 mmol) in dichlorobenzene (2.0 mL). Complex **10** (13 mg, 0.02 mmol) was transferred into a small glass vial and dissolved in dichlorobenzene (2.0 mL). Aryl iodide (0.4 mmol, 1eq), 1,3,5-trimethoxybenzene (67.0 mg, 0.4 mmol) and methanol (80µL) were added to the gold complex solution. This solution was loaded into a plastic syringe equipped with stainless steel needle. The syringe was closed by blocking the needle with a septum. Outside the glovebox, the Schlenk was cooled down to -10°C (Ethanol/N_2 cold bath). At this temperature, the solution of complex **10**, aryl iodide and 1,3,5-trimethoxybenzene was added. The reaction mixture was then stirred at 75°C. The yields were determined by GC-MS using *n*-dodecane as an internal standard. After complete conversion, silver salts were filtrated, and the solvent evaporated. Isolated yields were determined column chromatography (pentane/ethyl acetate). The fractions containing the biaryl product were then concentrated *in vaccuo* to yield the pure product.

With aryl bromides:

The same procedure as for aryl iodides was followed, except that five equivalents of aryl bromides were used and 10 mol% of complex **10.**

Characterization of biaryl products:

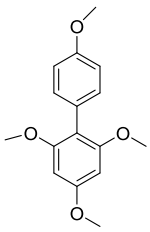

2,4,4',6-tetramethoxy-1,1'-biphenyl was prepared according to the general procedure described above using 4-iodoanisole with 1,3,5-trimethoxybenzene, and purified by column chromatography (pentane/ethyl acetate 100:0 to 95:5) to afford a white solid (70% isolated yield). Analytical data are consistent with that previously reported in the literature.[28] **^{1}H NMR** (300 MHz, $CDCl_3$): δ 7.29 (d, J_{HH} = 8.8 Hz, 2H), 6.93 (d, J_{HH} = 8.8 Hz, 2H), 6.23 (s, 2H), 3.86 (s, 3H), 3.83 (s, 3H), 3.72 (s, 6H).

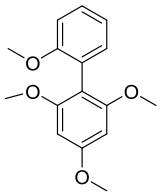

2,2',4,6-tetramethoxy-1,1'-biphenyl was prepared according to the general procedure described above using 2-iodoanisole with 1,3,5-trimethoxybenzene, and purified by column chromatography (pentane/ethyl acetate 100:0 to 95:5) to afford a white solid (82% isolated yield). Analytical data are consistent with that previously reported in the literature.[29] **^{1}H NMR** (300 MHz, $CDCl_3$): δ 7.37-7.32 (m, 1H), 7.21 (dd, J_{HH} = 7.46 Hz, J_{HH} = 1.66 Hz, 1H), 7.06-7.00 (m, 2H), 6.27 (s, 2H), 3.89 (s, 3H), 3.79 (s, 3H), 3.74 (s, 6H).

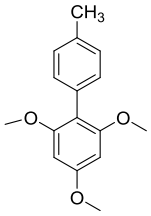

2,4,6-trimethoxy-4'-methyl-1,1'-biphenyl was prepared according to the general procedure described above using 4-iodotoluene with 1,3,5-trimethoxybenzene, and purified by column chromatography (pentane/ethyl acetate 100:0 to 95:5) to afford a white solid (77% isolated yield). Analytical data are consistent with that previously reported in the literature.[28] **^{1}H NMR** (300 MHz, $CDCl_3$): δ 7.23-7.19 (m, 4H), 6.25 (s, 2H), 3.88 (s, 3H), 3.74 (s, 6H), 2.40 (s, 3H).

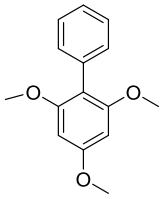

2,4,6-trimethoxy-1,1'-biphenyl was prepared according to the general procedure described above using iodobenzene with 1,3,5-trimethoxybenzene, and purified by column chromatography (pentane/ethyl acetate 100:0 to 95:5) to yield a afford solid (75% isolated yield). Analytical data are consistent with that previously reported in the literature.[28] **^{1}H NMR** (300 MHz, $CDCl_3$): δ 7.46-7.33 (m, 5H), 6.27 (s, 2H), 3.90 (s, 3H), 3.75 (s, 6H).

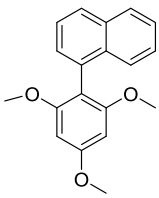

1-(2,4,6-trimethoxyphenyl)naphthalene was prepared according to the general procedure described above using 1-iodonapthalene with 1,3,5-trimethoxybenzene, and purified by column chromatography (pentane/ethyl acetate 100:0 to 90:10) to afford a white solid (74% isolated yield). Analytical data are consistent with that previously reported in the literature.[28] **^{1}H NMR** (300 MHz, $CDCl_3$): δ 7.87 (t, J_{HH} = 8.34 Hz, 2H), 7.58-7.53 (m, 2H), 7.48-7.43 (m, 1H), 7.40-7.36 (m, 2H), 6.32 (s, 2H), 3.93 (s, 3H), 3.64 (s, 6H).

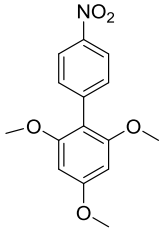

2,4,6-trimethoxy-4'-nitro-1,1'-biphenyl was prepared according to the general procedure described above using 1-iodo-4-nitrobenzene with 1,3,5-trimethoxybenzene, and purified by column chromatography (pentane/ethyl acetate 100:0 to 90:10) to afford a yellow solid (78% isolated yield). Analytical data are consistent with that previously reported in the literature.[30] **^{1}H NMR** (300 MHz, $CDCl_3$): δ 8.22 (d, J_{HH} = 9.10 Hz, 2H), 7.51 (d, J_{HH} = 9.10 Hz, 2H), 6.23 (s, 2H), 3.88 (s, 3H), 3.74 (s, 6H).

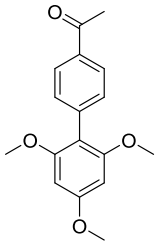

1-(2',4',6'-trimethoxybiphenyl-4-yl)ethanone was prepared according to the general procedure described above using 4'-bromoacetophenone (5eq), 1,3,5-trimethoxybenzene (1eq) and 10 mol% of complex **1** (reaction time 12 h), and purified by column chromatography (pentane/ethyl acetate 100:0 to 90:10) to afford a yellow solid (40% isolated yield). Analytical data are consistent with that previously reported in the literature.[31] **^{1}H NMR** (300 MHz, $CDCl_3$): δ 7.98 (d, J_{HH} = 8.10 Hz, 2H), 7.45 (d, J_{HH} = 8.10 Hz, 2H), 6.23 (s, 2H), 3.87 (s, 3H), 3.73 (s, 6H), 2.62 (s, 3H).

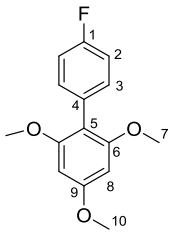

4'-fluoro-2,4,6-trimethoxy-1,1'-biphenyl was prepared according to the general procedure described above using 1-fluoro-4-iodobenzene with 1,3,5-trimethoxybenzene, and purified by column chromatography (pentane/ethyl acetate 100:0 to 90:10) to afford a white solid (65% isolated yield). Analytical data are consistent with that previously reported in the literature.[31] **^{1}H NMR** (300 MHz, $CDCl_3$): δ 7.32-7.27 (m, 2H), 7.07 (t, J = 8.86 Hz, 2H), 6.23 (s, 2H), 3.87 (s, 3H), 3.73 (s, 6H). **^{13}C{^{1}H} NMR** (100 MHz, $CDCl_3$): δ 160.5 (d, J_{C-F} = 245.4 Hz, C_1), 160.7 (s, C_9), 158.5 (s, C_6), 132.8 (d, J_{C-F} = 7.8 Hz, C_3), 129.9 (d, J_{C-F} = 3.4 Hz, C_4), 114.7 (d, J_{C-F} = 21.5 Hz, C_2), 111.5 (s, C_5), 91.0 (s, C_8), 55.9 (s, C_7), 55.5 (s, C_{10}). **^{19}F{^{1}H} NMR** (282 MHz, $CDCl_3$): δ -116.5 (s).

3.4.4 General procedure for gold-catalyzed direct arylation of indoles with aryl iodides

In a glovebox, a flame dried Schlenk equipped with a magnetic stirrer bar was charged with silver trifluoromethanesulfonate (134.0 mg, 0.52 mmol) and potassium phosphate tribasic (106.0 mg, 0.50 mmol) in dichlorobenzene (2.0 mL). Complex **10** (16.0 mg, 0.025 mmol) was transferred into a small glass vial and dissolved in dichlorobenzene (2.0 mL). Aryl iodide (0.5 mmol, 1eq), indole (1.0 mmol, 2eq) and methanol (80µL) were added to the gold complex solution. This solution was loaded into a plastic syringe equipped with stainless steel needle. The syringe was closed by blocking the needle with a septum. Outside the glovebox, the Schlenk was cooled down to -10°C (Ethanol/N_2 cold bath). At this temperature, the solution of complex **10**, aryl iodide and indole was added. The reaction mixture was then stirred at 75°C. After complete conversion, silver salts were filtrated, and the solvent evaporated. Isolated yields were determined after column chromatography (pentane/dichloromethane). The fractions containing the biaryl product were then concentrated *in vaccuo* to yield the pure product.

Characterization of biaryl products:

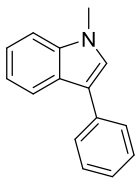

1-methyl-3-phenyl-1*H*-indole was prepared according to the general procedure described above using iodobenzene with 1-methy-1*H*-indole, and purified by column chromatography (pentane/dichloromethane 100:0 to 95:5) to afford a colorless oil (87% isolated yield). Analytical data are consistent with that previously reported in the literature.[32] **^{1}H NMR** (300 MHz, $CDCl_3$): δ 7.93 (d, J_{HH} = 8.0 Hz, 1H), 7.64 (d, J_{HH} = 7.7 Hz, 2H), 7.44-7.33 (m, 3H), 7.28-7.15 (m, 4H), 3.80 (s, 3H).

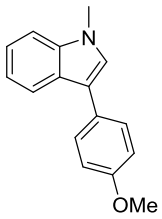

3-(4-methoxyphenyl)-1-methyl-1*H*-indole was prepared according to the general procedure described above using 4-iodoanisole with 1-methy-1*H*-indole, and purified by column chromatography (pentane/dichloromethane 85:15) to afford a white crystalline solid (37% isolated yield). Analytical data are consistent with that previously reported in the literature.[32] **^{1}H NMR** (300 MHz, $CDCl_3$): δ 7.91 (d, J_{HH} = 8.0 Hz, 1H), 7.58 (d, J_{HH} = 8.7 Hz, 2H), 7.37 (d, J_{HH} = 8.3 Hz, 1H), 7.31-7.26 (m, 1H), 7.21-7.17 (m, 2H), 7.00 (d, J_{HH} = 8.7 Hz, 2H), 3.87 (s, 3H), 3.84 (s, 3H).

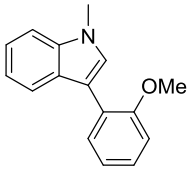

3-(2-methoxyphenyl)-1-methyl-*1H*-indole was prepared according to the general procedure described above using 2-iodoanisole with 1-methy-1*H*-indole, and purified by column chromatography (pentane/dichloromethane 95:5) to afford a white solid (50% isolated yield). Analytical data are consistent with that previously reported in the literature.[32] **^{1}H NMR** (300 MHz, $CDCl_3$): δ 7.80 (d, J_{HH} = 8.0 Hz, 1H), 7.65 (dd, J_{HH} = 7.4 Hz, J_{HH} = 1.7 Hz, 1H), 7.40-7.37 (m, 1H), 7.36 (br.s, 1H), 7.32-7.23 (m, 2H), 7.17 (t, J_{HH} = 7.5 Hz, 1H), 7.10-7.02 3.88 (m, 2H), 3.88 (s, 3H), 3.85 (s, 3H).

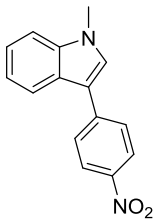

1-methyl-3-(4-nitrophenyl)-1*H*-indole was prepared according to the general procedure described above using 1-iodo-4-nitrobenzene with 1-methy-1*H*-indole, and purified by column chromatography (pentane/dichloromethane 90:10) to afford a yellow solid (52% isolated yield). Analytical data are consistent with that previously reported in the literature.[33] **^{1}H NMR** (300 MHz, $CDCl_3$): δ 8.27 (d, J_{HH} = 9.0 Hz, 2H), 7.96 (d, J_{HH} = 7.9 Hz, 1H), 7.78 (d, J_{HH} = 9.0 Hz, 2H), 7.43-7.26 (m, 4H), 3.88 (s, 3H).

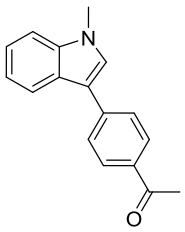

1-(4-(1-methyl-1*H*-indol-3-yl)phenyl)ethan-1-one was prepared according to the general procedure described above using 4'-iodoacetophenone with 1-methy-1*H*-indole, and purified by column chromatography (pentane/dichloromethane 80:20) to afford a yellow solid (71% isolated yield). Analytical data are consistent with that previously reported in the literature.[32] **^{1}H NMR** (300 MHz, $CDCl_3$): δ 7.96 (d, J_{HH} = 8.3 Hz, 2H), 7.90 (d, J_{HH} = 8.3 Hz, 1H), 7.68 (d, J_{HH} = 8.3 Hz, 2H), 7.34-7.27 (m, 2H), 7.25-7.13 (m, 2H), 3.81 (s, 3H), 2.58 (s, 3H).

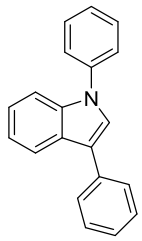

1,3-diphenyl-1*H*-indole was prepared according to the general procedure described above using iodobenzene with 1-phenyl-1*H*-indole, and purified by column chromatography (pentane/dichloromethane 90:10) to afford a yellow oil (31% isolated yield). Analytical data are consistent with that previously reported in the literature.[34] **^{1}H NMR** (300 MHz, $CDCl_3$): δ 8.01 (d, J_{HH} = 7.7 Hz, 1H), 7.74 (d, J_{HH} = 7.6 Hz, 2H), 7.64-7.47 (m, 8H), 7.42-7.24 (m, 4H).

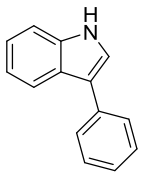

3-phenyl-1*H*-indole was prepared according to the general procedure described above using iodobenzene with 1*H*-indole, and purified by column chromatography (pentane/dichloromethane 95:5 to 90:10) to afford a light yellow solid (30% isolated yield). Analytical data are consistent with that previously reported in the literature.[33] **^{1}H NMR** (300 MHz, $CDCl_3$): δ 8.17 (br.s, 1H), 7.97 (d, J_{HH} = 7.7 Hz, 1H), 7.69 (d, J_{HH} = 7.5 Hz, 2H), 7.49-7.41 (m, 3H), 7.35-7.19 (m, 4H).

3.4.5 Procedure for gold-catalyzed direct arylation of 1-phneylpyrrole with PhI

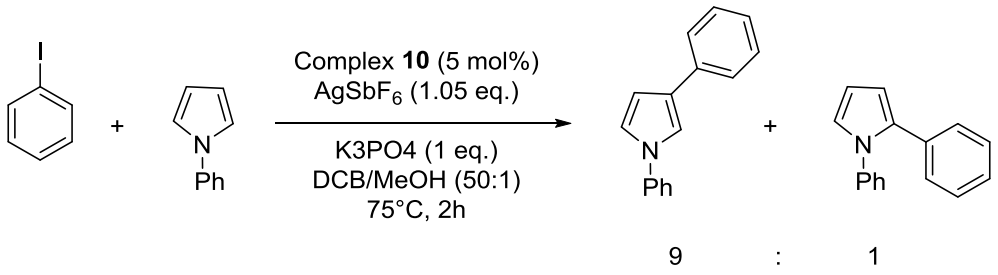

In a glovebox, a flame dried Schlenk equipped with a magnetic stirrer bar was charged with silver hexafluoroantimonate (289.0 mg, 0.84 mmol) and potassium phosphate tribasic (170.0 mg, 0.8 mmol) in dichlorobenzene (4.0 mL). Complex **10** (26.0 mg, 0.04 mmol) was transferred into a small glass vial and dissolved in dichlorobenzene (4.0 mL). Iodobenzene (90.0 µL, 0.8 mmol, 1eq), 1-phenyl-pyrrole (230.0 mg, 1.6 mmol) and methanol (160.0µL) were added to the gold complex solution. This solution was loaded into a plastic syringe equipped with stainless steel needle. The syringe was closed by blocking the needle with a septum. Outside the glovebox, the Schlenk was cooled down to –10°C (Ethanol/N2 cold bath). At this temperature, the solution of complex **10**, iodobenzene and 1-phenyl-pyrrole was added. The reaction mixture was then stirred at 75°C. After filtration of the silver salts, and a trap to trap to evaporate the dichlorobenzene, the sample was purified by column chromatography (pentane/ethyl acetate). The fractions containing the biaryl product were then concentrated *in vacuum* to give a mixture of α/β products in 61% yield. The two isomers were unambiguously identified by $^{13}C\{^{1}H\}$ NMR. Their relative proportion (1/9) was determined by ^{1}H NMR.

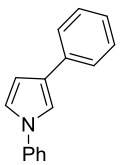

1,3-diphenyl-1*H*-pyrrole (β-isomer): Analytical data are consistent with those previously reported in the literature.[35] **$^{13}C\{^{1}H\}$ NMR** (125 MHz, $CDCl_3$): 140.6, 135.4, 129.7, 128.8, 127.0, 125.9, 125.8, 125.3, 120.6, 120.4, 115.9, 108.8.

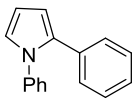

1,2-diphenyl-1*H*-pyrrole (*α*-isomer): Analytical data are consistent with those previously reported in the literature.[36] **$^{13}C\{^{1}H\}$ NMR** (125 MHz, $CDCl_3$): 140.8, 133.9, 133.1, 129.6, 128.4, 128.2, 126.7, 126.4,125.7, 124.5, 110.5, 109.4.

3.4.6 Procedure for gold-catalyzed direct arylation of 2,3-dimethylfuran with PhI

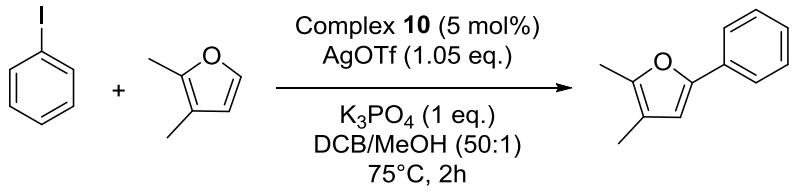

In a glovebox, a flame dried Schlenk equipped with a magnetic stirrer bar was charged with silver trifluoromethanesulfonate (134.0 mg, 0.52 mmol) and potassium phosphate tribasic (106.0 mg, 0.50 mmol) in dichlorobenzene (2.0 mL). Complex **10** (16.0 mg, 0.025 mmol) was transferred into a small glass vial and dissolved in dichlorobenzene (2.0 mL). Iodobenzene (56.0 µL, 0.5 mmol), 2,3-dimethylfuran (106.0 µL, 1.0 mmol) and methanol (80 µL) were added to the gold complex solution. This solution was loaded into a plastic syringe equipped with stainless steel needle. The syringe was closed by blocking the needle with a septum. Outside the glovebox, the Schlenk was cooled down to -10°C (Ethanol/N_2 cold bath). At this temperature, the solution of complex **10**, iodobenzene and 2,3-dimethylfuran was added. The reaction mixture was then stirred at 75°C. The yields were determined by GC-MS using *n*-dodecane as an internal standard. After complete conversion, silver salts were filtrated, and the solvent evaporated. Isolated yield was determined after column chromatography (pentane/dichloromethane). The fractions containing the biaryl product were then concentrated *in vaccuo* to yield the pure product as colorless oil (25%). Analytical data are consistent with those previously reported.[24]

^{1}H NMR (300 MHz, $CDCl_3$): δ δ 7.64 (d, J_{HH} = 8.2 Hz, 2H), 7.38 (t, J_{HH} = 7.5 Hz, 2H), 7.23 (t, J_{HH} = 7.5 Hz, 1H), 6.48 (s, 1H), 2.31 (s, 3H), 2.02 (s, 3H).

3.4.7 Control experiment: influence of the day light

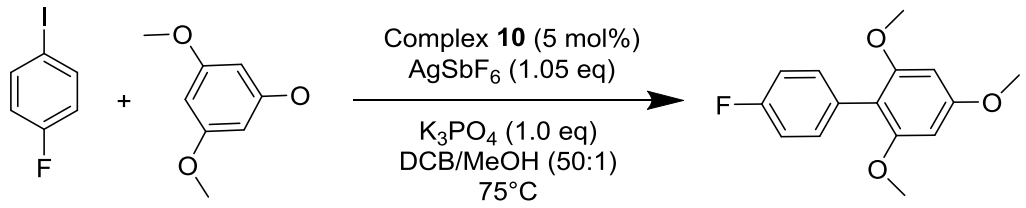

Two coupling experiments were carried out in parallel under exposure to day light and in the dark. In a glovebox, a flame dried Schlenk equipped with a magnetic stirrer bar was charged with silver hexafluoroantimonate (65.0 mg, 0.189 mmol) and potassium phosphate tribasic (38.0 mg, 0.180 mmol) in dichlorobenzene (1.0 mL). Complex **10** (6.0 mg, 0.009 mmol) was transferred into a small glass vial and dissolved in dichlorobenzene (1.0 mL). 1-Fluoro-4-iodobenzene (21.0 µL, 0.180 mmol), 1,3,5-trimethoxybenzene (30.0 mg, 0.180 mmol) and methanol (40 µL) were added to the gold complex solution. This solution was loaded into a plastic syringe equipped with stainless steel needle. The syringe was closed by blocking the needle with a septum. Outside the glovebox, the Schlenk was protected from light by wrapping it with aluminum foil and was cooled down to -10°C (Ethanol/N_2 cold bath). At this temperature, the solution of complex **10**, 1-fluoro-4-iodobenzene and 1,3,5-trimethoxybenzene was added. The reaction mixture was then stirred at 75°C for 2h. The yields were determined by GC-MS using *n*-dodecane as an internal standard. In both cases, the coupling product was formed in 95% yield.

3.4.8 Control experiment: mercury poisoning test

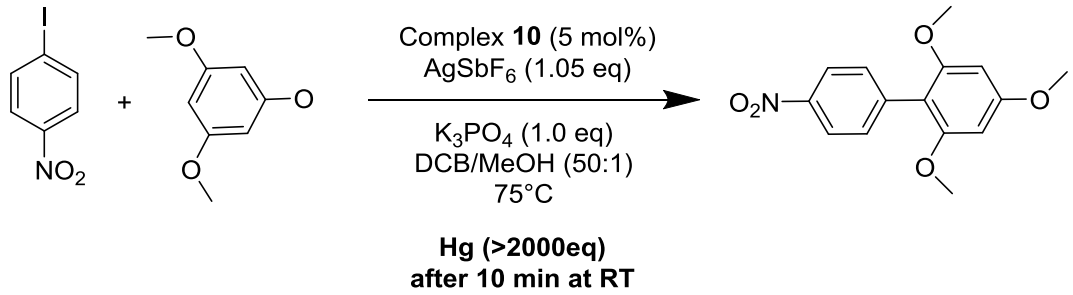

Two experiments with and without added Hg were carried out in parallel. In a glovebox, a flame dried Schlenk equipped with a magnetic stirrer bar was charged with silver hexafluoroantimonate (65.0 mg, 0.189 mmol) and potassium phosphate tribasic (38.0 mg, 0.180 mmol) in dichlorobenzene (1.0 mL). Complex **10** (6.0 mg, 0.009 mmol) was transferred into a small glass vial and dissolved in dichlorobenzene (1.0 mL). 1-Iodo-4-nitrobenzene (45.0 mg, 0.180 mmol), 1,3,5-trimethoxybenzene (30.0 mg, 0.18 mmol) and methanol (40 µL) were added to the gold complex solution. This solution was loaded into a plastic syringe equipped with stainless steel needle. The syringe was closed by blocking the needle with a septum. Outside the glovebox, the Schlenk was cooled down to – 10°C (Ethanol/N_2 cold bath). At this temperature, the solution of complex **10**, 1-iodo-4-nitrobenzene and 1,3,5-trimethoxybenzene was added. The reaction mixture was stirred at room temperature and after 10 minutes, one drop of Hg (>2000 equiv. relative to the catalyst) was added with a plastic Pasteur pipette. The reaction mixture was then stirred at 75°C. After the indicated times, aliquots were taken and analyzed by GC-MS. Yields were determined using *n*-dodecane as an internal standard.

3.4.9 Control experiment: radical scavenger test

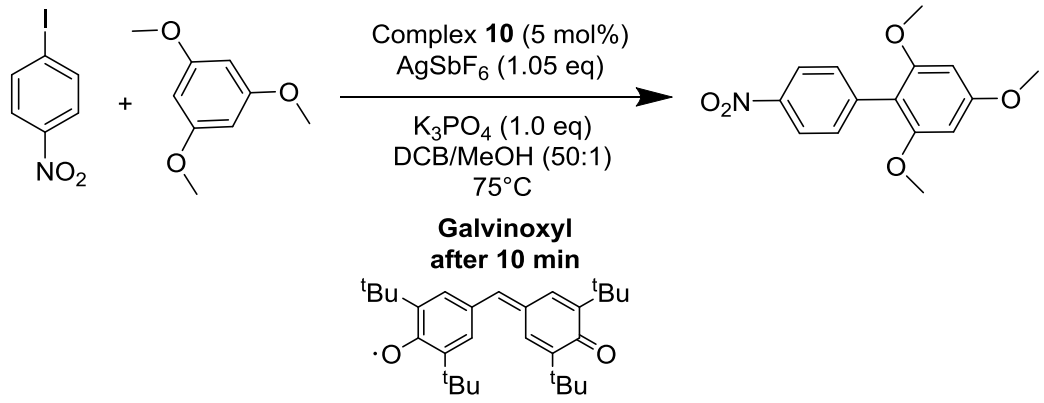

Two experiments with and without added galvinoxyl were carried out in parallel. In a glovebox, a flame dried Schlenk equipped with a magnetic stirrer bar was charged with silver hexafluoroantimonate (65.0 mg, 0.189 mmol) and potassium phosphate tribasic (38.0 mg, 0.180 mmol) in dichlorobenzene (1.0 mL). Complex **10** (6.0 mg, 0.009 mmol) was transferred into a small glass vial and dissolved in dichlorobenzene (1.0 mL). 1-Iodo-4-nitrobenzene (45.0 mg, 0.180 mmol), 1,3,5-trimethoxybenzene (30.0 mg, 0.180 mmol) and methanol (40 µL) were added to the gold complex solution. This solution was loaded into a plastic syringe equipped with stainless steel needle. The syringe was closed by blocking the needle with a septum. Outside the glovebox, the Schlenk was cooled down to – 10°C (Ethanol/N_2 cold bath). At this temperature, the solution of complex **10**, 1-iodo-4-nitrobenzene and 1,3,5-trimethoxybenzene was added. The reaction mixture was then stirred at 75°C. After 10 min, galvinoxyl (99.0 mg, 0.230 mmol) was added. After the indicated times, aliquots were taken and analyzed by GC-MS. Yields were determined using *n*-dodecane as an internal standard.

3.5 References

(1) Kharasch, M. S.; Isbell, H. S. *J. Am. Chem. Soc.* **1931**, *53*, 3053.

(2) Kramer, S. *Chem. Eur. J.* **2016**, *22*, 15584.

(3) He, Y.; Wu, H.; Toste, F. D. *Chem. Sci.* **2015**, *6*, 1194.

(4) de Haro, T.; Nevado, C. *J. Am. Chem. Soc.* **2010**, *132*, 1512.

(5) Hopkinson, M. N.; Tlahuext-Aca, A.; Glorius, F. *Acc. Chem. Res.* **2016**, *49*, 2261.

(6) Peng, H.; Xi, Y.; Ronaghi, N.; Dong, B.; Akhmedov, N. G.; Shi, X. *J. Am. Chem. Soc.* **2014**, *136*, 13174.

(7) Serra, J.; Whiteoak, C. J.; Acuña-Parés, F.; Font, M.; Luis, J. M.; Lloret-Fillol, J.; Ribas, X. *J. Am. Chem. Soc.* **2015**, *137*, 13389.

(8) Kar, A.; Mangu, N.; Kaiser, H. M.; Beller, M.; Tse, M. K. *Chem. Commun.* **2008**, *0*, 386.

(9) Kar, A.; Mangu, N.; Kaiser, H. M.; Tse, M. K. *J. Organomet. Chem.* **2009**, *694*, 524.

(10) Ball, L. T.; Lloyd-Jones, G. C.; Russell, C. A. *Science* **2012**, *337*, 1644.

(11) Ball, L. T.; Lloyd-Jones, G. C.; Russell, C. A. *J. Am. Chem. Soc.* **2014**, *136*, 254.

(12) Hata, K.; Ito, H.; Segawa, Y.; Itami, K. *Beilstein J. Org. Chem.* **2015**, *11*, 2737.

(13) Cambeiro, X. C.; Ahlsten, N.; Larrosa, I. *J. Am. Chem. Soc.* **2015**, *137*, 15636.

(14) Hofer, M.; Genoux, A.; Kumar, R.; Nevado, C. *Angew. Chem. Int. Ed.* **2017**, *56*, 1021.

(15) Wu, Q.; Du, C.; Huang, Y.; Liu, X.; Long, Z.; Song, F.; You, J. *Chem. Sci.* **2014**, *6*, 288.

(16) Gauchot, V.; Lee, A.-L. *Chem. Comm.* **2016**, *52*, 10163.

(17) Cai, R.; Lu, M.; Aguilera, E. Y.; Xi, Y.; Akhmedov, N. G.; Petersen, J. L.; Chen, H.; Shi, X. *Angew. Chem. Int. Ed.* **2015**, *54*, 8772.

(18) Witzel, S.; Xie, J.; Rudolph, M.; Hashmi, A. S. K. *Adv. Synth. Catal.* **2017**, *359*, 1522.

(19) Gauchot, V.; Sutherland, D. R.; Lee, A.-L. *Chem. Sci.* **2017**, *8*, 2885.

(20) Joost, M.; Amgoune, A.; Bourissou, D. *Angew. Chem. Int. Ed.* **2015**, *54*, 15022.

(21) Wolf, W. J.; Winston, M. S.; Toste, F. D. *Nat. Chem.* **2014**, *6*, 159.

(22) Lebrasseur, N.; Larrosa, I. *Adv. Heterocycl. Chem.* **2012**, *105*, 309.

(23) Stuart, D.R; Fagnou, K. *Science* **2007**, *316*, 1172

(24) Join, B.; Yamamoto, T.; Itami, K. *Angew. Chem. Int. Ed.* **2009**, *48*, 3644.

(25) Beck, E. M.; Hatley, R.; Gaunt, M. J. Angew. Chem., Int. Ed. 2008,47, 3004.

(26) Cresswell, A. J.; Lloyd-Jones, G. C. *Chem. Eur. J.* **2016**, *22*, 12641.

(27) Ueda, K.; Amaike, K.; Maceiczyk, R. M.; Itami, K.; Yamaguchi, J. *J. Am. Chem. Soc.* **2014**, *136*, 13226.

(28) Dai, J.-J.; Liu, J.-H.; Luo, D.-F.; Liu, L., *Chem. Comm.* **2011**, *47*, 677.

(29) Zhou, Z.; Zhang, Y.; Xia, W.; Chen, H.; Liang, H.; He, X.; Yu, S.; Cao, R.; Qiu, L., *Asian J. Org. Chem.*, **2016**, *5*, 1260.

(30) Dennis, E.G.; Jeffery, D.W.; Perkins, M.V.; Smith, P.A.; *Tetrahedron*, **2011**, *67*, 2125.

(31) Bunrit, A.; Sawadjoon, S.; Tšupova, S.; Sjöberg, P. J. R.; Samec, J. S. M. *J. Org. Chem.* **2016**, *81*, 1450.

(32) Zou, Y.; Yue, G.; Xu, J.; Zhou, J. *Eur. J. Org. Chem.* **2014**, *2014*, 5901.

(33) Phipps, R. J.; Grimster, N. P.; Gaunt, M. J. *J. Am. Chem. Soc.* **2008**, *130*, 8172.

(34) Gehrmann, T.; Lloret Fillol, J.; Scholl, S. A.; Wadepohl, H.; Gade, L. H. *Angew. Chem. Int. Ed.* **2011**, *50*, 5757.

(35) Bunrit, A.; Sawadjoon, S.; Tšupova, S.; Sjöberg, P. J. R.; Samec, J. S. M. *J. Org. Chem.* **2016**, *81*, 1450.

(36) Truong, T.; Daugulis, O. *J. Am. Chem. Soc.* **2011**, *133*, 4243.

4 Isolation of Reactive Gold(I) Carbene Complex

4.1 State of the Art

Gold carbene complexes are key intermediates, and their various transformations presented thereafter are one of the most versatile aspect of gold catalysis. These carbene species give access to a diverse range of compounds.[1-3] A handful of illustrating examples are discussed hereafter.

In 2004, Fürstner *et al.* reported the first gold(I)-catalyzed cycloisomerization of 1,5-enynes bearing an alcohol group at the propargylic position to form bicyclic ketones.[4] A gold(I) carbene species was proposed to be a key intermediate for this transformation (Scheme 4.1).

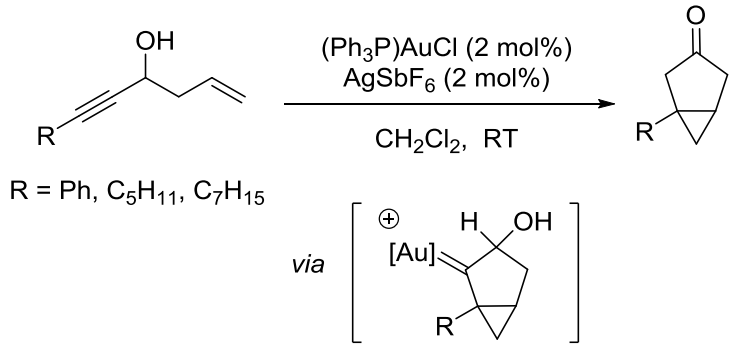

Scheme 4.1 Gold-catalyzed cycloisomerization of 1,5-enyes to form bicyclic ketones.

In 2010, J. Zhang and coworkers reported the gold-catalyzed tandem cycloisomerization/cyclopropanation of yne-enones in the presence of styrene to afford 3-acylfurans functionalized with a cyclopropane moiety.[5] The authors proposed the gold (2-furyl)carbene species as key reactive intermediate which undergoes the cyclopropanation reaction with styrene (Scheme 4.2).

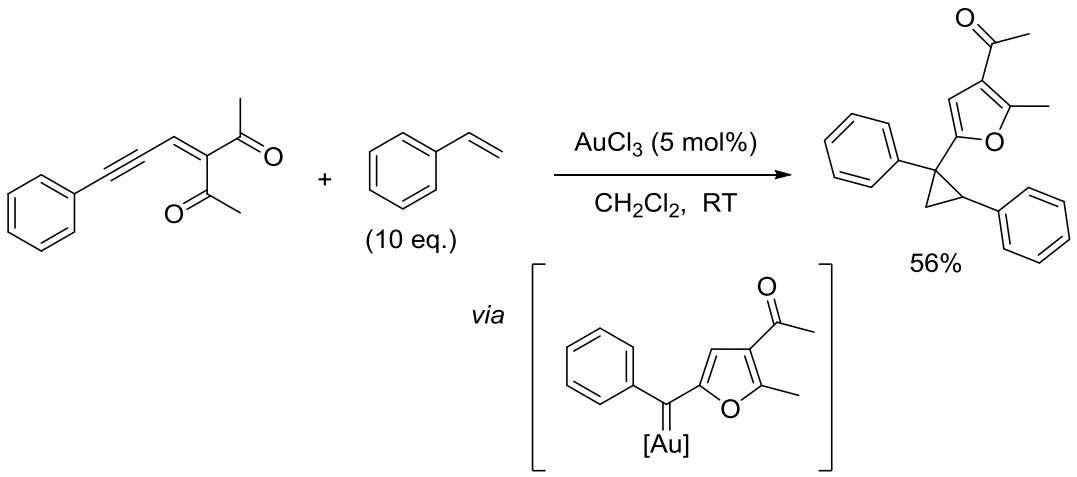

Scheme 4.2 Gold-catalyzed tandem cycloisomerization/cyclopropanation reaction.

As illustrated by these two examples, gold carbene species are usually pointed out as important (highly) reactive intermediates, but are rarely characterized or isolated. Over the past few years, several strategies have permitted the isolation and characterization of stable gold(I) carbene complexes, providing some essential structural information. Therefore, π-conjugation of the carbene center with heteroatoms (complex A)[6], π-delocalization (complex B)[7], and steric shielding of the carbene moiety with bulky ligands and substituents (complex C)[8] were noted as the main strategies to stabilize electrophilic gold carbenes (Scheme 4.3).

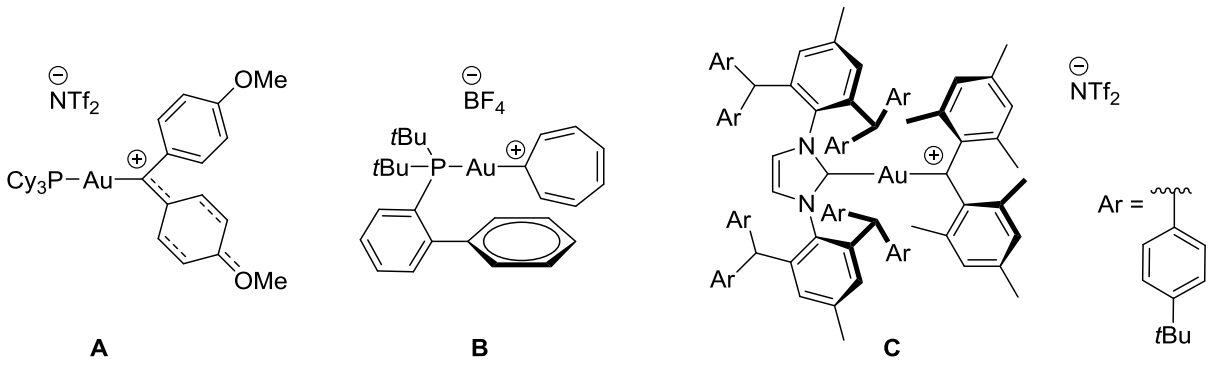

Scheme 4.3 Illustration of the strategies used to stabilize and isolate gold(I) carbenes.

Despite the progress in this field, an important class of gold carbene species, *i.e.* α-oxo gold carbene complexes have never been isolated or characterized. A variety of cascade transformations have substantiated the synthetic utility of α-oxo gold(I) carbene, and are usually pointed out as a key reactive intermediates.[9] Thus, the characterization and eventually the isolation of the α-oxo gold(I) carbene complex is of high interest not only from a synthetic point of view, but also from a fundamental point of view as it will allow to better understand the parameters that govern its reactivity.

Two main strategies have been developed to generate *in situ* α-oxo gold(I) carbene intermediates. These species can be synthesized *via* the classical extrusion of nitrogen from the corresponding diazo compounds in the presence of a gold species (Scheme 4.4, pathway a). Or, taking profit of the carbophilic Lewis acidic character of gold, the desired carbene complexes can be obtained *via* the attack of nucleophilic oxidants, typically N-oxides, on gold-activated alkynes (Scheme 4.4, pathway b).[2]

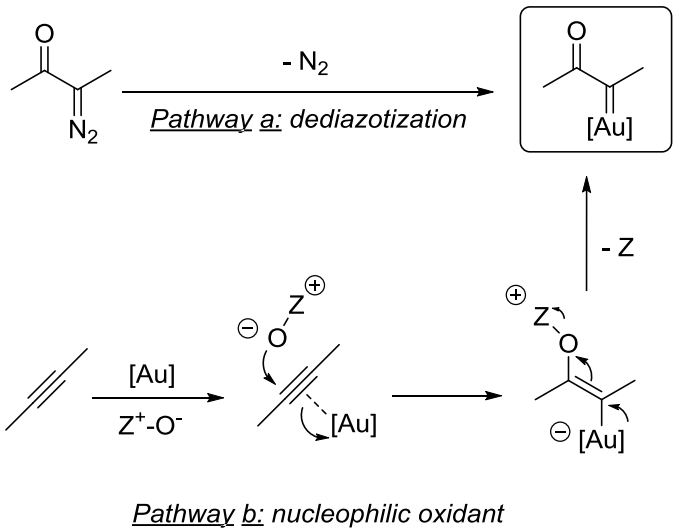

Scheme 4.4 Generation of α-oxo gold carbenes *via* dediazotization reaction or *via* alkyne oxidation.

As mentioned above, α-oxo gold(I) carbenes are highly reactive species and need to be trapped rapidly either in an intramolecular or intermolecular manner. Thus, numerous trapping strategies have been developed over the past few years and few examples are presented hereafter.

In 2010, the group of L. Zhang reported the first example of *in situ* generation α-oxo gold carbenes *via* intermolecular oxidation of propargylic alcohol, followed by an intramolecular O-H insertion by the gold carbene moiety to form the corresponding dihydrofuran-3-one.(10) With $Ph_3PAuNTf_2$ as the gold catalyst and pyridine *N*-oxide as external oxidants, the desired dihydrofuran-3-one compound was obtained in good yield and under mild reaction conditions (Scheme 4.5).

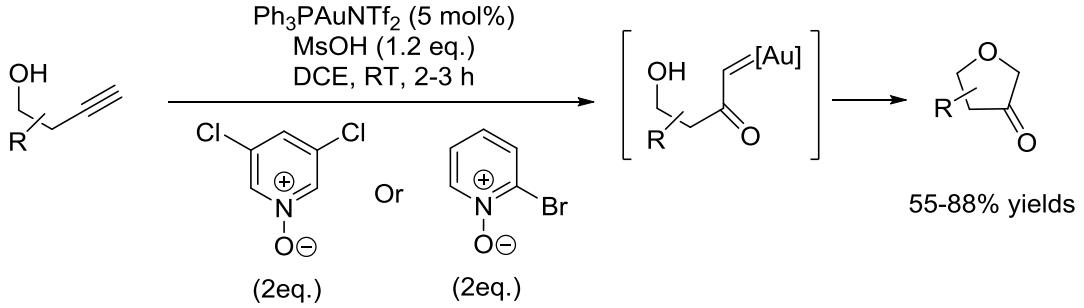

Scheme 4.5 Gold-catalyzed synthesis of dihydrofuran-3-ones *via* α-oxo gold carbene intermediates.

However, the basic pyridine formed during the reaction media was found to deactivate the gold catalyst and thus the addition of the strong acid MsOH (methanesulfonic acid) was found to be necessary. The reaction was shown to afford dihydrofuran-3-ones containing a broad range of functional groups in good yields (from 55% to 88%).

α-oxo gold(I) carbenes can also be trapped in an intermolecular manner as well. In fact, the carbene transfer reaction is one of the most effective strategies for aromatic C-H functionalization, and it is well known with transition metals. However, the functionalization

of phenols is very challenging because of the competitive O-H bond insertion reaction observed with various transition-metals catalysts (Rh, Cu, Ru, Fe and Pd).[11] In 2014, J. Zhang and coworkers investigated this reactivity with gold catalysts, and they reported the first example of highly site-selective direct C-H functionalization of phenols with diazoacetates *via* gold catalysis under mild conditions.[12] The use of tris(2,4-di-*tert*-butylphenyl)phosphite gold(I) chloride catalyst and silver hexafluoroantimonate as the halide scavenger were identified by the authors as the optimal conditions in terms of reactivity and selectivity, affording the *p*-C-H functionalization compounds as the sole products of the reaction (Scheme 4.6).

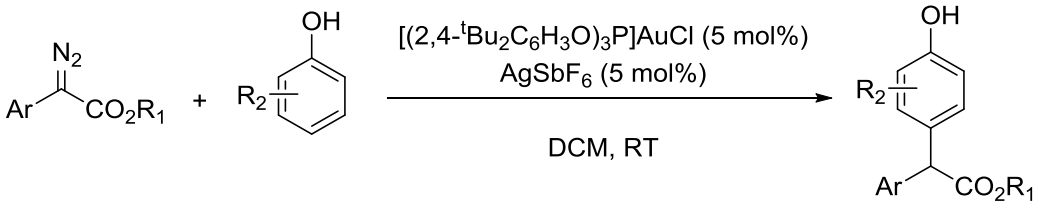

Scheme 4.6 Site selective C-H functionalization of phenols with diazo reagents *via* gold catalysis.

The reaction was found to be very efficient and selective with a wide range of phenols bearing different functional groups. For example, the reaction of the *ortho*-allyl phenol gave only the *para*-C-H bond functionalization product without the formation of any product stemming from the cyclopropanation reaction. The high selectivity observed was attributed by the authors to the carbocation like character of the *in situ* generated α-oxo gold(I) carbene, that reacts *via* the electrophilic addition pathway. Moreover, this transformation was thoroughly investigated by DFT calculations to further understand the origin of the unique selectivity observed.[13] Consistent with the experimental observations, with $[(PhO)_3PAuSbF_6]$, the *para*-C-H insertion was found to be more favorable than the O-H insertion pathway due to the

lower energy barriers and to the high thermodynamic stability of the intermediates and products. In contrast, with [(Ph_3P)$AuSbF_6$], both pathways were found to be in competition.

Very recently, the same authors substantiated the selectivity/electrophilicity relation while investigating the C-H functionalization of benzene derivatives.[14,15] In fact, when α-aryl-α-diazoacetate substrates and benzenes were reacted together in the presence of various gold(I) catalysts, only the dimerization of diazo reagents was observed. However, the installation of electron-withdrawing groups on the ester or the aryl group of the α-aryl-α-diazoacetate resulted in the *para*-selective functionalization of benzene derivatives. Very high yields and high selectivities were obtained with various arenes and diazo reagents. These reactions were realized at room temperature using cationic gold(I) complexes (Scheme 4.7).

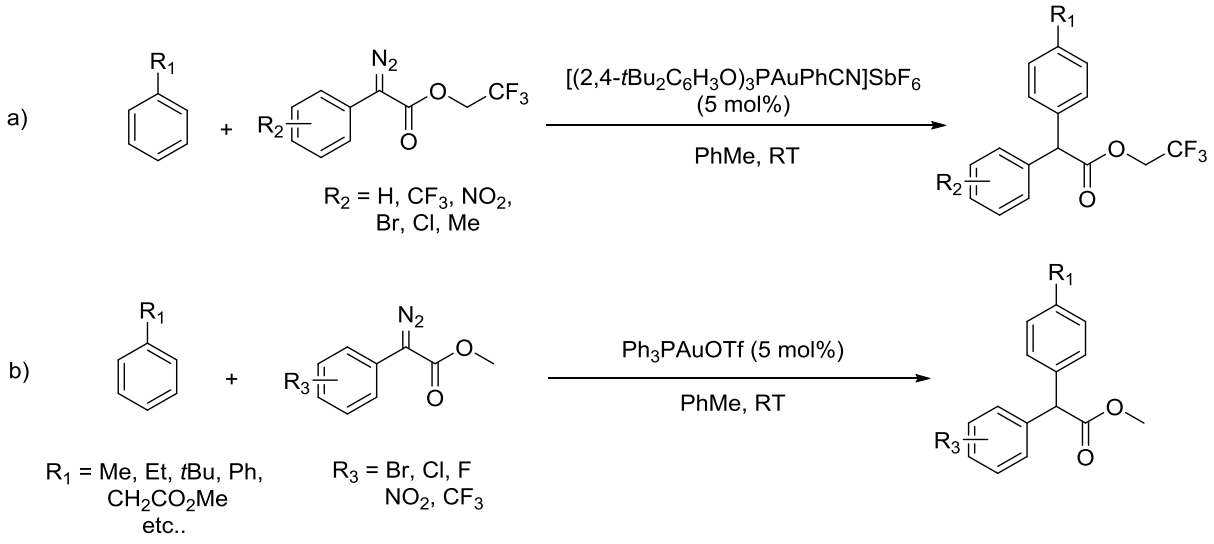

Scheme 4.7 Gold-catalyzed selective C-H functionalization of benzene derivatives with diazo reagents bearing a) EWG on the ester moiety and b) EWG on the aryl group.

The catalytic transfer of carbene fragments from diazo compounds to olefins is one of the most employed pathways in the synthesis of cyclopropane rings. These type of reactions have been reported with all transition metals,[16] and recently gold was shown to catalyze this

transformation as well. Echavarren *et al.* conducted an experimental study regarding the cyclopropanation of olefins with ethyl phenyldiazoacetate and gold(I) complexes bearing ligands with different electronic properties.[17] Thus, a series of gold complexes containing either phosphorus-based (phosphine or phosphite) or NHC (saturated or unsaturated) ligands was prepared and their reactivity towards the cyclopropanation of styrene was assessed (Scheme 4.8).

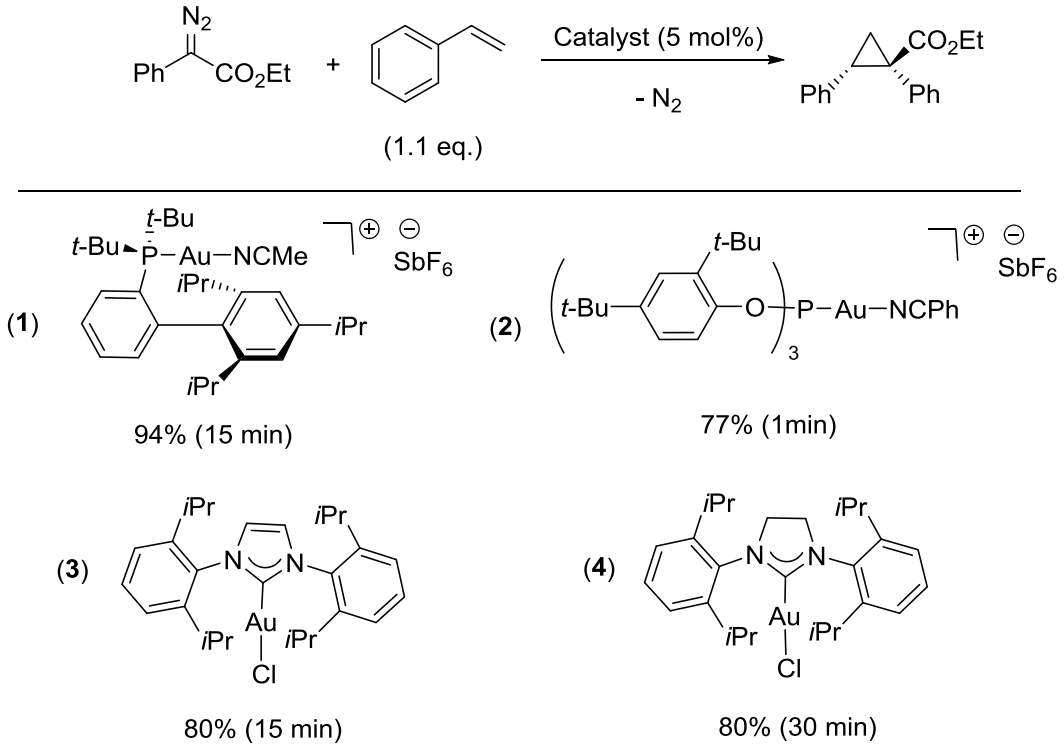

Scheme 4.8 Cyclopropanation of styrene with ethyl phenyldiazoacetate catalyzed by gold(I) complexes.

With nearly stoichiometric diazo/styrene ratio, the reaction afforded the functionalized cyclopropane in good to excellent yields, and the reaction times required for complete diazo consumption ranged from one to thirty minutes. Moreover, a unique diastereoisomer (the two phenyl rings in *cis* position) was obtained with the four gold(I) complexes. In this study, the authors compared the effect of the four different ligands on the carbene transfer reaction.

Thus, the activity of the catalysts was estimated based on the time required for complete consumption of the diazo reagent. In this respect, the phosphite-based gold(I) complex is the most active catalyst, since all the phenyldiazoacetate was consumed within one minute only (even at 0°C). These catalysts can also be compared based on the chemoselectivity: the relative amount of the cyclopropanes *vs.* the products derived from diazo coupling (carbene dimerization). Based on this parameter, the lowest chemoselectivity observed for the styrene cyclopropanation reaction was observed with the most active catalyst. This demonstrates that even though electrophilic catalysts are needed to promote these transformations, strong electrophilic character can also favors side reactions.

With the experience gained over the years in isolating and stabilizing reactive intermediates by a judicious choice of ligands, we got attracted by the possibility of characterizing the highly electrophilic α-oxo-gold(I) carbene.

4.2 Characterization of α-oxo gold(I) carbene

4.2.1 With (P,N) Ligand

As mentioned in chapter 2 *(section 2.4.2, scheme 2.21),* Zhang and coworkers reported the [3+2] annulation reaction between a terminal alkyne and a carboxamides for the formation of 2,4-disubstituted oxazoles.[18] When monophosphine gold(I) complexes were used as catalysts, the reaction didn't work. However, with gold(I) catalysts featuring bidentate (P,N) or (P,S) ligands, the reaction afforded the desired product in high yields. Therefore, bidentate ligands has been reported to play a key role in tempering the reactivity of α-oxo gold carbene intermediates *via* the generation of a tricoordinated gold intermediate, which is less electrophilic and thus more chemoselective when reacting with nucleophiles. This was further

supported by DFT calculations, and it was found that the three-coordinated gold(I) carbene complex is more stable than the dicoordinated one.

With 8-methylquinoline N-oxide, the postulated α-oxo gold carbene intermediate was generated but this species could not be detected. We envisioned to generate the α-oxo gold carbene at low temperature using the classical strategy, *i.e.* the decomposition of diazo reagents. To a solution of (Me-Dalphos)AuCl complex **10** and one equivalent of silver hexafluoroantimonate (*in situ* generation of the coordinatively unsaturated cationic gold(I) center), ethyl phenyldiazoacetate was added at low temperature (Scheme 4.9).

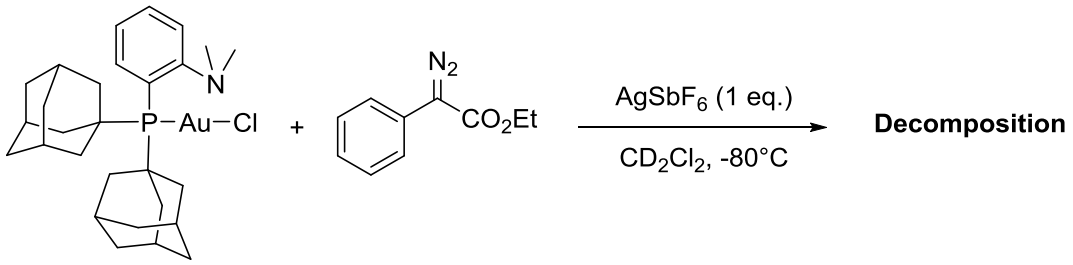

10

Scheme 4.9 Attempt to generate the α-oxo gold(I) carbene with complex **10** and ethyl phenyldiazoacetate.

After the addition of the diazo reagent, a change in color from colorless to dark orange was observed along with N_2 bubbling. The reaction was checked directly by NMR at -75°C, but unfortunately, the first check by $^{31}P\{^{1}H\}$ NMR displayed a peak forest, highlighting the instability of the α-oxo gold carbene even at very low temperatures. These experimental observations are consistent with that previously observed, and probably the nitrogen coordination to gold is too weak to stabilize this electrophilic species.

Since the α-oxo gold(I) carbene with the hemi-labile (P,N) ligand could not be characterized unambiguously at -75°C, we decided to use the *o*-carborane diphosphine ligand.

4.2.2 With (P,P) Ligand

4.2.2.1 Electronic Properties of bent (P,P) Gold(I) Complexes

As mentioned in chapter 2, the *o*-carborane diphosphine ligand induces a bent geometry around the gold center, and it was shown that the bending plays a key role in the oxidative addition process. Therefore, our group was interested to further explore the distinct electronic properties of the *o*-carborane diphosphine gold fragments.[19] A common experimental method used to quantify the electronic properties of a ligand and the degree of backdonation at a metal center consists in measuring the CO stretching frequency of a corresponding carbonyl complex. In that objective, a carbonyl complex was synthesized by reacting complex **6** with $GaCl_3$ (as halide scavenger) under 2 bar of carbon monoxide (Scheme 4.10).

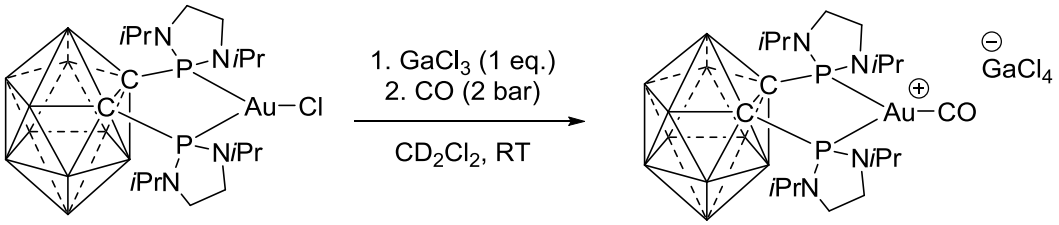

6

Scheme 4.10 Synthesis of the cationic bis(phosphine) gold(I) carbonyl complex.

The bis(phosphine) gold(I) carbonyl complex was fully characterized. The most important features of this carbonyl complex are the $^{13}C\{^1H\}$ NMR and IR data. The ^{13}C NMR displays a resonance signal at δ 191.8 ppm for the carbonyl moiety, which is shifted downfield compared to the signal for free CO (δ 184 ppm). Moreover, the ν(CO) stretching frequency (2113 cm^{-1}) is lower than that of free CO (2143 cm^{-1}), indicating a strong π-backdonation from gold to the carbonyl moiety. In fact, the bis(phosphine) gold(I) carbonyl complex stands as the first classical carbonyl gold complex, since all the previously reported carbonyl gold

species displayed CO stretching frequencies higher than that of free CO.[19] The bonding situation of this carbonyl complex was investigated computationally, and confirmed as well the major role of the *o*-carborane diphosphine ligand in the important Au→CO π-backdonation observed.

The unusual electronic properties of the *o*-carborane diphosphine ligand prompted our group to use this ligand to stabilize and isolate reactive species. In fact, our team reported in 2014 the isolation of an original gold(I) carbene complex.[19] Back in that time, most of the gold carbene complexes reported were stabilized by π-conjugation of the electro-deficient carbene center with[6] or without heteroatoms.[7,8] Moreover, gold(I) carbene stabilized by π-backdonation were not described and this is due to the weak π-backdonation from gold to the carbene moiety compared with other transition metals.[20] But the distinctive electronic properties of the *o*-carborane diphosphine ligand allowed the isolation and characterization of the first carbene complex stabilized by the gold fragment rather the carbene substituents. The gold(I) complex **6** reacted rapidly and cleanly with diphenyldiazomethane at -40°C to afford the gold(I) carbene complex (Scheme 4.11).

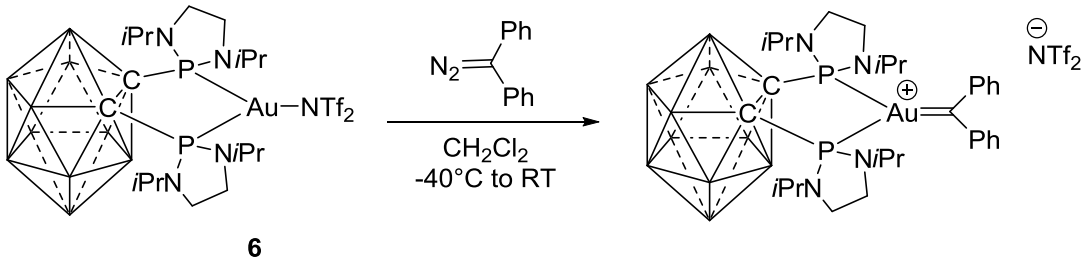

Scheme 4.11 Synthesis of the bis(phosphine) gold carbene complex.

The gold(I) carbene complex exhibited high thermal stability and thus it was fully characterized by means of multinuclear NMR, HRMS and X-ray diffraction analysis. Computational studies were carried out as well on the gold(I) carbene complex to assess the

role of the (P,P) bidentate ligand on the stability of the carbene species. A bonding interaction between the d_{xz}(Au) and $2p^{\pi}$(C) orbitals in the coordination plane of gold is apparent in the HOMO of the carbene complex. This indicates enhanced π-backdonation from the carborane diphosphine gold fragment, which results in an important contribution from the gold fragment to the stabilization of the carbene center.

These two examples highlight the peculiar electronic properties of the *o*-carborane diphosphine ligand and its crucial role in stabilizing reactive species. We were thus keen to take advantage of the electronic properties of the carborane diphosphine gold(I) complex (in particular the enhanced backdonation) to try to stabilize an α-oxo gold(I) carbene complex.

4.2.2.2 Synthesis of α-oxo Gold(I) Carbenes

We decided to generate the α-oxo gold(I) carbene first *via* the nucleophilic oxidant pathway, *i.e.* with an alkyne and pyridine *N*-oxide. To this end, an excess of diphenylacetylene was added to a solution of the bis(phosphine) gold(I) complex **1** and one equivalent of silver hexafluoroantimonate to generate the corresponding π-complex. After filtration of the silver salts generated in the reaction media, 3,5-dichloropyridine *N*-oxide was added. This reaction sequence was also performed with complex **2** (Scheme 4.12).

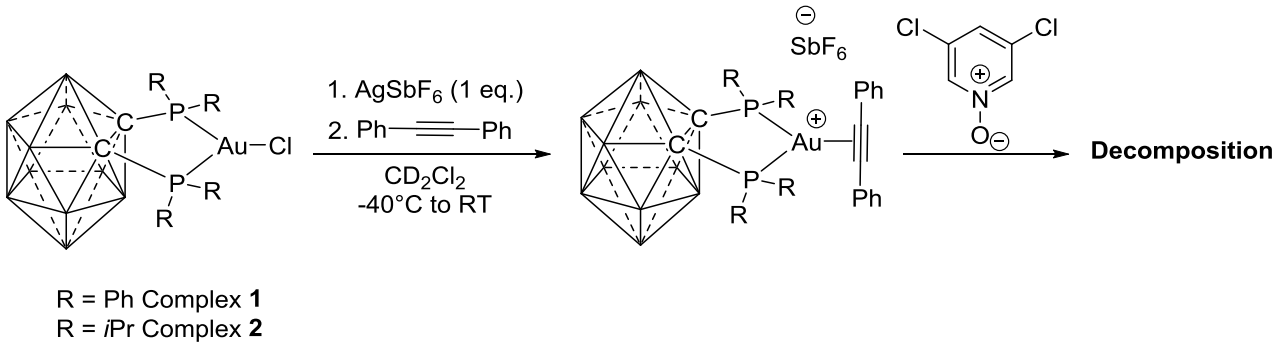

Scheme 4.12 Attempts to synthesize α-oxo gold(I) carbenes with complex **1** and **2**.

With both complexes, the corresponding π-species were formed instantly as pointed out by $^{31}P\{^{1}H\}$ NMR (δ 54.5 and 79.4 ppm for complex **1** and **2** respectively). However, the addition of pyridine *N*-oxide resulted in the formation of several phosphorus-containing species, and the precipitation of metallic gold could be observed. Thus, the formation of the α-oxo gold(I) carbene was not unambiguously confirmed, probably due to its rapid decomposition. Based on these experimental observations, we concluded that the electronic properties of complexes **1** and **2** were not suited for the stabilization of the α-oxo gold(I) carbene.

More electron-donating phosphorus substituents may prevent the decomposition observed with complex **1** and **2**, thus the same reaction sequence was performed again with complex **6** (Scheme 4.13).

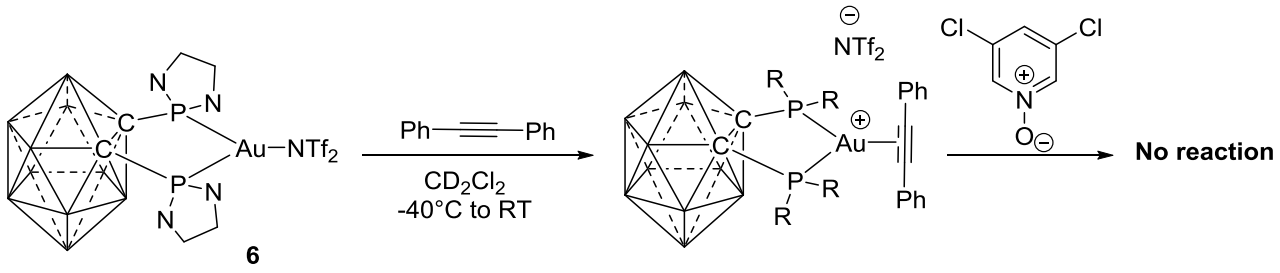

6

Scheme 4.13 Attempts to synthesize α-oxo gold(I) carbenes with complex **6**.

Once again, the formation of the π-complex was instantaneous and quantitative. However, no reaction was observed after the addition of 3,5-dichloropyridine *N*-oxide, even after heating at 50°C for several days. In fact, the π-complex seems to be too stable due to the strong π-backdonation from the bis(phosphine) gold(I) fragments to the coordinated alkyne, and thus the nucleophilic attack of the pyridine *N*-oxide could not take place. Thus, we decided to generate the α-oxo gold(I) carbene *via* the classical pathway, *i.e.* with diazo reagents.

In that objective, one equivalent of ethyl 2-diazo-2-phenylacetate was added at -40°C to a solution of complex **6** (Scheme 4.14). The reaction mixture turned immediately to dark violet along with N_2 bubbling, suggesting the formation of a carbene species, since the previously reported gold carbene complexes were strongly colored.[19] $^{31}P\{^1H\}$ monitoring of the reaction at low temperature, indicated the instantaneous formation of a new phosphorus containing species, displaying a singlet resonance at δ = 138.9 ppm.

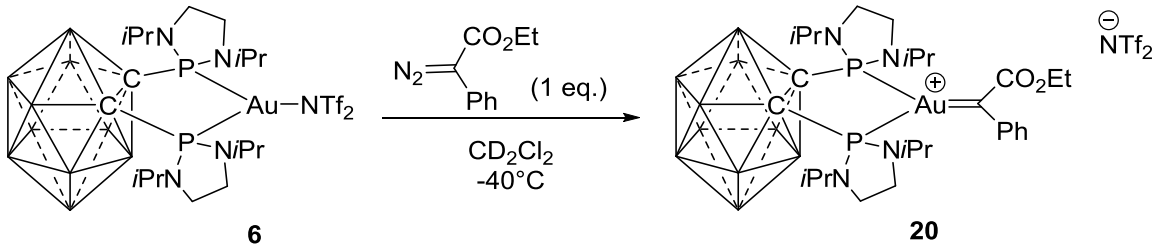

Scheme 4.14 Synthesis of the α-oxo gold carbene complex **20** at -40°C.

The single ^{31}P NMR signal implies symmetric coordination of the two phosphorus donor arms to gold. Complex **20** was revealed to be thermally unstable (decomposition above 0°C) and could not be isolated. However, it was completely characterized at low temperature by multinuclear NMR spectroscopy, and the formation of the carbene complex was clearly indicated by the $^{13}C\{^1H\}$ NMR spectrum. In fact, a characteristic resonance signal at δ = 283.4 ppm appears as a triplet (J_{CP} = 87.6 Hz), which is in the range of previously characterized gold carbene complexes (225-321 ppm).[6-8,19] Moreover, the resonance signals for the carbonyl moiety and all the C_{Ar} of the phenyl ring (except the *para*-carbon) appeared as triplets, and displayed coupling constants with the phosphorus atoms ranging from 7.6 to 15.8 Hz.

Satisfyingly, single crystals of **20** were grown by slow diffusion of pentane into a concentrated solution of this compound at -30°C, and an X-ray diffraction analysis was performed (Figure 4.1).

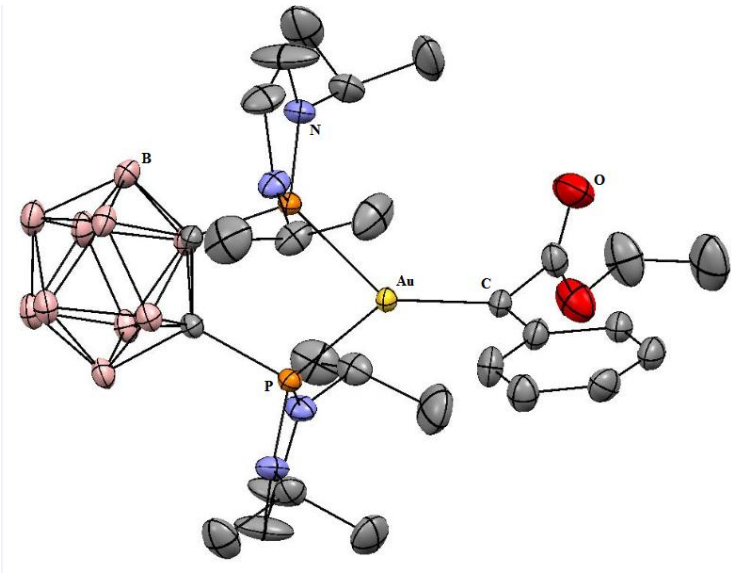

Figure 4.1 Molecular structure of complex **20** determined by single X-ray crystallography. Solvent molecules, the NTf^2 counter anion and hydrogen atoms were omitted for clarity. Selected bond lengths [Å] and angles [°]: P1Au 2.3567(7), P2Au 2.3551(6), AuC 1.961(2), P1AuP2 90.57(2).

κ^2-Coordination of the carborane diphosphine ligand to gold in a symmetric manner affords a tricoordinate α-oxo gold(I) carbene complex, and the gold sits in a trigonal planar geometry. The carbene center is perfectly planar and perpendicular to the PAuP coordination plane with a twist angle of 87.15°. This orientation minimizes steric repulsions between the carbene moiety and the substituents at phosphorus. The Au-C bond length (1.961(2) Å) is in the shortest range of reported Au-carbene bonds. Noteworthy, the phenyl ring is almost co-planar with the carbene center and the $C_{carbene}$-Ar_{ipso} is slightly contracted (1.449(4) Å) indicating that the π-system of the aromatic ring participates in the stabilization of the carbene species. On the other hand, the carbonyl fragment of the ester group is above the carbene plane and

points away from the electrophilic gold center, suggesting the absence of interaction between –CO and Au atoms.

Computational studies were carried out to gain insight into the electronic situation within the tricoordinated α-oxo gold carbene complex and to assess the role of the carborane diphosphine ligand in its stabilization. The optimized geometry fits nicely with that determined crystallographically. Moreover, the computed $^{13}C\{^{1}H\}$ NMR chemical shifts of the carbene atom (δ 292.6 ppm) and the associated P-C coupling constant also correlate well with experimental values. The frontier orbitals HOMO and LUMO of complex **20** correspond to bonding and anti-bonding interaction between the occupied the d_{xz}(Au) orbital at gold and the $2p^{\pi}$(C) orbital at the carbene center (Figure 4.2).

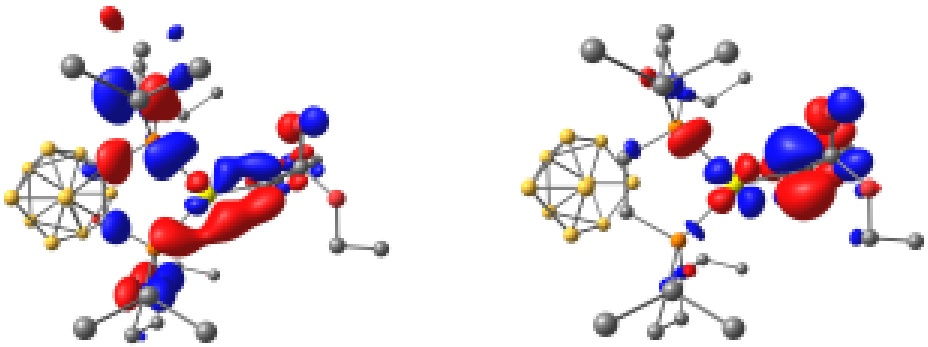

Figure 4.2 HOMO (left) and LUMO (right) of the α-oxo gold(I) carbene complex **20**.

NBO analysis displayed $\pi_{C=C}$(Ph) → $2p^{\pi}$(C) and n_C^{σ} → $\pi_{C=O}^{*}$(CO) donor-acceptor interactions (65.6 and 16.0 kcal/mol, respectively), indicative of the push-pull nature of the α-oxo gold carbene. Moreover, a significant d_{xz}(Au) → $2p^{\pi}$(C) back-donation (18.2 kcal/mol) was observed, which is also apparent in the considerable contribution of the $2p^{\pi}$(C) orbital (12.1%) in the corresponding NLMO (Natural Localized Molecular Orbital) associated to d_{xz}(Au). The significant π-backdonation from the carborane diphosphine gold fragment to the carbene was

also retrieved from the donation/backdonation ratio estimated by CDA (Charge-decomposition analysis) with a d/b ratio of 1.76, and from the absence of charge transfer between the carbene and gold fragments (CT = -0.07 e^-).

To highlight the key role of the carborane diphosphine ligand, the related α-oxo gold carbene complex featuring the MeDalphos ligand was also optimized, and its bonding situation was analyzed. In the optimized geometry, the Au···N (2.53 Å) distance is rather long [46% lower than the Σr_{VdW} (3.07 Å) but 22% longer than the Σr_{cov} (2.07 Å)]. Therefore, the P-Au-$C_{carbene}$ arrangement is almost linear (163.3°), and in the absence of significant N to Au coordination, the gold center is electron-deficient. As a consequence, with the (P,N) ligand, both the donation / back-donation ratio (d/b = 2.16) and the charge transfer between the carbene and the gold fragment (CT = 0.8 e^-) indicate a significantly lower contribution of the [(P,N)Au^+] fragment to the stabilization of the carbene species (Figure 4.3).

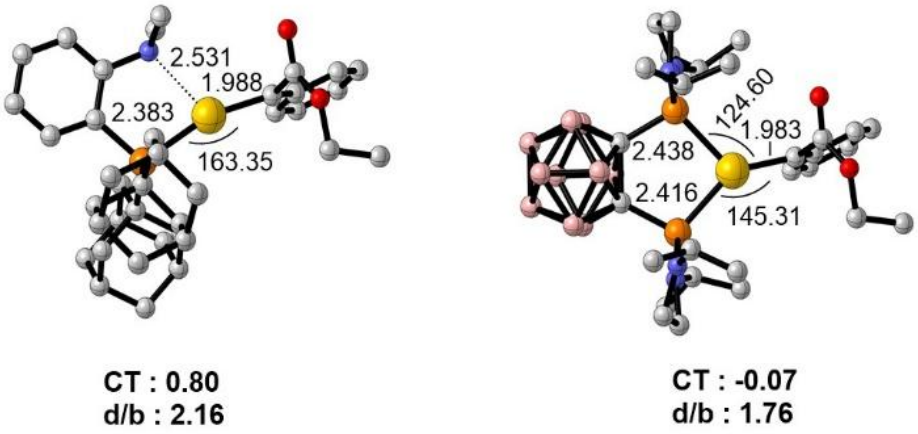

Figure 4.3 Optimized geometry of the (P,N) α-oxo gold(I) carbene complex (left) with key geometric and bonding parameters (distances in Å and bond angles in °) compared with the related (P,P) carbene complex **20** (right).

After substantiating the crucial role of the (P,P) bidentate ligand, we were keen to investigate to which extent the bidentate ligand could stabilize highly electrophilic α-oxo gold(I) carbenes. In that objective, the α-aryl-α-diazoacetate substrate featuring two CF_3 groups on

the phenyl ring was synthesized and reacted with complex **6** at low temperature to generate the corresponding carbene (Scheme 4.15).

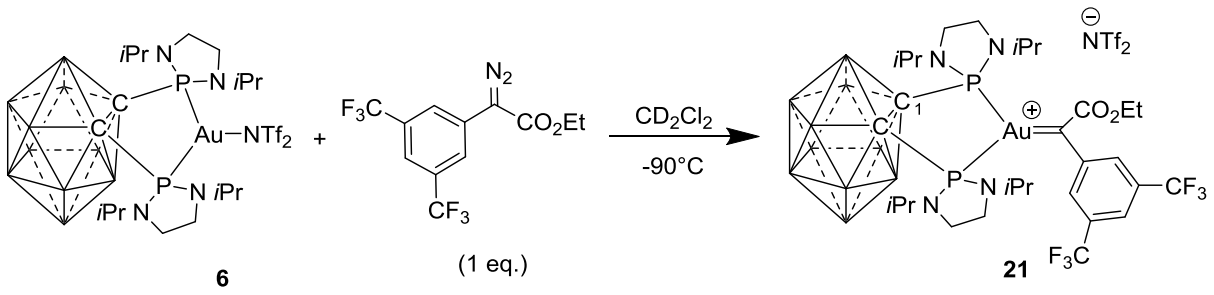

Scheme 4.15 Synthesis of the α-oxo gold carbene complex **21** at -90°C.

The α-oxo gold carbene complex **21** was much less stable than complex **20**, and decomposed very rapidly even at low temperature. Thus, complex **21** was only detected by $^{31}P\{^{1}H\}$ NMR spectroscopy at -90°C. More information about the electronic structure of complex **21** were provided by DFT. Its geometric features and bonding situation are similar to those of complex **20**. Here also, significant back-donation from gold to the carbene fragment was apparent in NBO [d_{xz}(Au) → $2p^{\pi}$(C) donor-acceptor interaction of 18.8 kcal/mol, 13.3% contribution of $2p^{\pi}$(C) in the corresponding NLMO d_{xz}(Au)] and CDA analysis (d/b = 1.70). The most apparent difference is the energy levels of the frontier orbitals, which stand at lower energetic level (by 0.2 – 0.3 eV) compared to that of complex **20**, and resembles that of the (P,N) gold(I) carbene complex (Figure 4.4).

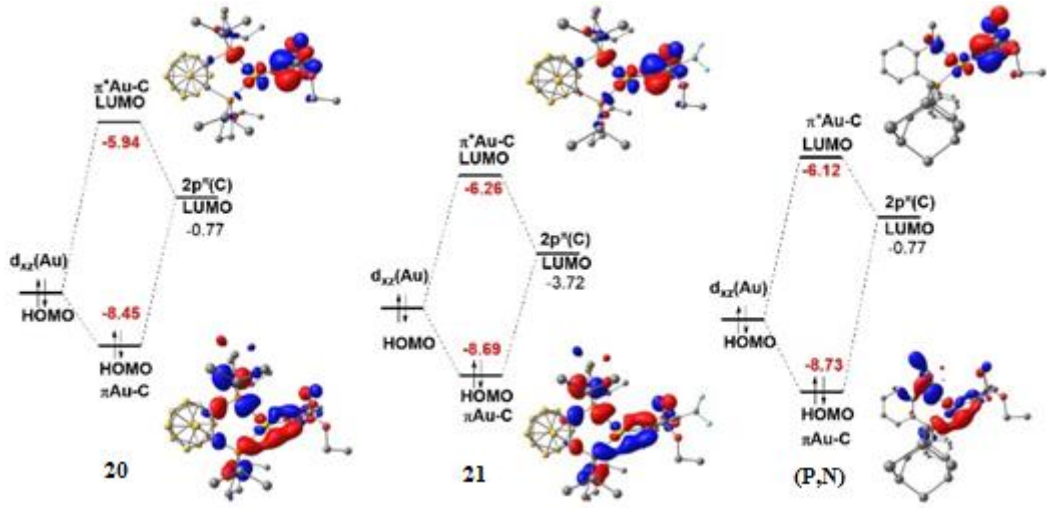

Figure 4.4 Schematic representation of the HOMO-LUMO energy levels of the α-oxo gold carbene complexes.

The experimental observations along with the computation data indicate that the (P,P) bidentate ligand plays a major role in stabilizing the α-oxo gold carbene species. In fact, enhanced back-donation from the *o*-carborane diphosphine gold fragment to the carbene moiety was observed, in contrast to the weak π-back-donation from the [(P,N)Au^{+}] fragment.

4.3 Reactivity of α-oxo Gold(I) Carbenes

After characterizing and examining closely the electronic properties of the α-oxo gold(I) carbene species, we were eager to investigate the consequences of the chelating coordination of the (P,P) ligand into the reactivity and/or selectivity of the carbene complex.

4.3.1 Towards Styrene

As mentioned-above, gold was shown recently to catalyze the transfer of carbene fragments to olefins to produce functionalized cyclopropane rings. The reported examples usually employ monodentate ligands (R_3P or NHC) and afford the desired products in good yields and with short reaction times (1 to 30 minutes) (*cf.* section 4.1). Therefore, after investigating the reactivity of complex **20** with phenols, we were interested to check its reactivity towards the cyclopropanation reaction of styrene.

Accordingly, to a solution of 2-diazo-2-phenylacetate was added 5 mol% of complex **6** in styrene over five minutes, at -40°C (Scheme 4.16).

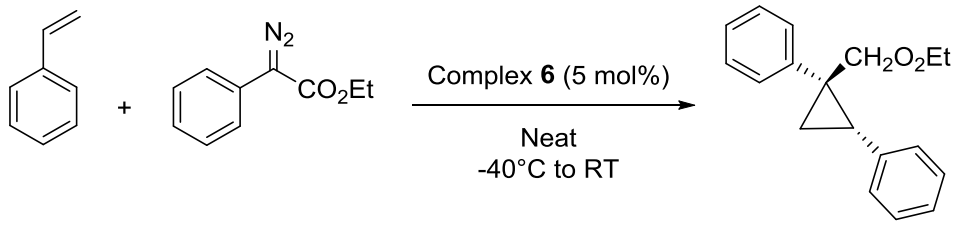

Scheme 4.16 Reactivity of the *in situ* generated α-oxo gold(I) carbene towards styrene.

Aliquots of the reaction mixture were submitted to GC-MS analysis, and the yields were determined *vs. n*-dodecane as internal standard. After one hour at room temperature, only 18% of the desired product was obtained, and after sixty four hours the reaction reached a maximum yield affording the *cis* isomer in 58% yield. The reaction with the (P,P) ligand is clearly slower than the previously reported gold-catalyzed cyclopropanation of styrene. This is probably due to the significant stabilization induced by the bidentate ligand, therefore tempering and attenuating the reactivity of the *in situ* generated α-oxo gold(I) carbene.

4.3.2 Towards Phosphine-Borane

Organoborons are among the most widely used substrates in organometallic chemistry and in modern organic synthesis. Furthermore, the development of new efficient catalytic methodologies for the preparation of these compounds is an active area of research. Recently, several reports described the metal (usually Rh or Cu) catalyzed carbene insertion reactions into B-H bonds for the formation of C-B bonds.[21,22] This transformation is described to be challenging, since the B-H bond does not readily undergo insertion with metal carbenes. However, upon formation of an adduct with an amine or a phosphine, the carbene insertion reaction into the B-H bond of borane becomes achievable.

To our knowledge, this transformation has never been reported with gold, and we were interested to investigate the behavior of the (P,P) gold(I) carbene towards the insertion reaction into the B-H bond of phosphine-borane. Accordingly, one equivalent of ethyl 2-diazo-2-phenylacetate was added to a solution of two equivalents of triphenylphosine-borane adduct and 5 mol% of complex **6**, over five minutes, at low temperature to generate the α-oxo gold carbene (Scheme 4.17).

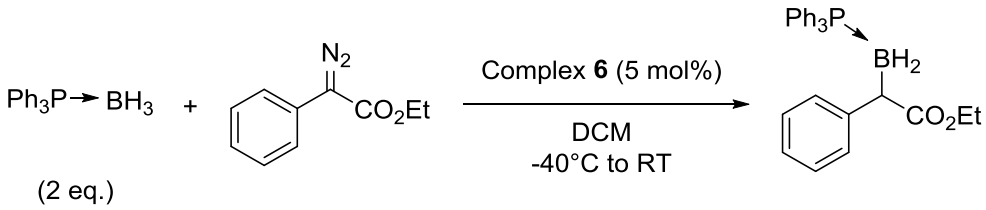

Scheme 4.17 Gold-catalyzed carbene insertion into the B-H bond of phosphine-borane.

The reaction was monitored by $^{31}P\{^{1}H\}$ NMR using an internal standard to determine the yield of the insertion product. The reaction was quiet fast, and after thirty minutes at room temperature, the desired product was obtained in 56% yield. In the literature, the same

reaction was reported with a Cu(I) catalyst, and the reaction afforded the insertion product in 80% yield but after 18h at room temperature.[21] Although, the yield is lower with the bidentate gold(I) catalyst, it seems to be more reactive, and maybe after optimization of the reaction conditions, higher yields could be obtained.

4.3.3 Towards Phenol

As mentioned in section 4.1, the carbene transfer reaction to phenols is of high synthetic interest, but remains a challenge for late transition metals due to the competitive O-H bond insertion reactions. And as illustrated by the example discussed above, monophosphine gold(I) complexes have been recently shown to catalyze the *p*-C-H bond functionalization, and high selectivity were observed with electron deprived phosphite ligands.

In order to check its reactivity and selectivity, the α-oxo gold(I) carbene was generated *in situ* at low temperature and one equivalent of phenol was added to the reaction mixture (Scheme 4.18). The GC-MS was calibrated with both O-H and C-H insertion products *vs. n*-dodecane as an internal standard.

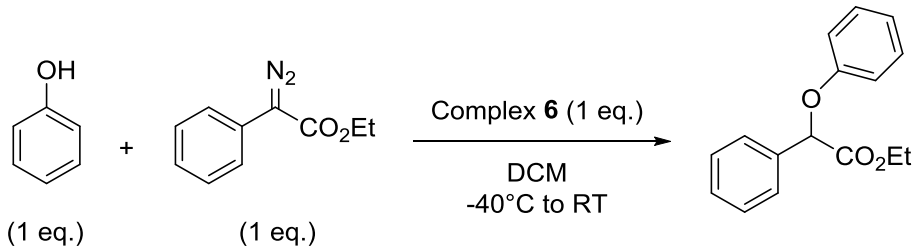

Scheme 4.18 Reactivity of the *in situ* generated α-oxo gold(I) carbene towards phenol.

Strikingly, after two hours, the reaction afforded exclusively the corresponding arylether product stemming from O-H insertion in 100% yield. Thus, a reverse chemoselectivity is observed with the (P,P) bidentate ligand compared to the reported examples with highly electrophilic gold(I) carbenes featuring electron-deprived monodentate phosphines. In fact, due to the enhanced backdonation induced by the diphosphine ligand, the electrophilicity of the gold carbene species was attenuated, and therefore its reactivity is more akin to other late transition metals.[11]

The next step was to translate the carbene transfer reaction with complex **6** from stoichiometric to catalytic conditions. To do so, a solution of ethyl 2-diazo-2-phenylacetate (1 eq.) and phenol (1 eq.) was added at -40°C to a solution of 5 mol% of the gold complex **6**. As indicated by GC-MS analysis, ethyl 2-(4-hydroxyphenyl)-2-phenylacetate was obtained in 29% yield after two hours. Based on this result, we surveyed the influence of two parameters: the injection time of diazo and phenol solution, as well as their ratio.

The first parameter inspected was the injection time of the solution of diazo and phenol substrates (Table 4.1). At -40°C, to a 5 mol% solution of complex **6** in DCM, was added an equimolar solution of phenol and diazo over 5, 20 and 90 minutes. Indeed, the injection time of the diazo and phenol solution affected the yield of the reaction, and the highest yield was obtained when the solution was injected over five minutes (entry 1). Increasing the injection time (entry 2 and 3) resulted in lower yields, probably due to the decomposition of the gold catalyst. Then, the ratio of diazo and phenol was optimized, and with a 5/1 ratio, a reasonable yield of 60% was obtained after two hours (entry 5). Noteworthy, only the product deriving from O-H insertion was obtained during the reactions catalyzed by complex **6**.

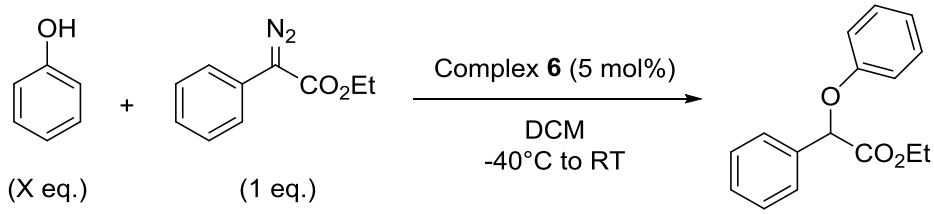

Table 4.1 Optimization of reaction conditions with phenol and ethyl 2-diazo-2-phenylacetate (injection time and diazo/phenol ratio).

Entry	Phenol (X eq.)	Injection Time	Yield (%)[a]
1	1	5 min	29%
2	1	20 min	7%
3	1	90 min	15%
4	2	5 min	35%
5	5	5 min	60%

[a]Yields determined after 2h using calibrated GC-MS analysis *vs. n*-dodecane as internal standard.

Next, to further confirm the gold electrophilicity/selectivity relationship for C-H *vs.* OH insertion, the reaction with ethyl 2-(3,5-bis(trifluoromethyl)phenyl)-2-diazoacetate was investigated. The electron-withdrawing CF_3 groups may counterbalance the electronic stabilization induced by the (P,P) bidentate ligand, and therefore restituting the classical electrophilic reactivity to the α-oxo gold(I) carbene.

With the optimized conditions in hands, a solution of ethyl 2-(3,5-bis(trifluoromethyl)phenyl)-2-diazoacetate (1 eq.) and phenol (5 eq.) was added at -40°C to a solution of 5 mol% of complex **6** (Scheme 4.19).

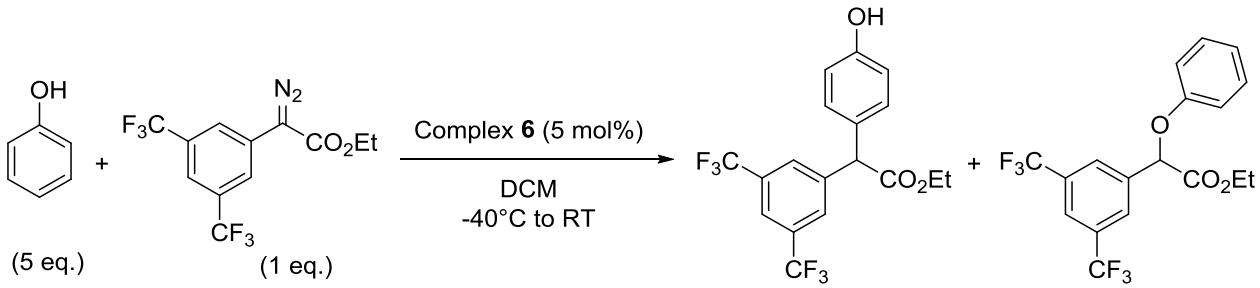

Scheme 4.19 Reactivity of the *in situ* generated α-oxo gold(I) carbene towards phenol.

The reaction proceeded faster, and after thirty minutes, GC-MS analysis revealed the presence of a mixture of products. Satisfyingly, the C-H bond insertion product was obtained as the major product in 68% yield, along with minor amount of the O-H insertion product (32% yield). Indeed, the electron-withdrawing groups on the phenyl ring of the diazo substrate outweighed the back-donation from the [(P,P)Au^{+}] fragment, and this result confirms that the selectivity of the α-oxo gold(I) species for C-H *vs.* O-H insertion is governed by the electrophilic character of the carbene.

4.4 Conclusion

With the *o*-carborane diphosphine ligand, the α-oxo gold(I) carbene was synthesized and characterized (NMR spectroscopy, X-ray and high resolution mass spectrometry) for the first time. On the other hand, with the hemi-labile (P,N) ligand, the α-oxo gold(I) carbene was unstable and decomposed in solution even at low temperature. DFT calculations were carried out on both gold(I) carbenes to compare their electronic situation and to assess the role of the ligand in stabilizing these highly electrophilic species. Consistent with the experimental observations, the (P,P) bidentate ligand was found to play a key role in stabilizing the gold carbene species due to an enhanced π-backdonation from the *o*-carborane diphosphine gold fragment to the carbene moiety. In contrast, a significantly lower contribution of the [(P,N)Au^{+}] fragment to the stabilization of the carbene complex was observed.

The cyclopropanation of styrene with the α-oxo gold carbene was tested. The reaction was slow compared to the previously reported monocoordinated gold(I) complexes. This suggest that the reactivity of the carbene was tempered by the significant stabilization induced by the (P,P) bidentate ligand. Then, the insertion of carbene into B-H bonds of phosphine-borane was conducted, and after half an hour the desired product was obtained in 56% yield. This unprecedented reaction with gold could be improved after optimizing the reaction conditions.

The reactivity of the *in situ* generated α-oxo gold(I) carbene complexes towards phenol was investigated. Interestingly, a reverse of chemoselectivity was observed in our case compared to the reported gold(I) carbene species featuring monodentate phosphines, and only the product deriving from O-H insertion was formed. In fact, the increased π-backdonation from the (P,P) bidentate ligand attenuated the electrophilicity of the α-oxo gold(I) carbene, and its reactivity is now similar to that of other late transition metals. Addition of electron-withdrawing groups on the α-aryl diazoacetate counterbalanced the electronic stabilization of

the bidentate ligand, and the C-H insertion compound was formed as the major product. This result confirmed that the selectivity of α-oxo gold carbenes for C-H *vs.* O-H insertion is controlled by the electrophilic character of the carbene.

4.5 Experimental Part

4.5.1 General Remarks

Ethyl 2-diazo-2-phenylacetate[23] and ethyl 2-(3,5-bis(trifluoromethyl)phenyl)-2-diazoacetate[24] were prepared according to reported procedures. Ethyl 2-phenoxy-2-phenylacetate[12], ethyl 2-(3,5-bis(trifluoromethyl)phenyl)-2-phenoxyacetate[12], ethyl 2-(3,5-bis(trifluoromethyl)phenyl)-2-(4-hydroxyphenyl)acetate[12], and ethyl 1,2-diphenylcyclopropane-1-carboxylate[25] were prepared according to reported procedures, and the GC-MS was calibrated with the authentic compounds *vs.* *n*-dodecane as internal standard. Phenol was dried prior to use.

General procedure for the synthesis of α-oxo gold (I) carbene with α-aryl-α-diazoacetates

In a glovebox, a screw-cap NMR tube was charged with complex **6** (20.0 mg, 0.021 mmol) in dichloromethane-d^2 (0.3 mL). α-aryl-α-diazoacetate (0.021 mmol) was transferred into a small glass vial and dissolved in dichloromethane-d^2 (0.3 mL). The prepared solution was loaded into a plastic syringe equipped with a stainless steel needle. Outside the glovebox, the NMR tube was cooled down to -40°C (Ethanol/ N_2 cold bath). At this temperature, the solution of α-aryl-α-diazoacetate was added to the complex **6** solution. Upon addition, the reaction mixture turned immediately dark violet. Due to thermal instability, all attempts to isolate it in pure form failed. The products were characterized by NMR spectroscopic analysis at low temperatures.

Single crystals of **20** were grown by slow diffusion of pentane into a concentrated solution of this complex in dichloromethane at -30°C.

Synthesis of α-oxo gold (I) carbene with ethyl-2-diazo-2-phenylacetate

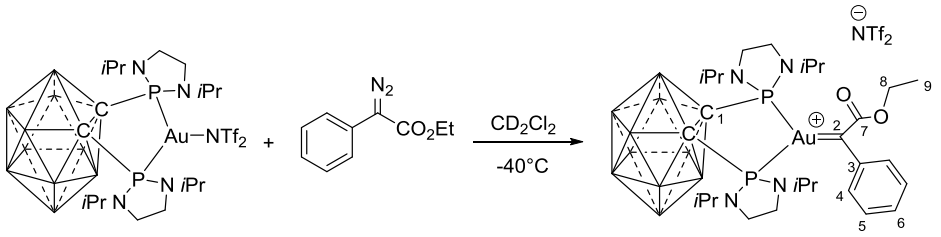

6 **20**

^{31}P{^{1}H} NMR (162 MHz, CD_2Cl_2): δ 138.9 (s). **^{1}H NMR** (400 MHz, CD_2Cl_2): δ 7.77-7.71 (m, 1H, H_{Ar}), 7.64-7.55 (m, 4H, H_{Ar}), 4.36 (q, J_{H-H} = 7.1 Hz, 2H, H_8), 3.64-3.51 (m, 4H, C*H*$(CH_3)_2$), 3.34-3.20 (m, 8H, N(C*H*$_2)_2$N), 2.84-1.96 (br.s, 10H, H_{BH}), 1.34-1.30 (m, 15H, CH(C*H*$_3)_2$ and H_9), 1.19 (d, J_{H-H} = 6.6 Hz, 6H, CH(C*H*$_3)_2$), 0.96 (d, J_{H-H} = 6.6 Hz, 6H, CH(C*H*$_3)_2$). **^{13}C{^{1}H} NMR** (100 MHz, CD_2Cl_2): δ 283.4 (t, J_{C-P} = 87.6 Hz, C_2), 173.0 (t, J_{C-P} = 11.5 Hz, C_7), 144.5 (t, J_{C-P} = 15.8 Hz, C_3), 139.0 (t, J_{C-P} = 9.6 Hz, C_4), 130.3 (t, J_{C-P} = 7.6 Hz, C_5), 129.8 (s, C_6), 119.6 (q, J_{C-F} = 319.1 Hz, CF_3), 90.8 (t, J_{C-P} = 25.2 Hz, C_1), 62.5 (s, C_8), 50.4 (t, J_{C-P} = 8.1 Hz, *C*H$(CH_3)_2$), 50.1 (t, J_{C-P} = 8.1 Hz, *C*H$(CH_3)_2$), 42.3 (s, N(*C*H$_2)_2$N), 21.4 (*pseudo* t, *N*= 2.8 Hz, CH(*C*H$_3)_2$), 21.1 (*pseudo* t, *N*= 2.8 Hz, CH(*C*H$_3)_2$), 20.8 (s, CH(*C*H$_3)_2$), 19.9 (s, CH(*C*H$_3)_2$), 14.3 (s, C_9). **^{19}F NMR** (282 MHz, CD_2Cl_2): δ -79.1 (s, CF_3). **^{11}B {^{1}H} NMR** (128 MHz, CD_2Cl_2): δ -2.8, -6.7, -9.6, -10.7. **HRMS (ESI+):** calculated for $[M]^+ = C_{28}H_{56}B_{10}N_4O_2P_2Au^+$: 847.4554. Found: 847.4561

Synthesis of α-oxo gold (I) carbene with ethyl 2-(3,5-bis(trifluoromethyl)phenyl)-2-diazoacetate

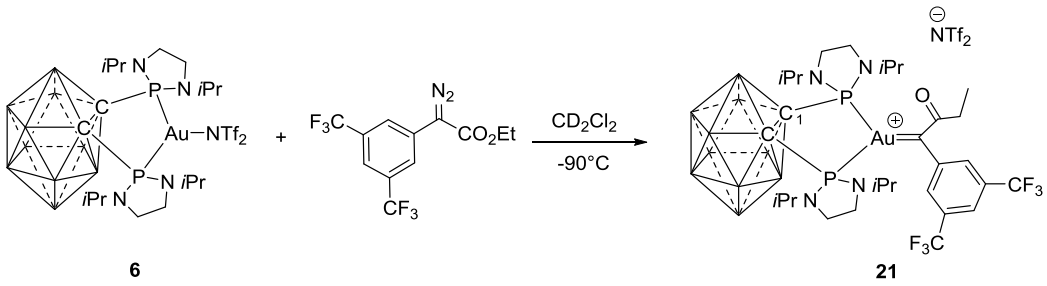

Attempts of synthesis of complex **21** were performed following the general procedure, except for the reaction's temperature: the solution of ethyl 2-(3,5-bis(trifluoromethyl)phenyl)-2-diazoacetate was added to the complex **6** solution at -90°C. Upon addition, the reaction mixture turned immediately dark violet with dinitrogen evolution. The reaction was monitored by $^{31}P\{^{1}H\}$ NMR at -90°C. The first check (t0) indicated the instantaneous formation of a major phosphorus-containing species (73%), displaying a resonance signal at δ 142.7 ppm (s), along with unidentified products (27%). After thirty minutes at -90°C, this resonance signal was not observed by $^{31}P\{^{1}H\}$ NMR, indicating the decomposition of complex **21**. $^{31}P\{^{1}H\}$ NMR (203 MHz, CD_2Cl_2): δ 142.7 ppm (s).

Cyclopropanation of styrene with ethyl 2-diazo-2-phenylacetate *via* gold catalysis

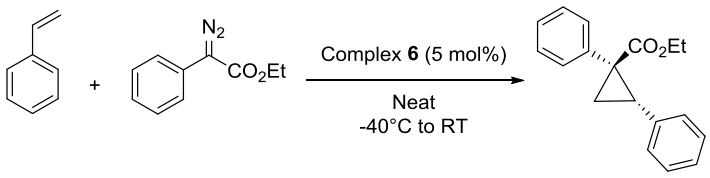

In a glovebox, a flame dried Schlenk equipped with a magnetic stirrer bar was charged with complex **6** (5.0 mg, 0.0055 mmol) in styrene (1.0 mL). Ethyl 2-diazo-2-phenylacetate (20.0 mg, 0.11 mmol) was transferred into a small glass vial and dissolved in styrene (1.0 mL). This solution was loaded into a plastic syringe equipped with stainless steel needle. This syringe was closed by blocking the needle with a septum. Outside the glovebox, the Schlenk was cooled down to -40°C (Ethanol/N_2 cold bath). At this temperature, the solution ethyl 2-diazo-2-phenylacetate was added drop-wise over five minutes. The reaction was then allowed to warm to room temperature. The yield was determined by GC-MS using *n*-dodecane as internal standard. After 64 hours at room temperature, the cyclopropane product was obtained in 58% yield.

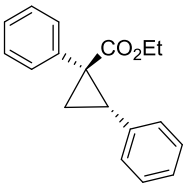

This compound was prepared according to reported procedure.[25] The relative configuration was determined by comparison with the known compounds.[26] **^{1}H NMR** (300 MHz, $CDCl_3$): δ 7.14-7.05 (m, 8H), 6.80-6.77 (m, 2H), 4.22-4.08 (m, 2H), 3.12 (dd, J_{H-H} = 7.5, 9.2 Hz, 1H), 2.15 (dd, J_{H-H} = 4.9, 9.5 Hz, 1H), 1.89 (dd, J_{H-H} = 4.9, 7.4 Hz, 1H), 1.19 (t, J_{H-H} = 7.0 Hz, 3H).

Carbene insertion into B-H bond *via* gold catalysis

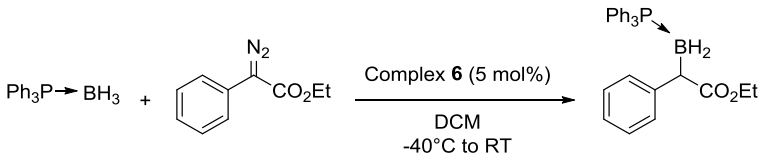

In a glovebox, a screw-cap NMR tube was charged with complex **6** (3.0 mg, 0.003 mmol) and the phosphine-borane adduct (30.0 mg, 0.110 mmol) in dichloromethane-d^2 (0.3 mL). Ethyl 2-diazo-2-phenylacetate (11.0 mg, 0.055 mmol) was transferred into a small glass vial and dissolved in dichloromethane-d^2 (0.3 mL). The prepared solution was loaded into a plastic syringe equipped with a stainless steel needle. Outside the glovebox, the NMR tube was cooled down to -40°C (Ethanol/ N_2 cold bath). At this temperature, the solution of ethyl 2-diazo-2-phenylacetate was added, over five minutes, to the complex **6** and the phosphine-borane solution. The reaction was then allowed to warm to room temperature and was monitored by $^{31}P\{^1H\}$ NMR using an internal standard. After 30 minutes, the reaction afforded the insertion product with 56% yield.(22)

General procedure for the functionalization of phenol with α-aryl-α-diazoacetates *via* gold catalysis

In a glovebox, a flame dried Schlenk equipped with a magnetic stirrer bar was charged with complex **6** (5.0 mg, 0.0055 mmol) in dichloromethane (0.5 mL). Phenol (52.0 mg, 0.55 mmol) and α-aryl-α-diazoacetate (0.11 mmol) were transferred into a small glass vial and dissolved in dichloromethane (1.0 mL). This solution was loaded into a plastic syringe equipped with stainless steel needle. This syringe was closed by blocking the needle with a septum. Outside the glovebox, the Schlenk was cooled down to -40°C (Ethanol/N_2 cold bath). At this temperature, the solution of phenol and α-aryl-α-diazoacetate was added drop-wise over five minutes. The reaction was then allowed to warm to room temperature. The yields were determined by GC-MS using *n*-dodecane as internal standard.

Functionalization of phenol with ethyl 2-diazo-2-phenylacetate

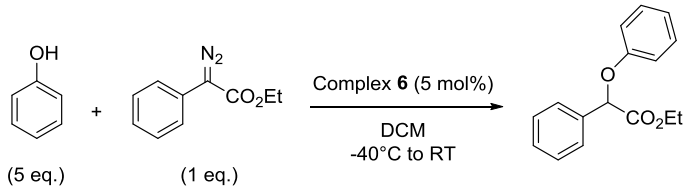

The general procedure was followed using ethyl 2-diazo-2-phenylacetate (0.11 mmol) and phenol (0.55 mmol). Aliquots of the reaction mixture were submitted to GC-MS analysis. After two hours, the reaction afforded the desired product in 60% yield.

Functionalization of phenol with ethyl 2-(3,5-bis(trifluoromethyl)phenyl)-2-diazoacetate

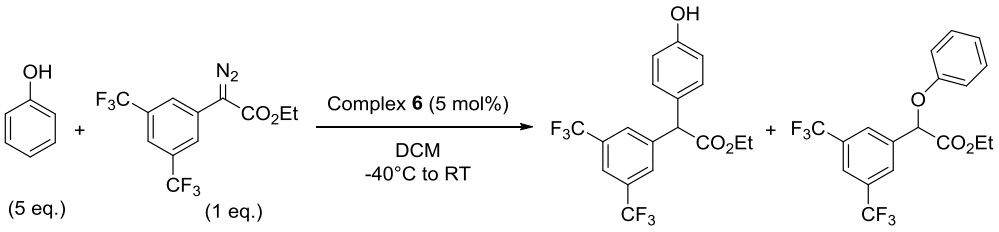

The general procedure was followed using ethyl 2-(3,5-bis(trifluoromethyl)phenyl)-2-diazoacetate (0.11 mmol) and phenol (0.55 mmol). Aliquots of the reaction mixture were submitted to GC-MS analysis. After 30 minutes, the reaction afforded the O-H insertion product in 32% yield and the C-H insertion product in 68% yield. After purification by column chromatography (Pentane/DCM 100:0 to 70:30), O-H insertion product was obtained as colorless oil (21% isolated yield) and C-H insertion product was obtained as a slightly yellow oil (50% isolated yield).

Ethyl 2-(3,5-bis(trifluoromethyl)phenyl)-2-phenoxyacetate:

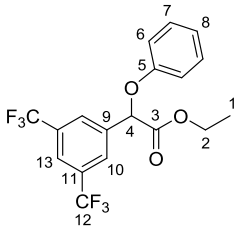

^{1}H NMR (300 MHz, $CDCl_3$): δ 8.10 (br.s, 2H, H_{Ar}), 7.90 (s, 1H, H_{Ar}), 7.32 (t, J_{H-H} = 8.0 Hz, 2H, H_{Ar}), 7.05 (t, J_{H-H} = 8.5 Hz, 1H, H_{Ar}), 6.97 (d, J_{H-H} = 8.0 Hz, 2H, H_{Ar}), 4.23 (q, J_{H-H} = 7.1 Hz, 2H, -C*H*$_2$CH$_3$), 1.21 (t, J_{H-H} = 7.1 Hz, 3H, -CH$_2$C*H*$_3$). **^{13}C{^{1}H} NMR** (125 MHz, $CDCl_3$): δ 168.8 (s, C_3), 156.9 (s, C_5), 138.3 (s, C_9), 132.3 (q, J_{C-F} = 33.7 Hz, C_{11}), 130.0 (s, C_7), 127.3 (d, J_{C-F} = 3.4 Hz, C_{10}), 123.2 (q, J_{C-F} = 275.2 Hz, C_{12}), 123.0 (sept, J_{C-F} = 3.8 Hz, C_{13}), 122.7 (s, C_8), 115.6 (s,C_6), 77.6 (s, C_4), 62.5 (s, C_2), 14.1 (s, C_1). **^{19}F NMR** (470 MHz, $CDCl_3$): δ -62.9 (s, CF_3).

Ethyl 2-(3,5-bis(trifluoromethyl)phenyl)-2-(4-hydroxyphenyl)acetate:

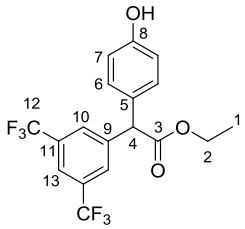

^{1}H NMR (300 MHz, $CDCl_3$): δ 7.77 (br.s, 3H, H_{Ar}), 7.16 (d, J_{H-H} = 8.8 Hz, 2H, H_{Ar}), 6.81 (d, J_{H-H} = 8.8 Hz, 2H, H_{Ar}), 5.27 (s, 1H), 5.04 (s, 1H), 4.24 (q, J_{H-H} = 7.2 Hz, 2H, -C*H*$_2$CH$_3$), 1.27 (t, J_{H-H} = 7.2 Hz, 3H, -CH$_2$C*H*$_3$). **^{13}C{^{1}H} NMR** (125 MHz, $CDCl_3$): δ 171.7 (s, C_3), 155.5 (s, C_8), 141.7 (s, C_9), 131.9 (q, J_{C-F} = 33.4 Hz, C_{11}), 129.8 (s, C_6), 129.3 (s, C_5), 129.0 (d, J_{C-F} = 3.4 Hz, C_{10}), 123.3 (q, J_{C-F} = 273.0 Hz, C_{12}), 121.5 (sept, J_{C-F} = 3.8 Hz, C_{13}), 116.1 (s, C_7), 62.0 (s, C_2), 55.9 (s, C_4), 14.2 (s, C_1). **^{19}F NMR** (470 MHz, $CDCl_3$): δ -62.8 (s, CF_3).

4.6 Computational Details

The B3PW91 (Becke 3-parameter-Perdew-Wang-1991) functional,[27] as implemented in Gaussian 09[28], was employed to locate *minima* structures on the potential energy surface.

The gold atom was described with the relativistic electron core potential SDD and the associated basis set,[29] augmented by a set of f polarization functions.[30] The 6-31G** basis set was employed for all other atoms.[31] All stationary points involved were fully optimized. Frequency calculations were undertaken to confirm the nature of the stationary points, yielding zero imaginary frequency for *minima*. All the geometrical structures were plotted with CYLview.[32]

The bonding situation in all systems was studied using Natural Bond Orbital[33] analysis (NBO, 5.9 version).[34] Charge transfer between the carbene and the metallic fragments have been calculated using atomic charges NPA. The Natural Localized Molecular Orbital (NLMO) associated to the Au↔C interaction (more specifically back-donation d_{xz}(Au) → $2p^{\pi}$(C)), $\pi_{C=C}{}^{aryl}$ → $2p^{\pi}$ (C) interaction, $n_C{}^{\sigma}$ →d(Au) interaction and $n_C{}^{\sigma}$ → $\pi^*_{C=C}$(CO) interaction have been determined. NLMO plot associated to the Au→C back-donation was drawn with the Molekel program for each complex ((PN)gold(I) α-oxo carbene, **20** and **21**).[35]

For each system, a charge decomposition analysis (CDA) was carried out with the CDA 2.2 program developed by G. Frenking.[36] The orbital contributions to the charge distributions are divided into four parts: *(i)* the mixing of the occupied orbitals of the ligand and the unoccupied MOs of the metal fragment (Ligand→Au donation *d*), *(ii)* the mixing of the unoccupied orbitals of the ligand and the occupied MOs of the metal fragment (Ligand←Au back-donation *b*), *(iii)* the mixing of the occupied orbitals of the ligand and the occupied orbitals of the metal fragment (ligand ↔Au repulsive polarization *r*), and *(iv)* the mixing of the unoccupied orbitals of the ligand and the unoccupied orbitals of the metal fragment (residual term Δ).

4.7 References

(1) Qian, D.; Zhang, J. *Chem. Soc. Rev.* **2015**, *44*, 677.

(2) Zheng, Z.; Wang, Z.; Wang, Y.; Zhang, L. *Chem. Soc. Rev.* **2016**, *45*, 4448.

(3) Asiri, A. M.; Hashmi, A. S. K. *Chem. Soc. Rev.* **2016**, *45*, 4471.

(4) Mamane, V.; Gress, T.; Krause, H.; Fürstner, A. *J. Am. Chem. Soc.* **2004**, *126*, 8654.

(5) Wang, T.; Zhang, J. *Dalton Trans.* **2010**, *39*, 4270.

(6) Seidel, G.; Fürstner, A. *Angew. Chem. Int. Ed.* **2014**, *53*, 4807.

(7) Harris, R. J.; Widenhoefer, R. A. *Angew. Chem. Int. Ed.* **2014**, *53*, 9369.

(8) Hussong, M. W.; Rominger, F.; Krämer, P.; Straub, B. F. *Angew. Chem. Int. Ed.* **2014**, *53*, 9372.

(9) Yeom, H.-S.; Shin, S. *Acc. Chem. Res.* **2014**, *47*, 966.

(10) Ye, L.; Cui, L.; Zhang, G.; Zhang, L. *J. Am. Chem. Soc.* **2010**, *132*, 3258.

(11) Gillingham, D.; Fei, N. *Chem. Soc. Rev.* **2013**, *42*, 4918.

(12) Yu, Z.; Ma, B.; Chen, M.; Wu, H.-H.; Liu, L.; Zhang, J. *J. Am. Chem. Soc.* **2014**, *136*, 6904.

(13) Liu, Y.; Yu, Z.; Zhang, J. Z.; Liu, L.; Xia, F.; Zhang, J. *Chem. Sci.* **2016**, *7*, 1988.

(14) Ma, B.; Chu, Z.; Huang, B.; Liu, Z.; Liu, L.; Zhang, J. *Angew. Chem. Int. Ed.* **2017**, *56*, 2749.

(15) Ma, B.; Wu, J.; Liu, L.; Zhang, J. *Chem. Commun.* **2017**, *53*, 10164.

(16) Lebel, H.; Marcoux, J.-F.; Molinaro, C.; Charette, A. B. *Chem. Rev.* **2003**, *103*, 977.

(17) Prieto, A.; Fructos, M. R.; Mar Díaz-Requejo, M.; Pérez, P. J.; Pérez-Galán, P.; Delpont, N.; Echavarren, A. M. *Tetrahedron* **2009**, *65*, 1790.

(18) Luo, Y.; Ji, K.; Li, Y.; Zhang, L. *J. Am. Chem. Soc.* **2012**, *134*, 17412.

(19) Joost, M.; Estévez, L.; Mallet-Ladeira, S.; Miqueu, K.; Amgoune, A.; Bourissou, D. *Angew. Chem. Int. Ed.* **2014**, *53*, 14512.

(20) Celik, M. A.; Dash, C.; Adiraju, V. A. K.; Das, A.; Yousufuddin, M.; Frenking, G.; Dias, H. V. R. *Inorg. Chem.* **2013**, *52*, 729.

(21) Cheng, Q.-Q.; Zhu, S.-F.; Zhang, Y.-Z.; Xie, X.-L.; Zhou, Q.-L. *J. Am. Chem. Soc.* **2013**, *135*, 14094.

(22) Chen, D.; Zhang, X.; Qi, W.-Y.; Xu, B.; Xu, M.-H. *J. Am. Chem. Soc.* **2015**, *137*, 5268.

(23) Peng, C.; Cheng, J.; Wang, J. *J. Am. Chem. Soc.* **2007**, *129*, 8708.

(24) Ye, F.; Qu, S.; Zhou, L.; Peng, C.; Wang, C.; Cheng, J.; Hossain, M. L.; Liu, Y.; Zhang, Y.; Wang, Z.-X.; Wang, J. *J. Am. Chem. Soc.* **2015**, *137*, 4435.

(25) de Fremont, P.; Stevens, E. D.; Fructos, M. R.; Mar Diaz-Requejo, M.; Perez, P. J.; Nolan, S. P. *Chem. Commun.* **2006**, *19*, 2045.

(26) The *trans* and *cis* isomers can be distinguished unambiguously by ^{1}H NMR. For the *cis* isomer see: a) Xu, Z.-H.; Zhu, S.-N.; Sun, X.-L.; Tang, Y.; Dai, L.-X. *Chem. Commun.* **2007**, *0*, 1960. b) Two related isomers were also distinguished by optical rotation: Davies, H. M. L.; Lee, G. H. *Org. Lett.*

2004, *6*, 1233.c) For the *trans* isomer see: Su, Y.; Li, Q.-F.; Zhao, Y.-M.; Gu, P. *Org. Lett.* **2016**, *18*, 4356.

(27) a) Becke, A. D. *J. Chem. Phys.* **1993**, *98*, 5648-5652; b) Perdew, J. P. Unified Theory of Exchange and Correlation Beyond the Local Density Approximation. In *Electronic Structure of Solids '91*; Ziesche, P.; Eschrig, H.; Eds.; Akademie Verlag: Berlin, **1991**, 11.

(28) Frisch, M. J.; Trucks, G. W.; Schlegel, H. B.; Scuseria, G. E.; Robb, M. A.; Cheeseman, J. R.; Scalmani, G.; Barone, V.; Mennucci, B.; Petersson, G. A.; Nakatsuji, H.; Caricato, M.; Li, X.; Hratchian, H. P.; Izmaylov, A. F.; Bloino, J.; Zheng, G.; Sonnenberg, J. L.; Hada, M.; Ehara, M.; Toyota, K.; Fukuda, R.; Hasegawa, J.; Ishida, M.; Nakajima, T.; Honda, Y.; Kitao, O.; Nakai, H.; Vreven, T.; Montgomery, J. A. Jr.; Peralta, J. E.; Ogliaro, F.; Bearpark, M.; Heyd, J. J.; Brothers, E.; Kudin, K. N.; Staroverov, V. N.; Kobayashi, R.; Normand, J.; Raghavachari, K.; Rendell, A.; Burant, J. C.; Iyengar, S. S.; Tomasi, J.; Cossi, M.; Rega, N.; Millam, J. M.; Klene, M.; Knox, J. E.; Cross, J. B.; Bakken, V.; Adamo, C.; Jaramillo, J.; Gomperts, R.; Stratmann, R. E.; Yazyev, O.; Austin, A. J.; Cammi, R.; Pomelli, C.; Ochterski, J. W.; Martin, R. L.; Morokuma, K.; Zakrzewski, V. G.; Voth, G. A.; Salvador, P.; Dannenberg, J. J.; Dapprich, S.; Daniels, A. D.; Farkas, O.; Foresman, J. B.; Ortiz, J. V.; Cioslowski, J.; Fox, D. J. Gaussian 09; Gaussian, Inc., Wallingford, CT, **2009**, Revision D.01.

(29) Andrae, D.; Häussermann, U. M. Dolg, H. Stoll, Preuss, H. *Theor. Chim. Acta* **1990**, *77*, 123.

(30) Ehlers, A.W.; Biihme, M.; Dapprich, S.; Gobbi, A.; Hijllwarth, A.; Jonas, V.; Kiihler, K.F.; Stegmann, R.; Veldkamp, A.; Frenking, G. *Chem. Phys. Chem.* **1993**, *208*, 111.

(31) Hariharan, P. C.; Pople, J.A. *Theor. Chim. Acta* **1973**, *28*, 213.

(32) Legault, C.Y. CYLview, 1.0b, Université de Sherbrooke, **2009** (http://www.cylview.org).

(33) a) Reed, E.; Curtiss, L.A.; Weinhold, F. *Chem. Rev*., **1988**, *88*, 899; b) Foster, J. P.; Weinhold, F. *J. Am. Chem. Soc.* **1980**, *102*, 7211; c) Reed, A. E.; Weinhold, F. *J. Chem. Phys.* **1985**, *83*, 1736.

(34) Glendening, E. D.; Badenhoop, J.K.; Reed, A.E.; Carpenter, J.E.; Bohmann, J.A.; Morales, C.M.; Weinhold, F. Theoretical Chemistry Institute, University of Wisconsin, Madison, **2001**.

(35) Molekel 4.3, Flükiger, P.; Lüthi, H.P.; Portmann, S,; Weber, J. Swiss Center for Scientific Computing, Manno, Switzerland, **2000-2002**. (b) Portmann, S.; Lüthi, H.P. *Chimica* **2000**, *54*, 766.

(36) Dapprich, S.; Frenking, G. *J. Phys. Chem.* **1995**, *99*, 9352.

5 General Conclusion and Perspectives

The main objectives of this research project were focused on the elucidation of the impact of ancillary ligands on the reactivity of gold(I) complexes towards the intermolecular oxidative addition of aryl halides, and also on the stabilization of highly reactive gold(I) intermediates. These two main topics were studied in detail by experimental means and supported by theoretical analyses carried out by the group of Dr. Karinne Miqueu.

Taking advantage of the experience gained in our group on the fundamental parameters governing the reactivity of gold towards oxidative addition, we defined geometrical and electronic requirements to trigger the redox activity of gold(I) and to stabilize the resulting gold(III) complexes. Two strategies have been elaborated. For the first one, we speculated that a dicoordinated gold(I) complex featuring a bidentate ligand inducing a small bite angle may be active for the oxidative addition reaction. Indeed, gold(I) complexes bearing *o*-carboranyl diphosphine ligands were found to undergo the intermolecular oxidative addition of aryl iodides and C-C bonds under very mild conditions (Scheme 5.1). The resulting gold(III) complexes were isolated and completely characterized, but were found to be unstable and to decompose over time.

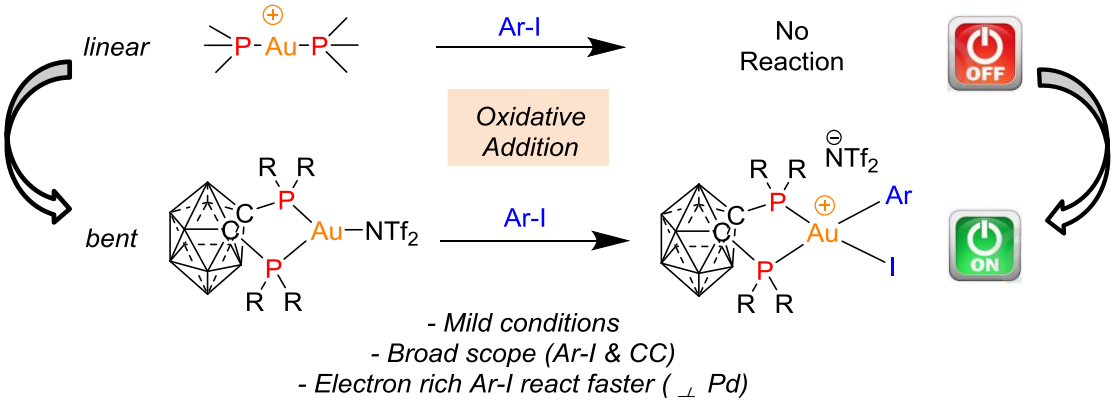

Scheme 5.1 Bending turns on the reactivity: the first strategy elaborated to trigger the reactivity of gold(I) towards oxidative addition.

For the second strategy, taking advantage of the soft/hard character of Au(I)/Au(III), we envisioned that bidentate ligands bearing soft and hard donor groups may feature a hemi-labile character. In fact, we hypothesized that the coordination of a monophosphine to a soft Au(I) center would grant a reactive cationic complex, and upon oxidative addition, the pendant hard group would coordinate the resulting hard Au(III) center to form a stable tetracoordinate complex (Scheme 5.2). Gratifyingly, with a commercially available (P,N) gold(I) complex, the oxidative addition of aryl halides (iodides and bromides) and C-C bonds was achieved. This gold(I) complex exhibited high reactivity and the corresponding gold(III) species were found to be very stable (several days in solution). Moreover, a strong counter anion effect was observed on the reaction rate of the oxidative addition, which allowed to modulate the reactivity and extend the scope to challenging substrates for which the oxidative addition reaction was not feasible with the (P,P) gold(I) complex.

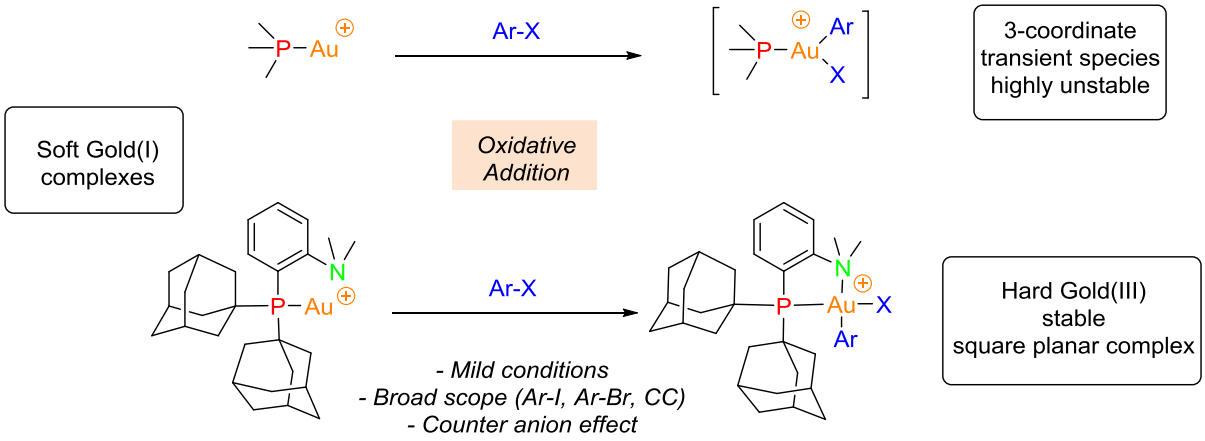

Scheme 5.2 Hemi-labile ligand: the second strategy elaborated to trigger the reactivity of gold(I) towards oxidative addition.

Having proved that the oxidative addition step is actually a favorable process when an adequate ancillary ligand is used, we were eager to further explore the reactivity of the (P,P) and (P,N) gold(I) complexes and go beyond this fundamental elementary step. In that objective, we aimed to construct a new Au(I)/Au(III) catalytic cycle involving a sequence of

Csp^2-X oxidative addition, Csp^2-H auration and reductive elimination. The reaction of iodobenzene with trimethoxybenzene was explored as a prototype transformation in the presence of [(P,P)Au^+] and [(P,N)Au^+] complexes. Although, the oxidative addition was feasible with the (P,P) gold(I) complex, the cross-coupling products could not be obtained, probably due to the decomposition of the *o*-carboranyl bis(phosphine) gold(III) complexes in solution. In contrast, the (P,N) gold(I) complex readily reacted to give the biaryl product, providing the first example of gold-mediated direct arylation using aryl halides as electrophiles. After optimization of the reaction parameters (the catalytic loading, the ratio of coupling partners, the temperature, the halide scavenger, the solvent, the co-solvent and the presence of a base), various aryl halides bearing an electron-donating or an electron-withdrawing groups were successfully coupled with electron-rich arenes (TMB) and heteroarenes (indoles, pyrroles and furans) under mild conditions compared to other transition metals. Moreover, the mechanistic studies are in agreement with a 2-electron Au(I)/Au(III) redox catalytic cycle akin to that encountered with palladium complexes (Scheme 5.3).

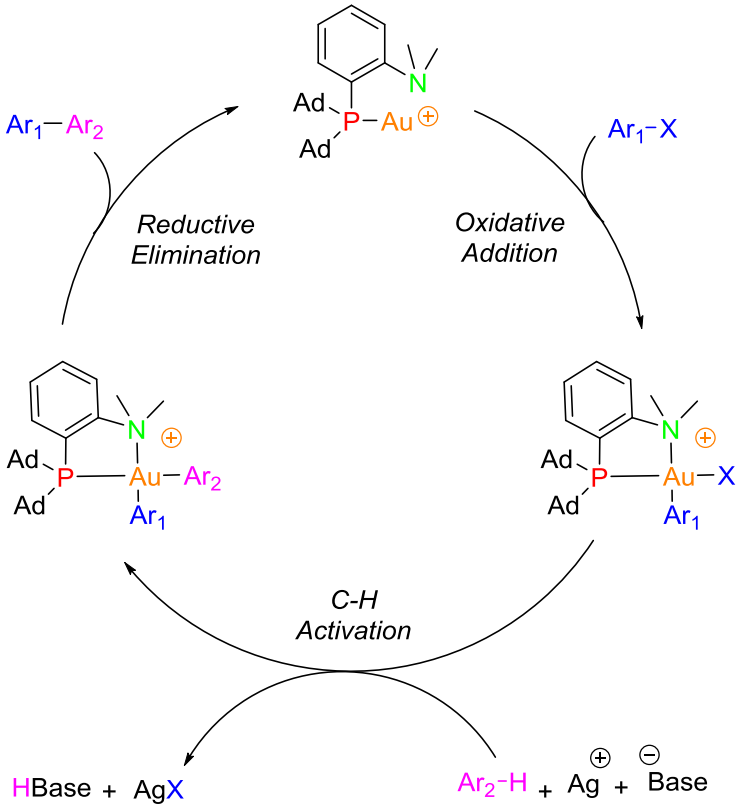

Scheme 5.3 Proposed reaction mechanism for the Au(I)/Au(III)-mediated direct arylation reaction.

The oxidative addition reaction is the common entry point to various cross-coupling catalytic cycles. Having in hands two gold(I) complexes that undergo the oxidative addition reaction, currently in the lab, 2-electron redox processes are being developed, aiming at constructing new gold-catalyzed cross-coupling reactions (Csp^2-Csp^3, Csp^2-N, Csp^2-O...). For example, we started to investigate the reactivity of the (P,N) gold(I) complexes towards the heteroarylation of olefins, involving a sequence of oxidative addition, nucleophilic attack on π-activated alkenes and reductive elimination. We found that using 10 mol% of the (P,N) gold(I) complex, silver hexafluoroantimonate as the halide scavenger and K_3PO_4 as the base, the reaction between 4-penten-1-ol and iodobenzene afforded the desired product in 82% yield after nine hours at room temperature (Scheme 5.4).

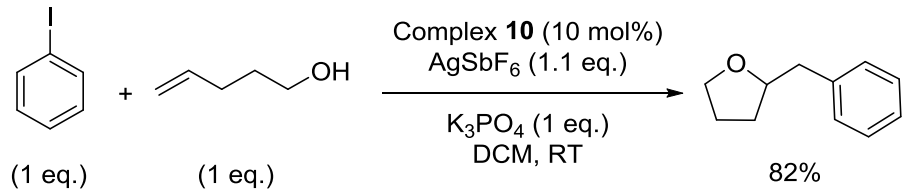

Scheme 5.4 Au(I)/Au(III)-mediated oxyarylation of alkene.

In 2010, the group of L. Zhang described the first gold-catalyzed Csp^3-Csp^2 bond formation in an intermolecular oxidative cross-coupling manner.(1) Zhang *et al.* realized amino- and oxyarylation of terminal alkenes with arylboronic acids. Using a monophosphine gold(I) complex and two equivalents of Selectfluor as strong external oxidant to access the +III oxidation state of gold, the desired products were obtained in moderate to excellent yields (Scheme 5.5).

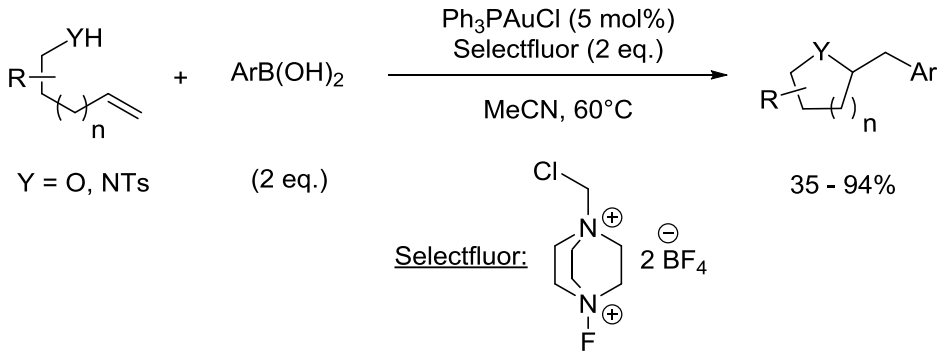

Scheme 5.5 Gold-catalyzed oxy- and aminoarylations of alkenes using an external oxidant.

The proposed catalytic cycle (Scheme 5.6) involves a Au(I)/Au(III) oxidation (step A), followed by a transmetallation from boron to the gold(III) species facilitated by the formation of a strong B-F bond (step B). Alternatively, the authors proposed as well that the transmetallation step could occur before the Au(I)/Au(III) oxidation. The generated cationic

aryl gold(III) species activates the alkene (step C), followed by the nucleophilic attack (step D). After reductive elimination, the desired product is formed and the initial gold(I) catalyst is regenerated (step E).

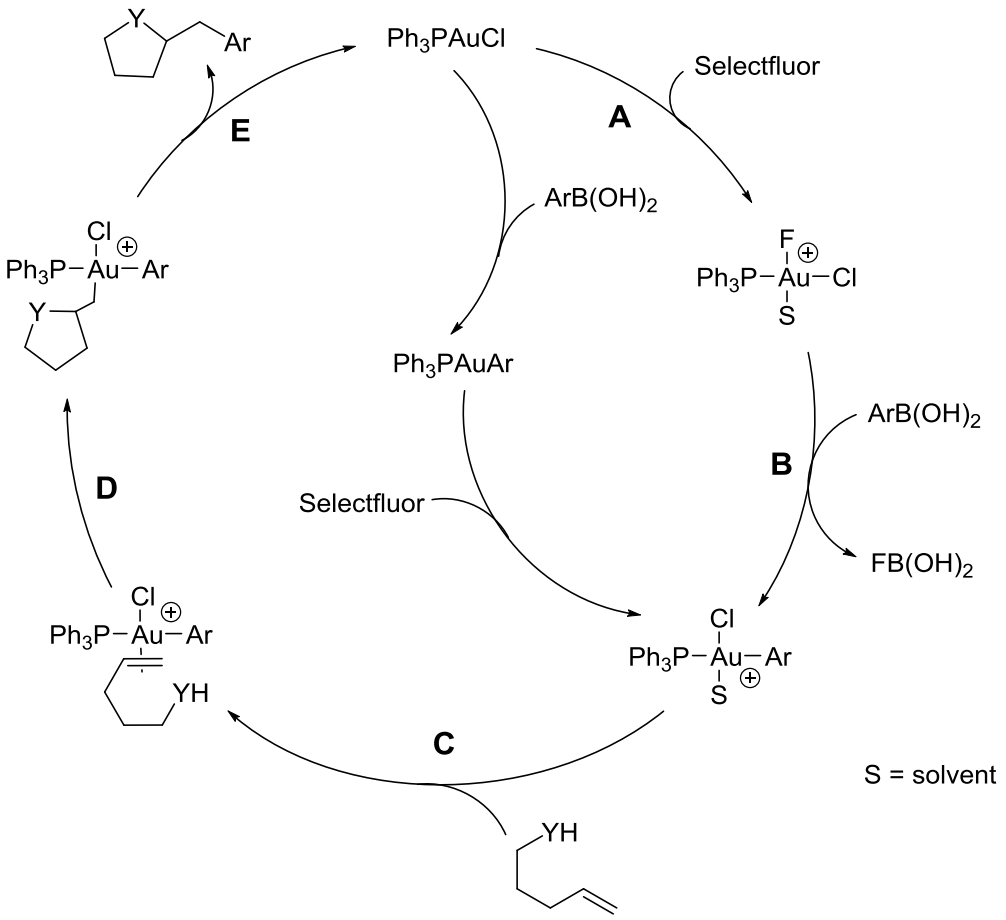

Scheme 5.6 Proposed reaction mechanism for the gold-catalyzed oxy- and aminoarylations of alkenes using an external oxidant.

As mentioned before, the use of strong external oxidants is a major drawback, due to their incompatibility with several functional groups. Thus, there's a great interest to develop alternative strategies to perform cross-coupling reactions without the use of sacrificial oxidants.

Lastly, we were interested in the stabilization of highly reactive gold(I) complexes, such as α-oxo gold(I) carbenes. This species, due to its high electrophilic character, has never been isolated or characterized. The use of the bidentate diphosphine gold(I) complex and ethyl diazoacetate compounds allowed the quick formation of the α-oxo gold(I) carbene at low temperature. Gratifyingly, this gold(I) carbene was completely characterized for the first time in solution (at -40°C) and in the solid state (Scheme 5.6).

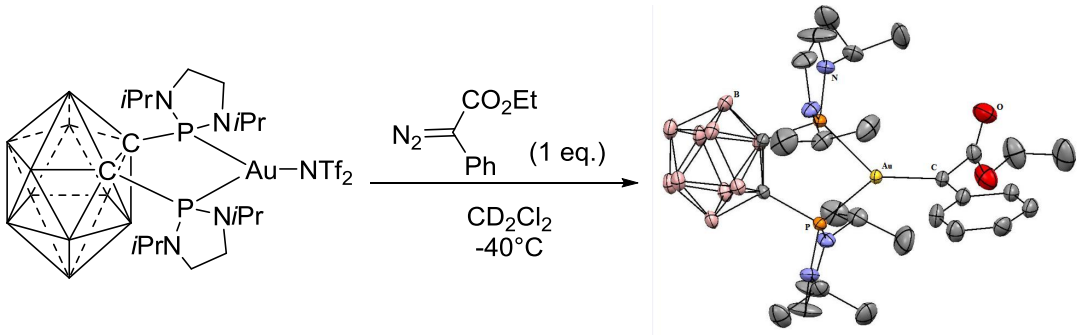

Scheme 5.6 Synthesis of the α-oxo gold carbene complex and its X-ray structure.

Moreover, computational studies were conducted to gain more insight into the electronic situation within the tricoordinated α-oxo gold(I) carbene complex and to assess the role of the ligand in its stabilization. A significant π-backdonation from the *o*-carboranyl diphosphine gold fragment to the carbene moiety was observed, highlighting the crucial role of the (P,P) bidentate ligand. Finally, the reactivity of the *in situ* generated α-oxo gold(I) carbene complex towards insertion and cyclopropanation reactions was investigated. Interestingly, the increased π-backdonation from the (P,P) bidentate ligand attenuated the electrophilicity of the α-oxo gold(I) carbene, and its reactivity resembles that of other late transition metals. In contrast, with the (P,N) gold(I) complex, the α-oxo gold(I) carbene species was not unambiguously characterized due to its decomposition at low temperature.

Overall, this study shows that bidentate ligands are promising ligand scaffolds for gold. The (P,P) and (P,N) ligands are complementary, since the diphosphine ligand allows the stabilization of highly reactive intermediates due to the enhanced backdonation from the [(P,P)Au^{+}] fragment, whereas the hemi-labile (P,N) ligand allows the access to Au(I)/Au(III) mediated cross-coupling reactions. The interest in the coordination chemistry and the catalytic application of gold complexes was revived at the end of the 1990s and since then, there was an explosive growth of gold catalysis. More recently, the use of multidentate ligands in gold complexes has been shown to offer promising opportunities in terms of stabilization and reactivity. We hope that the work summarized in this manuscript provides more insight on the key roles of bidentate ligands in triggering the reactivity of gold complexes.

(1) Zhang, G.; Cui, L.; Wang, Y.; Zhang, L. *J. Am. Chem. Soc.* **2010**, *132*, 1474.

6 Compte-rendu en Langue Française

6.1 Introduction Générale

L'or est sans doute l'un des premiers métaux connus par les humains. En raison de sa couleur brillante, sa ductilité, sa malléabilité et sa haute résistance à la corrosion, l'utilisation de l'or a été consacrée aux systèmes d'échange monétaires, l'odontologie et l'électronique. Dans toutes ces applications, l'or est utilisé dans son état métallique. Malgré la disponibilité d'autres états d'oxydation stables, notamment les états +I et +III, l'or était considéré comme un métal inerte pendant longtemps, et sa chimie était peu développée.

Cependant, l'or a connu un essor dans la chimie et surtout dans le domaine de la catalyse. Cette expansion a commencée à peu près dans la dernière décennie, après que les chercheurs ont découvert que l'or est un acide de Lewis carbophile permettant d'activer des liaisons π vis-à-vis d'une attaque nucléophile (Schéma 6.1).

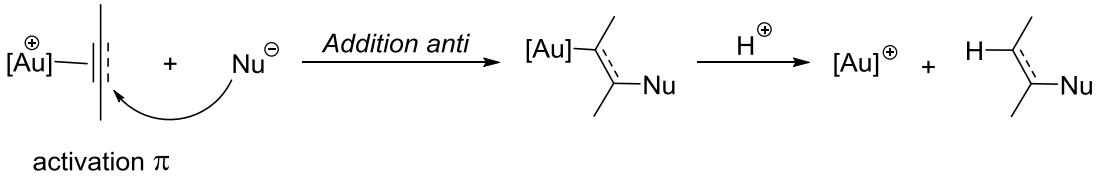

Schéma 6.1 Mécanisme généralement proposé pour les processus classiques de catalyse à l'or par activation π.

Après cette découverte, des progrès spectaculaires en catalyse à l'or s'en suivis et maintenant les complexes d'or sont très utilisés dans la synthèse organique. Néanmoins, dans toutes ces transformations, des complexes d'or(I) cationiques avec des ligands monodentés (L = R_3P ou NHC) de formule générale [LAu^+], ont été utilisés comme espèces actives. Pendant un certain temps, la modulation des ligands et les études concernant la relation structure/réactivité ont été limitées à ces ligands monodentés. Cependant, récemment, l'utilisation de complexes

d'or(I) et d'or(III) supportés par des ligands multidentés a permis des progrès significatifs pour la caractérisation d'espèces actives et pour le développement des nouvelles transformations catalytiques à l'or.

6.2 Objectif du Projet de Thèse

Ce travail de thèse porte sur la chimie organométallique des complexes d'or(I) et sur l'étude de leurs réactivités. Plus particulièrement, le travail présenté ici dans ce manuscrit avait pour objectif d'approfondir nos connaissances sur l'impact des ligands bidentés (P,P) et (P,N) sur (i) la réactivité de l'or vis-à-vis de l'addition oxydante intermoléculaire et (ii) la stabilisation d'intermédiaires catalytiques d'or(I) hautement réactifs. Le travail expérimental a été appuyé par des études théoriques menées par le l'équipe du Dr. Karinne Miqueu (Université de Pau) qui ont permis de confirmer et de mieux comprendre les résultats expérimentaux obtenus.

6.3 Design de Ligand pour Déclencher l'Addition Oxydante à l'Or(I)

6.3.1 Introduction

L'addition oxydante par une activation concertée d'une liaison σ est une des étapes fondamentales de la chimie organométallique. Alors que cette étape clé de nombreux cycles catalytiques est bien établie avec les autres métaux de transition, l'or se montre réticent au processus d'addition oxydante. Cette doctrine générale repose principalement sur le potentiel rédox de l'or qui est beaucoup plus élevé par rapport à celui de ses voisins proches comme le palladium et le platine (E_0: Au^{3+}/Au^{+} = 1.41 V, Pd^{2+}/Pd = 0.91 V, Pt^{2+}/Pt = 1.18 V).

6.3.2 Synthèse et Réactivité du complexe (P,P)Au(I)

Après avoir réalisé l'addition oxydante intramoléculaire à l'or(I), nous avons commencé à étudier si cette transformation est faisable de manière intermoléculaire. Sur la base de nos résultats précédents, nous avons cherché à en savoir plus sur les paramètres (géométriques et électroniques) principaux qui régissent la réactivité des complexes d'or(I) vis-à-vis de la réaction d'addition oxydante. En effet, un complexe d'or(I) cationique monocoordinés est capable d'effectuer l'addition oxydante, mais les espèces d'or(III) tricoordinées résultantes sont très instables. En revanche, les complexes d'or(I) dicoordinés neutres ou cationiques (LAuCl ou bien L_2Au^+ avec L = PR_3 ou NHC) sont pas actifs pour l'addition oxydante intermoléculaire. Ces complexes dicoordinés linéaire sont très stables. On trouve dans la littérature que les complexes bidentés de palladium(0) et platine(0) présentant une géométrie coudée sont plus réactifs pour la réaction d'addition oxydante. Ceci est expliqué par le faite que dans ces complexes, le métal adopte une géométrie proche de celle de l'état de transition et qu'un angle L-M-L plus contraint augmente le niveau énergétique de l'HOMO. Du coup, nous nous sommes demandé si des complexes (P,P) bidentés d'or(I) avec un angle de morsure faible pourraient à la fois favoriser l'addition oxydante et stabiliser les complexes d'or(III) générés (Schéma 6.2).

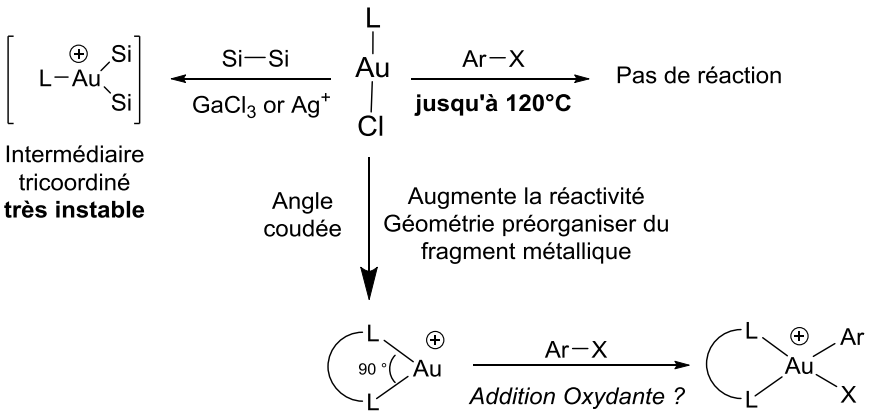

Schéma 6.2 Les principes de conception que nous avons établis pour déclencher la réactivité de l'or(I) vis-à-vis de la réaction d'addition oxydante.

Il est intrinsèquement difficile de chélater des ligands à l'or(I) en raison de sa préférence pour la géométrie linéaire. En effet, des nombreux ligands bidentés, qui sont utilisés avec d'autres métaux de transition pour former des structures chélatantes, forment des espèces dinucléaires avec l'or(I) afin de préserver la géométrie linéaire. Ces complexes dinucléaires sont favorisés thermodynamiquement grâce à la formation d'interactions aurophiles (Schéma 6.3).

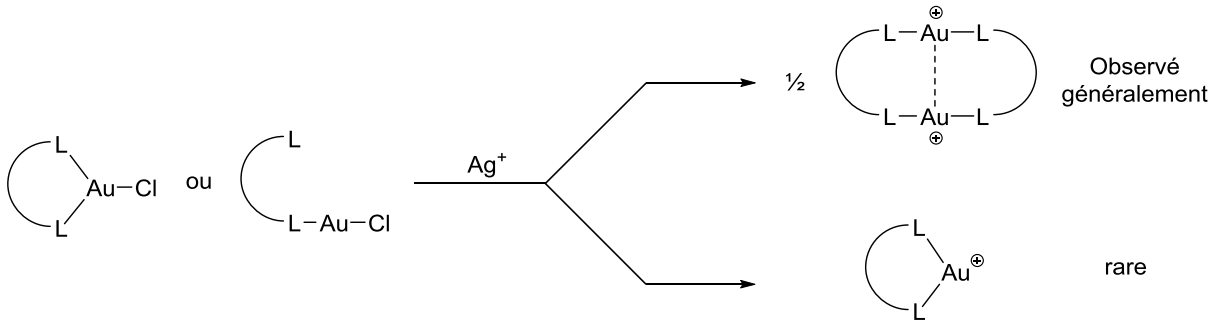

Schéma 6.3 Comportement habituel des complexes d'or(I) avec des ligands bidentés.

Il existe quelques rares exemples de ligands diphosphines décrits dans la littérature qui impose une coordination bidentée sur l'or (I) pour former des complexes mononucléaires. Parmi ces ligands, un ligand diphosphine basé sur un squelette *o*-carborane a attiré notre attention.

Dans un premier temps, nous avons synthétisé les ligands 1,2-bis(diphenylphoshpino)-1,2-dicarba-*closo*-dodecarborane, 1,2-bis(diisopropylphoshpino)-1,2-dicarba-*closo*-dodecarborane et 1,2-bis(diaminophoshpino)-1,2-dicarba-*closo*-dodecarborane afin d'examiné l'influence des substituants des bras phosphorés sur la réactivité. Les complexes d'or(I) chlorés **1**, **2** et **3** ont été préparés en faisant réagir le ligand correspondant avec [(SMe_2)AuCl] (Schéma 6.4).

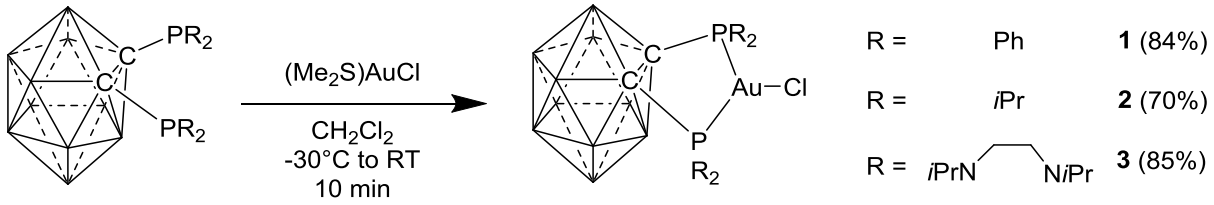

Schéma 6.4 Synthèse des complexes *o*-carborane diphosphine d'or(I).

Dans le but d'étudier leurs réactivités vis-à-vis de l'activation de la liaison Csp^2-I, nous avons mis les complexes **1**, **2** et **3** en présence de $GaCl_3$ (pour abstraire le chlorure lié à l'atome de l'or) et d'iodobenzene. Avec les complexes **1** et **2**, l'isolement du produit formé s'est relevé compliqué à cause de leurs instabilités à la température, mais la formation des complexes d'or(III) en provenance de l'addition oxydante de la liaison carbone-iode a été confirmée par spectroscopie RMN multi-noyaux à -30°C. En revanche, avec le complexe **3**, les espèces d'or(III) étaient relativement stables et ont été caractérisé en solution et en état solide (Schéma 6.5).

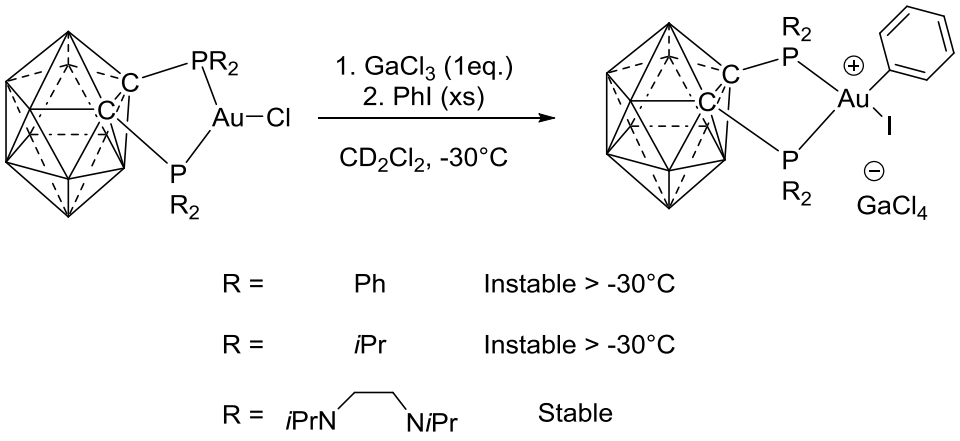

Schéma 6.5 Synthèse des complexes *o*-carborane diphosphine d'or(III).

L'influence du contre-anion sur la stabilité et la réactivité du complexe **3** a également été étudiée. En effet, nous nous sommes aperçus que l'utilisation du triflimidate comme un contre-anion faiblement coordinant permettait de stabiliser le complexe d'or(I) et de garder sa réactivité vis-à-vis de l'addition oxydante (Schéma 6.6).

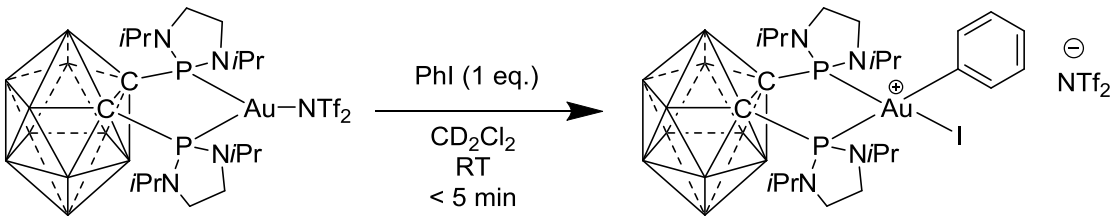

6 **7**

Schéma 6.6 Synthèse du complexe d'or(III) par addition oxydante à partir du complexe triflimidate d'or(I).

Le complexe **6** réagit spontanément et rapidement avec l'iodobenzene à température ambiante : une conversion complète a été obtenue en moins de cinq minutes. En outre, la réaction d'addition oxydante est générale et une variété d'iodure d'aryle ont été activés. En effet, la réaction est compatible avec plusieurs groupes fonctionnels (OMe, NHAc, F, CN et NO_2) et fonctionne aussi avec des substrats hétérocycliques (Schéma 6.7). De manière surprenante, l'addition oxydante des iodobenzenes substitués en position *para* est plus rapide avec les substituents électron-donneurs qu'avec les substituents électron-attracteurs. Cette tendance de réactivité est opposée à celle rencontrée lors de l'addition oxydante des halogénures d'aryles aux complexes $L_2Pd(0)$. La réaction du complexe **6** vis-à-vis de l'activation des liaisons plus fortes (Csp^2-Br et Csp^2-Cl) a ensuite été étudiée. Malheureusement, l'addition oxydante des bromures et chlorures d'aryles est restée un obstacle car aucun signe d'activation de la liaison Csp^2-halogène n'a été observé et un chauffage prolongé a provoqué la décomposition du complexe **6**.

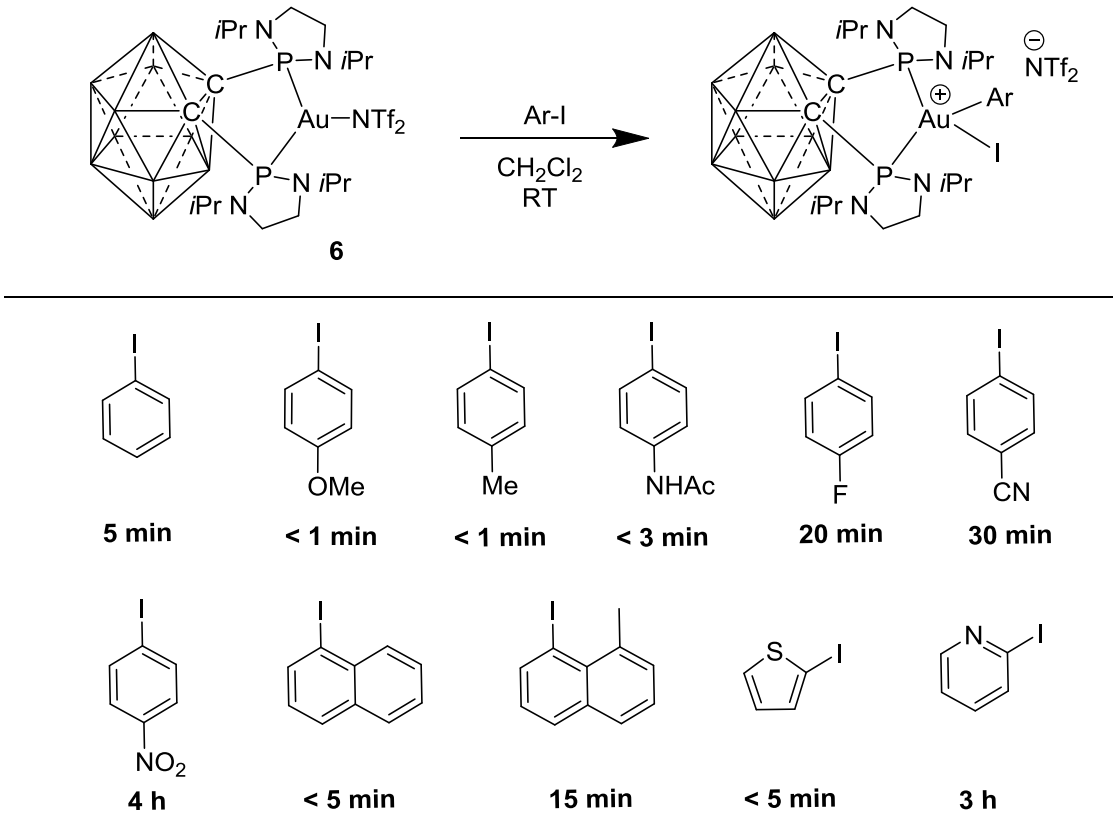

Schéma 6.7 Scope de l'addition oxydante des iodures d'aryles avec le complexe **6**.

Pour mieux comprendre le mécanisme de l'addition oxydante des iodures d'aryles au complexe **6**, des calculs DFT ont été réalisés en collaboration avec le groupe du Dr. Karinne Miqueu. La réaction passe par un état de transition concerté avec une barrière d'activation remarquablement faible ($\Delta E^{\ddagger}$ = 10.3 kcal/mol et $\Delta G^{\ddagger}$ = 10.7 kcal/mol) en accord avec les conditions douces dans lesquelles la réaction se produit expérimentalement.

6.3.3 Synthèse et Réactivité du complexe (P,N)Au(I)

Comme mentionné ci-dessus, les complexes cationiques d'or(I) portés par des ligands monodentés (L = R_3P ou NHC) sont actifs pour l'addition oxydante, mais les espèces d'or(III) tricoordinés résultants sont très instables et difficiles à isoler et à exploiter leurs réactivités. Ainsi, nous avons supposé que les ligands bidentés hémi-labiles pourraient fournir un équilibre approprié entre la réactivité et la stabilité de ces espèces clés. Profitant du caractère mou/dur de l'Au(I)/Au(III), nous avons envisagé d'utiliser des ligands bidentés (P,L) (L étant un groupement donneur dur). La coordination d'une monophosphine à l'or(I) mou conférerait un complexe cationique réactif, et après l'addition oxydante, le groupement dur (L) coordonnerait l'or(III) dur pour former un complexe stable tetra-coordiné adoptant une géométrie plan carrée.

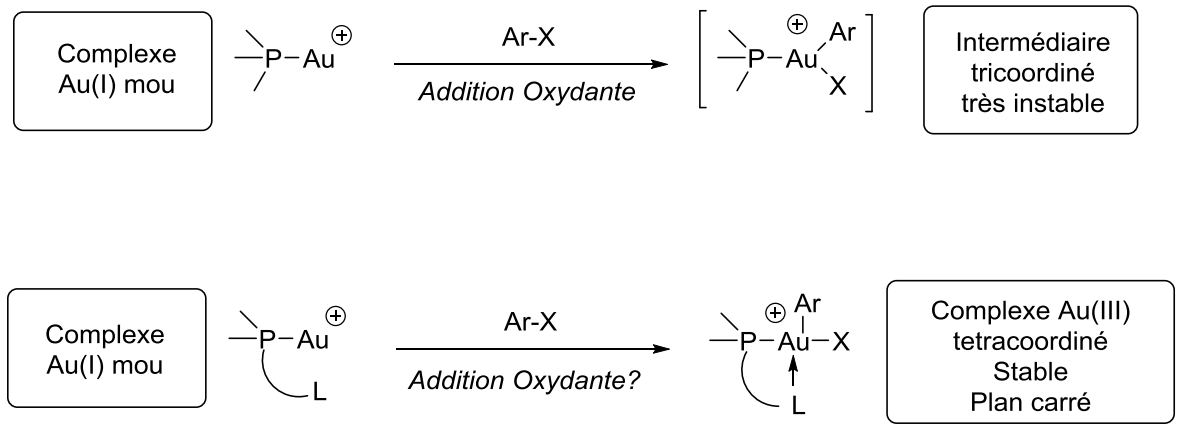

Schéma 6.8 Les principes de conception pour l'addition oxydante à des complexes Au(I) monocoordinés.

Parmi les complexes testés portant des ligands hémi-labiles, un complexe commercial, le (MeDalphos)AuCl, s'est montré réactif vis-à-vis de l'addition oxydante. En effet, en présence d'$AgNTf_2$ (pour générer un or(I) cationique monocoordiné), l'addition oxydante d'iodobenzene a été réalisée (Schéma 6.9). Le contrôle de la réaction par RMN $^{31}P\{^1H\}$ a indiqué la formation progressive du complexe **11** (δ 74.1 ppm). Après 48 heures à température

ambiante, la réaction est terminée, et le complexe **11** est formé avec 92% de rendement (spectroscopique). La RMN ^{1}H indique également la formation de l'or(III) par addition oxydante, puisque le signal de résonance de –N(CH_3)$_2$ est blindé (par rapport au complexe **10**) indiquant la coordination de l'azote à l'or(III). Le complexe **11** est très stable (plusieurs jours en solution sans traces de décomposition) et a été entièrement caractérisé en solution (RMN et HRMS) et à l'état solide (par diffraction des rayons X).

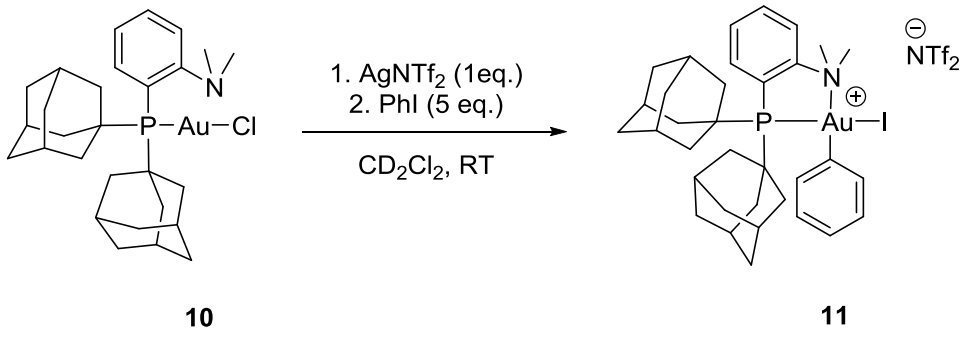

10 **11**

Schéma 6.9 Addition oxydante de l'iodobenzene au complexe **10**.

Dans le but d'augmenter la vitesse de la réaction d'addition oxydante tout en maintenant des conditions douces, des contre-anions non-coordinants ont été testés. Avec SbF_6^-, qui est moins coordinant que le NTf_2^-, l'addition oxydante de l'iodobenzene se produit instantanément, et le complexe d'or(III) est obtenu comme le seul produit de la réaction. Ce résultat suggère que la première étape du processus d'addition oxydante est le déplacement du contre-anion par l'iodobenzene pour former un adduit avec le centre métallique. Ceci a été confirmé par les calculs DFT, qui montrent aussi que le processus d'addition oxydante passe par un état de transition concerté avec une barrière d'activation remarquablement faible ($\Delta G^{\ddagger}$ = 11.2 kcal/mol). Le processus est thermodynamiquement favorable et conduit au complexe d'or(III) tetra-coordiné obtenu expérimentalement.

Le complexe **10** réagissait facilement avec une série d'iodure d'aryles, et des réactions instantanées ont été observés aves des iodobenzenes comportant des substituants électro-attracteurs et électro-donneurs. En outre, le scope des iodures d'aryles a été étendue à des substrats très pauvres en électrons tels que l'iodopentafluorobenzene, et fonctionne aussi avec des substrats hétérocycliques. L'addition oxydante intermoléculaire des bromures d'aryles a été également démontrée pour la première fois avec l'or grâce au ligand (P,N) bidenté (Schéma 6.10). Dans les mêmes conditions et avec plusieurs chlorures d'aryles, l'activation de la liaison Csp^2-Cl n'a pas été réalisée.

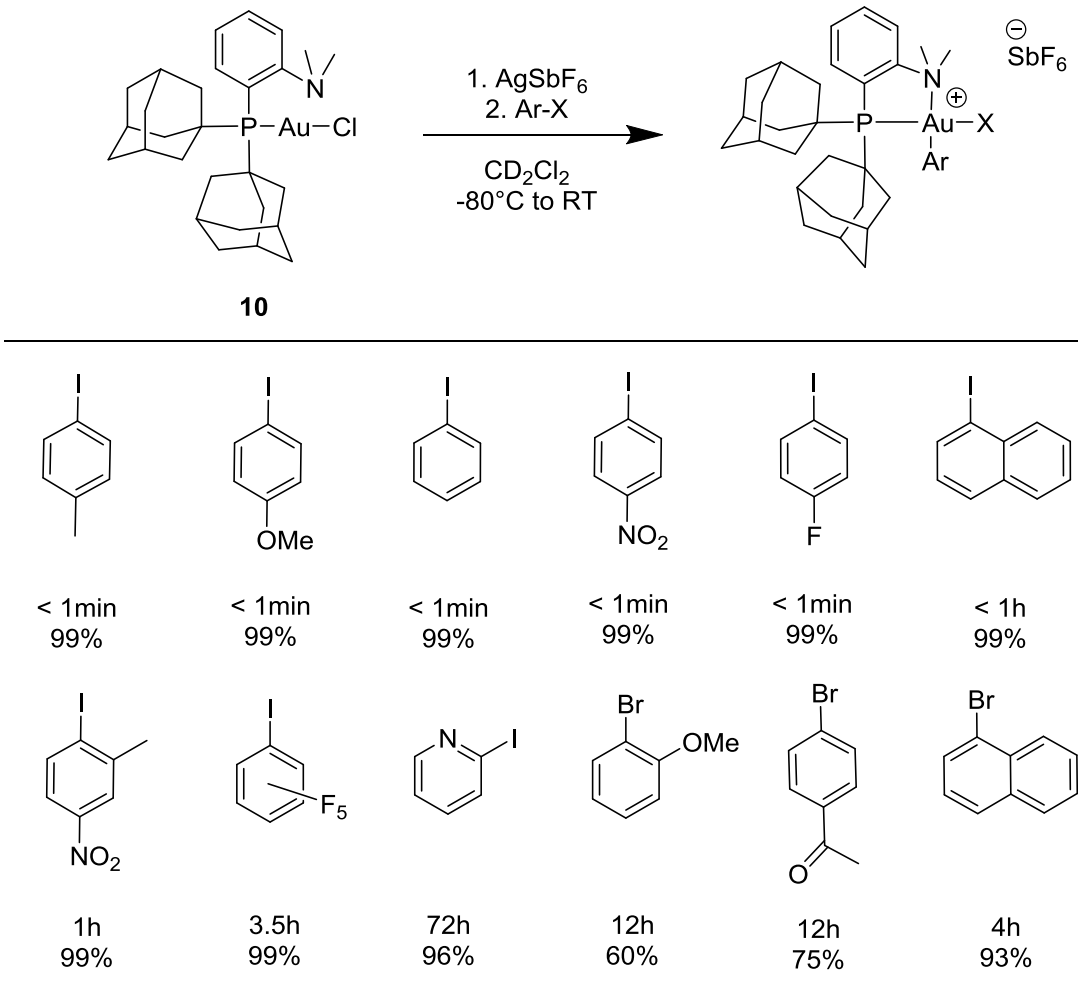

Schéma 6.10 Scope de l'addition oxydante des halogénures d'aryles avec le complexe **10**.

6.4 Développement de Réactions de Couplage Croisé C-C avec Ar-X

Dans la littérature, plusieurs exemples de réactions de couplage croisés Csp^2-Csp^2 catalysées à l'or peuvent être trouvés. Cependant, ces réactions nécessitent l'utilisation des oxydants externes ou bien des électrophiles forts (et certains sont explosifs) pour accéder à l'état d'oxydation +III de l'or. Les produits de couplage sont généralement obtenus avec de bons rendements, mais les conditions de réactions sont dures et le scope des substrats est limité.

Après avoir confirmé que l'addition oxydante d'halogénures d'aryles à l'or(I) se produit facilement avec les complexes **6** et **10**, nous avons alors cherché à aller au-delà de cette étape élémentaire. Puisque les complexes d'or(III) sont connus pour l'activation de liaison Csp^2-H des arènes et hétéroarènes et puisque l'élimination réductrice Csp^2-Csp^2 est un processus favorable à partir des complexes d'or(III) bi(aryle), il était très intéressant d'étudier la réactivité de nos complexes d'or(III) pour la réaction d'arylation directe. Nous avons donc envisagé de construire un cycle catalytique ou la première étape serait l'addition oxydante d'halogénures d'aryles pour générer le complexe d'or(III) aryle (étape A), suivie d'une activation électrophile de la liaison C-H d'un arène riche (étape B). L'élimination réductrice à partir du complexe d'or(III) bi(aryle) fermerait alors le cycle (étape C) avec la formation du produit biaryle et la régénération du catalyseur d'or(I) (Schéma 6.11).

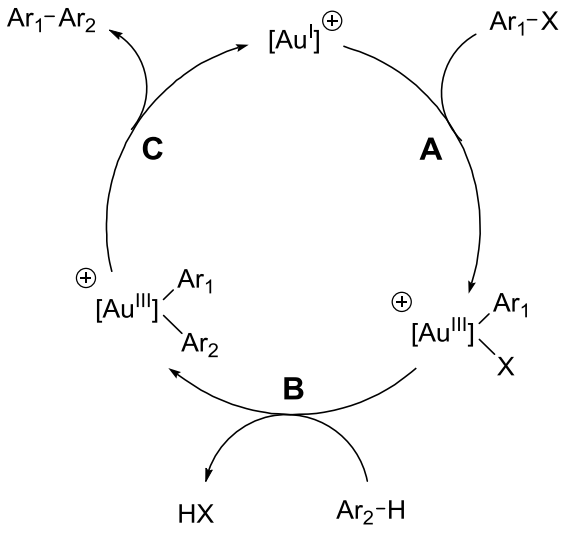

Schéma 6.11 Cycle catalytique Au(I)/Au(III) hypothétique pour le couplage croisé les halogénures d'aryles et les arènes riches.

6.4.1 Réactions Stœchiométriques Modèles

Puisque l'addition oxydante des iodures d'aryles au complexe **10** donnent des complexes d'or(III) stables (par rapport au complexe **7**), nous avons évalué en premier le couplage entre l'iodobenzene et le 1,3,5-trimethoxybenzene (TMB) avec le complexe **10**. Après l'addition oxydante de PhI, un équivalent de TMB a été ajouté au complexe d'or(III) à température ambiante. L'analyse GC-MS d'aliquotes prélevées du milieu réactionnel a révélé la formation d'un fragment organique ayant la même masse molaire du produit de couplage croisé souhaité, mais il se formé très lentement. Cependant, l'addition d'un équivalent d'$AgSbF_6$ a augmenté considérablement la vitesse de la réaction. Ceci est probablement du a l'augmentation de l'éléctrophilie de l'or(III) après l'extraction de l'iode. Après douze heures de réaction, le produit de couplage a été isolé avec un rendement de 90%. Encouragés par ce résultat préliminaire, nous avons testé la même réaction mais en 'one pot', puisque notre objectif est de développer un cycle catalytique. Dans ces conditions, la réaction de couplage croisé s'est également bien déroulée (Schéma 6.12).

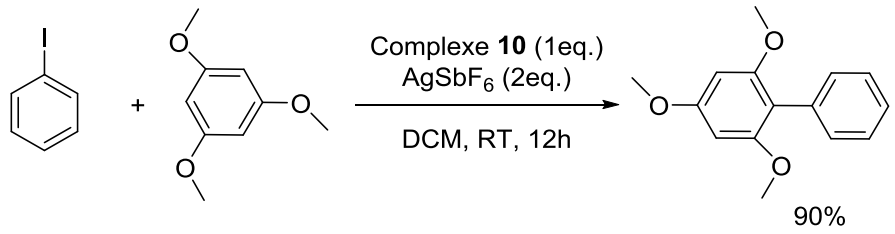

Schéma 6.12 Couplage croisé de PhI et TMB avec le complexe **10**.

A ce stade, nous avons décidé de commencer à optimiser les conditions de la réaction et plusieurs paramètres (substituants portés par le phosphore, l'abstracteur d'halogène, le solvant et le co-solvant) ont ainsi été examinés.

L'effet des substituants du phosphore sur la réaction d'arylation directe était le premier paramètre que nous avons examiné en comparant les substituants adamantyl, isopropyle et phényle. Dans tous les cas, le produit de couplage désiré a été formé, mais avec les substituants adamantyl un meilleur rendement a été obtenu. L'influence de différents sels d'argent sur l'efficacité et la vitesse de la réaction a ensuite été examinée. Avec Ag_2O et AgCSA, le produit de couplage n'a pas été détecté par GC-MS même après douze heures à température ambiante. Ceci peut s'expliquer par la forte coordination des anions CSA^- et AgO^- au centre métallique après l'abstraction du chlorure, empêchant ainsi la réaction d'addition oxydante. Lorsque le tetrafluoroborate est utilisé comme contre-anion non coordinant, la réaction de couplage croisé se produit, mais le composé souhaité est formé avec un rendement très faible (10%). Du coup, $AgSbF_6$ était l'abstracteur d'halogène le plus approprié pour la réaction de couplage croisé. Nous avons ensuite étudié l'effet de différents solvants (DMSO, DMF, DCE et TFA) et co-solvants (DMSO, TFA et MeOH) sur la réaction du couplage croisé. L'impact positif le plus significatif sur la vitesse de réaction a été obtenu en effectuant la réaction dans le dichlorométhane avec une petite quantité de méthanol (50 :1).

Ainsi dans ces conditions, et après cinq heures à température ambiante, un rendement de 97% du produit de couplage pourrait être atteint (Schéma 6.13).

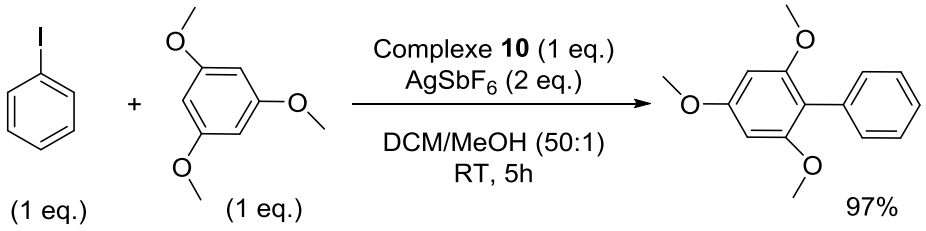

Schéma 6.13 Couplage croisé de PhI et TMB avec le complexe **10** après l'optimisation.

6.4.2 De la Stœchiométrie à la Catalyse

Après avoir réalisé la réaction stœchiométrique du couplage croisé, l'étape suivante consistait à passer à des conditions catalytiques. Une nouvelle optimisation des conditions de la réaction a été effectuée, et différents paramètres ont été examinés comme la charge catalytique, la température, le ratio PhI / TMB, l'abstracteur d'halogène et la présence d'une base. Ainsi, les nouvelles conditions expérimentales sont : 5 mol% du catalyseur, 1.05 équivalent d'AgSbF6, 1 équivalent de chaque partenaire de couplage et 1 équivalent de K_3PO_4. Les réactions sont effectuées à 75°C en utilisant le 1,2-dichlorobenzène (DCB) comme solvant avec une petite quantité de MeOH (50 :1). Après deux heures de réactions, les produits de couplages sont obtenus avec des bons rendements. La réaction de couplage tolère les iodures d'aryles portant des groupes électro-attracteurs (*p*-nitro et *p*-fluoro iodobenzenes) et électro-donneurs (*p*-methoxy and *p*-methyl iodobenzenes), ainsi que des substrats substitués en ortho tels que le 8-iodonaphtalène. L'arylation du 1,3,5-trimethoxybenzene a été testée avec les bromures d'aryles aussi. Pour maintenir des conditions réactionnelles douces et des temps de réaction raisonnablement courts, le couplage croisé d'ArBr et TMB a été réalisé avec 10 mol% du catalyseur et 5 équivalents du bromure d'aryle. Dans ces conditions, les produits biaryl ont

également été obtenus avec des bons rendements après quelques heures à 75°C. Outre l'avantage d'éviter l'utilisation d'oxydants externes ou des électrophiles forts, cette stratégie de couplage n'a aucune contrainte électronique pour les partenaires de couplages et donne accès à des composes biaryl avec des substituants électro-donneurs sur les deux aryles (Schéma 6.14).

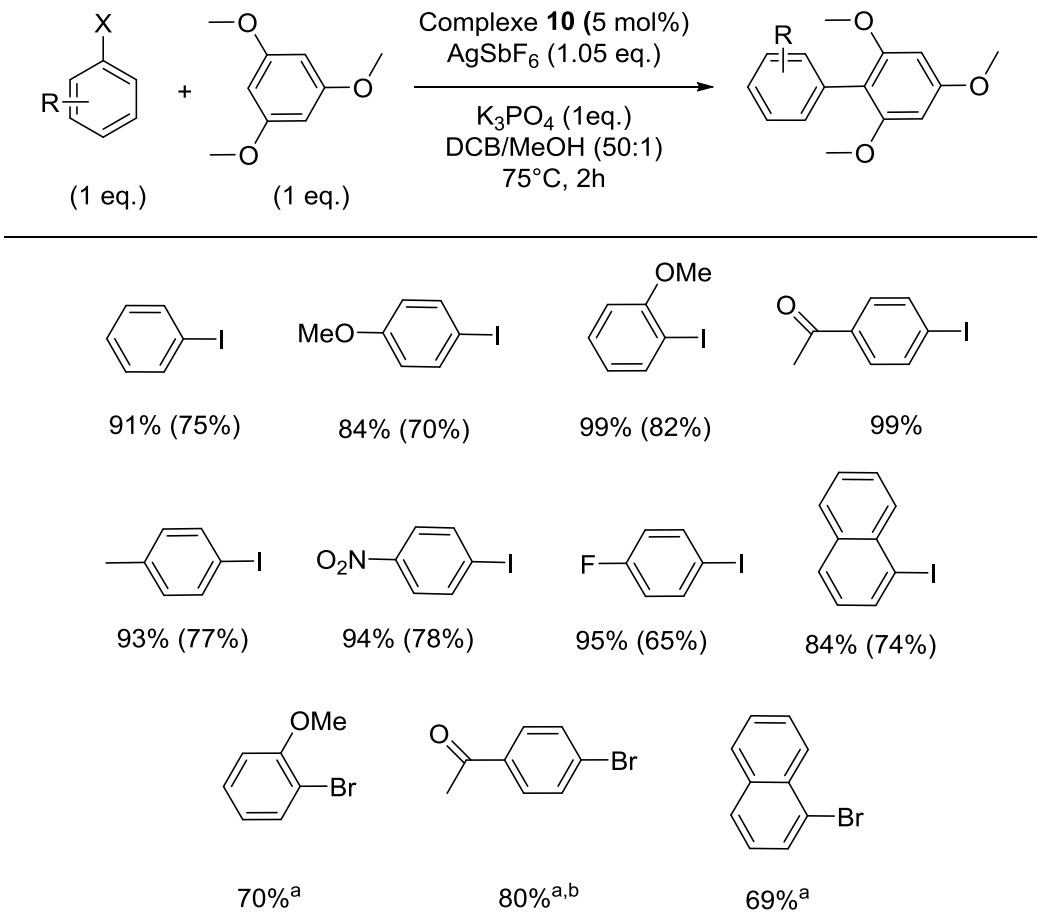

Schéma 6.14 Couplage croisé d'halogénures d'aryles (X = I, Br) et TMB catalysés par le complexe **10**. Les rendements ont été déterminés par GC-MS (étalonnée *vs. n*-dodecane), et les rendements isolés entre parenthèse. [a] Conditions: [Au] 10 mol%, 5 eq. ArBr. [b] Temps de réaction: 12h.

La réaction de couplage croisé Csp^2-Csp^2 fonctionne aussi avec des hétéroarènes riches comme les pyrroles. En effet, le 1-phényle-1*H*-pyrrole et l'iodobenzene ont été couplés en utilisant 5 mol% du complexe **10** et 1 équivalent d'$AgSbF_6$ dans les conditions douces standard (Schéma 6.15). Sans optimisation, un rendement isolé de 61% a été obtenu et une

sélectivité élevée a été observée (β:α = 9/1). Les deux isomères ont été identifiés sans ambigüité par RMN ^{13}C et leur proportion relative a été déterminée par RMN ^{1}H.

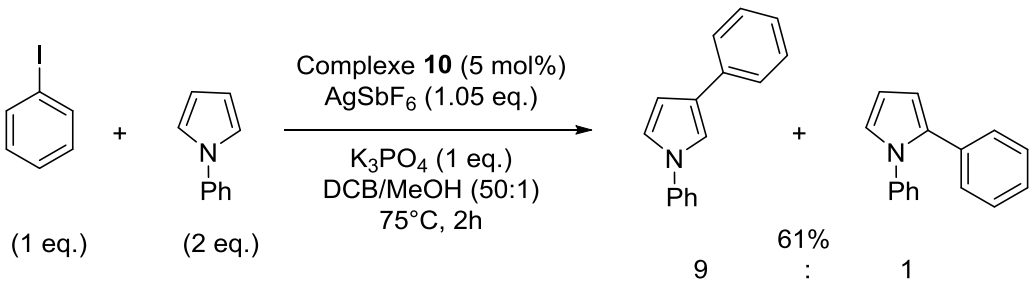

Schéma 6.15 Couplage croisé de PhI et 1-phényle-1*H*-pyrrole avec le complexe **10**.

Le couplage croisé entre les indoles et les iodures d'aryles a été réalisé aussi. Même si $AgSbF_6$ est l'abstracteur d'halogène le plus adapté pour la réaction d'arylation du TMB, mais pour les indoles, des meilleurs résultats ont été obtenus avec AgOTf (Schéma 6.16).

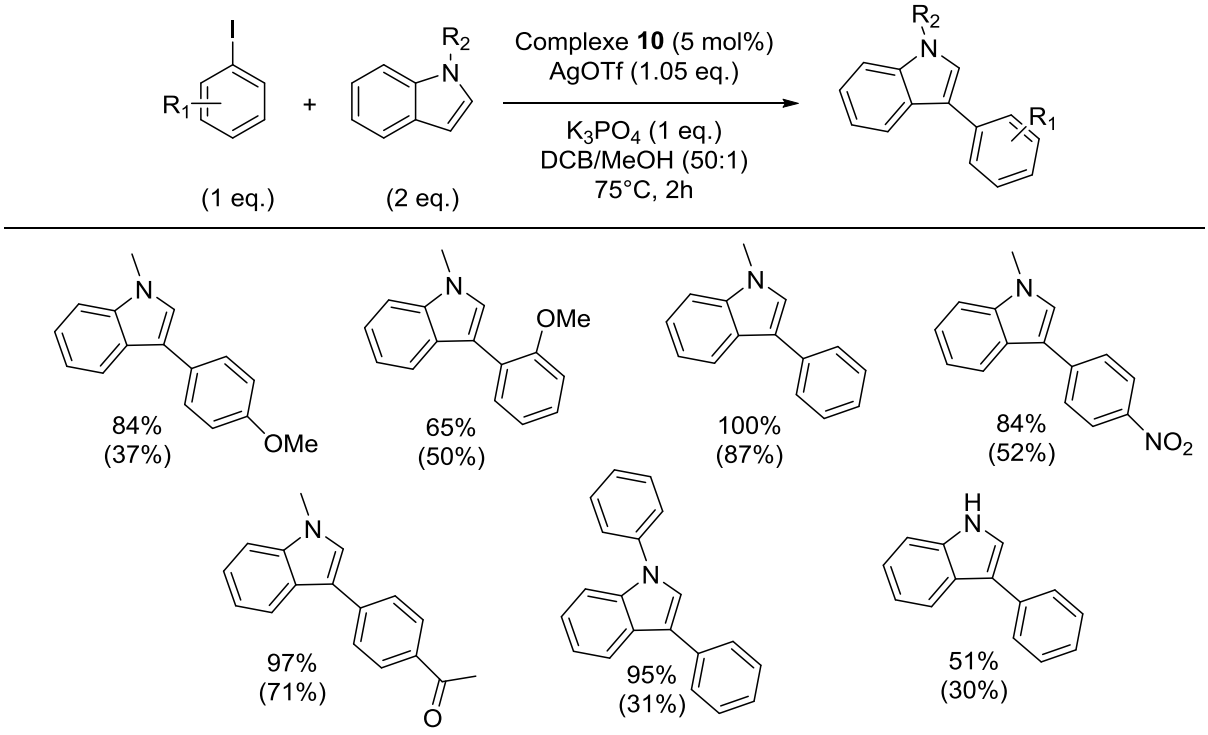

Schéma 6.16 Couplage croisé d'iodures d'aryles et les indoles catalysés par le complexe **10**. Les rendements ont été déterminés par GC-MS (étalonnée *vs. n*-dodecane), et les rendements isolés entre parenthèse.

Le scope de cette réaction n'est pas limité aux hétérocycles à base d'azote et peut être étendu à des substrats à base d'oxygène. En effet, l'arylation directe du 2,3-diméthylfurane avec de l'iodobenzene a donné le produit de couplage croisé avec un rendement de 71% après deux heures à 75°C (Schéma 6.17). Une régiosélectivité élevée a également été observée, et seul le furane arylé en position C2 a été formé.

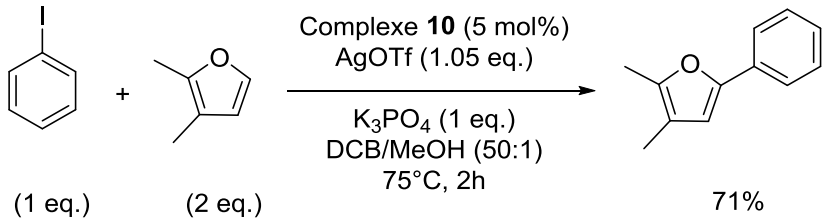

Schéma 6.17 Couplage croisé de PhI et 2,3-diméthylfurane avec le complexe **10**.

6.5 Isolation d'un Carbène d'or(I) Réactif

6.5.1 Introduction

Les complexes carbéniques d'or sont des intermédiaires clés, et leurs transformations diverses constituent l'un des aspects les plus polyvalent de la catalyse à l'or donnant accès à une gamme variée de composés. Malgré les progrès dans ce domaine, une famille importante d'espèces carbéniques, les complexes α-oxo d'or(I), n'a jamais été isolée ou caractérisée. Une variété de transformations cascades ont prouvé l'utilité synthétiques des complexes α-oxo carbène d'or(I), et sont généralement soulignées comme des intermédiaires clés. Ainsi, la caractérisation et éventuellement l'isolement d'un complexe carbène α-oxo d'or(I) représente un grand intérêt non seulement d'un point de vue synthétique, mais aussi d'un point de vue fondamentale car cela permettra de mieux comprendre les paramètres qui réagissent sa réactivité.

6.5.2 Caractérisation d'un complexe α-oxo carbène d'or(I)

6.5.2.1 Avec le Ligand (P,N)

Nous avons envisagé de générer le carbène α-oxo d'or(I) à basse température en utilisant la stratégie classique, c'est-à-dire la décomposition d'un réactif diazo. A une solution du complexe **10** (Me-Dalphos)AuCl et à un équivalent d'$AgSbF_6$ (génération *in situ* du complexe d'or(I) cationique insaturé), une équivalent d'éthylphenyldiazoacétate a été ajouté à -80°C (Schéma 6.18).

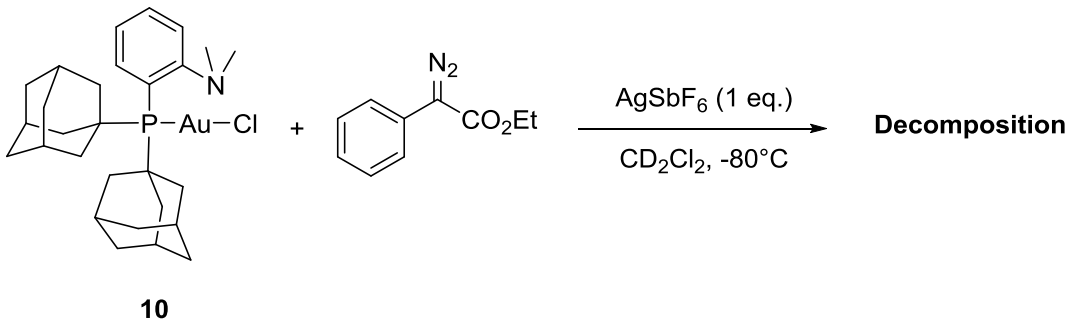

Schéma 6.18 Tentative de générer le carbène α-oxo d'or(I) avec le complexe **10** et l'éthylphenyldiazoacétate.

Après l'addition du diazo, un changement de couleur (d'incolore à l'orange foncé) et un dégagement de N_2 ont été observés. La réaction a été contrôlée directement par RMN à -75°C, mais le premier contrôle par RMN $^{31}P\{^1H\}$ a révélé la présence de plusieurs espèces, mettant en évidence l'instabilité du carbène α-oxo d'or(I) même a très basses températures.

Puisque le carbène α-oxo d'or(I) n'a pas pu être caractérisé sans ambigüité à -75°C avec le ligand (P,N), nous avons décidé d'utiliser le ligand *o*-carborane diphosphine.

6.5.2.2 Avec le Ligand (P,P)

Le ligand *o*-carborane diphosphine a déjà été utilisé par notre équipe pour isoler et caractériser des complexes carbonyles et carbéniques d'or(I). En plus, les calculs théoriques ont révélés la présence d'une retro-donation importante du fragment [(P,P)Au^{+}] expliquant la stabilité de ces espèces.

Comme avec le ligand (P,N), un équivalent d'éthylphenyldiazoacétate a été ajouté à basse température à une solution du complexe **6** (Schéma 6.19). Le mélange réactionnel a immédiatement changé de couleur en violet foncé avec un bullage concomitant de N_2, suggérant la formation d'une espèce carbéniques. Le suivie de la réaction par RMN $^{31}P\{^{1}H\}$ à -40°C, a indiqué la formation instantanée d'une seule nouvelle espèce avec un déplacement chimique de 138.9 ppm.

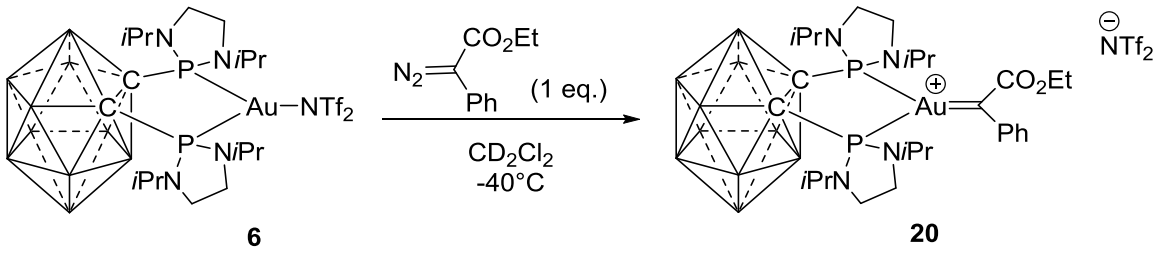

Schéma 6.19 Synthèse du carbène α-oxo d'or(I) **20** à -40°C.

Le complexe **20** s'est révélé d'être thermiquement instable (décomposition au-dessus de 0°C) et n'a pas pu être isolé. Cependant, il a été entièrement caractérisé à basse température par spectrométrie RMN multinucléaire, et la formation du complexe carbénique était clairement indiquée par la RMN $^{13}C\{^{1}H\}$. En fait, un signal de résonance caractéristique à δ = 283.4 ppm apparait sous la forme d'un triplet (J_{CP} = 87.6 Hz), et se situe dans la zone des complexes d'or(I) carbéniques précédemment caractérisés. La formation du complexe **20** a été confirmée

aussi par diffraction des rayons X. La coordination-κ^2 symétrique du ligand diphosphine à l'or donne un complexe α-oxo d'or(I) tricoordiné, et l'or se trouve dans une géométrie trigonale planaire.

Des études computationnelles ont été menées afin de mieux comprendre la situation électronique du complexe α-oxo d'or(I) tricoordiné et d'évaluer le rôle du ligand diphosphine dans sa stabilisation. Les orbitales frontières HOMO et LUMO du complexe **20** correspondent a une interaction de liaison et anti-liaison entre l'orbitale occupée d_{xz}(Au) et l'orbitale $2p^{\pi}$(C) du carbène. De plus, une rétro-donation d_{xz}(Au)→ $2p^{\pi}$(C) significatif a été observé, ce qui reflète aussi dans la contribution considérable de l'orbitale $2p^{\pi}$(C) (12.1%) dans la NLMO associé à d_{xz}(Au). La rétro-donation significatif du fragment [(P,P)Au^{+}] au carbène a également été retrouvée dans le rapport donation/rétro-donation estimé par CDA (d/b = 1.76) et dans l'absence de transfert de charge entre le carbène et le fragment de l'or (CT = -0.07 e). Ces résultats expérimentales et théoriques souligne le rôle important du ligand (P,P) dans la stabilisation de l'espèce réactif α-oxo carbène d'or(I).

Après avoir confirmé le rôle crucial du ligand (P,P) bidenté, nous avons essayé de stabiliser des carbènes α-oxo d'or(I) encore plus électrophile. Dans cet objectif, le substrat α-aryle-α-diazoacétate comportant deux groupes CF_3 sur le noyau aromatique a été synthétisé et réagi avec le complexe **6** à basse température pour générer le carbène correspondant (Schéma 6.20).

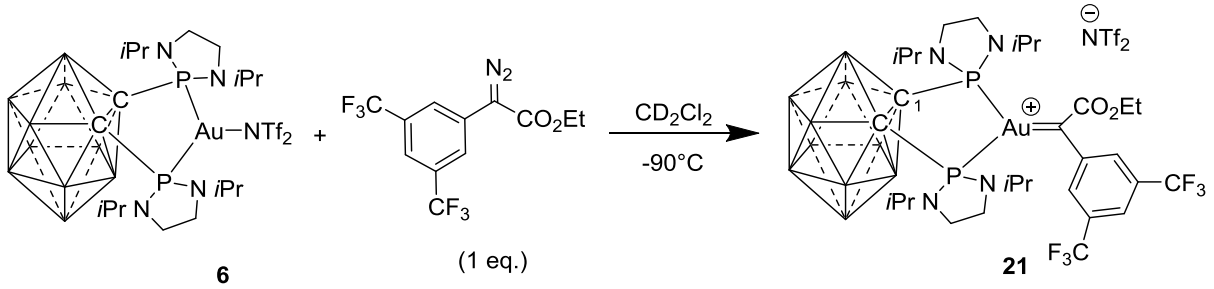

Schéma 6.20 Synthèse du carbène α-oxo d'or(I) **21** à -90°C.

Le complexe **21** était beaucoup moins stable que le complexe **20** et décomposait très rapidement même à basse température. Ainsi, le complexe **21** n'a été détecté que par spectroscopie RMN $^{31}P\{^{1}H\}$ à -90°C. Plus d'informations sur sa structure électronique ont été fournis par calculs DFT, qui ont confirmé sa haute instabilité.

Ensuite, nous avons étudié les conséquences de la coordination chélate du ligand (P,P) sur la réactivité et/ou sélectivité du complexe **20**. La réaction de transfert du fragment carbène aux phénols reste un défi pour les métaux de transition en raison des réactions compétitives d'insertion O-H *vs.* C-H. Il a été récemment montré que les complexes monophosphine d'or(I) catalysaient la fonctionnalisation de la liaison *p*-C-H des phénols d'une manière très sélective.

En utilisant 5 mol% du complexe **6**, le carbène α-oxo d'or(I) a été généré *in situ* à basse température et 5 équivalents de phénol ont été ajoutés au mélange réactionnel (Schéma 6.21). Après deux heures à température ambiante, la réaction a fourni exclusivement le produit issu de l'insertion O-H avec un rendement de 60%. Ainsi, une chimiosélectivité inverse est observé avec le ligand (P,P) comparé aux autres exemples rapportés avec des complexes d'or(I) comportant des phosphines monodentes dépourvues d'électrons. En raison de la rétro-donation importante induite par le ligand (P,P), l'électrophilie du carbène α-oxo d'or(I) a été atténuée, et donc sa réactivité est plus proche des autres métaux de transition.

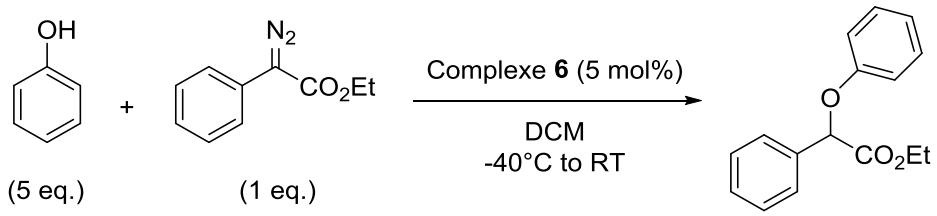

Schéma 6.21 Réactivité du carbène α-oxo d'or(I) avec le phénol.

Ensuite, pour confirmer la relation électrophilie / sélectivité de l'or pour l'insertion C-H *vs.* O-H, la réaction avec le diazo-CF_3 a été étudiée. Les groupes CF_3 électro-attracteurs peuvent contrebalancer la stabilisation électronique induite par le ligand (P,P) et par conséquent restituer la réactivité électrophile classique au carbène α-oxo d'or(I). Ainsi, une solution du diazo-CF_3 (1 eq.) et de phénol (5 eq.) a été ajoutée a -40°C à une solution du complexe **6** (Schéma 6.22)

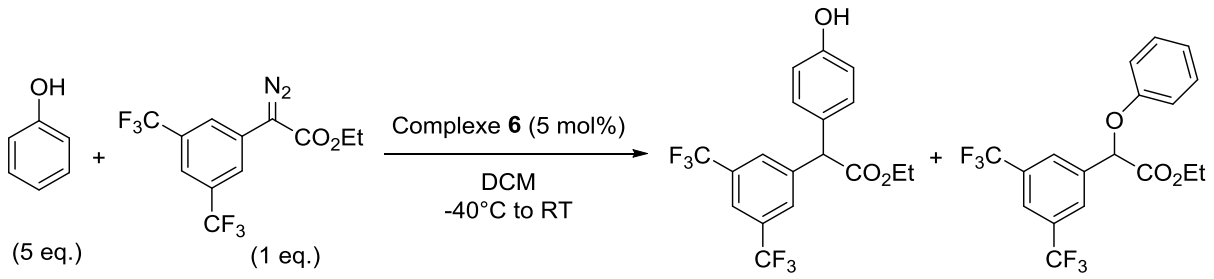

Schéma 6.22 Réactivité du carbène α-oxo d'or(I) avec le phénol.

La réaction s'est déroulée plus rapidement, et après 30 minutes, le produit d'insertion C-H a été obtenu comme le produit majoritaire (68%) avec une quantité mineure du produit issu de l'insertion O-H (32%). En effet, les groupes électro-attracteurs sur le phényle du substrat diazo ont contrebalancés la rétro-donation du fragment [(P,P)Au^+], et ce résultat confirme que la sélectivité des espèces α-oxo d'or(I) pour l'insertion C-H *vs.* O-H est régie par le caractère électrophile du carbène.

6.6 Conclusion

Grâce à cette étude, nous avons pu montrer que l'addition oxydante des liaisons Csp^2-X (X = I, Br) est un processus favorable et faisable avec les complexes d'or à condition que le ligand soit adapté à cette transformation. Le couplage croisé mettant en jeu une étape d'addition oxydante a été réalisé, et plusieurs arènes et hétéroarènes ont été couplés avec des halogénures d'aryles pour former des biaryls avec de très bons rendements et dans des conditions douces. Finalement, avec le ligand (P,P) bidenté, on a pu caractérisé a basse température pour la première fois un complexe α-oxo carbène d'or(I). Ainsi, ces résultats montrent que l'utilisation des ligands bidentés est la clé pour stabiliser des intermédiaires d'or clés et pour développer des réactions considérer auparavant impossible à l'or.